# BACTERIAL IRON AND MANGANESE REDUCTION DRIVEN BY ORGANIC SULFUR ELECTRON SHUTTLES

A Dissertation
Presented to
The Academic Faculty

by

Rebecca Elizabeth Cooper

In Partial Fulfillment
of the Requirements for the Degree
Doctor of Philosophy in the
School of Biology

Georgia Institute of Technology
May 2015

**BACTERIAL IRON AND MANGANESE REDUCTION DRIVEN BY**

**ORGANIC SULFUR ELECTRON SHUTTLES**

Approved by:


Dr. Thomas DiChristina, Advisor
School of Biology
*Georgia Institute of Technology*

Dr. Brian Hammer
School of Biology
*Georgia Institute of Technology*

Dr. Jim Spain
School of Civil and Environmental Engineering
*Georgia Institute of Technology*

Dr. Frank Stewart
School of Biology
*Georgia Institute of Technology*

Dr. Martial Taillefert
School of Earth and Atmospheric Sciences
*Georgia Institute of Technology*


Date Approved: March 31, 2015

## ACKNOWLEDGEMENTS

First, I would like to thank my advisor, Dr. Tom DiChristina. Thank you for taking a chance on me, twice. I appreciate your understanding, patience, and your ability to make me think outside of the box and grow both as a person and scientist. You have given me the confidence to become successful and I thank you for giving me the opportunity to realize my own potential as a scientist.

Thank you to my committee member: Brian Hammer, Jim Spain, Frank Stewart, and Martial Taillefert. Thank you for your time, patience, and advice.

Thank you to my current and former labmates in the DiChristina lab: Seng Kew Wee, Ramanan Sekar, Nadia Szeinbaum, Dawayland Cobb, and Jennifer Goff. Thank you for the moral support and advice along the way. I have had such a great time working beside all of you.

To my mom, thank you for the constant support, encouragement, and always believing in me. Thank you for reminding me that as long as I am doing the best I can do I can and will accomplish great things. To my brother and sister, thank you for your never-ending support. You both mean more to me that I can ever express with words. To my Mema, thank you for the unconditional love you have for me, Kimberly, and Jamie. I am forever appreciative for everything you have done for us. To my Papa, thank for always believing in me, for the crossword puzzles you always finished for me, and the constant love you had for me. You are the smartest man I will ever know and I am a better person for having had you in my life. To the rest of my family, thank you for the unconditional love and support.

## TABLE OF CONTENTS

## LIST OF TABLES

## LIST OF FIGURES

## LIST OF SYMBOLS AND ABBREVIATIONS

| | |
|---|---|
| ADP | adenosine diphosphate |
| AI-2 | autoinducer-2 |
| AMC | activated methyl cycle |
| ATP | adenosine triphosphate |
| AQDS | anthraquinone-2,6-disulfonate |
| CAH | cystamine |
| CAAC | cystamine |
| CBL | cystathionine β-lyase |
| CGS | Cystathionine γ-synthase |
| CLSM | confocal laser scanning microscopy |
| CSH | cysteine |
| CSSC | cystine |
| DMRB | dissimilatory metal-reducing bacteria |
| DMSP | dimethylsulfoniopropionate |
| DNA | deoxyribonucleic acid |
| DSP | direct sulfurylation pathway |
| DTDG | dithiodiglycolate |
| DTDP | dithiodipropionate |
| DTNB | 5-(3-Carboxy-4-nitrophenyl)disulfanyl-2-nitrobenzoic acid |

| | |
|---|---|
| FAD | flavin adenine dinucleotide |
| Fe | iron |
| GSH | glutathione |
| GSSG | oxidized glutathione |
| HFO | hydrous Fe(III) oxide |
| HSH | homocysteine |
| HSSH | homocystine |
| HSST | homoserine succinyltransferase |
| IM | inner membrane |
| LB | Luria-Bertani medium |
| Mn | manganese |
| OAHS | O-acetyl-L-homoserine sulfhydrolase |
| OAS | O-acetyl-L-serine |
| OASS | O-acetylserine sulfhydrolase |
| OM | outer membrane |
| OPHS | O-phospho-L-homoserine |
| OSHS | O-succinyl-L-homosrine |
| PCR | polymerase chain reaction |
| PMF | proton motive force |
| RNA | ribonucleic acid |
| SAH | S-adenosylhomocysteine |

| | |
|---|---|
| SAM | S-adenosylmethionine |
| SRB | sulfate-reducing bacteria |
| SRH | S-ribosylhomocysteine |
| TSP | transulfurylation pathway |

## SUMMARY

Dissimilatory metal-reducing bacteria (DMRB) play an important role in the biogeochemical cycling of metals. DMrB are unique in that they possess the ability to couple metal reduction with their metabolism. Microbial Fe(III) respiration is a central component of a variety of environmentally important processes, including the biogeochemical cycling of iron and carbon in redox stratified water and sediments, the bioremediation of radionuclide-contaminated water, the degradation of toxic hazardous pollutants, and the generation of electricity in microbial fuel cells. In addition, microbial Fe(III) respiration is postulated to be one of the first respiratory processes to have evolved on early earth. Despite this environmental and evolutionary importance, the molecular mechanism of microbial Fe(III) respiration is poorly understood. Current models of the molecular mechanism of microbial metal respiration are based on direct enzymatic, Fe(III) solubilization, and flavin-based electron shuttling pathways. Further understanding of the mechanism by which DMRB mediate metal reduction will provide further insight into their roles in the environment and to the development of applications such as generation of electricity via microbial fuel cells and the bioremediation of metal- and radionuclide contaminated sites. Since Fe(III) oxides are solid at circumneutral pH and therefore unable to come into direct contact with the microbial inner membrane, these bacteria must utilize an alternative strategy for iron reduction. Reduced organic compounds such as thiols are prominent in natural environments where DMRB are found. These thiol compounds are redox reactive and are capable of abiotically reducing Fe(III) oxides at high rates. These

thiol compounds provide an DMRB a suite of external electron shuttles for Fe(III) reduction, thereby enabling the bacteria to shuttle electrons to external Fe(III) oxides during Fe(III) respiration.

The main objectives of the thesis research were to i) determine if bacterial cell-Fe(III) oxide contact and biofilm formation are required for Fe(III) oxide reduction by *S. oneidensis* (Chapter 2), ii) determine if *S. oneidensis* produces and utilizes Autoinducer-2 under anaerobic growth conditions as an alternate carbon and electron source (Chapter 3), and iii) determine if extracellular thiols produced by *S. oneidensis* shuttle electrons to external Fe(III) and Mn(III,IV) oxides during anaerobic respiration (Chapter 4).

*S. oneidensis* wild-type and Δ*luxS* anaerobic biofilm formation phenotypes were assessed under a variety of electron donor-electron acceptor pairs, including lactate or formate as the electron donor and fumarate, thiosulfate, or Fe(III) oxide-coated silica surfaces as the terminal electron acceptor. The rates of biofilm formation under the aforementioned growth conditions as well as in the presence of exogenous thiol compounds indicate that Δ*luxS* formed biofilms at rates only 5-10% of the wild-type strain, Δ*luxS* displayed a biofilm-deficient mutant phenotype regardless of electron donor (lactate or formate), and Δ*luxS* biofilm formation rates were restored to wild-type levels by addition of a variety of exogenous compounds including cysteine, glutathione, homocysteine, methionine, serine, and homoserine. Lastly, cell adsorption isotherm analyses were conducted to determine the attachment phenotype of the wild-type and Δ*luxS* to Fe(III) oxide surface. The results of Chapter 2 indicate that neither biofilm formation nor Fe(III) oxide attachment are required for Fe(III) oxide reduction by *S. oneidensis*, and suggest that

electron transport pathways other than direct enzymatic reduction may dominate during Fe(III) oxide respiration by *S. oneidensis.*

*S. oneidensis* Δ*luxS* displays a deficient biofilm phenotype when grown under anaerobic growth conditions. Δ*luxS* anaerobic biofilm formation rates were restored to wild-type levels by addition of exogenous auntoinducer-2 (AI-2). This discovery led to subsequent experiments performed to detect the production of AI-2 by both wild-type and Δ*luxS* strains under both aerobic and anaerobic growth conditions as well as the depletion of AI-2. AI-2 production experiments showed that the concentration of AI-2 produced by *S. oneidensis* were equivalent to the *Vibrio harveyi* negative controls (AI-2$^-$ strains). The addition of exogenous AI-2 to both wild-type and Δ*luxS* resulted in the swift depletion of AI-2 from the media. The results of Chapter 3 indicate that *S. oneidensis* is capable of utilizing AI-2 as carbon source that can be taken up and used as a metabolite.

*S. oneidensis* produced and secreted a variety of thiol compounds, including cysteine, homocysteine, glutathione, and cyteamine when grown under Fe(III)-reducing and Mn(III) and Mn(IV)-reducing conditions. Both reduced and oxidized forms of the aforementioned thiol compounds were detected, indicating that the thiols are in a constant state of flux between the reduced and oxidized forms and that the concentration of reduced thiols to its' oxidized counterpart is indicative of the state of metal reduction by the microorganisms. The results of Chapter 4 indicate that endogenous thiols produced by *S. oneidensis* when utilizing Fe(III) oxides or Mn (III, IV) oxides as the terminal electron acceptor are used as an effective electron shuttles, which ultimately increase the efficiency of electron transfer to external metal oxides during anaerobic Fe(III)-, Mn(III)-, and Mn(IV)-oxide respiration.

The *S. oneidensis* genome contains genes that comprise the activated methyl cycle (AMC) and transsulfurylation pathways (TSP). The AMC is a metabolic cycle that produces the methyl donor S-adenosyl-L-methionine (SAM) and recycles methionine via S-adenosyl homocysteine (SAH) and homocysteine. The TSP is a metabolic pathway responsible for the interconversion of cysteine and homocysteine via cystathionine. In *S. oneidensis,* theses cycles are imperative for the production of thiol compounds, including homocysteine, glutathione, and cysteine, that can serve as electron shuttles for Fe(III) oxide reduction. The results indicate that the components of the AMC and TSP of *S. oneidensis* yield extracellular thiols during anaerobic growth on Fe(III) oxides as the terminal electron acceptors and these extracellular thiols can also be used as an electron shuttle.

# CHAPTER 1

## INTRODUCTION

Microbial iron (Fe(III)) respiration is a fundamental component of a variety of environmentally important processes, including biogeochemical cycling of iron and carbon, bioremediation of radionuclide-contaminated water, and degradation of toxic hazardous pollutants (1). Microbial Fe(III) reduction also drives the generation of electricity in microbial fuel cells (2-5). Bacterial energy conservation requires generation of a proton motive force (PMF) across the inner membrane (IM). Electrons originating from oxidation of electron donors are transported down the redox gradient of an electron transport chain to IM- or periplasmic- localized terminal reductases coupled to proton translocation across the IM to generate PMF. PMF drives ATP synthesis as protons are translocated back into the cytoplasm through IM-localized ATPases, catalyzing the phosporylation of ADP to ATP (6). Fe(III)-respiring bacteria are therefore presented with a unique physiological problem: they are required to respire anaerobically on insoluble terminal electron acceptors that are unable to contact IM-localized electron transport systems (1). In anaerobic marine and freshwater environments, dissimilatory metal-reducing bacteria (DMRB) produce energy by coupling the oxidation of molecular hydrogen ($H_2$) to the reduction of alternate electron acceptors, such as soluble and insoluble forms of Fe(III), Mn(III), and Mn(IV) (1).

### Phylogeny of *Gammaproteobacteria*

The phylum *Proteobacteria* is composed of gram-negative bacteria that encompass a diversity of physiological traits (7, 8). The predominant gram-negative members of the phylum *Proteobacteria* include phototrophs, heterotrophs, and lithotrophs (9). *Proteobacteria* can be phylogenetically divided into *Alpha, Beta, Delta, Epsilon, Gamma,* and *Zeta* classes based on comparative analysis of 16S rRNA sequences (7, 9-12). Within the classes that comprise the *Proteobacteria* phylum, *Gammaproteobacteria* are more closely related to *Betaproteobacteria* than to any other clases in the phylum (9, 13, 14). The *Gammaproteobacteria* class includes many of the most widely studied model organisms, including *Escherichia coli, Vibrio, Salmonella, Yersinia, Pseudomonas,* and *Shewanella* (8, 9, 13, 15, 16). In addition, the *Gammaproteobacteria* are comprised of close to 250 genera, which equates to one of the highest numbers of genera within all bacteria phyla (16, 17).

**Phylogenetic diversity of DMRB**

*Shewanella oneidensis* MR-1 and *Geobacter sulfurreducens* were two of first bacterial strains reported to utilize metals, such as iron and manganese, as the sole terminal electron acceptor (18, 19). Further study of DMRB led to identification of DMRB throughout the domains *Bacteria* and *Archaea* (20, 21). DMRB have been identified in all major classes of *Proteobacteria,* including the class *Alpha* (e.g., *Acidiphilium acidophilum*), *Beta* (e.g., *Ferribacterium limneticum* and *Rhodoferax ferrireducens*), *Delta* (e.g., *Geobacter sulfurreducens, Pelobacter carbinolicus, Desulfuromonas acetoxidans, Desulfovibrio profundus,* and *Geothermobacter ehrlichii*), *Epsilon* (e.g., *Sulfurospirilllum barnesii*), and *Gamma* (e.g., *Shewanella oneidensis, Aeromonas hydrophila, Pantoea*

*agglomerans* SP1, and *Ferrimonas balearica*) (Figure 1.1). The most comprehensively studied DMRB include facultative anaerobes from the genus *Shewanella* and obligate anaerobes from the genus *Geobacter*, which belong to *Gammaproteobacteria* and *Deltaproteobacteria* classes, respectively. Recent studies involving the metabolism of *S. oneidensis* MR-1, *G. sulfurreducens*, and some related strains have provided substantial insight into the mechanisms of metal respiration utilized by these microorganisms.

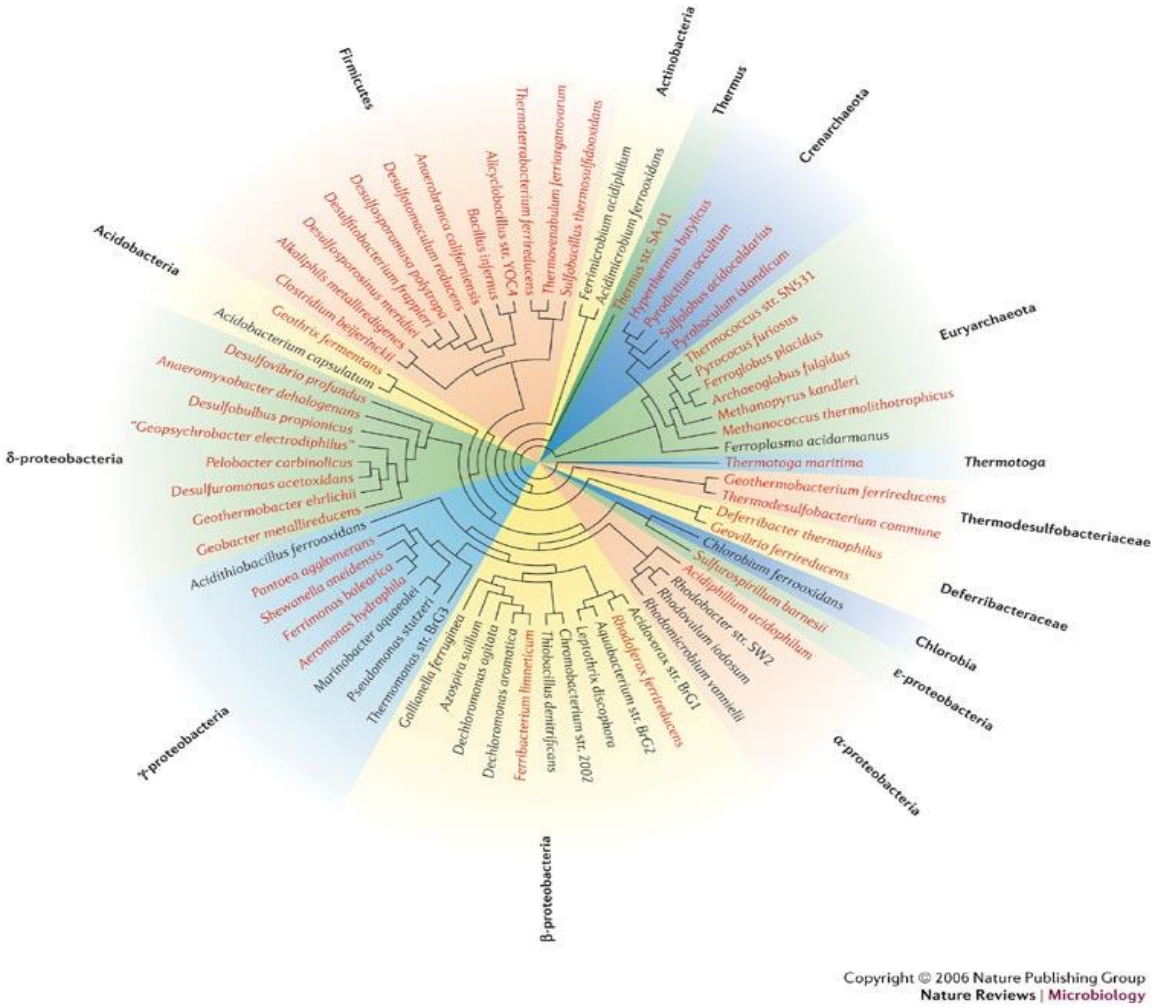


**Figure 1.1 Phylogenetic affiliations of microorganisms contributing to iron cycling (21).**

**Metal-reducing members of the Genus *Shewanella***

*S. oneidensis* MR-1 is a gram-negative facultative anaerobe, previously known as *Alteromonas putrefaciens* MR-1. *S. oneidensis* MR-1 was isolated from anaerobic

sediments in a metal-rich Oneida Lake (NY); it was the first microorganisms found to produce energy via electron transport chain-linked metal reduction (19). Most known *Shewanella* species have been isolated from marine environments (22), including the tissues of rotting squid and fish, however (22), *S. oneidensis* MR-1 was isolated from freshwater sediments (22). *S. oneidensis* MR-1 utilizes a variety of terminal electron acceptors, including $O_2$, fumarate, nitrate, nitrite, trimethylamine *N*-oxide, dimethyl sulfoxide, sulfite, thiosulfate, elemental sulfur, and soluble and insoluble transition metals such as Fe(III) citrate, Fe(III) oxide, goethite, hematite, Mn(IV) oxide, and Mn(III) (19, 23-28). The respiratory versatility displayed by *Shewanella* enables the microorganism to survive in environments with fluctuating redox conditions (29). Human infections by *Shewanella* species are uncommon, but several infections have been associated with *S. algae* and *S. putrefaciens* (30). In the food industry, however, *Shewanella* species have been branded as the microorganisms responsible for food spoilage when fish are stored at low temperatures (31-33).

**Molecular mechanisms of microbial metal respiration**

Respiration in gram-negative bacteria is derived from the generation of a proton-motive force (PMF) across the inner membrane (IM). Electrons originating from the oxidation of electron donors are transported down the redox gradient of an electron transport chain to terminal reductases, at the same time proton are translocated across the IM to generate PMF. PMF provides the energy for ATP synthesis as protons are translocated back to the cytoplasm via IM-localized ATPases, catalyzing the phosphorylation of ADP to ATP (6). Bacterial terminal reductases for soluble electron

acceptors, including $O_2$, nitrate, and fumarate, are localized to the IM or periplasmic space. DMRB are unique in that they are required to respire anaerobically on terminal electron acceptors found mostly in solid forms that are ostensibly unable to contact IM-localized electron transport systems (1). *S. oneidensis* employs a variety of novel respiratory strategies to overcome the problem of respiring solid Fe(III) oxides including i) direct enzymatic reduction via outer membrane (OM) or nanowire-localized metal reductases (34-38), ii) Fe(III) chelation (solubilization) pathways in which the solid Fe(III) oxides are first non-reductively dissolved by endogenously synthesized organic ligands prior to reduction (39), iii) nanowire pathways in which electrically conductive pili (nanowires) transfer electrons to external metal oxides (38), and iv) electron shuttling pathways mediated by exogenous or endogenous electron shuttling compounds (40-44).

**1. Direct enzymatic reduction pathways.** Direct enzymatic reduction of Fe(III) oxides requires OM-localized terminal Fe(III) reductases (Fig. 1.2). *S. oneidensis* has developed extracellular electron transfer strategies that require multiheme *c*-type cytochromes (45). The *S. oneidensis* OM proteins involved in terminal steps of the electron transfer to insoluble electron acceptors include several decaheme *c*-type cytochromes (MtrC OmcA, MtrA) (37, 45-47) that are a subset of 42 predicted *c*-type cytochromes encoded by the *S. oneidensis* genome (24). One of the proposed electron-transfer pathways to insoluble Fe(III) oxides is through OM-localized decaheme *c*-type cytochromes encoded by the *omcA-mtrCAB* gene cluster (19, 48-50). Disruption of the *mtrC* or *omcA* genes does not affect the ability of *S. oneidensis* to reduce soluble electrons acceptors such as nitrate or fumarate, while the *mtrC* deletion mutant displays 33% less Fe(III) reduction activity than the wild type strain. While deletion of *omcA* does not affect

Fe(III) oxide reduction activity, the *mtrC-omcA* double mutant is severely impaired in Fe(III) oxide reduction activity. Thus, MtrC is postulated to be involved in direct electron transfer to extracellular Fe(III) oxides (51, 52) or to extracellular electron shuttles which then reduce the insoluble Fe(III) oxides (41, 53). MtrC and OmcA are translocated across the periplasm to the OM via a type II protein secretion system (T2SS) (Fig. 1.2) (54). MtrC is hypothesized to bind and transfer electrons to flavins secreted by *S. oneidensis* as electron shuttles to transfer electron to external Fe(III) oxides (55, 56).

MtrA is located in the *S. oneidensis* periplasm (34), while MtrC and OmcA are translocated across the periplasm to the OM via the type II protein secretion system (Fig. 1.2) (35). Amino acid sequence analyses indicate that MtrA displays a high degree of similarity to NrfB, a *c*-type cytochrome involved in formate-dependent nitrite reduction in *E. coli* (34). MtrA associates in the OM as part of the extracellular electron conduit comprised of MtrABC in a 1:1:1 stoichiometry (51). Purified MtrA and MtrC associate with MtrB in proteoliposomes as part of the MtrCAB complex that directs electrons from internal reduced methyl viologen to external Fe(III) substrates (51, 57, 58). MtrB is a central component in the metal reduction pathway, and the absence of *mtrB* gene results in a severe loss in respiratory activity for both soluble and insoluble metals (34). MtrB does not contain heme groups and it is proposed to function as a OM anchor that aids in electron transport from MtrA in the periplasm to MtrC or OmcA at the cell surface (45). The MtrB β-barrel may serve as a structural sheath for embedding MtrA and MtrC at the inner and outer faces of the OM, thus facilitating electron transfer to external Fe(III) oxides (Fig. 1.2) (59, 60). MtrA and MtrB homologs have been reported in Fe(II)-oxidizing bacteria including *Rhodopseudomonas palustris*, *Sideroxydans lithotropicus*, and *Dechloromonas*

*aromatic* (61-63). The presence of MtrAB homologs across species of Fe(III)-reducing and Fe(II)-oxidizing bacteria imply that electron transfer across the OM via the Mtr pathway may be bidirectional (64).

Electron transfer reactions to Fe(III) substrates are exceedingly slow at distances > 15 Å (65-67). Direct enzymatic Fe(III) reduction may therefore require bacterial cell-Fe(III) oxide surface contact that is enhanced by biofilm formation. Aerobic biofilm formation by *S. oneidensis* is similar to that observed in *Pseudomonas aeruginosa* and *Escherichia coli* (68-71): After initial cell attachment, microcolonies and small 3-dimensional (3D) structures are formed. Total surface coverage is achieved in biofilms growing horizontally and vertically, ultimately maturing to 3D mushroom-like protrusions and valley-shaped indentations (70). Previous studies have assessed the impact of both genetic and environmental factors on biofilm development, including surface topography (72), shear stress (73), temperature, quorum sensing signals (74), and nutrient concentration (75, 76). The impact of these factors on the mechanisms associated with biofilm formation is not well characterized(77). In *P. aeruginosa* and *E.coli*, biofilm formation requires S-ribosylhomocysteinase (LuxS)-catalyzed formation of autoinducer-2 (AI-2), a quorum-sensing signal that facilitates cell-cell communication between bacteria carrying out cell density-dependent activities (78-83). LuxS converts S-ribosylhomocysteine (SRH) to homocysteine and the AI-2 precursor metabolite 4,5-dihydroxy-2,3-pentadione, which subsequently undergoes a series of abiotic reactions to form AI-2 (84-86). Although LuxS-dependent *S. oneidensis* biofilm formation on silica surfaces has been examined under aerobic conditions (87), LuxS-dependent biofilm formation on Fe(III) oxide surfaces under anaerobic conditions has yet to be examined.

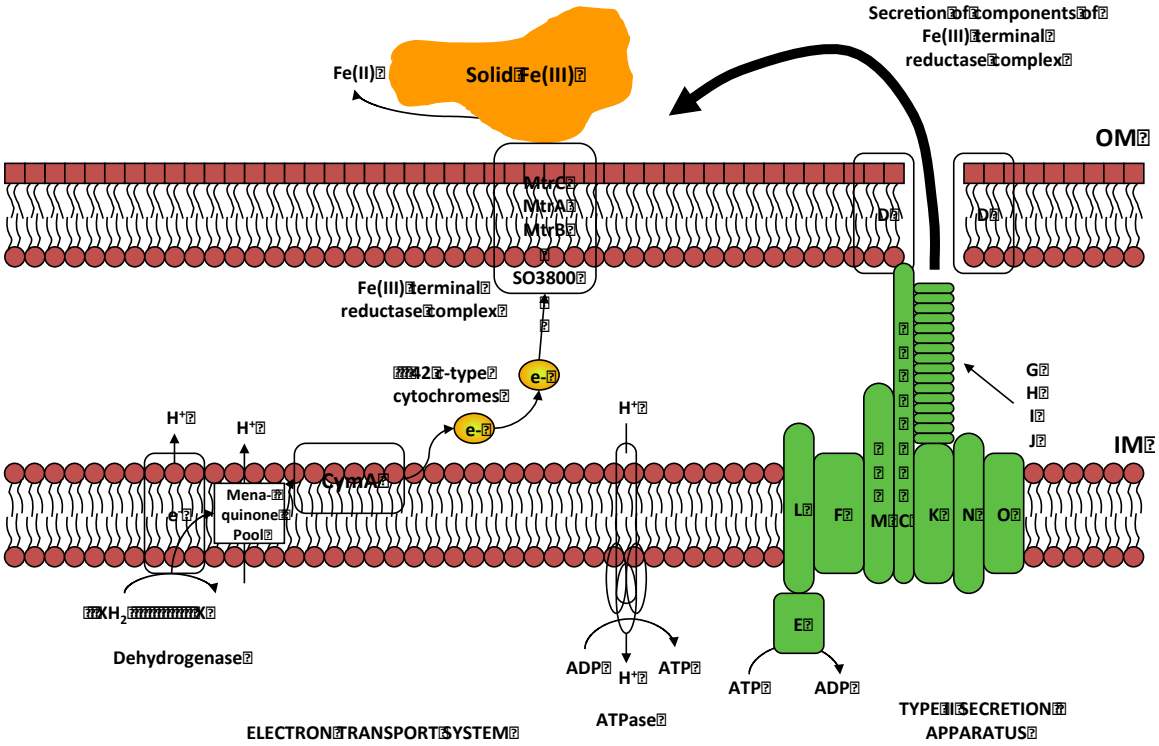


**Figure 1.2. Working model of the *S. oneidensis* electron transport chain terminating with reduction of external Fe(III) oxides via direct contact mechanism (1, 88).**

**2. Fe(III) solubilization pathways.** The Fe(III) oxide chelation (solubilization) pathway is the least characterized of the Fe(III) oxide reduction pathway. In this pathway (Fig. 1.3), *S. oneidensis* is postulated to secrete organic ligands that subsequently form more readily reducible soluble organic-Fe(III) complexes. The resulting soluble organic-Fe(III) complexes may be reduced at the OM or taken into the cell and reduced by periplasmic or IM-localized Fe(III) reductases. Soluble organic-Fe(III) is detected electrochemically in *S. oneidensis* and S. *putrefaciens* cultures incubated anaerobically with solid Fe(III) oxides (89). Detection of soluble organic-Fe(III) prior to Fe(II) production indicates that soluble organic-Fe(III) is an intermediate in the reduction of solid Fe(III) oxides (Fig. 1.3) (1). Genetic and biochemical analyses have indicated that Fe(III)-chelating siderophores do not function as Fe(III)-solubilizing ligands during anaerobic

Fe(III) oxide reduction (90). The identity of the Fe(III)-solubilizing organic ligands and the proteins involved in ligand biosynthesis have yet to be identified.

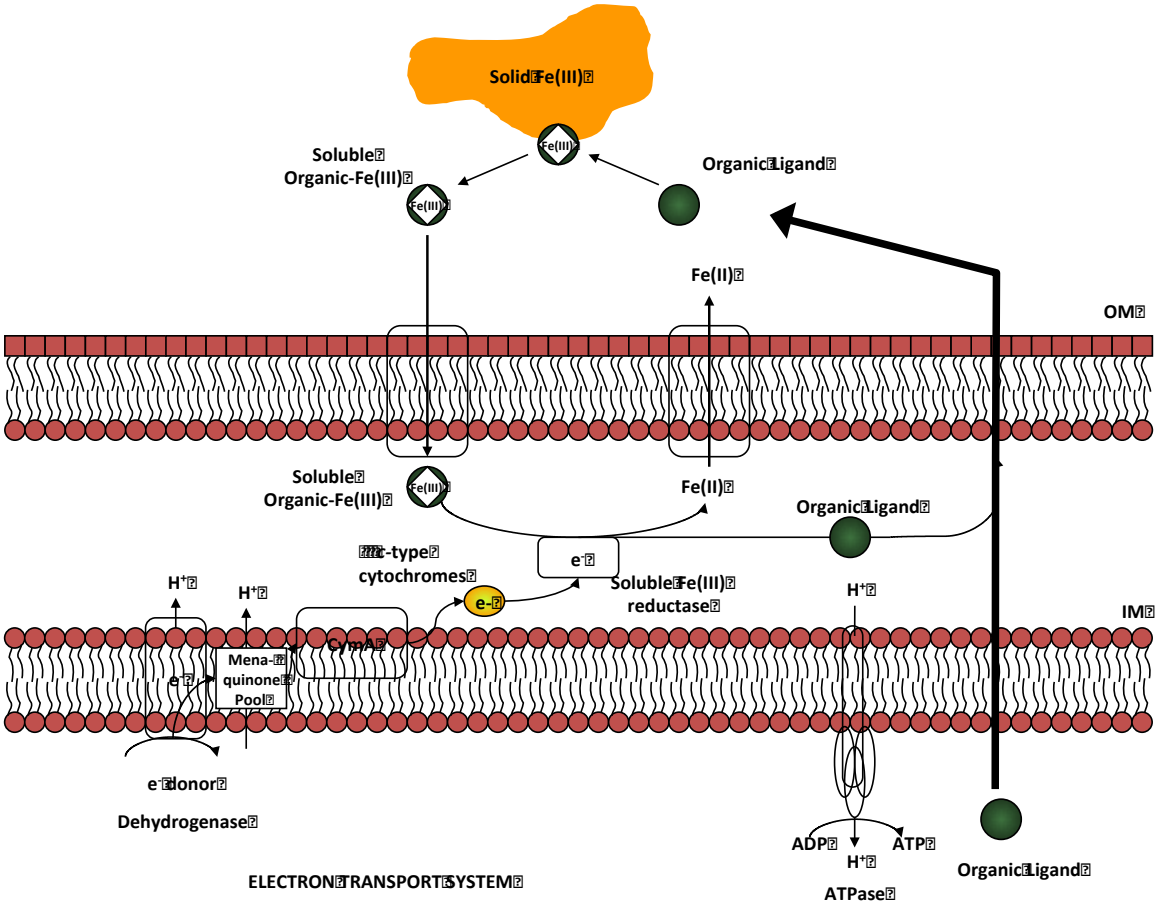


**Figure 1.3. Working model of the *S. oneidensis* electron transport chain terminating with reduction of external Fe(III) oxides via Fe(III) solubilization pathways (88).**

**3. Extracellular electron transfer via nanowires.** *S. oneidensis* cultures grown in rich medium under $O_2$-limiting conditions produce pilus-like external appendages known as nanowires, which have been shown to range in size from 50-to-150 nm iin diameter and tens of microns in length (91). Scanning tunneling microscopy (92) analyses revealed that nanowires are electrically conductive (93). The nanowires formed by *S. oneidensis* may facilitate electron transfer from the cell surface to external Fe(III) oxides without the need for direct contact between the bacterial cell and the Fe(III) oxide surface. Mutants lacking MtrC and OmcA, as well as those lacking a functional Type II protein

secretion system, produce poorly conductive nanowires. Further studies are necessary to decipher the roles of MtrC, OmcA, and Type II protein secretion in nanowire architecture and conductivity.

**4. Electron shuttling pathways.** *S. oneidensis* transfers electrons to Fe(III) oxides located more than 50 μm (i.e., 50 cell diameters) from the cell surface (94, 95). Since electron transfer reactions are exceedingly slow at distances >15Å (65-67), electron transfer to external Fe(III) oxides may be enhanced by exogenous or endogenous electron shuttling compounds. *S. oneidensis* utilizes naturally-occurring humic acids (40, 96, 97), phenazines (e.g., pyocyanin) (98), and redox-active antibiotics (e.g., tetracyclines) (98) as exogenous electron shuttles to extracellular Fe(III) oxides (40). Potential endogenous electron shuttles produced by *Shewanella* include menaquinone (42), melanin (43), flavins (FMN, FAD, riboflavin) (40, 44), and organic sulfur (thiol) compounds (Fig. 1.3). The ability of these compounds to function as endogenous electron shuttles, however, has recently been brought into question. *S. oneidensis* was initially postulated to secrete menaquinone as an endogenous electron shuttle (42), yet these findings were subsequently attributed to inadvertent cell lysis (99). Melanin is also produced extracellularly by *Shewanella* but only in the presence of high amounts (1g/L) of tyrosine, thus limiting its effectiveness as an electron shuttle in natural environments (43, 44). *S. oneidensis* also produces extracellular flavins under aerobic or anaerobic conditions (100). Evidence for electron shuttling by flavins includes the findings that oxidized flavins are reduced by *S. oneidensis c*-type cytochrome MtrC (44, 100) and that reduced flavins abiotically reduce Fe(III) oxides (99). The rate limiting step in flavin-based electron shuttling is the microbial reduction of oxidized flavin, as opposed to the abiotic reduction of Fe(III) oxides by

reduced flavin (101). More recent studies with *S. oneidensis*, however, have demonstrated that extracellular flavin remain bound to surface-exposed MtrC (i.e., flavin functions as a bound redox co-factor), thus limiting its utility to function as an electron shuttle to external Fe(III) oxides (55). The electron shuttling pathways of *S. oneidensis* thus remain poorly understood.

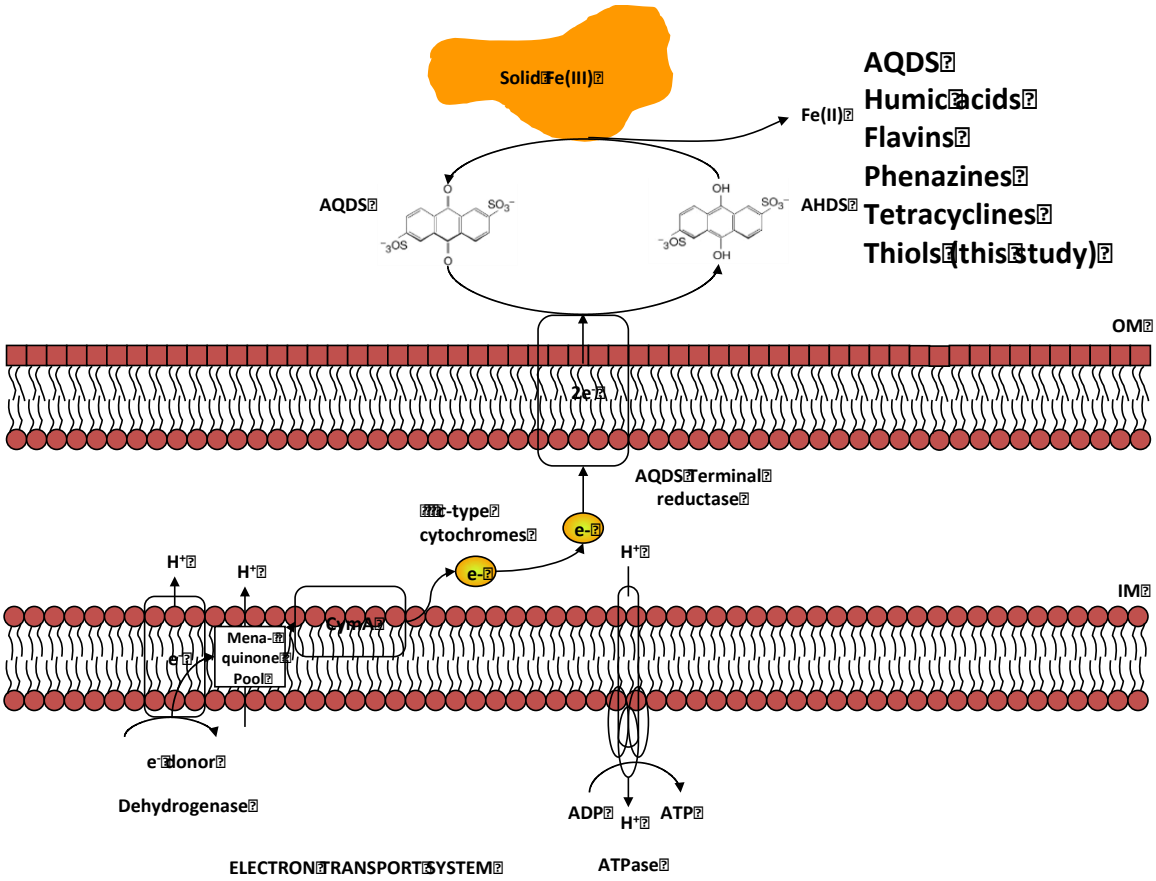


**Figure 1.4. Working model of the *S. oneidensis* electron transport chain terminating with reduction of external Fe(III) oxides via direct electron shuttling (88).**

*Shewanella* proteins engaged in thiol-based electron shuttling have not been identified and the molecular mechanisms of the electron shuttling pathway are subject to current debate. Reduced organic sulfur compounds, such as thiols, are pervasive in both freshwater and marine environments. Thiols have been reported in freshwater (102), marine water (103-105), and estuarine and salt marsh porewaters (106-109), with

concentrations ranging from nanomolar to micromolar levels (110). Thiols frequently identified in these environments include cysteine, glutathione, mercaptoproionate, mercaptoacetate, mercaptosuccinate, mercaptoethanol, and mathanethiol (102, 105, 107, 110) (Fig. 1.5).

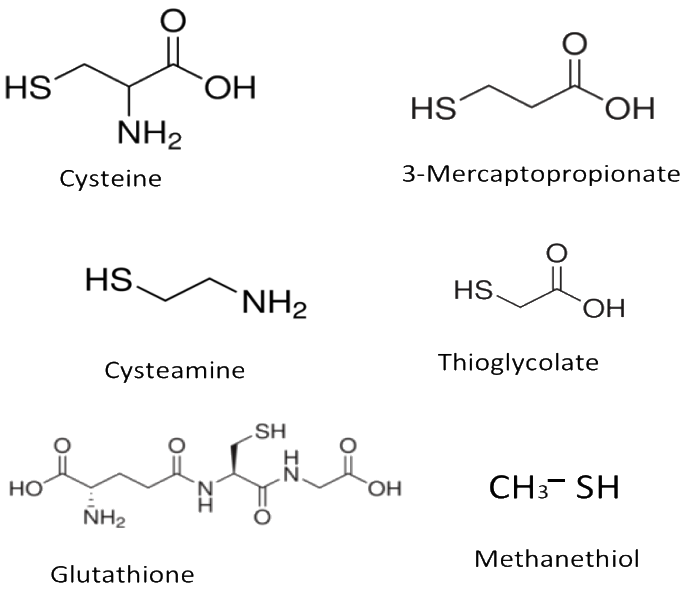


**Figure 1.5. Chemical structure of naturally occurring thiols found in freshwater, marine water, and estuarine and salt marsh pore waters.**

Thiol compounds have been shown to play an important role in biogeochemical processes, and their importance in natural environments has received immense attention due to the ability of thiol compounds to form complexes with mercury (110) and copper (104, 106, 111). Naturally occurring thiol compounds found in the environment are derived from both biological and abiotic sources. Mercaptopropionate and methanethiol are generated by microbial degradation of dimethylsulfoniopropionate (DMSP) (112, 113). The role of DMSP is most often attributed to maintenance of intracellular osmotic balance in macro and micro algae (114, 115) and in halophytic plants (114, 116). Cysteine (CSH) and Glutathione (GSH) are prominent intracellular thiols found in my prokaryotic and

eukaryotic organism (117); the detection of CSH and GSH in aquatic environments is more than likely due to secretion by metabolically active microorganisms or via discharge from decaying microorganisms (103, 118). Mercaptoacetate, mercaptoethanol, and mercaptopyruvate are typically generated via microbial degredation of CSH and GSH (112). Thiol compounds also arise abiotically via reactions between sulfide or polysulfide and unsaturated organic compounds (119).

Interestingly, thiol compounds abiotically reduce Fe(III) oxides to form Fe(II) and their analogous disulfide (120). Addition of CSH to anaerobic cultures of Fe(III)-reducing bacteria, such as *S. oneidensis* and *G. sulfurreducens*, boost Fe(III) oxide reduction activity (3, 121). The abundance of thiols in the environments where Fe(III)-reducing bacteria are found, the use of naturally occurring thiols as electron shuttles to Fe(III) oxides may afford Fe(III)-reducing bacteria with a competitive advantage in anaerobic, metal-rich environments.

**Organic sulfur metabolism in *S. oneidensis.***

Recent findings by our research group indicate that *S. oneidensis* secretes organic sulfur (thiol) compounds extracellularly under anaerobic growth conditions (Fig. 1.6). Extracellular thiols were detected at bulk concentrations of approximately 9 µM via application of the thiol reactive stain 5,5'-Dithiobis-(2-Nitrobenzoic acid) (DTNB, Ellman's reagent; reduced form produces yellow color in Fig. 1.6) to *S. oneidensis* cultures grown anaerobically on agar or liquid growth media. The detection of extracellular thiols was surprising since thiols are generally involved in a variety of intracellular processes, including maintenance of redox homeostasis and proper protein thiol-disulfide ratios, and to protect against reactive oxygen (ROS), nitrogen (RNS), and electrophilic (RES) species

(122). The dominant intracellular thiols in eukaryotes and gram-negative bacteria include cysteine and gluthathione (117, 123). In gram-positive bacteria, glutathione may be replaced by alternative thiols such as mycothiol in *Actinobacteria* (124, 125) and bacilithiol in *Bacillus* (126). We postulate that determining the composition and identifying the metabolic pathways involved in extracellular thiol production may provide clues to their function.

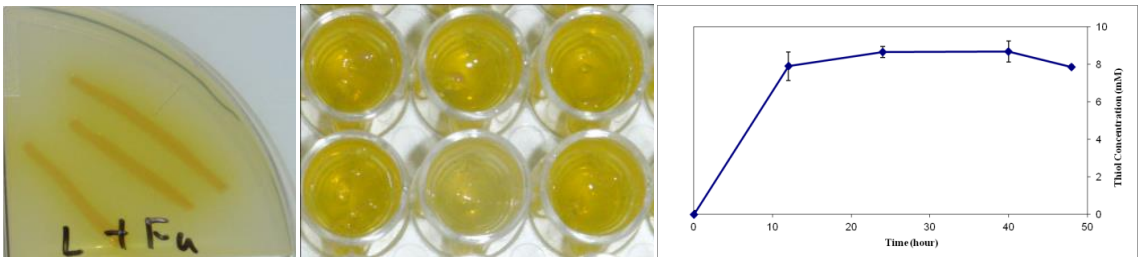


**Figure 1.6. Thiol production phenotypes of *S. oneidensi*s after anaerobic incubation on agar (left panel) and liquid (middle panel) growth medium supplemented with fumarate as electron acceptor and 5,5'-Dithiobis-(2-Nitrobenzoic acid) (DTNB; Ellman's Reagent) as thiol-specific stain (yellow color). Extracellular thiol production by wild-type *S. oneidensis* incubated anaerobically with lactate as electron donor and fumarate as electron acceptor (right panel). Data in this figure was provided by Seng Kew Wee of the DiChristina laboratory.**

Interestingly, LuxS is a component of the activated methyl cycle (AMC) and transulfurylation pathways (Fig. 1.7) which metabolize the precursor amino acids serine or homoserine to produce a variety of organic sulfur compounds, thiols, and other amino acids (e.g., cystathionine, homocysteine, S-adenosyl methionine (SAM), and methionine) many of which are critical to intracellular processes in both eukaryotes and prokaryotes (127, 128). The *S. oneidensis* AMC and transsulfurylation pathways are composed of a series of enzymatic reactions that ultimately lead to the production of methionine Fig. 1.7) and the activated methyl donor SAM (Fig. 1.7). Methionine synthesis requires the production of homocysteine, which is produced via one of three pathways: 1) LuxS-catalyzed hydrolysis

of SRH to yield homocysteine (reaction 14, Fig. 1.7), 2) MetC-catalyzed conversion of cystathionine to yield homocysteine (reaction 7, Fig. 1.7), and 3) MetY catalyzed formation of homocysteine from O-acetyl-L-homoserine (OAHS) and $H_2S$. (Fig. 1.7). In addition to homocysteine biosynthesis, the AMC and Transsulfurylation pathways in *S. oneidensis* are responsible for conversion of homoserine into threonine via homoserine kinase and threonine (reactions 1 and 2, Fig. 1.7). Cysteine is produced from CysK- and CysM-catalyzed sulfurylation of O-acetyl-L-serine with either $H_2S$ or thiosulfate as the S-donor (Fig. 1.7). Cysteine is then incorporated into the Transsulfurylation pathway via MetB-catalyzed addition of cysteine to either O-succinyl-L-homoserine (OSHS) or O-phospho-L-homoserine (OPHS) to produce cystathionine (Fig. 1.7).

In some gram-negative bacteria, (e.g., *Vibrio harveyi*, *E. coli*, and *Salmonella typhimurium)*, LuxS plays a critical role in producing the quorum sensing signal AI-2 (as described above), (78-83), while in other gram-negative bacteria (e.g., *Rhodobacter sphaeroides* and *Neptuniibacter caesariensis* (127)), LuxS plays a critical role in SRH detoxification via LuxS conversion of SRH to 4,5-dihydroxy-2,3-pentadione and homocysteine (Fig. 1.7) (127), and subsequent recovery of homocysteine to produce SAM (127, 128).

Thiols are potent chemical reductants of Fe(III), rapidly coupling Fe(III) reduction to production of the corresponding disulfide (3). Cysteine, for example, reduces Fe(III) oxides abiotically via electron transfer reactions that produce Fe(II) and cystine (120). The initial rate and extent of Fe(III) reduction correlate linearly with cysteine concentration (3, 120). In previous studies, the addition of cysteine to Fe(III)-reducing *S. oneidensis* cultures increased the rate and extent of Fe(III) reduction by *S. oneidensis* (129), and the addition

of cysteine to *S. oneidensis*-driven microbial fuel cells increased power generation (4). In addition, exogenous cysteine functioned as an electron carrier between *Geobacter sulfurreducens* and *Wolinella succinogenes* in an acetate-oxidizing, Fe(III)-reducing syntrophic co-culture (130). The detection of extracellular thiols in anaerobic Fe(III)-reducing *S. oneidensis* cultures, and the ability of thiols to rapidly reduce Fe(III) oxides forms the basis our new hypothesis which incorporates a novel electron shuttling system: thiol-driven (abiotic) reduction of external Fe(III) oxides is sustained via catalytic (biotic) reduction of the resulting disulfides (Fig. 1.8).

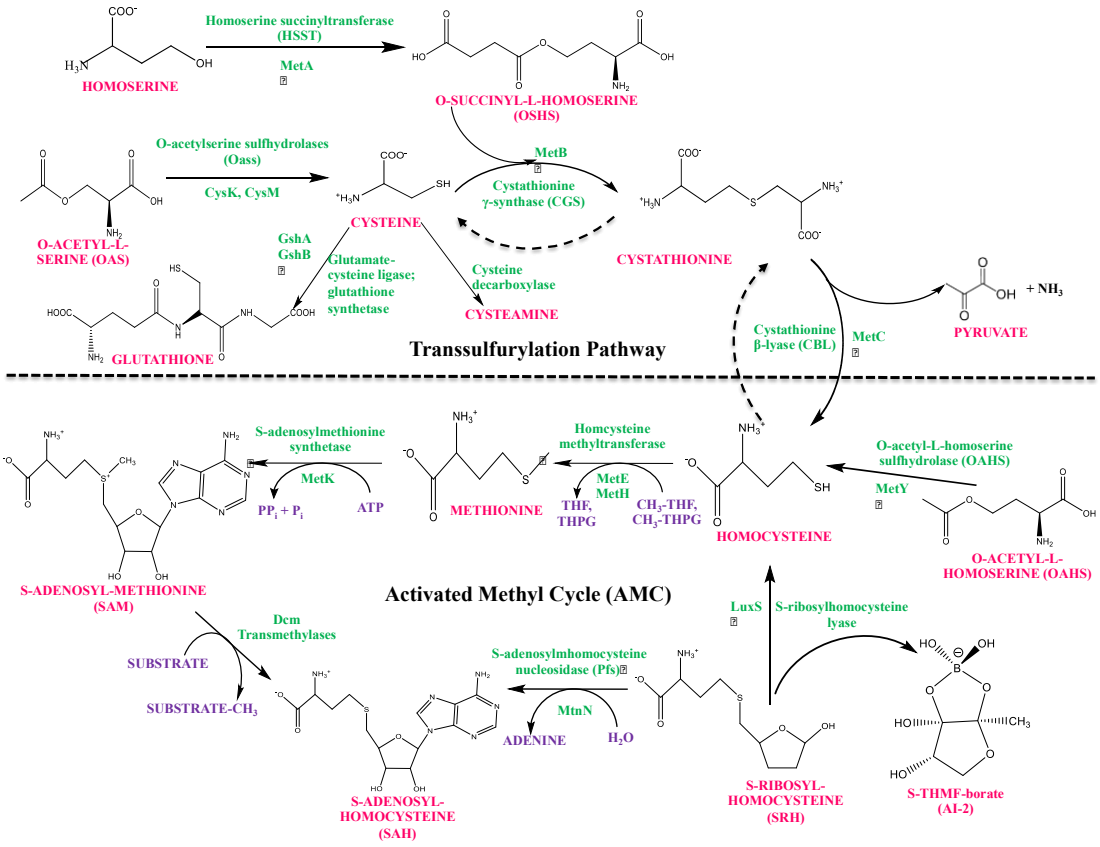


**Figure 1.7. Activated Methyl Cycle (AMC) and Transsulfuration pathways predicted by BLAST analysis of the *S. oneidensis* genome.**

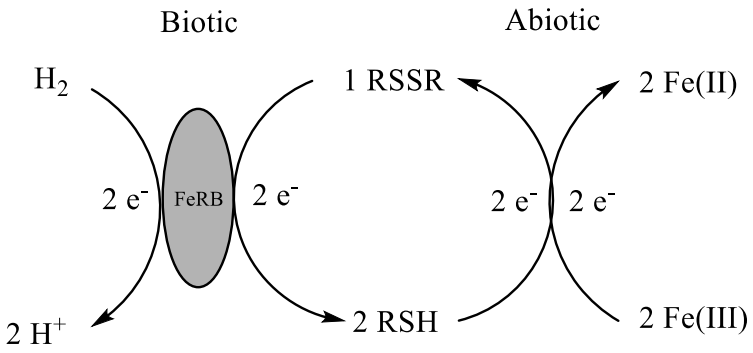


**Figure 1.8. Proposed electron shuttling pathway of *S. oneidensis*: thiol (RSH)-driven (abiotic) reduction of external Fe(III) oxides is sustained via catalytic (biotic) reduction of the resulting disulfides (RSSR).**

The main objectives of the thesis research were to i) determine if bacterial cell-Fe(III) oxide contact and biofilm formation are required for Fe(III) oxide reduction by *S. oneidensis* (Chapter 2), ii) determine if *S. oneidensis* produces and utilizes Autoinducer-2, the universal quorum sensing signal used by other gram negative bacteria including *Vibrio* and *E. coli* to regulate biofilm formation activity, under anaerobic growth conditions as an alternate carbon and electron source for biofilm restoration and respiration on a variety of terminal electron acceptors, including thiosulfate, nitrate, fumarate, and ferrihydrite (Chapter 3), and iii) determine if extracellular thiols produced by the activated methyl cycle and transulfurylation pathway enzymes found in *S. oneidensis* influence Fe(III) reduction by functioning as an shuttle electron to external Fe(III) and Mn(III,IV) oxides during anaerobic respiration (Chapter 4).

## References

1. **DiChristina TJ, Fredrickson JK, Zachara JM.** 2005. Enzymology of electron transport: Energy generation with geochemical consequences. Molecular Geomicrobiology **59:**27-52.
2. **Bretschger O, Obraztsova A, Sturm CA, Chang IS, Gorby YA, Reed SB, Culley DE, Reardon CL, Barua S, Romine MF, Zhou J, Beliaev AS, Bouhenni R, Saffarini D, Mansfeld F, Kim BH, Fredrickson JK, Nealson KH.**

2007. Current production and metal oxide reduction by *Shewanella oneidensis* MR-1 wild type and mutants. Appl. Environ. Microbiol. **73:**7003-7012.

3. **Doong RA, Schink B.** 2002. Cysteine-mediated reductive dissolution of poorly crystalline iron(III) oxides by Geobacter sulfurreducens. Environ. Sci. Technol. **36:**2939-2945.
4. **Logan BE, Murano C, Scott K, Gray ND, Head IM.** 2005. Electricity generation from cysteine in a microbial fuel cell. Water Res **39:**942-952.
5. **Logan BE, Hamelers B, Rozendal RA, Schrorder U, Keller J, Freguia S, Aelterman P, Verstraete W, Rabaey K.** 2006. Microbial fuel cells: Methodology and technology. Environ. Sci. Technol. **40:**5181-5192.
6. **Madigan MT, J.M. Martinko, and T.D. Brock.** 2005. *Brock Biology of Microorganisms*, 11th ed. Prentice Hall/Pearson Education, Upper Saddle River, NJ.
7. **Stackebrandt E, Murray RGE, Truper HG.** 1988. Proteobacteria-Classis Nov, a Name for the Phylogenetic Taxon That Includes the Purple Bacteria and Their Relatives. International Journal of Systematic Bacteriology **38:**321-325.
8. **Woese CR, Weisburg WG, Hahn CM, Paster BJ, Zablen LB, Lewis BJ, Macke TJ, Ludwig W, Stackebrandt E.** 1985. The Phylogeny of Purple Bacteria - the Gamma-Subdivision. Syst. Appl. Microbiol. **6:**25-33.
9. **Gupta RS.** 2000. The phylogeny of proteobacteria: relationships to other eubacterial phyla and eukaryotes. FEMS Microbiol. Rev. **24:**367-402.
10. **Emerson D, Rentz JA, Lilburn TG, Davis RE, Aldrich H, Chan C, Moyer CL.** 2007. A Novel Lineage of Proteobacteria Involved in Formation of Marine Fe-Oxidizing Microbial Mat Communities. PLoS One **2**.
11. **Woese CR.** 1987. Bacterial Evolution. Microbiol. Rev. **51:**221-271.
12. **Woese CR, Stackebrandt E, Macke TJ, Fox GE.** 1985. A Phylogenetic Definition of the Major Eubacterial Taxa. Syst. Appl. Microbiol. **6:**143-151.
13. **Gao B, Mohan R, Gupta RS.** 2009. Phylogenomics and protein signatures elucidating the evolutionary relationships among the Gammaproteobacteria. Int J Syst Evol Micr **59:**234-247.
14. **Gupta RS, Sneath PHA.** 2007. Application of the character compatibility approach to generalized molecular sequence data: Branching order of the proteobacterial subdivisions. J. Mol. Evol. **64:**90-100.
15. **Ivanova EP, Flavier S, Christen R.** 2004. Phylogenetic relationships among marine Alteromonas-like proteobacteria: emended description of the family Alteromonadaceae and proposal of Pseudoalteromonadaceae fam. nov., Colwelliaceae fam. nov., Shewanellaceae fam. nov., Montellaceae fam. nov., Ferrimonadaceae fam. nov., Idiomarinaceae fam. nov and Psychromonadaceae fam. nov. Int J Syst Evol Micr **54:**1773-1788.
16. **Williams KP, Gillespie JJ, Sobral BWS, Nordberg EK, Snyder EE, Shallom JM, Dickerman AW.** 2010. Phylogeny of Gammaproteobacteria. J. Bacteriol. **192:**2305-2314.
17. **Garrity GM, Bell JA, Lilburn TG.** 2005. Class III. *Gammaproteobacteria class. nov. In* Brendel PJ, Krieg NR, Staley JT, Garrity GM (ed.), Bergey's manual of systematic bacteriology 2nd ed, vol. 2. Springer, New York, NY.

18. **Lovley DR, Phillips EJP.** 1988. Novel Mode of Microbial Energy-Metabolism - Organic-Carbon Oxidation Coupled to Dissimilatory Reduction of Iron or Manganese. Appl. Environ. Microbiol. **54:**1472-1480.
19. **Myers CR, Nealson KH.** 1988. Bacterial manganese reduction and growth with manganese oxide as the sole electron acceptor. Science **240:**1319-1321.
20. **Lovley DR.** 2000. *Fe(III)- and Mn(IV)-reducing prokaryotes*. *In* S. Falkow ea (ed.), *The Prokaryotes*. Springer-Verlag.
21. **Weber KA, Achenbach LA, Coates JD.** 2006. Microorganisms pumping iron: anaerobic microbial iron oxidation and reduction. Nat Rev Microbiol **4:**752-764.
22. **Hau HH, Gralnick JA.** 2007. Ecology and biotechnology of the genus *Shewanella*. Annu. Rev. Microbiol. **61:**237-258.
23. **Burnes BS, Mulberry MJ, DiChristina TJ.** 1998. Design and application of two rapid screening techniques for isolation of Mn(IV) reduction-deficient mutants of *Shewanella putrefaciens*. Appl. Environ. Microbiol. **64:**2716-2720.
24. **Heidelberg JF, Paulsen IT, Nelson KE, Gaidos EJ, Nelson WC, Read TD, Eisen JA, Seshadri R, Ward N, Methe B, Clayton RA, Meyer T, Tsapin A, Scott J, Beanan M, Brinkac L, Daugherty S, DeBoy RT, Dodson RJ, Durkin AS, Haft DH, Kolonay JF, Madupu R, Peterson JD, Umayam LA, White O, Wolf AM, Vamathevan J, Weidman J, Impraim M, Lee K, Berry K, Lee C, Mueller J, Khouri H, Gill J, Utterback TR, McDonald LA, Feldblyum TV, Smith HO, Venter JC, Nealson KH, Fraser CM.** 2002. Genome sequence of the dissimilatory metal ion-reducing bacterium Shewanella oneidensis. Nat. Biotechnol. **20:**1118-1123.
25. **Moser DP, Nealson KH.** 1996. Growth of the facultative anaerobe Shewanella putrefaciens by elemental sulfur reduction. Appl. Environ. Microbiol. **62:**2100-2105.
26. **Saffarini DA, DiChristina TJ, Bermudes D, Nealson KH.** 1994. Anaerobic respiration of *Shewanella putrefaciens* requires both chromosomal and plasmid-borne genes. FEMS Microbiol. Lett. **119:**271-277.
27. **Taillefert M, Beckler JS, Carey E, Burns JL, Fennessey CM, DiChristina TJ.** 2007. *Shewanella putrefaciens* produces an Fe(III)-solubilizing organic ligand during anaerobic respiration on insoluble Fe(III) oxides. J. Inorg. Biochem. **101:**1760-1767.
28. **Taratus EM, Eubanks SG, DiChristina TJ.** 2000. Design and application of a rapid screening technique for isolation of selenite reduction-deficient mutants of *Shewanella putrefaciens*. Microbiol. Res. **155:**79-85.
29. **Beliaev AS, Klingeman DM, Klappenbach JA, Wu L, Romine MF, Tiedje JA, Nealson KH, Fredrickson JK, Zhou J.** 2005. Global transcriptome analysis of Shewanella oneidensis MR-1 exposed to different terminal electron acceptors. J. Bacteriol. **187:**7138-7145.
30. **Holt HM, Gahrn-Hansen B, Bruun B.** 2005. Shewanella algae and Shewanella putrefaciens: clinical and microbiological characteristics. Clin. Microbiol. Infect. **11:**347-352.
31. **Gram L, Ravn L, Rasch M, Bruhn JB, Christensen AB, Givskov M.** 2002. Food spoilage - interactions between food spoilage bacteria. Int. J. Food Microbiol. **78:**79-97.

32. **Vogel BF, Holt HM, Gerner-Smidt P, Bundvad A, Sogaard P, Gram L.** 2000. Homogeneity of Danish environmental and clinical isolates of Shewanella algae. Appl. Environ. Microbiol. **66:**443-448.
33. **Vogel BF, Venkateswaran K, Satomi M, Gram L.** 2005. Identification of Shewanella baltica as the most important H2S-producing species during iced storage of Danish marine fish. Appl. Environ. Microbiol. **71:**6689-6697.
34. **Beliaev AS, Saffarini DA.** 1998. *Shewanella putrefaciens mtrB* encodes an outer membrane protein required for Fe(III) and Mn(IV) reduction. J. Bacteriol. **180:**6292-6297.
35. **DiChristina TJ, Moore CM, Haller CA.** 2002. Dissimilatory Fe(III) and Mn(IV) reduction by *Shewanella putrefaciens* requires *ferE*, a homolog of the *pulE* (*gspE*) type II protein secretion gene. J. Bacteriol. **184:**142-151.
36. **Myers JM, Myers CR.** 2001. Role for outer membrane cytochromes OmcA and OmcB of *Shewanella putrefaciens* MR-1 in reduction of manganese dioxide. Appl. Environ. Microbiol. **67:**260-269.
37. **Myers CR, Myers JM.** 1992. Localization of cytochromes to the outer-membrane of anaerobically grown *Shewanella putrefaciens* MR-1. J. Bacteriol. **174:**3429-3438.
38. **Gorby YA.** 2007. Bacterial nanowires: Extracellular electron transfer and mineral transformation. Geochim. Cosmochim. Acta **71:**A345-A345.
39. **Jones ME, Fennessey CM, DiChristina TJ, Taillefert M.** 2010. *Shewanella oneidensis* MR-1 mutants selected for their inability to produce soluble organic-Fe(III) complexes are unable to respire Fe(III) as anaerobic electron acceptor. Environmental Microbiology **12:**938-950.
40. **Lovley DR, Coates JD, BluntHarris EL, Phillips EJP, Woodward JC.** 1996. Humic substances as electron acceptors for microbial respiration. Nature **382:**445-448.
41. **Marsili E, Baron DB, Shikhare ID, Coursolle D, Gralnick JA, Bond DR.** 2008. *Shewanella* secretes flavins that mediate extracellular electron transfer. Proc. Natl. Acad. Sci. U. S. A. **105:**3968-3973.
42. **Newman DK, Kolter R.** 2000. A role for excreted quinones in extracellular electron transfer. Nature **405:**94-97.
43. **Turick CE, Tisa LS, Caccavo F.** 2002. Melanin production and use as a soluble electron shuttle for Fe(III) oxide reduction and as a terminal electron acceptor by Shewanella algae BrY. Appl. Environ. Microbiol. **68:**2436-2444.
44. **von Canstein H, Ogawa J, Shimizu S, Lloyd JR.** 2008. Secretion of flavins by *Shewanella* species and their role in extracellular electron transfer. Appl. Environ. Microbiol. **74:**615-623.
45. **Shi L, Squier TC, Zachara JM, Fredrickson JK.** 2007. Respiration of metal (hydr)oxides by *Shewanella* and *Geobacter*: a key role for multihaem *c*-type cytochromes. Mol. Microbiol. **65:**12-20.
46. **Myers CR, Myers JM.** 2003. Cell surface exposure of the outer membrane cytochromes of Shewanella oneidensis MR-1. Lett. Appl. Microbiol. **37:**254-258.
47. **Myers JM, Myers CR.** 2003. Overlapping role of the outer membrane cytochromes of Shewanella oneidensis MR-1 in the reduction of manganese(IV) oxide. Lett. Appl. Microbiol. **37:**21-25.

48. **Myers CR, Myers JM.** 1997. Outer membrane cytochromes of *Shewanella putrefaciens* MR-1: Spectral analysis, and purification of the 83-kDa c-type cytochrome. Biochimica Et Biophysica Acta-Biomembranes **1326:**307-318.
49. **Myers JM, Myers CR.** 2000. Role of the tetraheme cytochrome CymA in anaerobic electron transport in cells of *Shewanella putrefaciens* MR-1 with normal levels of menaquinone. J. Bacteriol. **182:**67-75.
50. **Pitts KE, Dobbin PS, Reyes-Ramirez F, Thomson AJ, Richardson DJ, Seward HE.** 2003. Characterization of the Shewanella oneidensis MR-1 decaheme cytochrome MtrA. J. Biol. Chem. **278:**27758-27765.
51. **Ross DE, Ruebush SS, Brantley SL, Hartshorne RS, Clarke TA, Richardson DJ, Tien M.** 2007. Characterization of protein-protein interactions involved in iron reduction by *Shewanella oneidensis* MR-1. Appl. Environ. Microbiol. **73:**5797-5808.
52. **Lower BH, Yongsunthon R, Shi L, Wildling L, Gruber HJ, Wigginton NS, Reardon CL, Pinchuk GE, Droubay TC, Boily JF, Lower SK.** 2009. Antibody Recognition Force Microscopy Shows that Outer Membrane Cytochromes OmcA and MtrC Are Expressed on the Exterior Surface of Shewanella oneidensis MR-1. Appl. Environ. Microbiol. **75:**2931-2935.
53. **Shi L, Deng S, Marshall MJ, Wang ZM, Kennedy DW, Dohnalkova AC, Mottaz HM, Hill EA, Gorby YA, Beliaev AS, Richardson DJ, Zachara JM, Fredrickson JK.** 2008. Direct involvement of type II secretion system in extracellular translocation of *Shewanella oneidensis* outer membrane cytochromes MtrC and OmcA. J. Bacteriol. **190:**5512-5516.
54. **DiChristina TJ.** 2002. New insights into the molecular mechanism of microbial metal reduction. Abstr Pap Am Chem S **223:**U595-U595.
55. **Okamoto A, Hashimoto K, Nealson KH, Nakamura R.** 2013. Rate enhancement of bacterial extracellular electron transport involves bound flavin semiquinones. Proc. Natl. Acad. Sci. U. S. A.
56. **White GF, Shi Z, Shi L, Wang ZM, Dohnalkova AC, Marshall MJ, Fredrickson JK, Zachara JM, Butt JN, Richardson DJ, Clarke TA.** 2013. Rapid electron exchange between surface-exposed bacterial cytochromes and Fe(III) minerals. Proc. Natl. Acad. Sci. U. S. A. **110:**6346-6351.
57. **Hartshorne RS, Jepson BN, Clarke TA, Field SJ, Fredrickson J, Zachara J, Shi L, Butt JN, Richardson DJ.** 2007. Characterization of *Shewanella oneidensis* MtrC: a cell-surface decaheme cytochrome involved in respiratory electron transport to extracellular electron acceptors. J. Biol. Inorg. Chem. **12:**1083-1094.
58. **White GF, Shi Z, Shi L, Wang Z, Dohnalkova AC, Marshall MJ, Fredrickson JK, Zachara JM, Butt JN, Richardson DJ, Clarke TA.** 2013. Rapid electron exchange between surface-exposed bacterial cytochromes and Fe(III) minerals. Proceedings of the National Academy of Sciences of the United States of America **110:**6346-6351.
59. **Hartshorne RS, Reardon CL, Ross D, Nuester J, Clarke TA, Gates AJ, Mills PC, Fredrickson JK, Zachara JM, Shi L, Beliaev AS, Marshall MJ, Tien M, Brantley S, Butt JN, Richardson DJ.** 2009. Characterization of an electron

conduit between bacteria and the extracellular environment. Proc. Natl. Acad. Sci. U. S. A. **106:**22169-22174.

60. **Richardson DJ, Butt JN, Fredrickson JK, Zachara JM, Shi L, Edwards MJ, White G, Baiden N, Gates AJ, Marritt SJ, Clarke TA.** 2012. The porin-cytochrome' model for microbe-to-mineral electron transfer. Mol. Microbiol. **85:**201-212.
61. **Jiao Y, Newman DK.** 2007. The pio operon is essential for phototrophic Fe(II) oxidation in Rhodopseudomonas palustris TIE-1. J. Bacteriol. **189:**1765-1773.
62. **Liu J, Wang Z, Belchik SM, Edwards MJ, Liu C, Kennedy DW, Merkley ED, Lipton MS, Butt JN, Richardson DJ, Zachara JM, Fredrickson JK, Rosso KM, Shi L.** 2012. Identification and Characterization of MtoA: A Decaheme c-Type Cytochrome of the Neutrophilic Fe(II)-Oxidizing Bacterium Sideroxydans lithotrophicus ES-1. Frontiers in microbiology **3:**37.
63. **Shi L, Rosso KM, Zachara JM, Fredrickson JK.** 2012. Mtr extracellular electron-transfer pathways in Fe(III)-reducing or Fe(II)-oxidizing bacteria: a genomic perspective. Biochem. Soc. Trans. **40:**1261-1267.
64. **Ross DE, Flynn JM, Baron DB, Gralnick JA, Bond DR.** 2011. Towards Electrosynthesis in Shewanella: Energetics of Reversing the Mtr Pathway for Reductive Metabolism. PLoS One **6**.
65. **L. G, A. L, T. L, D. MF, T. R, I. G.** 1999. DIrect electron transfer between heme-containing enzymes and electrodes as a basis for third generation biosensors. Anal. Chim. Acta **400:**91-108.
66. **S. FR, A. PC, D. ML, T. KL.** 2003. DIrect electron transfer: an approach for electrochemical biosensors with higher selectivity and sensitivity. Journal of the Brazilian Chemical Society **14:**230-243.
67. **B. GH, R. WJ.** 1996. Electron transfer in proteins. Annu. Rev. Biochem. **65:**537-561.
68. **Klausen M, Heydorn A, Ragas P, Lambertsen L, Aaes-Jorgensen A, Molin S, Tolker-Nielsen T.** 2003. Biofilm formation by Pseudomonas aeruginosa wild type, flagella and type IV pili mutants. Mol. Microbiol. **48:**1511-1524.
69. **Sauer K, Camper AK, Ehrlich GD, Costerton JW, Davies DG.** 2002. Pseudomonas aeruginosa displays multiple phenotypes during development as a biofilm. J. Bacteriol. **184:**1140-1154.
70. **Thormann KM, Saville RM, Shukla S, Pelletier DA, Spormann AM.** 2004. Initial phases of biofilm formation in Shewanella oneidensis MR-1. J. Bacteriol. **186:**8096-8104.
71. **Tolker-Nielsen T, Brinch UC, Ragas PC, Andersen JB, Jacobsen CS, Molin S.** 2000. Development and dynamics of Pseudomonas sp biofilms. J. Bacteriol. **182:**6482-6489.
72. **Puckett SD, Taylor E, Raimondo T, Webster TJ.** 2010. The relationship between the nanostructure of titanium surfaces and bacterial attachment. Biomaterials **31:**706-713.
73. **Rochex A, Godon JJ, Bernet N, Escudie R.** 2008. Role of shear stress on composition, diversity and dynamics of biofilm bacterial communities. Water Res **42:**4915-4922.

74. **Dickschat JS.** 2010. Quorum sensing and bacterial biofilms. Nat. Prod. Rep. **27:**343-369.
75. **Sawyer LK, Hermanowicz SW.** 1998. Detachment of biofilm bacteria due to variations in nutrient supply. Water Sci Technol **37:**211-214.
76. **Skolimowski M, Nielsen MW, Emneus J, Molin S, Taboryski R, Sternberg C, Dufva M, Geschke O.** 2010. Microfluidic dissolved oxygen gradient generator biochip as a useful tool in bacterial biofilm studies. Lab on a chip **10:**2162-2169.
77. **Jefferson KK.** 2004. What drives bacteria to produce a biofilm? FEMS Microbiol. Lett. **236:**163-173.
78. **Bassler B.** 2002. How bacteria talk to each other. Mol. Biol. Cell **13:**2a-2a.
79. **Joyce EA, Bassler BL, Wright A.** 2000. Evidence for a signaling system in Helicobacter pylori: detection of a luxS-Encoded autoinducer. J. Bacteriol. **182:**3638-3643.
80. **Surette MG, Miller MB, Bassler BL.** 1999. Quorum sensing in Escherichia coli, Salmonella typhimurium, and Vibrio harveyi: A new family of genes responsible for autoinducer production. Proc. Natl. Acad. Sci. U. S. A. **96:**1639-1644.
81. **Waters CM, Bassler BL.** 2005. Quorum sensing: Cell-to-cell communication in bacteria. Annu. Rev. Cell Dev. Biol. **21:**319-346.
82. **Bassler B, Hammer BK.** 2003. Quorum sensing controls biofilm formation in Vibrio cholerae. Mol. Microbiol. **501:**101-104.
83. **Miller MB, Bassler BL.** 2001. Quorum sensing in bacteria. Annu. Rev. Microbiol. **55:**165-199.
84. **Emerson D, Floyd MM.** 2005. Enrichment and isolation of iron-oxidizing bacteria at neutral pH. Environmental Microbiology **397:**112-123.
85. **Miller ST, Xavier KB, Campagna SR, Taga ME, Semmelhack MF, Bassler BL, Hughson FM.** 2004. Salmonella typhimurium recognizes a chemically distinct form of the bacterial quorum-sensing signal Al-2. Mol. Cell **15:**677-687.
86. **Schauder S, Shokat K, Surette MG, Bassler BL.** 2001. The LuxS family of bacterial autoinducers: biosynthesis of a novel quorum-sensing signal molecule. Mol. Microbiol. **41:**463-476.
87. **Learman DR, Yi H, Brown SD, Martin SL, Geesey GG, Stevens AM, Hochella MF.** 2009. Involvement of *Shewanella oneidensis* MR-1 LuxS in Biofilm Development and Sulfur Metabolism. Appl. Environ. Microbiol. **75:**1301-1307.
88. **Cooper RE, Goff JL, Reed BC, Sekar R, DiChristina TJ.** 2014. Breathing metals: Molecular mechanisms of microbial iron reduction, Manual of Environmental Microbiology. ASM Press.
89. **Carey E, Burns J, DiChristina TJ, Taillefert M.** 2005. Formation of soluble organic-Fe(III) complexes during microbial iron reduction. Geochim. Cosmochim. Acta **69:**A225-A225.
90. **Fennessey CM, Jones ME, Taillefert M, DiChristina TJ.** 2010. Siderophores are not involved in Fe(III) solubilization during anaerobic Fe(III) respiration by *Shewanella oneidensis* MR-1. Appl. Environ. Microbiol. **76:**2425-2432.
91. **Gorby YA, Yanina S, McLean JS, Rosso KM, Moyles D, Dohnalkova A, Beveridge TJ, Chang IS, Kim BH, Kim KS, Culley DE, Reed SB, Romine MF, Saffarini DA, Hill EA, Shi L, Elias DA, Kennedy DW, Pinchuk G,**

**Watanabe K, Ishii S, Logan B, Nealson KH, Fredrickson JK.** 2006. Electrically conductive bacterial nanowires produced by *Shewanella oneidensis* strain MR-1 and other microorganisms. Proc. Natl. Acad. Sci. U. S. A. **103:**11358-11363.

92. **Chin KJ, Hahn D, Hengstmann U, Liesack W, Janssen PH.** 1999. Characterization and identification of numerically abundant culturable bacteria from the anoxic bulk soil of rice paddy microcosms. Appl. Environ. Microbiol. **65:**5042-5049.
93. **El-Naggar MY, Wanger G, Leung KM, Yuzvinsky TD, Southam G, Yang J, Lau WM, Nealson KH, Gorby YA.** 2010. Electrical transport along bacterial nanowires from *Shewanella oneidensis* MR-1. Proc. Natl. Acad. Sci. U. S. A. **107:**18127-18131.
94. **Lies DP, Hernandez ME, Kappler A, Mielke RE, Gralnick JA, Newman DK.** 2005. *Shewanella oneidensis* MR-1 uses overlapping pathways for iron reduction at a distance and by direct contact under conditions relevant for biofilms. Appl. Environ. Microbiol. **71:**4414-4426.
95. **Nevin KP, Lovley DR.** 2002. Mechanisms for Fe(III) oxide reduction in sedimentary environments. Geomicrobiol J **19:**141-159.
96. **Lovley DR, Kashefi K, Vargas M, Tor JM, Blunt-Harris EL.** 2000. Reduction of humic substances and Fe(III) by hyperthermophilic microorganisms. Chem Geol **169:**289-298.
97. **Roden EE.** 2012. Microbial iron-redox cycling in subsurface environments. Biochem. Soc. Trans. **40:**1249-1256.
98. **Hernandez ME, Kappler A, Newman DK.** 2004. Phenazines and other redox-active antibiotics promote microbial mineral reduction. Appl. Environ. Microbiol. **70:**921-928.
99. **Myers CR, Myers JA.** 2004. *Shewanella oneidensis* MR-1 restores menaquinone synthesis to a menaquinone-negative mutant. Appl. Environ. Microbiol. **70:**5415-5425.
100. **Coursolle D, Baron DB, Bond DR, Gralnick JA.** 2010. The Mtr Respiratory Pathway Is Essential for Reducing Flavins and Electrodes in Shewanella oneidensis. Journal of Bacteriology **192:**467-474.
101. **Shi Z, Zachara JM, Shi L, Wang ZM, Moore DA, Kennedy DW, Fredrickson JK.** 2012. Redox Reactions of Reduced Flavin Mononucleotide (FMN), Riboflavin (RBF), and Anthraquinone-2,6-disulfonate (AQDS) with Ferrihydrite and Lepidocrocite. Environ. Sci. Technol. **46:**11644-11652.
102. **Hu HY, Mylon SE, Benoit G.** 2006. Distribution of the thiols glutathione and 3-mercaptopropionic acid in Connecticut lakes. Limnol Oceanogr **51:**2763-2774.
103. **Al-Farawati R, Van Den Berg CMG.** 2001. Thiols in coastal waters of the western North Sea and English Channel. Environ. Sci. Technol. **35:**1902-1911.
104. **Chapman CS, Capodaglio G, Turetta C, van den Berg CMG.** 2009. Benthic fluxes of copper, complexing ligands and thiol compounds in shallow lagoon waters. Mar. Environ. Res. **67:**17-24.
105. **Dupont CL, Moffett JW, Bidigare RR, Ahner BA.** 2006. Distributions of dissolved and particulate biogenic thiols in the subartic Pacific Ocean. Deep-Sea Res Pt I **53:**1961-1974.

106. **Dryden CL, Gordon AS, Donat JR.** 2007. Seasonal survey of copper-complexing ligands and thiol compounds in a heavily utilized, urban estuary: Elizabeth River, Virginia. Mar. Chem. **103:**276-288.
107. **Luther GW, Church TM.** 1988. Seasonal Cycling of Sulfur and Iron in Porewaters of a Delaware Salt-Marsh. Mar. Chem. **23:**295-309.
108. **Luther GW, Church TM, Scudlark JR, Cosman M.** 1986. Inorganic and Organic Sulfur Cycling in Salt-Marsh Pore Waters. Science **232:**746-749.
109. **Tang DG, Shafer MM, Karner DA, Overdier J, Armstrong DE.** 2004. Factors affecting the presence of dissolved glutathione in estuarine waters. Environ. Sci. Technol. **38:**4247-4253.
110. **Zhang JZ, Wang FY, House JD, Page B.** 2004. Thiols in wetland interstitial waters and their role in mercury and methylmercury speciation. Limnol Oceanogr **49:**2276-2286.
111. **Leal MFC, Van den Berg CMG.** 1998. Evidence for strong copper(I) complexation by organic ligands in seawater. Aquat Geochem **4:**49-75.
112. **Kiene RP, Malloy KD, Taylor BF.** 1990. Sulfur-Containing Amino-Acids as Precursors of Thiols in Anoxic Coastal Sediments. Appl. Environ. Microbiol. **56:**156-161.
113. **Kiene RP, Taylor BF.** 1988. Biotransformations of Organosulfur Compounds in Sediments Via 3-Mercaptopropionate. Nature **332:**148-150.
114. **Moran MA, Reisch CR, Kiene RP, Whitman WB.** 2012. Genomic Insights into Bacterial DMSP Transformations. Annu Rev Mar Sci **4:**523-542.
115. **Yoch DC.** 2002. Dimethylsulfoniopropionate: Its sources, role in the marine food web, and biological degradation to dimethylsulfide. Appl. Environ. Microbiol. **68:**5804-5815.
116. **Otte ML, Wilson G, Morris JT, Moran BM.** 2004. Dimethylsulphoniopropionate (DMSP) and related compounds in higher plants. J Exp Bot **55:**1919-1925.
117. **Fahey RC.** 2001. Novel thiols of prokaryotes. Annu. Rev. Microbiol. **55:**333-356.
118. **Morel FMMH, J. G.** 1993. Principles and Applications of Aquatic Chemistry. Wiley-Interscience Press, New York.
119. **Vairavamurthy A, Mopper K.** 1987. Geochemical Formation of Organosulfur Compounds (Thiols) by Addition of H2s to Sedimentary Organic-Matter. Nature **329:**623-625.
120. **Amirbahman A, Sigg L, vonGunten U.** 1997. Reductive dissolution of Fe(III) (hydr)oxides by cysteine: Kinetics and mechanism. J. Colloid Interface Sci. **194:**194-206.
121. **Liu D, Dong HL, Zhao LD, Wang HM.** 2014. Smectite Reduction by Shewanella Species as Facilitated by Cystine and Cysteine. Geomicrobiol J **31:**53-63.
122. **Hand CE, Honek JF.** 2005. Biological chemistry of naturally occurring thiols of microbial and marine origin. J. Nat. Prod. **68:**293-308.
123. **Fahey RC, Sundquist AR.** 1991. Evolution of Glutathione Metabolism. Adv. Enzymol. Relat. Areas Mol. Biol. **64:**1-53.

124. **Newton GL, Buchmeier N, Fahey RC.** 2008. Biosynthesis and functions of mycothiol, the unique protective thiol of *Actinobacteria*. Microbiol. Mol. Biol. Rev. **72:**471-+.
125. **Rawat M, Av-Gay Y.** 2007. Mycothiol-dependent proteins in actinomycetes. FEMS Microbiol. Rev. **31:**278-292.
126. **Newton GL, Rawat M, La Clair JJ, Jothivasan VK, Budiarto T, Hamilton CJ, Claiborne A, Helmann JD, Fahey RC.** 2009. Bacillithiol is an antioxidant thiol produced in Bacilli. Nat. Chem. Biol. **5:**625-627.
127. **Rezzonico F, Duffy B.** 2008. Lack of genomic evidence of AI-2 receptors suggests a non-quorum sensing role for luxS in most bacteria. BMC Microbiol. **8**.
128. **Winzer K, Hardie KR, Burgess N, Doherty N, Kirke D, Holden MTG, Linforth R, Cornell KA, Taylor AJ, Hill PJ, Williams P.** 2002. LuxS: its role in central metabolism and the in vitro synthesis of 4-hydroxy-5-methyl-3(2H)-furanone. Microbiol-Sgm **148:**909-922.
129. **Doong RA, Chiang HC.** 2005. Transformation of carbon tetrachloride by thiol reductants in the presence of quinone compounds. Environ. Sci. Technol. **39:**7460-7468.
130. **Kaden J, Galushko AS, Schink B.** 2002. Cysteine-mediated electron transfer in syntrophic acetate oxidation by cocultures of Geobacter sulfurreducens and Wolinella succinogenes. Arch. Microbiol. **178:**53-58.

# CHAPTER 2

## S-Ribosylhomocysteine Lyase (LuxS)-Dependent Biofilm Formation on Fe(III) Oxide Surfaces Does Not Enhance Fe(III) Oxide Reduction Activity of *Shewanella oneidensis*

[Submitted for publication, currently under review]

**Summary**

The γ-proteobacterium *Shewanella oneidensis* respires a variety of terminal electron acceptors, including solid Fe(III) oxides. *S. oneidensis* transfers electrons to Fe(III) oxides via direct (*c*-type cytochrome) and indirect (electron shuttling and Fe(III) solubilization) pathways. To test the hypothesis that Fe(III) oxide reduction is enhanced by formation of anaerobic biofilms on Fe(III) oxide surfaces, the gene encoding the activated methyl cycle (AMC) enzyme S-ribosylhomocysteine lyase (LuxS) was deleted in-frame from the *S. oneidensis* genome to generate the corresponding mutant Δ*luxS*. Conventional biofilm assays and visual inspection via confocal laser scanning microscopy indicated that wild-type *S. oneidensis* formed anaerobic biofilms on polystyrene and bare and Fe(III) oxide-coated silica surfaces, while Δ*luxS* was severely impaired in anaerobic biofilm formation. Rates of anaerobic biofilm formation by Δ*luxS* were restored to wild-type levels by addition of AMC and Transsulfurylation pathway intermediates involved in organic sulfur metabolism. Cell-hematite attachment isotherms demonstrated that Δ*luxS* was also impaired in attachment to hematite surfaces under anaerobic conditions. Despite its deficiencies in anaerobic biofilm formation and

hematite attachment, Δ*luxS* retained wild-type Fe(III) oxide and hematite reduction activities. LuxS is therefore required for anaerobic biofilm formation on Fe(III) oxide surfaces, yet LuxS-dependent biofilm formation does not enhance Fe(III) oxide reduction activity.

## Introduction

Microbial Fe(III) reduction is a fundamental component of a variety of environmentally important processes, including the biogeochemical cycling of iron, carbon, and other elements, the bioremediation of radionuclide-contaminated waters, and the generation of electricity in microbial fuel cells (1-4). At circumneutral pH, Fe(III) is found in a variety of solid forms ranging from amorphous (e.g., ferrihydrite) to highly crystalline (e.g., $\alpha$-$Fe_2O_3$, hematite) Fe(III) oxides (5). Fe(III)-reducing gram-negative bacteria, such as the $\gamma$–proteobacterium *Shewanella oneidensis*, are thus presented with the physiological problem of transferring electrons to Fe(III) oxides located outside the cell (4, 6-8). *S. oneidensis* employs a variety of novel respiratory strategies to overcome the problem of transferring electrons to external Fe(III) oxides, including i) direct enzymatic reduction via *c*-type cytochromes associated with the extracellular electron conduit (EEC) located on the surface or surface extensions of the *S. oneidensis* outer membrane (OM) (9-16), ii) extracellular electron transfer via endogenous or exogenous electron shuttling compounds (17-20), and iii) non-reductive Fe(III) solubilization by organic ligands to produce more readily reducible soluble organic-Fe(III) complexes (21-23).

In marine and freshwater environments, microorganisms are often found as surface-attached biofilm communities (24, 25). The biofilm matrix is composed of exopolymeric substances that promote adhesion to surfaces and provide the biofilm microbial communities with hydrated microenvironments that enhance metabolic activity, potentially including microbial Fe(III) oxide reduction activity (8, 26, 27). Under aerobic conditions, *S. oneidensis* forms biofilms on silica glass surfaces in a

manner similar to *Pseudomonas aeruginosa* and *Escherichia coli* (24, 25, 28-32). After attachment of individual cells, spatially isolated *S. oneidensis* microcolonies form, followed by fusion of the microcolonies to form small three-dimensional (3D) structures that ultimately cover the entire silica surface. Further horizontal and vertical cell growth results in formation of a mature biofilm consisting of mushroom-like protrusions (also referred to as cell piles or towers) and valley-shaped indentations (31, 33-35). Under anaerobic (fumarate-reducing) conditions, *S. oneidensis* forms similar biofilms on silica surfaces that actively reduce fumarate during anaerobic biofilm formation, maintenance, and stabilization (36). The formation of anaerobic *S. oneidensis* biofilms on Fe(III) oxide surfaces, and the influence of anaerobic biofilm formation on Fe(III) oxide reduction activity, however, has yet to be fully examined. Previous studies have examined the role of *S. oneidensis* attachment to the surface of hematite particles via hematite attachment isotherm experiments, however, little work has been done to examine the role of biofilm formation on ferrihydrite and hematite surfaces under anaerobic growth conditions. For example, the *S. oneidensis* ΔSO3800 (outer-membrane associated serine protease) mutant was shown to display an adhesion deficient phenotype to hematite via hematite adsorption isotherm experiments (37). Despite the inability of ΔSO3800 to adhere to hematite surfaces, they retained the ability to reduce all anaerobic electron acceptors, including ferrihydrite (37). The mechanism through which SO3800 initiates adhesion of *S. oneidensis* to the surfaces of Fe(III) oxides is not fully known, but could include a direct contact mechanism in which an electrostatic charge or Fe(III) binding motif initiates the adhesion to hematite surfaces or the adhesion could occur via indirect mechanisms in which SO3800 protease activity remodels the cell surface (i.e. excess EPS

removel) of *S. oneidensis* to facilitate binding to the oxide surfaces (37). Furthermore, SO3800 lacks a Thr-Pro-Thr motif which indicates any type of direct Fe(III)-binding motif in SO3800 must be different than predicted for MtrC (37). It is more likely that an indirect mechanism influences SO3800 ability to facilitate adhesion to Fe(III) oxide surfaces based on observed evidence, including decrease in cell surface charge, increase in electrophoretic softness, and increase in capsular exopolysaccharide (EPS) in the ΔSO3800 compared to wild-type. It is possible that the SO3800-controlled removal of EPS could enable surface-exposed MtrC and OmcA to adhere directly to and transfer electron to hematite surfaces (37).

The activated methyl cycle (AMC) enzyme S-ribosylhomocysteine lyase (LuxS; Fig. 2.1) is required for *S. oneidensis* biofilm formation under aerobic conditions (35, 38, 39). In the early stages of aerobic biofilm formation, *S. oneidensis* wild-type cells form microcolonies and aggregated cell clusters on silica surfaces, while *S. oneidensis* mutants lacking LuxS (Δ*luxS*) form a monolayer of unevenly distributed (patchy) single cells (31, 35). In the latter stages of aerobic biofilm development, wild-type *S. oneidensis* continues to form larger 3D structures, while the Δ*luxS* mutant remains as a monolayer of patchy single cells (33, 35). Although LuxS enzymatically converts S-ribosylhomocysteine (SRH) to homocysteine and 4,5-dihydroxy-2,3-pentanedione (DPD; the metabolic precursor of the quorum sensing signal autoinducer-2 (AI-2); Fig. 2.1), the aerobic biofilm formation-deficiencies displayed by *S. oneidensis* Δ*luxS* are not caused by disruption of AI-2-mediated quorum sensing, but rather by build of toxic AMC intermediates that are otherwise metabolized to sub-toxic levels by the wild-type strain (25, 33, 35). The involvement of *S. oneidensis* LuxS in formation of anaerobic biofilms

on Fe(III) oxide surfaces and the influence of LuxS-mediated anaerobic biofilm formation on Fe(III) oxide reduction activity have yet to be investigated.

The main objective of the present study was to test the hypothesis that Fe(III) oxide reduction by *S. oneidensis* is enhanced by anaerobic biofilm formation on Fe(III) oxide surfaces. The experimental strategy to test the hypothesis included i) generation of a *S. oneidensis* Δ*luxS* mutant strain via in-frame gene deletion mutagenesis, ii) visual inspection and quantification of Δ*luxS* anaerobic biofilm formation rates on polystyrene and bare and Fe(III) oxide-coated silica surfaces, iii) quantification of the ability of Δ*luxS* to attach to hematite surfaces under anaerobic conditions, and iv) determination of the Fe(III) oxide reduction activity of Δ*luxS* on Fe(III) oxide-coated silica surfaces and in batch cultures with Fe(III) oxide or hematite as electron acceptor.

## Materials and Methods

**Bacterial strains and cultivation conditions.** The bacterial strains and plasmids used in this study are listed in Supplementary Information, Table S4. For genetic manipulations, *S. oneidensis* was cultured at 30°C in Luria-Bertani (LB) medium. For anaerobic growth experiments, cells were grown in M1 minimal medium (40) supplemented with lactate (18 mM), formate (18 mM), or hydrogen (anaerobic gas mixture consisting of 5% $H_2$, 10% $CO_2$, 85% $N_2$) as electron donor. When hydrogen was used as the electron donor, incubations were conducted inside an anaerobic chamber with no additional electron donors present in the anaerobic gas mix or media. Electron acceptors were added from anaerobic stock solutions synthesized as previously described (41-45): Fe(III) citrate (50 mM), ferrihydrite (10 mM), hematite (10 mM), fumarate (10 mM), $NO_3^-$ (15 mM), $NO_2^-$

(2 mM), TMAO (25 mM), and $S_2O_3^{2-}$ (10 mM). When required, gentamicin (Gm) was added at a final concentration of 15 μg $ml^{-1}$. For growth of *Escherichia coli* β2155 λ *pir*, diaminopimelate (DAP) was added at a final concentration of 100 μg $ml^{-1}$. Aerobic growth was monitored spectrophotometrically by measuring changes in absorbance at 600 nm ($A_{600}$).

**Nucleotide and amino acid sequence analyses.** Genome sequence data for *S. oneidensis* MR-1 was obtained from the National Center for Biotechnology Information (NCBI, http://www.ncbi.nlm.nih.gov) and the Department of Energy Joint Genome Institute (DOE-JGI, http://jgi.doe.gov). AMC and Transsulfurylation pathway homologs in the NCBI databases were identified via BLAST analysis (46) using the corresponding *S. oneidensis* enzymes as the search queries.

**In-frame gene deletion mutagenesis and genetic complementation analysis.** The gene encoding LuxS (SO_1101) was deleted in-frame from the *S. oneidensis* genome via previously described procedures (Table 2.4) (47). The primers used for construction of Δ*luxS* are listed in Table 2.5. Regions corresponding to approximately 750 bp upstream and downstream of each open reading frame (ORF) were PCR-amplified with primers D1 and D2 for the upstream region and D3 and D4 for the downstream region with iProof ultrahigh-fidelity polymerase (Bio-Rad, Hercules, CA), generating fragments F1 and F2, which were fused by overlap extension PCR to generate fragment F3. Fragment F3 was cloned into pKO2.0 (containing *sacB*) with BamHI and SalI restriction endonucleases to generate recombinant plasmid pKO2.0-F3, which was electroporated into *E. coli* strain

β2155 λ *pir*. pKO2.0-F3 was mobilized into recipient *S. oneidensis* wild-type cells via conjugal transfer from *E. coli* donor strain β2155 λ pir. *S. oneidensis* recipient strains containing the plasmid integrated into the genome were selected on LB agar medium supplemented with 15 μg $ml^{-1}$ Gm. Single plasmid integrants were identified via PCR with primers D1-DTR and D4-DTF that flank the targeted recombination region. Plasmids were resolved from the genomes of the single integrants by plating on LB agar medium containing sucrose (10% w/v). Following counter selection on sucrose-containing LB agar medium, the corresponding in-frame deletion mutant (designated strain Δ*luxS*) was isolated and confirmed via PCR amplification and direct DNA sequencing (University of Nevada, Reno Genomics Facility). Genetic complementation of Δ*luxS* was carried out by cloning wild-type *luxS* into broad-host-range cloning vector pBBR1MCS (48) and conjugally transferring the recombinant vector into Δ*luxS* via bi-parental mating procedures (16).

**Visual inspection of anaerobic biofilm formation on bare and Fe(III) oxide-coated silica surfaces via confocal laser scanning microscopy (CLSM).** *S. oneidensis* wild-type and Δ*luxS* mutant strains were incubated anaerobically on bare and Fe(III) oxide-coated silica surfaces and biofilm formation was visualized via CLSM. Biofilm formation experiments (to be used for CLSM imaging) were inoculated using *S. oneidensis* MR-1 or *ΔluxS* grown in LB media at 30˚C to $OD_{600}$ 1.0. 12 mL of the aforementioned culture was added to bare silica surfaces or Fe(III) oxide-coated silica surfaces in sterile petri dishes. The slides were incubated at 30˚C for 45 min. Next, the slides were transferred to fresh media and placed in an anaerobic chamber. M1 minimal

growth medium supplemented with either lactate or formate as the electron donor and containing the previously prepared bare and Fe(III) oxide-coated silica slides. Fumarate or thiosulfate was used as the terminal electron acceptor for biofilms grown on bare silica and Fe(III) oxides were used as the electron acceptor for biofilms grown on Fe(III) oxide-coated silica slides. Strains were incubated anaerobically for 48 h at 25˚C in M1 minimal growth medium containing the previously prepared bare silica surfaces. At pre-determined time points, replicate silica slides were sacrificed for CLSM imaging and determination of electron acceptor reduction activity. At pre-determined time points, replicate silica slides were sacrificed for CLSM imaging and analysis of Fe(III) oxide reduction activity.

To prepare the Fe(III) oxide-coated silica surfaces, silica glass microscope slides were washed with 30% (w/v) hydrogen peroxide ($H_2O_2$) and subsequently etched by washing with 5 M NaOH (49, 50). The etched silica surfaces were coated with Fe(III) oxides by slowly oxidizing a 1 M $FeSO_4$ solution with 30% (w/v) $H_2O_2$. The microscope slides were heated to 100ºC to fix the Fe(III) oxide coating to the silica surface and then cleaned via sonication (49, 50). Strains were incubated anaerobically inside an anaerobic chamber for 48 h at 25˚C in M1 minimal growth medium supplemented with either lactate or formate as the electron donor and containing the previously prepared bare and Fe(III) oxide-coated silica slides. At pre-determined time points, replicate silica slides were sacrificed for CLSM imaging and analysis of Fe(III) oxide reduction activity.

Fe(II) production by *S. oneidensis* incubated on the Fe(III) oxide-coated silica slides was monitored by measurement of HCl-extractable Fe(II) via the Ferrozine method (51). Fe(II) production by *S. oneidensis* on Fe(III) oxide-coated surfaces was measured

under two separate conditions, the first conditions ensured planktonic cells remained unperturbed and the second conditions required the planktonic cells to be decanted every 12 hours in order to identify the impact of cells adhered to the Fe(III) oxide-coated silica surfaces and the planktonic cells on Fe(III) reduction activity.

For CLSM imaging, the bare and Fe(III) oxide-coated silica slides were washed with sterile, anaerobic PBS buffer (NaCl (8 g $l^{-1}$), KCl (0.2 g $l^{-1}$), $Na_2HPO_4$ (1.44 g $l^{-1}$), $KH_2PO_4$ (0.24 g $l^{-1}$, pH 7) and attached cells were fixed with 4% paraformaldehyde. The fixed cells were stained with 0.1% (w/v) anaerobic acridine orange solution for 20 min and then washed with anaerobic PBS buffer for 10 min prior to examination of biofilm structure via CLSM. CLSM imaging was carried out with a Zeiss 510 Vis system comprised of a Zeiss Axio Observer inverted microscope and an argon laser source with excitation wavelengths of 453, 477, 488, and 514 nm. 3D digitized images were generated with Zeiss Zen 2009 software (Carl Zeiss Microscopy, Inc.).

**Quantification of the rates of aerobic and anaerobic biofilm formation**. Rates of aerobic and anaerobic biofilm formation by *S. oneidensis* wild-type and Δ*luxS* mutant strains were determined by conventional biofilm assays in polystyrene microtiter plates (33, 52, 53). Washed cell suspensions were inoculated at initial cell densities of $1.0 \times 10^7$ cells $ml^{-1}$ in the individual wells of microtiter plates in M1 minimal growth medium supplemented with lactate (18 mM), formate (18 mM), or $H_2$ (anaerobic gas mixture consisting of 5% $H_2$, 10% $CO_2$, 85% $N_2$) as electron donor. Fumarate and $S_2O_3^{2-}$ (10 mM final concentration) were added as electron acceptors from anaerobic, filter-sterilized stocks, and the microtiter plates were incubated at 30˚C. Anaerobic biofilm experiments

were incubated inside an anaerobic chamber for the duration of the experiment. Cells adhered to the polystyrene walls of the microtiter plates were measured via staining with 0.01% (v/v) crystal violet (CV). After removal of the unattached cells remaining in the well solution, the well walls were washed twice with deionized water to remove any excess CV and any remaining planktonic cells. Acetic acid (33%, v/v) was then added to each well to solubilize the cell wall-associated CV for 10 min. The addition of acetic acid ensures cell material does not remain adhered to the polystyrene walls thereby preventing interference/scattering of light at 550nm. The total number of attached bacterial cells was determined by measuring absorbance at 550 nm ($A_{550}$) with a microtiter plate (BioTek Synergy HT Multidetection Microplate Reader). To rescue the anaerobic biofilm formation-deficiencies displayed by Δ*luxS*, a suite of AMC and Transsulfurylation pathway intermediates involved in organic sulfur metabolism were added at final concentrations of 150-300 μM to M1 minimal medium and biofilm formation rates were determined via the CV-based biofilm assay described above. The AMC and Transsulfurylation pathway intermediates included cystine, cysteine, oxidized and reduced glutathione, homocysteine, methionine, serine, and homoserine (39, 54, 55). The amino acids alanine and lysine were added as control metabolites not involved in organic sulfur metabolism.

**Quantification of *S. oneidensis* wild-type and ΔluxS mutant cell attachment to hematite surfaces via adsorption isotherm analyses.** *S. oneidensis* wild-type and Δ*luxS* mutant strains were tested for the ability to attach to hematite surfaces via adsorption isotherm experiments as previously described for *S. oneidensis* serine protease

mutant ΔSO3800 (37). *S. oneidensis* wild-type and Δ*luxS* mutant strains were grown anaerobically to late-log phase in M1 minimal medium with lactate (18 mM) as electron donor and fumarate (10 mM) as electron acceptor, harvested via centrifugation, and washed and resuspended in anaerobic 50 mM KCl buffer (pH 7) to a final cell concentration of $1.8 \times 10^8$ cells $ml^{-1}$. The cell suspensions were incubated anaerobically in the presence of 2 mg ml hematite for 2 h to reach pre-determined equilibria (37). Hematite stock solutions were prepared by washing and resuspending 1 g of hematite in 10 ml of anaerobic 50 mM KCl buffer (pH 7). To determine the number of cells attached to the hematite surfaces, samples were removed from the anaerobic incubations at pre-selected time intervals and gently centrifuged at 800 × *g* to remove the hematite particles and hematite-bound cells. The concentration of cells remaining in solution was measured by $A_{600}$, and the number of cells attaching to the hematite surfaces was calculated by subtracting the concentration of cells remaining in the cell suspension supplemented with hematite from an otherwise identical control suspensions with hematite omitted (37).

**Determination of the overall anaerobic respiratory capability of Δ*luxS* in batch cultures.** *S. oneidensis* wild-type and Δ*luxS* mutant strains were grown anaerobically (initial inoculum of $1.0 \times 10^7$ cells $ml^{-1}$) in M1 minimal medium supplemented with either lactate (18 mM), formate (15 mM), or $H_2$ (anaerobic gas mixture consisting of 5% $H_2$, 10% $CO_2$, 85% $N_2$) as electron donor and either Fe(III)-citrate (50 mM), ferrihydrite (10 mM), or hematite (10 mM) as electron acceptor. Fe(II) production was monitored by measurement of HCl-extractable Fe(II) via the Ferrozine method (51). Δ*luxS* was also tested for the ability to respire anaerobically on a suite of five additional electron

acceptors, including Mn(III) pyrophosphate, Mn(IV) oxide, TMAO, fumarate, $NO_3^-$, $NO_2^-$, and $S_2O_3^{2-}$. Mn(III) pyrophosphate was measured colorimetrically as previously described (56). Mn(IV) reduction was measured spectrophotometrically after reaction with benzidine as previously described (41). Growth on TMAO and fumarate was monitored by $A_{600}$ measurements. $NO_2^-$ was measured (for both $NO_3^-$ and $NO_2^-$ reduction experiments) spectrophotometrically with sulfinilic acid-*N*-1-naphthyl-ethylene-diamine dihydrochloride solution (57). $NO_3^-$ reduction (i.e. $NO_2^-$ production) is measured as the increase in $NO_2^-$ production over time; $NO_2^-$ reduction (i.e. $NO_2^-$ depletion) is measured as a decrease in $NO_2^-$ over time. $S_2O_3^{2-}$ concentration was measured by cyanolysis as previously described (47, 58). Under $S_2O_3^{2-}$ reducing conditions, the decrease in $S_2O_3^{2-}$ concentration is measured over time. Rates for aerobic growth and anaerobic respiration were measured in the linear range observed during aerobic growth activity or anaerobic reduction activity.

## Results

**Identification of the AMC and Transsulfurylation pathway enzymes via BLASTp analyses.** The genes encoding putative AMC and Transulfurylation pathway enzymes were identified in the *S. oneidensis* genome via BLASTp analyses. Homologs with high amino acid sequence similarity (94-100%), sequence identity (57-88%), and e-values ($e^{-100}$-0.0) of the complete AMC and nearly complete Transsulfurylation pathway enzymes were identified in the *S. oneidensis* genome (Table 2.1, Fig. 2.1). The complete AMC pathway included SO_1101, a LuxS homolog which displayed 100% sequence similarity,

82% sequence identity, and a strong e-value ($e^{-100}$) to the LuxS homolog of *Vibrio parahaemolyticus* (Table 2.1). Cystathionine β-synthase (CBS) and cystathionine γ-lyase (CGL) were the only Transsulfurylation pathway enzymes missing from the *S. oneidensis* genome, potentially indicating that the Transsulfurylation pathway is dedicated to operating in the forward direction to produce homocysteine with cysteine and O-succinyl-L-homoserine as substrates and cystathionine as intermediate (and not operating in the reverse direction to produce cysteine and α-ketobutyrate with homocysteine as substrate and cystathionine as intermediate) (Table 2.1, Fig 2.1).

**Visual inspection of anaerobic biofilm formation on bare and Fe(III) oxide-coated silica surfaces**. Confocal laser scanning microscopy (CLSM) image analyses indicated that *S. oneidensis* wild-type and Δ*luxS* mutant strains displayed widely varying biofilm architectures during anaerobic growth on bare (Figs. 2.2A-B; fumarate- or thiosulfate ($S_2O_3^{2-}$)-amended) and Fe(III) oxide-coated (Fig. 2.2C) silica surfaces. With lactate as electron donor, *S. oneidensis* wild-type and Δ*luxS*+*luxS* strains (top and bottom row of images, respectively) formed microcolonies that subsequently developed into larger 3D structures until the bare and Fe(III) oxide-coated silica surfaces were completely covered with mushroom-like protrusions (cell piles or towers) after a 48 h anaerobic incubation period with lactate as electron donor. The Δ*luxS* mutant cells (Fig. 2.2, middle row of images), on the other hand, were severely impaired in anaerobic biofilm formation during the 48 h incubation period with lactate as electron donor, with patches of both the bare and Fe(III) oxide-coated silica surfaces remaining uncovered. Compared to the *S. oneidensis* wild-type and Δ*luxS*+*luxS* strains, Δ*luxS* was also severely impaired in

anaerobic biofilm formation on both bare and Fe(III) oxide-coated silica surfaces with formate replacing lactate as electron donor (Supporting Information, Fig. 2.S2).

**Fe(III) reduction activity of *S. oneidensis* wild-type and ΔluxS mutant strains on Fe(III) oxide-coated silica surfaces**. Under anaerobic growth conditions with $H_2$ and lactate as electron donors, *S. oneidensis* wild-type and Δ*luxS* mutant strains reduced the Fe(III) oxides coated on the silica surfaces at nearly identical rates (Fig. 2.3A): The wild-type strain reduced the Fe(III) oxides coated on the silica surfaces at a rate of 38 (± 9) μM $hr^{-1}$, while Δ*luxS* reduced the Fe(III) oxides coated on the silica surfaces at a rate of 37 (± 7) μM $hr^{-1}$. Under anaerobic growth conditions with $H_2$ and formate as electron donors, *S. oneidensis* WT and Δ*luxS* reduced the Fe(III) oxides coated on the silica surfaces at nearly identical rates (Fig. 2.3A): The wild-type strain reduced the Fe(III) oxides coated on the silica surfaces at a rate of 24 (± 6) μM $hr^{-1}$, while Δ*luxS* reduced the Fe(III) oxides coated on the silica surfaces at a rate of 23 (± 5) μM $hr^{-1}$. Under anaerobic growth conditions with $H_2$ as electron donor, *S. oneidensis* WT and Δ*luxS* reduced the Fe(III) oxides coated on the silica surfaces at nearly identical rates (Fig. 2.3A): The wild-type strain reduced the Fe(III) oxides coated on the silica surfaces at a rate of 26 (± 2) μM $hr^{-1}$, while Δ*luxS* reduced the Fe(III) oxides coated on the silica surfaces at a rate of 26 (± 3) μM $hr^{-1}$. For the these specific experiments, the rates of Fe(III) reduction were calculated by dividing the final Fe(II) concentration by the total incubation time. Results of the decanting experiment shows that during the first 12 hours of reduction, cells in direct contact to the Fe(III) oxide-coated silica surfaces are important to Fe(III) reduction, however, after 12 hours planktonic cells dominate Fe(III) reduction pathways (Fig. 2.3B).

**Rates of aerobic and anaerobic biofilm formation on polystyrene surfaces**. Rates of aerobic and anaerobic biofilm formation on polystyrene surfaces were determined using conventional CV-based biofilm assays in polystyrene microtiter plates. Under aerobic conditions with lactate or formate as electron donor, the rates of biofilm formation by Δ*luxS* were approximately half (47-63%) of the corresponding wild-type rates of biofilm formation (wild-type $A_{550}$ increase of 0.056 $hr^{-1}$ with lactate, and 0.008 $hr^{-1}$ with formate; Table 2.2, Supporting Information, Fig. 2.S2). However, under anaerobic conditions with lactate or formate as electron donor, Δ*luxS* biofilm formation rates ranged from 10-13% of the wild-type rate with $S_2O_3^{2-}$ as electron acceptor (wild-type $A_{550}$ increase of 0.017 $hr^{-1}$ with lactate and 0.010 $hr^{-1}$ with formate) and from 6-23% of the wild-type rate with fumarate as electron acceptor (wild-type $A_{550}$ increase of 0.004 $hr^{-1}$ with lactate and 0.003 $hr^{-1}$ with formate; Fig. 2.4A, Table 2.2).

Regardless of electron donor (lactate and formate) or electron acceptor ($S_2O_3^{2-}$ and fumarate), the rates of anaerobic biofilm formation by Δ*luxS* were restored to near wild-type levels by addition of either cysteine (99-106% of wild-type rates), cystine (91-117%), oxidized glutathione (99-105%), reduced glutathione (80-108%), homocysteine (76-86%), methionine (108-125%), serine (105-123%), or homoserine (103-115% ) (Figs. 2.4B-C, Supporting Information, Table 2.S3). Rates of anaerobic biofilm formation by Δ*luxS*, on the other hand, remained at mutant levels (7-15% of wild-type rates) after addition of alanine or lysine (Figs. 2.4B-C, Table 2.3).

***S. oneidensis* cell-hematite attachment isotherms.** To determine the ability of *S. oneidensis* wild-type and Δ*luxS* mutant strains to attach to hematite surfaces, a series of

bacterial cell-hematite adsorption isotherm analyses were carried out. Under anaerobic conditions, fumarate-grown Δ*luxS* cells adhered to hematite at levels approximately 32% of the fumarate-grown *S. oneidensis* wild-type cells (Fig. 2.5). As previously reported, fumarate-grown cells of serine protease mutant ΔSO3800 adhered to hematite at levels approximately 34% of fumarate-grown *S. oneidensis* wild-type cells (Fig. 2.5) (37). The bacterial cell-hematite adsorption isotherm analyses thus indicate that wild-type *S. oneidensis* readily attaches to hematite surfaces under anaerobic conditions, while Δ*luxS* displayed hematite attachment deficiencies nearly identical to that displayed by ΔSO3800 (37).

**Overall respiratory capability of Δ*luxS* in anaerobic batch cultures**. In anaerobic batch cultures inoculated with $10^7$ cells $mL^{-1}$ initial inoculum with $H_2$, lactate, or formate as electron donor, Δ*luxS* reduced ferrihydrite at near wild-type rates (88%, 72%, and 104% of the wild-type strain, respectively)(Fig. 2.6, Supporting Information, Fig. 2.S4). In anaerobic batch cultures with $H_2$, lactate, or formate as electron donor, Δ*luxS* also reduced hematite at near wild-type rates (87%, 104%, and 96% of the wild-type strain, respectively) (Fig. 2.6, Supporting Information, Fig. 2.S4). In addition, Δ*luxS* reduced the alternate electron acceptors Mn(III) pyrophosphate, trimethylamine-*N*-oxide (TMAO), fumarate, nitrate ($NO_3^-$), nitrite ($NO_2$), and thiosulfate ($S_2O_3^{2-}$) at wild-type rates (80-120%) with either lactate, formate, or $H_2$ as electron donor (Supporting Information, Fig. 2.S5). Thus, in anaerobic batch cultures, Δ*luxS* reduced all electron acceptors at wild type rates, regardless of electron donor. Additionally, in aerobic batch cultures with lactate or formate as the electron donor, Δ*luxS* grew at near wild-type rates.

**Discussion**

*S. oneidensis* biofilm formation has been previously examined on bare silica surfaces under both aerobic and anaerobic (fumarate-reducing) conditions (33-36). The present study is the first to investigate *S. oneidensis* biofilm formation on Fe(III) oxide surfaces under anaerobic conditions, and subsequently to examine the influence of anaerobic biofilm formation on Fe(III) oxide reduction activity. Previous studies of *S. oneidensis* biofilm formation on bare silica surfaces under aerobic and anaerobic (fumarate-reducing) conditions indicated that *S. oneidensis* initially formed aggregated cell clusters (microcolonies) that subsequently developed into larger 3D structures until the surface was completely covered in a mature biofilm (33-35). Results of the present study indicate that *S. oneidensis* biofilms develop under anaerobic conditions on bare and Fe(III) oxide-coated silica surfaces in a manner similar to aerobic biofilm formation on bare silica surfaces (Fig 2.2, Supporting Information, Fig. 2.S1). In addition, the rates of anaerobic biofilm formation on polystyrene surfaces with $S_2O_3^{2-}$ as electron acceptor ($A_{550}$ increase of 0.015 $hr^{-1}$) were approximately 5-fold greater than the rates of anaerobic biofilm formation with fumarate as electron acceptor ($A_{550}$ increase of 0.003 $hr^{-1}$) (Fig. 2.4, Table 2.4). The biogeochemical factors driving the differences in these rates of anaerobic biofilm formation may be due to the differences in midpoint redox potentials ($E'_0$) between fumarate ($E'_0$ = +0.02 V) and $S_2O_3^{2-}$ ($E'_0$ = -0.40 V)(see discussion below).

The molecular details associated with *S. oneidensis* biofilm formation have been examined only under aerobic conditions (33). The AMC enzyme LuxS is involved in aerobic biofilm formation by a wide range of bacteria, including *S. oneidensis* (33, 59). LuxS catalyzes the conversion of SRH to homocysteine and the AI-2 precursor DPD (60)

(Fig. 2.1). Mature AI-2 functions as a quorum sensing signal that regulates a myriad of cellular processes including virulence factor production, pathogenicity, bioluminescence, sporulation, DNA uptake competence, and biofilm formation (59, 61-67). *S. oneidensis* produces AI-2 under aerobic conditions, but does not produce AI-2 under anaerobic Fe(III) citrate-reducing conditions (35, 68). In addition, AI-2 involvement in *S. oneidensis* biofilm formation is not predicted by genome analyses, which have demonstrated that homologs similar to the AI-2 sensor (LuxPQ), transporter (Lsr ABC-type), kinase (LsrK), and cognate transcriptional repressor (LsrR) are not present in the *S. oneidensis* genome (33, 60).

In other bacterial AMC systems, however, homocysteine production via LuxS catalyzed conversion of S-ribosyl homocysteine is more important that the LuxS mediated production of AI-2. Homocysteine is enzymatically converted step-wise to methionine by cobalamine-dependent (MetH) and cobalamine-independent (MetE) methionine synthases and to the universal methyl donor S-adenosyl-methionine (SAM) by S-adenosylmethionine synthase (MetK) (Fig. 2.1) (60). Due to aberrant intracellular pools of methionine and SAM, Δ*luxS* mutant strains display a wide array of pleiotropic mutant phenotypes, including deficiencies in aerobic biofilm formation. For example, previous studies have reported that the aerobic biofilms of *S. oneidensis* Δ*luxS* on bare silica surfaces contain approximately 66% of the wild-type biofilm biomass (33). In the present study, Δ*luxS* formed aerobic biofilms on polystyrene and bare silica surfaces with lactate or formate as electron donor at rates approximately 43-63% of the wild-type strain (Supporting Information, Fig. 2.S2). Δ*luxS* formed anaerobic biofilms on polystyrene and bare silica surfaces with lactate or formate as electron donor and fumarate or

thiosulfate as electron acceptor at rates approximately 6-23% of the wild-type strain (Fig. 2.4A, Supporting Information, Fig. 2.S3). In addition, visual inspection of biofilm architecture via CLSM demonstrated that Δ*luxS* was severely impaired in anaerobic biofilm formation on Fe(III) oxide-coated silica surfaces (Fig. 2.2, Supporting Information, Fig. 2.S1), and cell-hematite adsorption isotherm analyses indicated that Δ*luxS* was deficient in attachment to hematite surfaces (Fig. 2.5). LuxS is thus required for *S. oneidensis* biofilm formation on polystyrene and bare and Fe(III)-coated silica surfaces under both aerobic and anaerobic (fumarate-, $S_2O_3^{2-}$- and Fe(III) oxide-reducing) conditions.

The involvement of LuxS in anaerobic biofilm formation, and the absence of proteins involved in AI-2 sensing, uptake, phosphorylation, and transcriptional regulation led us to hypothesize that anaerobic biofilm production by *S. oneidensis* required LuxS-dependent homocysteine production. Regardless of electron donor (lactate and formate) or electron acceptor ($S_2O_3^{2-}$, fumarate, or Fe(III) oxides), the rates of anaerobic biofilm formation by Δ*luxS* were restored to wild-type levels by addition of homocysteine and a variety of other AMC and Transsulfurylation pathway metabolites, including cysteine, cystine, reduced glutathione, oxidized glutathione, methionine, serine, and homoserine (Fig. 2.1, Figs. 2.4B-C, Table 2.3). Homocysteine (and AI-2) is produced by LuxS via conversion of S-ribosylhomocysteine. In order for homocysteine to be present in sufficient amounts within the cell to maintain a proper concentration, *luxS* must be present in *S. oneidensis*. In the absence of endogenous homocysteine, the addition of exogenous homocysteine restored biofilm formation in part modulating the redox homoestasis within the cell. Rates of anaerobic biofilm formation by Δ*luxS* remained at

mutant levels, on the other hand, after addition of alanine or lysine, two amino acids which are not intermediates in the AMC or transulfurylation pathways nor are they involved in organic sulfur metabolism (Figs. 2.4B-C, Table 2.3). These results suggest that maintenance of a proper intracellular pool of AMC and Transsulfurylation pathway metabolites is required for anaerobic biofilm formation by *S. oneidensis*. Reasons for this finding are unclear, however, the organic sulfur compounds produced by the AMC and Transulfurylation pathways have been previously implicated in maintenance of redox homeostasis in a variety of other bacteria (69-72).

*S. oneidensis* biofilm formation on bare and Fe(III) oxide-coated silica surfaces also appears similar to *S. oneidensis* biofilm formation on graphite anode surfaces in microbial fuel cells (MFC) where *S. oneidensis* rapidly forms thick biofilms with more negative anode potentials on the harder to reduce anode surfaces (i.e., MFC with higher applied external resistance) (73). In a similar fashion, results of the present study demonstrate that the rates of anaerobic biofilm formation on polystyrene surfaces were 5-fold greater in the presence of electron acceptors with more negative $E'_0$ values (e.g., $S_2O_3^{2-}$ versus fumarate; Fig. 4; see discussion above). Results of the present study also indicate that the highly reducing conditions required for formation of thicker *S. oneidensis* biofilms on Fe(III) oxide surfaces is driven by LuxS-mediated production of homocysteine and other AMC and Transulfurylation pathway metabolites involved in organic sulfur metabolism. AMC and Transsulfurylation pathway metabolites such as homocysteine, cysteine, and glutathione are well known for their ability to maintain intracellular reducing conditions to combat oxidative stress (72, 74, 75), and cysteine and glutathione are often added as external reducing agents to maintain redox poise in

anaerobic growth medium (76, 77). The ability of both reduced thiols and oxidized disulfides to rescue anaerobic biofilm formation in the *luxS* mutant indicates *S. oneidensis* is capable of reducing disulfides, thus is capable of using both reduced and oxidized thiols during anaerobic growth as a way to maintain the internal thiol pool and redox homeostasis within the cells. The potential link between redox homeostasis and LuxS-dependent biofilm formation warrants further examination with *S. oneidensis* gene deletion mutants lacking other AMC and Transsulfurylation pathway enzymes.

The anaerobic biofilm formation-deficient phenotype displayed by *S. oneidensis* Δ*luxS* was leveraged to determine the influence of LuxS-dependent biofilm formation on Fe(III) oxide reduction activity. *S. oneidensis* transfers electrons to external Fe(III) oxides via EEC- or surface extension-associated *c*-type cytochromes (11, 14), endogenous or exogenous electron shuttles (17-20), and soluble organic-Fe(III) complexes produced by endogenous or exogenous Fe(III)-chelating ligands (21-23). The *S. oneidensis* electron transport system consists of inner membrane (IM)-localized dehydrogenases, menaquinone, and CymA, a menaquinol-oxidizing *c*-type cytochrome that functions as a central branch point for electron transport to Fe(III) oxides, $NO_3^-$, $NO_2^-$, dimethylsulfoxide, and fumarate (78). In the Fe(III) oxide reduction system, electron transfer proceeds from CymA to MtrA (79), which forms the OM-localized EEC with MtrB and MtrC (14).

MtrC-catalyzed electron transfer to Fe(III) oxides requires distances of <15 Å for efficient electron transfer between the catalytically active heme groups of MtrC and the Fe(III) oxide surface (80). In the present study, we hypothesized that the Fe(III) oxide reduction activity of *S. oneidensis* may be enhanced by anaerobic biofilm formation on

Fe(III) oxide surfaces. In the direct electron transfer pathway, the anaerobic biofilm may provide a hydrated microenvironment that enhances MtrC-catalyzed Fe(III) reduction activity. The electron shuttling and Fe(III) solubilization pathways may also be enhanced by formation of anaerobic biofilms on Fe(III) oxide surfaces (8). In these two pathways, either electron shuttling flavins (17) or Fe(III)-chelating organic ligands (21, 23) are secreted into the anaerobic biofilm where they deliver electrons to or solubilize Fe(III) from the Fe(III) oxide surface, respectively. The anaerobic biofilm may provide a hydrated microenvironment for catalytic re-reduction of oxidized flavins after electron delivery to the Fe(III) oxide surface (electron shuttling pathway) or for organic ligand-promoted Fe(III) chelation reactions at the Fe(III) oxide surface (Fe(III) solubilization pathway). The anaerobic biofilm may also impede diffusional loss of flavins and organic ligands to the biofilm external environment, and thus facilitate sharing of flavins and organic ligands between cells in the multiple cell layers of *S. oneidensis* biofilms. In this manner, *S. oneidensis* cells located several cell layers away from the Fe(III) oxide surface may maintain Fe(III) oxide reduction activity without direct contact with the Fe(III) oxide surface. Anaerobic biofilm formation, however, does not appear to enhance the overall Fe(III) oxide reduction activity of *S. oneidensis* since Δ*luxS* is severely impaired in the ability to form anaerobic biofilms, yet displays wild-type Fe(III) oxide reduction activity on Fe(III) oxide-coated silica surfaces and in anaerobic batch cultures with ferrihydrite or hematite as electron acceptor (Fig. 2.3, Fig. 2.4, Fig. 2.6, Table 2.2, Supporting Information, Fig. 2.S3, Supporting Information, Fig. 2.S4).

One potential explanation for the inability of anaerobic biofilms to enhance Fe(III) oxide reduction activity is that the small proportion of Δ*luxS* cells remaining

attached to the Fe(III) oxides in a patchy cell monolayer (Fig. 2.2, Supporting information, Fig. 2.S1) contributes nearly 100% of the reducing power required to produce the Fe(II) signals detected in the anaerobic incubations with Fe(III) oxide-coated silica surfaces and in batch cultures with ferrihydrite or hematite as electron acceptor. In this case, only those cells interacting directly with the Fe(III) oxide surface contribute to the overall Fe(III) oxide reduction activity. On the other hand, the inability of anaerobic biofilm formation to enhance Fe(III) oxide reduction activity may also indicate that unattached (planktonic) *S. oneidensis* cells are able to deliver electrons over long (μm) distances to the Fe(III) oxide surface via overlapping electron shuttling or Fe(III) solubilization pathways (4, 8, 81). To examine these two possibilities, current work is focused on application of (anaerobic) single cell fluorescent technology to detect the metabolic activity of single *S. oneidensis* wild-type and Δ*luxS* biofilm formation-deficient mutant cells interacting at short (nm) and long (μm) distances from the Fe(III) oxide surface.

**References**


1. **Hau HH, Gralnick JA.** 2007. Ecology and biotechnology of the genus *Shewanella*. Annu. Rev. Microbiol. **61:**237-258.
2. **Logan BE.** 2010. Scaling up microbial fuel cells and other bioelectrochemical systems. Appl Microbiol Biot **85:**1665-1671.
3. **Lovley DR, Holmes DE, Nevin KP.** 2004. Dissimilatory Fe(III) and Mn(IV) reduction. Adv. Microb. Physiol. **49:**219-286.
4. **Cooper RE, Goff JL, Reed BC, Sekar R, DiChristina TJ.** 2014. Breathing metals: Molecular mechanisms of microbial iron reduction, Manual of Environmental Microbiology. ASM Press.
5. **Stumm W, Morgan JJ.** 1996. Aquatic Chemistry: Chemical equilibria and rates in natural waters, 3rd ed. Wiley, New York.
6. **Richter K, Schicklberger M, Gescher J.** 2012. Dissimilatory reduction of extracellular electron acceptors in anaerobic respiration. Appl. Environ. Microbiol. **78:**913-921.

7. **Shi L, Rosso KM, Clarke TA, Richardson DJ, Zachara JM, Fredrickson JK.** 2012. Molecular underpinnings of Fe(III) oxide reduction by *Shewanella oneidensis* MR-1. Frontiers in microbiology **3:**50.
8. **Melton ED, Swanner ED, Behrens S, Schmidt C, Kappler A.** 2014. The interplay of microbially mediated and abiotic reactions in the biogeochemical Fe cycle. Nat Rev Microbiol **12:**797-808.
9. **Beliaev AS, Saffarini DA.** 1998. *Shewanella putrefaciens mtrB* encodes an outer membrane protein required for Fe(III) and Mn(IV) reduction. J. Bacteriol. **180:**6292-6297.
10. **Myers CR, Myers JM.** 1992. Localization of cytochromes to the outer-membrane of anaerobically grown *Shewanella putrefaciens* MR-1. J. Bacteriol. **174:**3429-3438.
11. **Pirbadian S, Barchinger SE, Leung KM, Byun HS, Jangir Y, Bouhenni RA, Reed SB, Romine MF, Saffarini DA, Shi L, Gorby YA, Golbeck JH, El-Naggar MY.** 2014. *Shewanella oneidensis* MR-1 nanowires are outer membrane and periplasmic extensions of the extracellular electron transport components. Proc. Natl. Acad. Sci. U. S. A. **111:**12883-12888.
12. **Shi L, Deng S, Marshall MJ, Wang ZM, Kennedy DW, Dohnalkova AC, Mottaz HM, Hill EA, Gorby YA, Beliaev AS, Richardson DJ, Zachara JM, Fredrickson JK.** 2008. Direct involvement of type II secretion system in extracellular translocation of *Shewanella oneidensis* outer membrane cytochromes MtrC and OmcA. J. Bacteriol. **190:**5512-5516.
13. **Hartshorne RS, Reardon CL, Ross D, Nuester J, Clarke TA, Gates AJ, Mills PC, Fredrickson JK, Zachara JM, Shi L, Beliaev AS, Marshall MJ, Tien M, Brantley S, Butt JN, Richardson DJ.** 2009. Characterization of an electron conduit between bacteria and the extracellular environment. Proc. Natl. Acad. Sci. U. S. A. **106:**22169-22174.
14. **White GF, Shi Z, Shi L, Wang ZM, Dohnalkova AC, Marshall MJ, Fredrickson JK, Zachara JM, Butt JN, Richardson DJ, Clarke TA.** 2013. Rapid electron exchange between surface-exposed bacterial cytochromes and Fe(III) minerals. Proc. Natl. Acad. Sci. U. S. A. **110:**6346-6351.
15. **Wee SK, Burns JL, DiChristina TJ.** 2014. Identification of a molecular signature unique to metal-reducing Gammaproteobacteria. FEMS Microbiol. Lett. **350:**90-99.
16. **DiChristina TJ, Moore CM, Haller CA.** 2002. Dissimilatory Fe(III) and Mn(IV) reduction by *Shewanella putrefaciens* requires *ferE*, a homolog of the *pulE* (*gspE*) type II protein secretion gene. J. Bacteriol. **184:**142-151.
17. **Marsili E, Baron DB, Shikhare ID, Coursolle D, Gralnick JA, Bond DR.** 2008. *Shewanella* secretes flavins that mediate extracellular electron transfer. Proc. Natl. Acad. Sci. U. S. A. **105:**3968-3973.
18. **von Canstein H, Ogawa J, Shimizu S, Lloyd JR.** 2008. Secretion of flavins by *Shewanella* species and their role in extracellular electron transfer. Appl. Environ. Microbiol. **74:**615-623.
19. **Flynn TM, O'Loughlin EJ, Mishra B, DiChristina TJ, Kemner KM.** 2014. Sulfur-mediated electron shuttling during bacterial iron reduction. Science **344:**1039-1042.

20. **Roden EE, Kappler A, Bauer I, Jiang J, Paul A, Stoesser R, Konishi H, Xu HF.** 2010. Extracellular electron transfer through microbial reduction of solid-phase humic substances. Nat Geosci **3:**417-421.
21. **Jones ME, Fennessey CM, DiChristina TJ, Taillefert M.** 2010. *Shewanella oneidensis* MR-1 mutants selected for their inability to produce soluble organic-Fe(III) complexes are unable to respire Fe(III) as anaerobic electron acceptor. Environmental Microbiology **12:**938-950.
22. **Taillefert M, Beckler JS, Carey E, Burns JL, Fennessey CM, DiChristina TJ.** 2007. *Shewanella putrefaciens* produces an Fe(III)-solubilizing organic ligand during anaerobic respiration on insoluble Fe(III) oxides. J. Inorg. Biochem. **101:**1760-1767.
23. **Fennessey CM, Jones ME, Taillefert M, DiChristina TJ.** 2010. Siderophores are not involved in Fe(III) solubilization during anaerobic Fe(III) respiration by *Shewanella oneidensis* MR-1. Appl. Environ. Microbiol. **76:**2425-2432.
24. **Flemming HC, Wingender J.** 2010. The biofilm matrix. Nat Rev Microbiol **8:**623-633.
25. **Karatan E, Watnick P.** 2009. Signals, regulatory networks, and materials that build and break bacterial biofilms. Microbiol. Mol. Biol. Rev. **73:**310-347.
26. **Hall-Stoodley L, Costerton JW, Stoodley P.** 2004. Bacterial biofilms: from the natural environment to infectious diseases. Nat Rev Microbiol **2:**95-108.
27. **Halan B, Buehler K, Schmid A.** 2012. Biofilms as living catalysts in continuous chemical syntheses. Trends Biotechnol. **30:**453-465.
28. **McDougald D, Rice SA, Barraud N, Steinberg PD, Kjelleberg S.** 2012. Should we stay or should we go: mechanisms and ecological consequences for biofilm dispersal. Nature Rev Microbiol **10:**39-50.
29. **Klausen M, Heydorn A, Ragas P, Lambertsen L, Aaes-Jorgensen A, Molin S, Tolker-Nielsen T.** 2003. Biofilm formation by Pseudomonas aeruginosa wild type, flagella and type IV pili mutants. Mol. Microbiol. **48:**1511-1524.
30. **Sauer K, Camper AK, Ehrlich GD, Costerton JW, Davies DG.** 2002. Pseudomonas aeruginosa displays multiple phenotypes during development as a biofilm. J. Bacteriol. **184:**1140-1154.
31. **Thormann KM, Saville RM, Shukla S, Pelletier DA, Spormann AM.** 2004. Initial phases of biofilm formation in Shewanella oneidensis MR-1. J. Bacteriol. **186:**8096-8104.
32. **Tolker-Nielsen T, Brinch UC, Ragas PC, Andersen JB, Jacobsen CS, Molin S.** 2000. Development and dynamics of Pseudomonas sp biofilms. J. Bacteriol. **182:**6482-6489.
33. **Learman DR, Yi H, Brown SD, Martin SL, Geesey GG, Stevens AM, Hochella MF.** 2009. Involvement of *Shewanella oneidensis* MR-1 LuxS in Biofilm Development and Sulfur Metabolism. Appl. Environ. Microbiol. **75:**1301-1307.
34. **Majors PD, McLean JS, Pinchuk GE, Fredrickson JK, Gorby YA, Minard KR, Wind RA.** 2005. NMR methods for in situ biofilm metabolism studies. J. Microbiol. Methods **62:**337-344.
35. **Bodor AM, Jansch L, Wissing J, Wagner-Dobler I.** 2011. The luxS mutation causes loosely-bound biofilms in Shewanella oneidensis. BMC Res. Notes **4:**180.

36. **McLean JS, Majors PD, Reardon CL, Bilskis CL, Reed SB, Romine MF, Fredrickson JK.** 2008. Investigations of structure and metabolism within Shewanella oneidensis MR-1 biofilms. J. Microbiol. Methods **74:**47-56.
37. **Burns JL, Ginn BR, Bates DJ, Dublin SN, Taylor JV, Apkarian RP, Amaro-Garcia S, Neal AL, Dichristina TJ.** 2010. Outer Membrane-Associated Serine Protease Involved in Adhesion of *Shewanella oneidensis* to Fe(III) Oxides. Environ. Sci. Technol. **44:**68-73.
38. **Kouzuma A, Oba H, Tajima N, Hashimoto K, Watanabe K.** 2014. Electrochemical selection and characterization of a high current-generating Shewanella oneidensis mutant with altered cell-surface morphology and biofilm-related gene expression. BMC Microbiol. **14:**190.
39. **Pereira CS, Thompson JA, Xavier KB.** 2013. AI-2-mediated signalling in bacteria. FEMS Microbiol. Rev. **37:**156-181.
40. **Myers CR, Nealson KH.** 1988. Bacterial manganese reduction and growth with manganese oxide as the sole electron acceptor. Science **240:**1319-1321.
41. **Burnes BS, Mulberry MJ, DiChristina TJ.** 1998. Design and application of two rapid screening techniques for isolation of Mn(IV) reduction-deficient mutants of *Shewanella putrefaciens*. Appl. Environ. Microbiol. **64:**2716-2720.
42. **Neal AL, Dublin SN, Taylor J, Bates DJ, Burns L, Apkarian R, DiChristina TJ.** 2007. Terminal electron acceptors influence the quantity and chemical composition of capsular exopolymers produced by anaerobically growing *Shewanella* spp. Biomacromolecules **8:**166-174.
43. **Taratus EM, Eubanks SG, DiChristina TJ.** 2000. Design and application of a rapid screening technique for isolation of selenite reduction-deficient mutants of *Shewanella putrefaciens*. Microbiol. Res. **155:**79-85.
44. **Blakeney MD, Moulaei T, DiChristina TJ.** 2000. Fe(III) reduction activity and cytochrome content of *Shewanella putrefaciens* grown on ten compounds as sole terminal electron acceptor. Microbiol. Res. **155:**87-94.
45. **Payne AN, DiChristina TJ.** 2006. A rapid mutant screening technique for detection of technetium [Tc(VII)] reduction-deficient mutants of *Shewanella oneidensis* MR-1. FEMS Microbiol. Lett. **259:**282-287.
46. **Altschul SF, Madden TL, Schaffer AA, Zhang JH, Zhang Z, Miller W, Lipman DJ.** 1997. Gapped BLAST and PSI-BLAST: a new generation of protein database search programs. Nucleic Acids Res. **25:**3389-3402.
47. **Burns JL, DiChristina TJ.** 2009. Anaerobic Respiration of Elemental Sulfur and Thiosulfate by *Shewanella oneidensis* MR-1 Requires *psrA*, a Homolog of the *phsA* Gene of *Salmonella enterica* Serovar Typhimurium LT2. Appl. Environ. Microbiol. **75:**5209-5217.
48. **Kovach ME, Elzer PH, Hill DS, Robertson GT, Farris MA, Roop RM, Peterson KM.** 1995. Four new derivatives of the broad-host-range cloning vector PBBR1MCS, carrying different antibiotic-resistance cassettes. Gene **166:**175-176.
49. **Zhang MN, Dale JR, DiChristina TJ, Stack AG.** 2009. Dissolution Morphology of Iron (Oxy)(Hydr)Oxides Exposed to the Dissimilatory Iron-Reducing Bacterium *Shewanella oneidensis* MR-1. Geomicrobiol J **26:**83-92.

50. **Grantham MC, Dove PM, DiChristina TJ.** 1997. Microbially catalyzed dissolution of iron and aluminum oxyhydroxide mineral surface coatings. Geochim. Cosmochim. Acta **61:**4467-4477.
51. **Stookey LL.** 1970. Ferrozine - a new spectrophotometric reagent for iron. Anal. Chem. **42:**779-781.
52. **Hammer BK, Bassler BL.** 2003. Quorum sensing controls biofilm formation in Vibrio cholerae. Mol. Microbiol. **50:**101-114.
53. **O'Toole GA, Pratt LA, Watnick PI, Newman DK, Weaver VB, Kolter R.** 1999. Genetic approaches to study of biofilms. Biofilms **310:**91-109.
54. **Leyn SA, Suvorova IA, Kholina TD, Sherstneva SS, Novichkov PS, Gelfand MS, Rodionov DA.** 2014. Comparative genomics of transcriptional regulation of methionine metabolism in proteobacteria. PLoS One **9:**e113714.
55. **Doherty NC, Shen F, Halliday NM, Barrett DA, Hardie KR, Winzer K, Atherton JC.** 2010. In Helicobacter pylori, LuxS is a key enzyme in cysteine provision through a reverse transsulfuration pathway. J. Bacteriol. **192:**1184-1192.
56. **Kostka JE, Luther GW, Nealson KH.** 1995. Chemical and biological reduction of Mn(III)-pyrophosphate complexes - potential importance of dissolved Mn(III) as an environmental oxidant. Geochim. Cosmochim. Acta **59:**885-894.
57. **Montgomery HAC, Dymock JF.** 1962. Rapid determination of nitrate in fresh and saline waters. Analyst **87:**374-378.
58. **Kelly DP, Wood AP.** 1994. Synthesis and determination of thiosulfate and polythionates. Inorganic Microbial Sulfur Metabolism **243:**475-501.
59. **Waters CM, Bassler BL.** 2005. Quorum sensing: Cell-to-cell communication in bacteria. Annu. Rev. Cell Dev. Biol. **21:**319-346.
60. **Rezzonico F, Duffy B.** 2008. Lack of genomic evidence of AI-2 receptors suggests a non-quorum sensing role for luxS in most bacteria. BMC Microbiol. **8**.
61. **Miller MB, Skorupski K, Lenz DH, Taylor RK, Bassler BL.** 2002. Parallel quorum sensing systems converge to regulate virulence in Vibrio cholerae. Cell **110:**303-314.
62. **Davies DG, Parsek MR, Pearson JP, Iglewski BH, Costerton JW, Greenberg EP.** 1998. The involvement of cell-to-cell signals in the development of a bacterial biofilm. Science **280:**295-298.
63. **Passador L, Cook JM, Gambello MJ, Rust L, Iglewski BH.** 1993. Expression of Pseudomonas-Aeruginosa Virulence Genes Requires Cell-to-Cell Communication. Science **260:**1127-1130.
64. **Vlamakis H, Chai YR, Beauregard P, Losick R, Kolter R.** 2013. Sticking together: building a biofilm the Bacillus subtilis way. Nat Rev Microbiol **11:**157-168.
65. **Lo Scrudato M, Blokesch M.** 2012. The Regulatory Network of Natural Competence and Transformation of Vibrio cholerae. Plos Genet **8**.
66. **Antonova ES, Bernardy EE, Hammer BK.** 2012. Natural competence in Vibrio cholerae is controlled by a nucleoside scavenging response that requires CytR-dependent anti-activation. Mol. Microbiol. **86:**1215-1231.
67. **Antonova ES, Hammer BK.** 2011. Quorum-sensing autoinducer molecules produced by members of a multispecies biofilm promote horizontal gene transfer to Vibrio cholerae. FEMS Microbiol. Lett. **322:**68-76.

68. **Bodor A, Elxnat B, Thiel V, Schulz S, Wagner-Doebler I.** 2008. Potential for luxS related signalling in marine bacteria and production of autoinducer-2 in the genus Shewanella. BMC Microbiol. **8**.
69. **Green J, Paget MS.** 2004. Bacterial redox sensors. Nat Rev Microbiol **2:**954-966.
70. **Ritz D, Beckwith J.** 2001. Roles of thiol-redox pathways in bacteria. Annu. Rev. Microbiol. **55:**21-48.
71. **Antelmann H, Helmann JD.** 2011. Thiol-based redox switches and gene regulation. Antioxidants & Redox Signaling **14:**1049-1063.
72. **Norambuena J, Flores R, Cardenas JP, Quatrini R, Chavez R, Levican G.** 2012. Thiol/Disulfide system plays a crucial role in redox protection in the acidophilic iron-oxidizing bacterium Leptospirillum ferriphilum. PLoS One **7:**e44576.
73. **McLean JS, Wanger G, Gorby YA, Wainstein M, McQuaid J, Ishii SI, Bretschger O, Beyenal H, Nealson KH.** 2010. Quantification of Electron Transfer Rates to a Solid Phase Electron Acceptor through the Stages of Biofilm Formation from Single Cells to Multicellular Communities. Environ. Sci. Technol. **44:**2721-2727.
74. **Newton GL, Fahey RC, Cohen G, Aharonowitz Y.** 1993. Low-Molecular-Weight Thiols in *Streptomycetes* and Their Potential Role as Antioxidants. J. Bacteriol. **175:**2734-2742.
75. **Joe-Wong C, Shoenfelt E, Hauser EJ, Crompton N, Myneni SCB.** 2012. Estimation of Reactive Thiol Concentrations in Dissolved Organic Matter and Bacterial Cell Membranes in Aquatic Systems. Environ. Sci. Technol. **46:**9854-9861.
76. **Postgate JR.** 1963. Versatile medium for the enumeration of sulfate-reducing bacteria. Appl. Microbiol. **11:**265-267.
77. **Tremblay PL, Lovley DR.** 2012. Role of the NiFe hydrogenase Hya in oxidative stress defense in Geobacter sulfurreducens. J. Bacteriol. **194:**2248-2253.
78. **Myers CR, Myers JM.** 1997. Cloning and sequence of *cymA* a gene encoding a tetraheme cytochrome *c* required for reduction of iron(III), fumarate, and nitrate by *Shewanella putrefaciens* MR-1. J. Bacteriol. **179:**1143-1152.
79. **Schuetz B, Schicklberger M, Kuermann J, Spormann AM, Gescher J.** 2009. Periplasmic electron transfer via the *c*-type cytochromes MtrA and FccA of *Shewanella oneidensis* MR-1. Appl. Environ. Microbiol. **75:**7789-7796.
80. **Breuer M, Rosso KM, Blumberger J.** 2014. Electron flow in multiheme bacterial cytochromes is a balancing act between heme electronic interaction and redox potentials. Proc. Natl. Acad. Sci. U. S. A. **111:**611-616.
81. **Lies DP, Hernandez ME, Kappler A, Mielke RE, Gralnick JA, Newman DK.** 2005. *Shewanella oneidensis* MR-1 uses overlapping pathways for iron reduction at a distance and by direct contact under conditions relevant for biofilms. Appl. Environ. Microbiol. **71:**4414-4426.

## Figures

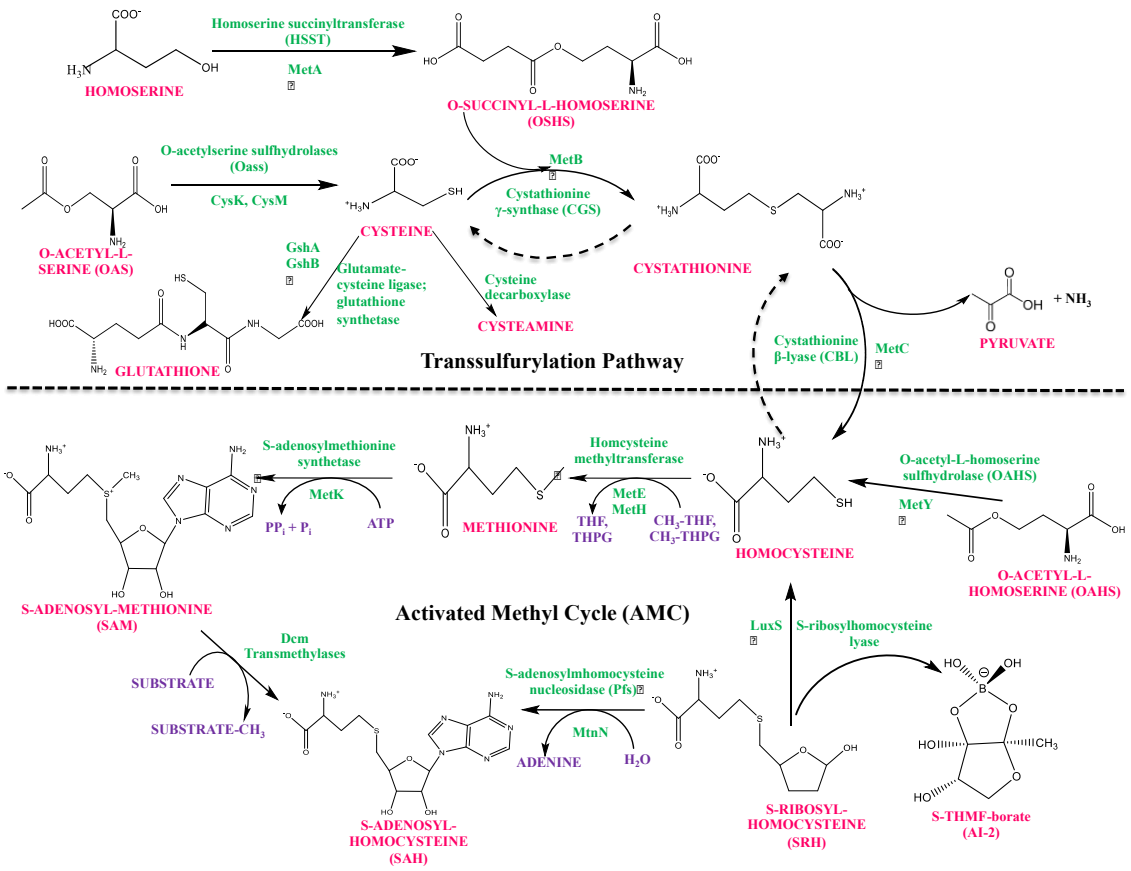


**Figure 2.1. Activated methyl cycle (AMC) and Transsulfurylation pathway enzymes predicted by BLASTp analysis of the *S. oneidensis* genome. Dotted lines indicate that two enzymes (Cystathionine β-synthase, CBS and Cystathionine γ-lyase, CGL) are missing from the *S. oneidensis* genome.**

**A.**

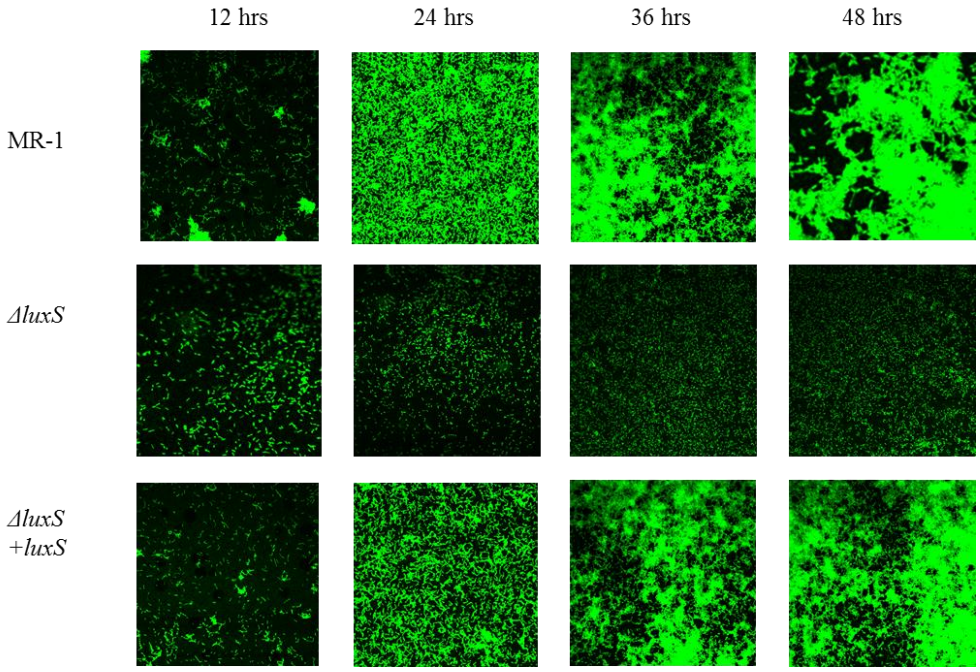
12 hrs
24 hrs
36 hrs
48 hrs
MR-1
ΔluxS
ΔluxS
+luxS

**B.**

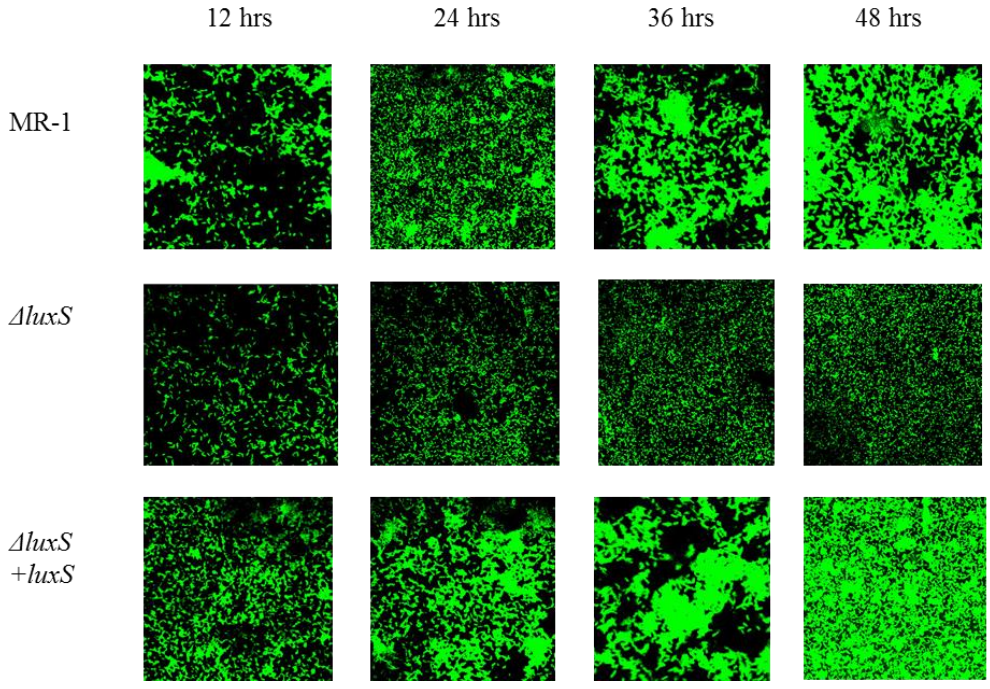
12 hrs
24 hrs
36 hrs
48 hrs
MR-1
ΔluxS
ΔluxS
+luxS

**C.**

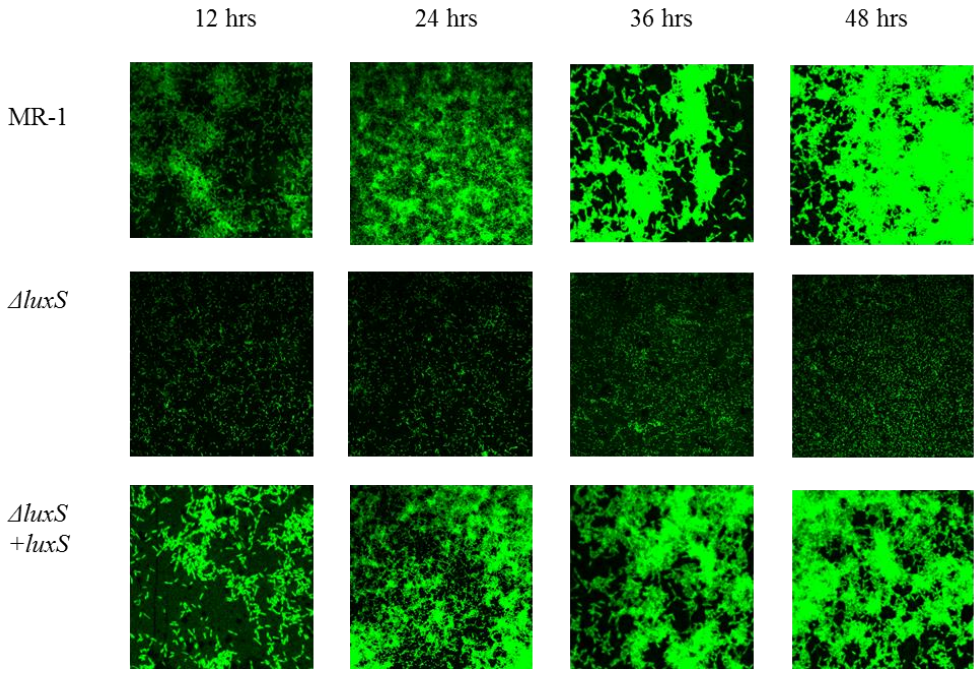


**Figure 2.2. CLSM images of anaerobic biofilms formed by *S. oneidensis* wild-type (MR-1), Δ*luxS*, and Δ*luxS*+*luxS* strains during a 48 hr anaerobic growth period on bare silica surfaces amended with lactate as electron donor and thiosulfate (A), fumarate (B), or Fe(III) oxide-coated silica surfaces (C) as electron acceptor.**

**A.**

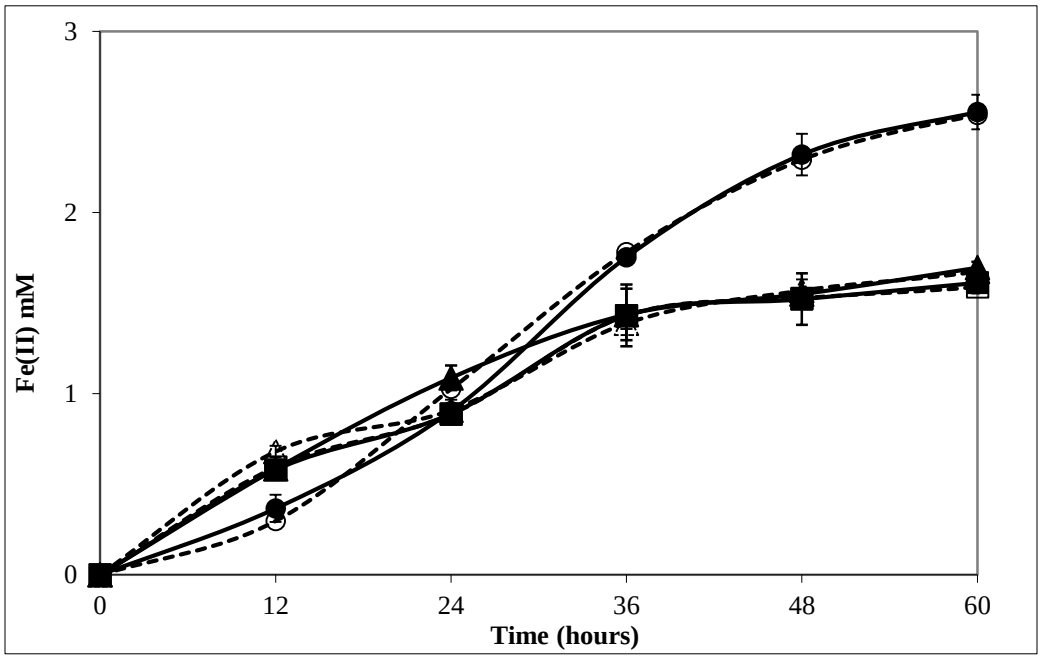


**B.**

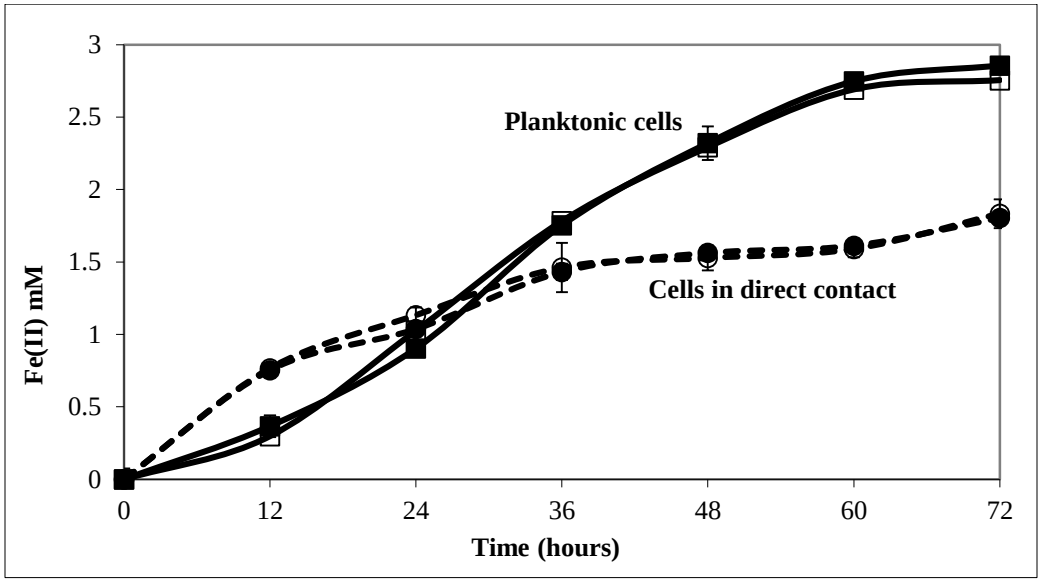


**Figure 2.3. Fe(III) reduction by *S. oneidensis* wild-type (lactate, solid circles; formate, solid squares; $H_2$ as electron donor, solid triangles) and Δ*luxS* (lactate, open circles/dashed line; formate, open squares/dashed line; $H_2$, open triangles/dashed lines) with Fe(III) oxide-coated silica as anaerobic electron acceptor with unperturbed planktonic cells (A). Fe(III) reduction by *S. oneidensis* wild-type (dashed line, closed circles) and *luxS* (dashed line, open circles) under anaerobic conditions with lactate and Fe(III) oxide-coated silica in decanting conditions (planktonic cells removed every 12 hours). *S. oneidensis* wild-type (solid, closed squares) and *luxS* (solid line, open squares) unperturbed experiments used for comparison. Values are means of two parallel yet independent anaerobic incubations, and each time point in the two parallel incubations represent triplicate**

**samples. Error bars represent range of errors. In some cases, error bars are smaller than the symbol.**

**A.**

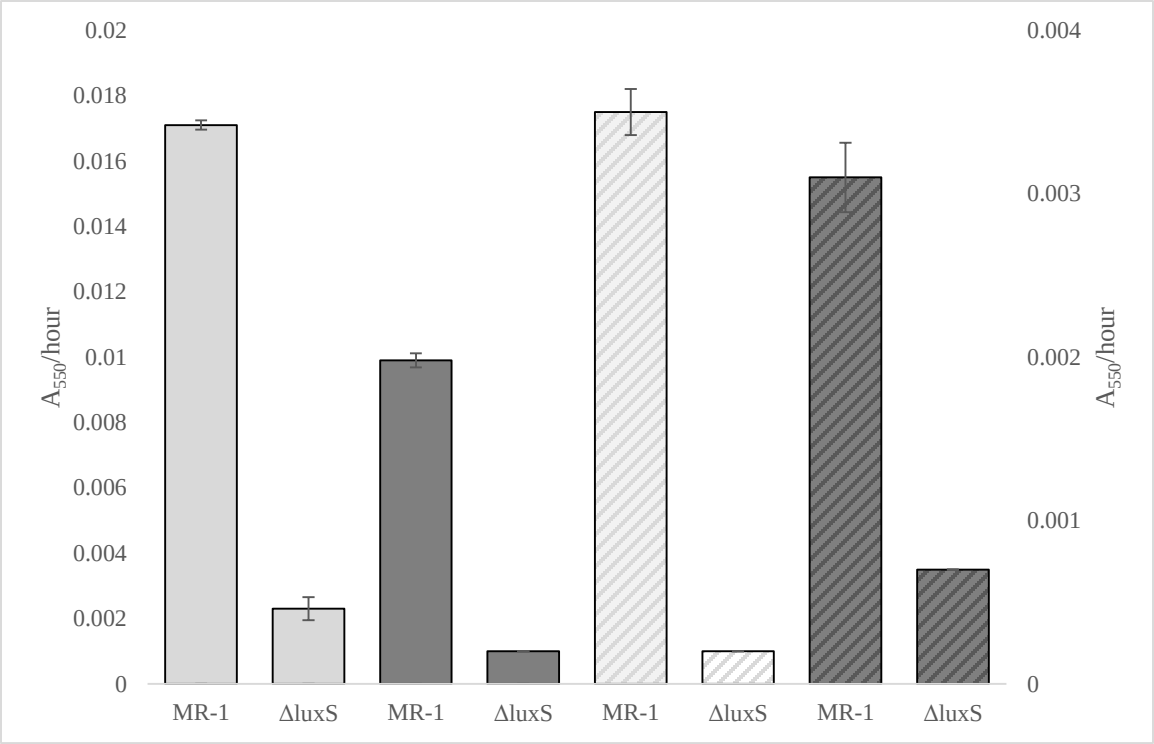


**B.**

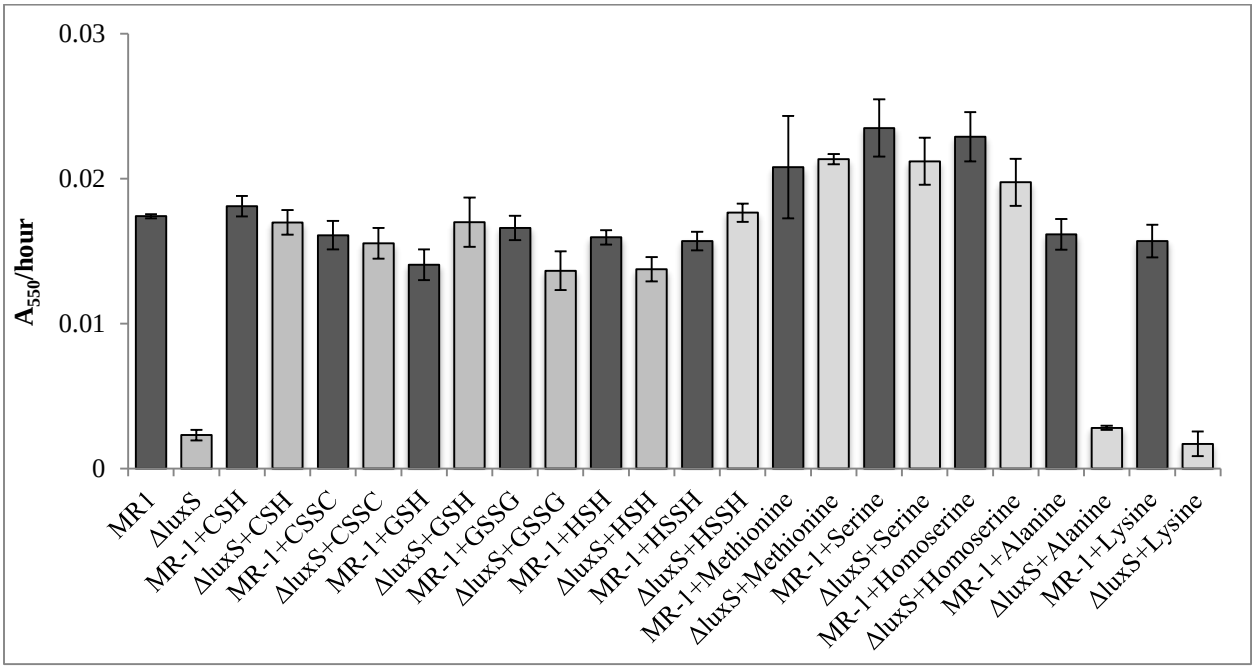

**C.**

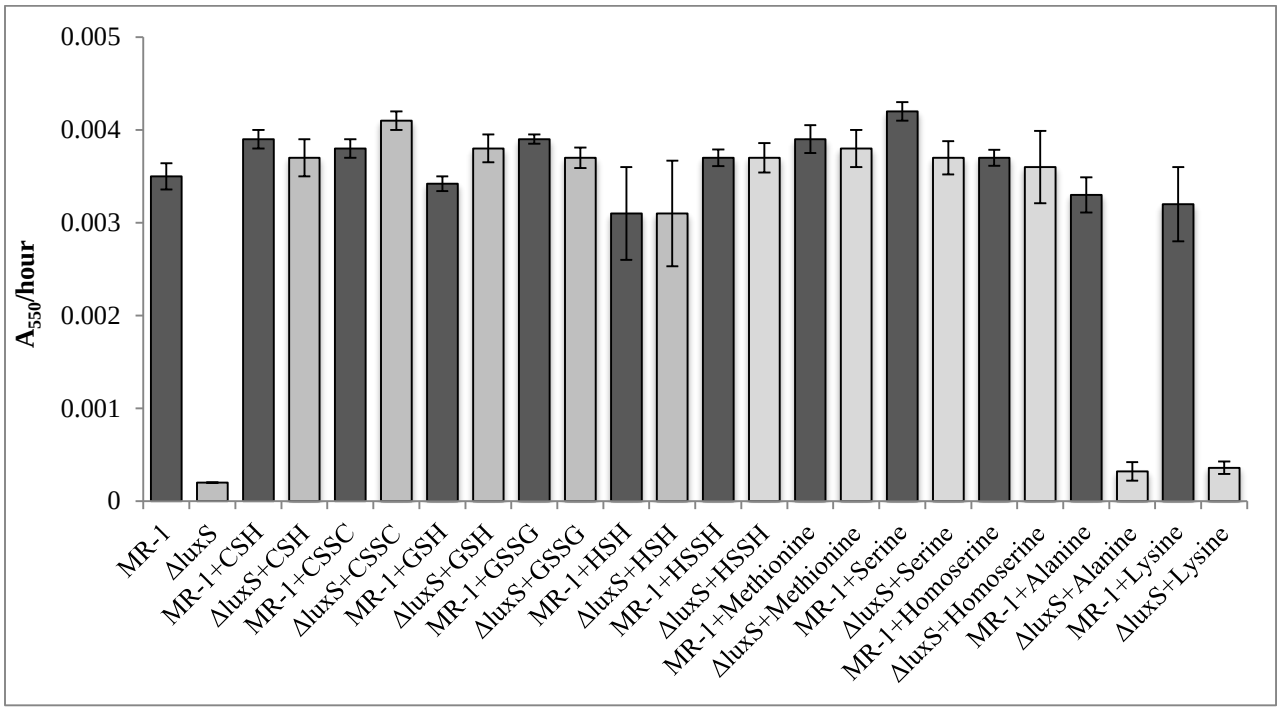


**Figure 2.4. Rates of anaerobic biofilm formation (measured via the CV assay as increases in $A_{550}$ per hour) by *S. oneidensis* wild-type and Δ*luxS* mutant strains with various electron donor and electron acceptor pairs, including lactate and thiosulfate (light gray, left axis), formate and thiosulfate (dark gray, left axis), lactate and fumarate (light gray, hashed, right axis), and formate and fumarate (black, hashed, right axis) (A). Rates of anaerobic biofilm formation with lactate as electron donor and thiosulfate (B) or fumarate (C) as electron acceptor (wild-type, dark gray bars; Δ*luxS*, light gray bars) amended with exogenous cysteine (CSH), cystine (CSSC), reduced glutathione (GSH), oxidized glutathione (GSSG), homocysteine (HSH), homocystine (HSSH), methionine, serine, homoserine, alanine, and lysine. Values are means of two parallel yet independent anaerobic incubations, and each time point in the two parallel incubations represent triplicate samples. Error bars represent range of errors. In some cases, error bars are smaller than the symbol**.

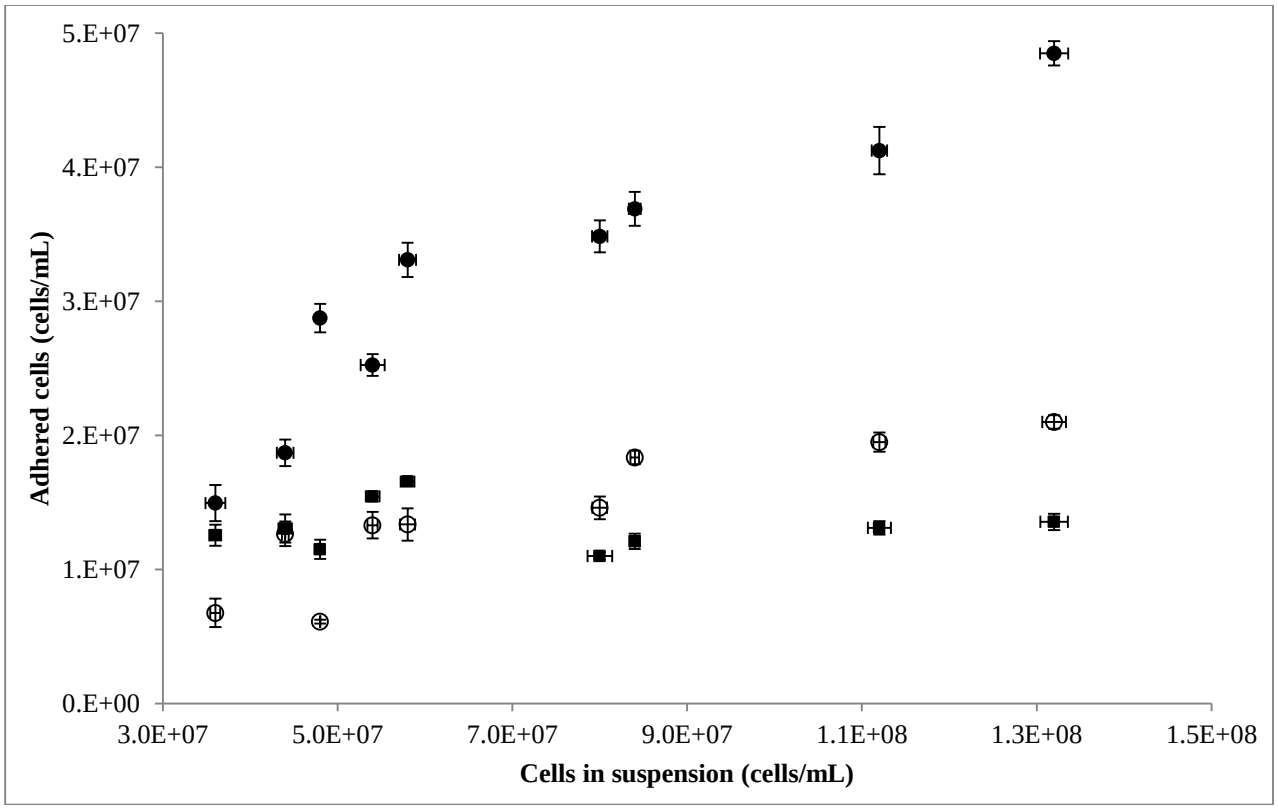


**Figure 2.5. Hematite adsorption isotherms of *S. oneidensis* wild-type (filled circles), Δ*luxS* (open circles), and ΔSO3800 (closed squares) mutant strains incubated anaerobically in the presence of hematite. Values are means of two parallel yet independent anaerobic incubations, and each time point in the two parallel incubations represent triplicate samples. Error bars represent range of errors. In some cases, error bars are smaller than the symbol.**

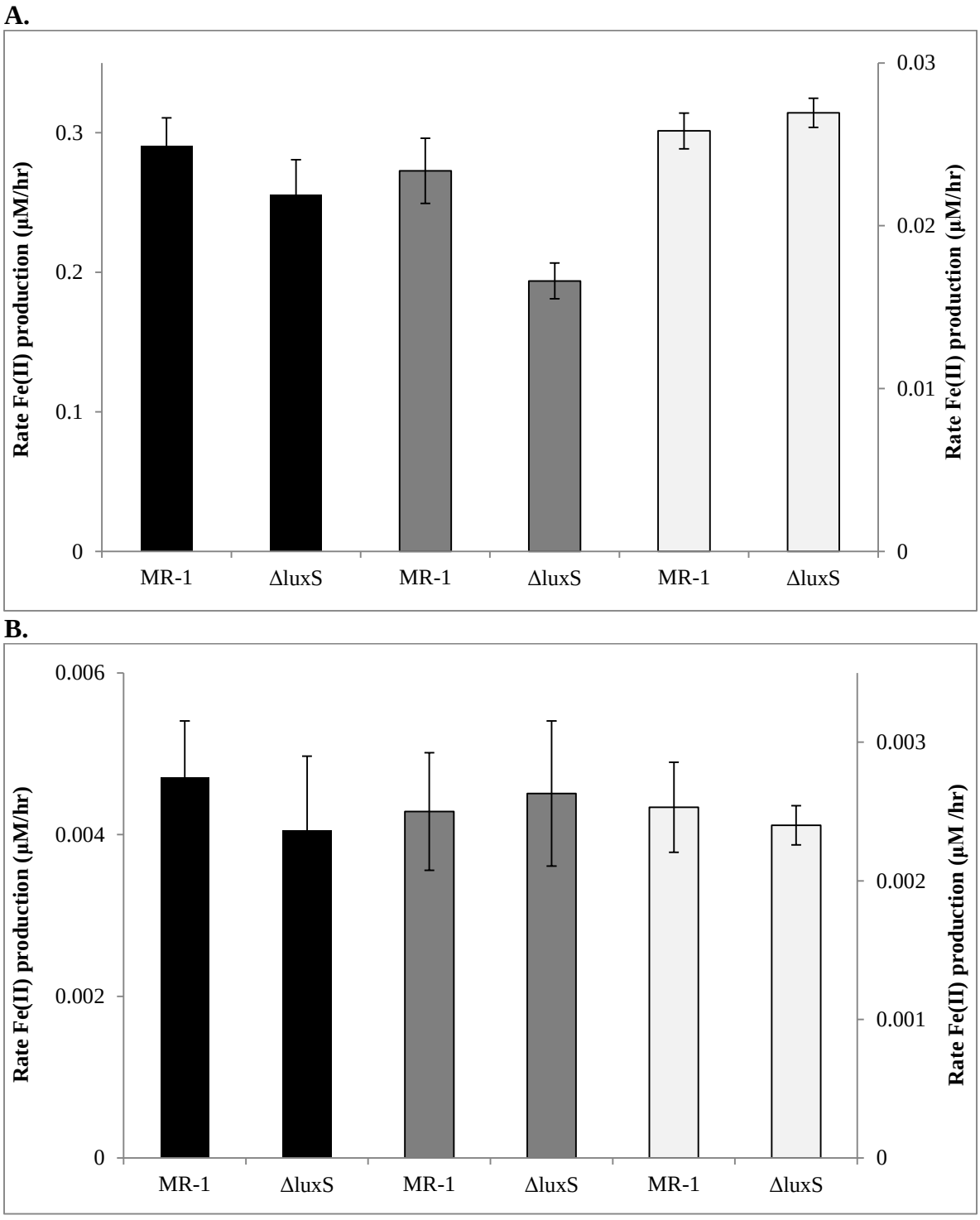


**Figure 2.6. Fe(III) reduction rates by *S. oneidensis* wild-type and Δ*luxS* mutant strains in anaerobic batch cultures with (A) HFO as electron acceptor with either $H_2$ (black bars, left axis), lactate (gray bars, right axis), or formate (white bars, right axis) as electron donor, and (B) hematite as electron acceptor with either $H_2$ (black bars, left axis), lactate (gray bars, right axis), or formate (white bars, right axis) as**

**electron donor. Values are means of two parallel yet independent anaerobic incubations, and each time point in the two parallel incubations represent triplicate samples. Error bars represent range of errors. In some cases, error bars are smaller than the symbol.**

## Tables

**Table 2.1. Activated Methyl Cycle (AMC) and Transsulfurylation pathway homologs identified in the *S. oneidensis* genome via BLASTp analysis.**

| ORF/Gene | Result for GenBank Analysis | | | | |
|---|---|---|---|---|---|
| | Best Hit | Sim | ID | E value | Putative Function |
| SO1101 (*luxS*) | *Vibrio parahaemolyticus* | 100 | 82 | $1^{-100}$ | S-ribosylhomocysteinase |
| SO0818 (*metE*) | *Proteus mirabilis* | 99 | 59 | 0.0 | 5-methyltetrahydropterolytriglutamate/ homocysteine S-methyltransferase |
| SO1030 (*metH*) | *Ferrimonas balearica* | 98 | 74 | 0.0 | B12-dependent methionine synthase |
| SO0929 (*metK*) | *Ferrimonas balearica* | 100 | 88 | 0.0 | Methionine adenosyltransferase |
| SO3006 (Dcm Transmethylase) | *Yersinia pseudotuberculosis* | 99 | 57 | 0.0 | C-5 cytosine-specific DNA methylase family protein |
| SO1322 (*mtnN*) | *Ferrimonas kyonanensis* | 97 | 70 | $4^{-113}$ | 5-methylthioadenosine nucleosidase |
| SO1676 (*metA*) | *Ferrimonas balearica* | 99 | 70 | $1^{-164}$ | Homoserine O-succinyltransferase |
| SO4056 (*metB*) | *Ferrimonas balearica* | 96 | 71 | 0.0 | Cystathionine beta-lyase |
| SO2191 (*metC*) | *Psychromonas hadalis* | 97 | 81 | 0.0 | O-acetylhomoserine aminocarboxypropyltransferase |
| SO1095 (*metY*) | *Cobetia martina* | 99 | 87 | 0.0 | Cysteine synthase |
| SO2903 (*cysK*) | *Oceanimonas smirnovii* | 99 | 82 | 0.0 | Cysteine synthase B |
| SO3598 (*cysM*) | *Vibrio cholerae* | 100 | 80 | $9^{-171}$ | Glutamate-cysteine ligase |
| SO3559 (*gshA*) | *Aeromonas diversa* | 94 | 54 | 0.0 | Glutathione synthetase |
| SO0831 (*gshB*) | *Aliagarivorams taiwanensis* | 99 | 75 | $4^{-179}$ | Glutathione synthetase |

Designations:

1. Orf/gene: open reading frame identified in *S. oneidensis* genome
2. Best Hit: Homolog with highest similarity value identified in genomes outside the genus *Shewanella*.
3. Sim: Similarity
4. ID: Identity
5. E value: expect value
6. Putative function: Annotated function

**Table 2.2. Rates of aerobic and anaerobic biofilm formation ($A_{550}$/hour) in *S. oneidensis* wild-type and Δ*luxS* mutant strains with formate or lactate as electron donor and fumarate, thiosulfate, or $O_2$ as electron acceptor.**

| | Fumarate | | Thiosulfate | | $O_2$ | |
|---|---|---|---|---|---|---|
| **Strains** | **Formate** | **Lactate** | **Formate** | **Lactate** | **Formate** | **Lactate** |
| **MR-1** | 0.0031 (±0.0002) | 0.0035 (±0.0001) | 0.0099 (±0.0002) | 0.0171 (±0.0001) | 0.0081 (±0.0003) | 0.0562 (±0.0021) |
| **Δ*luxS*** | 0.0007 (±0.0000) | 0.0002 (±0.0000) | 0.001 (±0.0000) | 0.0023 (±0.0004) | 0.0037 (±0.0001) | 0.0355 (±0.0033) |

Notes:

1. Values indicate $A_{550}$ measured via the CV assay
2. Values are means of two parallel yet independent anaerobic incubations. Error bars represent range of errors.

**Table 2.3. Rates of anaerobic biofilm formation ($A_{550}$/hour) by *S. oneidensis* wild-type and Δ*luxS* mutant strains with lactate as electron donor and fumarate or thiosulfate as electron acceptor in anaerobic incubations amended with cysteine (CSH), cystine (CSSC), reduced glutathione (GSH), oxidized glutathione (GSSG), homocysteine (HSH), homocystine (HSSH), methionine, serine, homoserine, alanine, and lysine.**

| | Lactate | | | Lactate | |
|---|---|---|---|---|---|
| **Strains** | **Fumarate** | **Thiosulfate** | **Strains** | **Fumarate** | **Thiosulfate** |
| **MR-1+CSH** | 0.0039 (±0.0001) | 0.0181 (±0.0007) | **Δ*luxS*+CSH** | 0.0037 (±0.0002) | 0.0170 (±0.0008) |
| **MR-1+CSSC** | 0.0038 (±0.0001) | 0.016 (±0.0009)1 | **Δ*luxS*+CSSC** | 0.0041 (±0.0001) | 0.0156 (±0.0011) |
| **MR-1+GSH** | 0.00142 (±0.0001) | 0.01405 (±0.0011) | **Δ*luxS*+GSH** | 0.0038 (±0.0002) | 0.0170 (±0.0017) |
| **MR-1+GSSG** | 0.0039 (±0.0001) | 0.0166 (±0.0008) | **Δ*luxS*+GSSG** | 0.0037 (±0.0001) | 0.0137 (±0.0013) |
| **MR-1+HSH** | 0.0031 (±0.0005) | 0.0159 (±0.0005) | **Δ*luxS*+HSH** | 0.0031 (±0.0006) | 0.0138 (±0.0008) |
| **MR-1+HSSH** | 0.0037 (±0.0001) | 0.0157 (±0.0006) | **Δ*luxS*+HSSH** | 0.0037 (±0.0002) | 0.0177 (±0.0006) |
| **MR-1+Methionine** | 0.0039 (±0.0002) | 0.0208 (±0.0035) | **Δ*luxS*+Methionine** | 0.0038 (±0.0002) | 0.0214 (±0.0004) |
| **MR-1+Serine** | 0.0042 (±0.0001) | 0.0235 (±0.0019) | **Δ*luxS*+Serine** | 0.0037 (±0.0002) | 0.0212 (±0.0016) |
| **MR-1+Homoserine** | 0.0037 (±0.0001) | 0.0229 (±0.0017 | **Δ*luxS*+Homoserine** | 0.0036 (±0.0004) | 0.0198 (±0.0016) |
| **MR-1+Alanine** | 0.0033 (±0.0002) | 0.0162 (±0.0011) | **Δ*luxS*+Alanine** | 0.0003 (±0.0001) | 0.0028 (±0.0001) |
| **MR-1+Lysine** | 0.0032 (±0.0004) | 0.0157 (±0.0011) | **Δ*luxS*+Lysine** | 0.0004 (±0.0001) | 0.0017 (±0.0008) |

Notes:

1. Values indicate $A_{550}$ measured via the CV assay
2. Values are means of two parallel yet independent anaerobic incubations. Error bars represent range of errors.

## Table 2.4. Bacterial strains and plasmids used in this study.

| Bacterial strain or plasmid | Description | Source or Reference |
|---|---|---|
| *S. oneidensis* | | |
| MR-1 | Wild-type strain | ATCC |
| Δ*luxS* | In-frame deletion mutant | This study |
| ΔSO3800 | In-frame deletion mutant | Burns and DiChristina, 2009 |
| Δ*lux+luxS* | *luxS*-complemented mutant | This study |
| *E. coli* | | |
| EC100D *pir-116* | F⁻ *mcrA* Δ(*mrr-hsdRMS-mcrBC*) φ80d*laxZ*ΔM15 Δ*lacX74 recA1 end A1 araD139* Δ(*ara leu*) *7697 galU galK* λ⁻ *rpsL nupG pir-116*(DHFR) | Epicentre |
| β2155 λ *pir* | *thrB1004 pro thi strA hsdS laxZ*ΔM115 (F9 *lacZ*ΔM115 *lacI*$^{q}$ *traD36 proA1 proB1)* Δ*dapA::erm pir::*RP4 Km$^{r}$ | Dehio and Meyer, 1997 |
| Plasmids | | |
| pKO2.0 | 4.5-kb γR6K *mob*RP4 *sacB* Gm$^{r}$ *lacZ* | Burns and DiChristina, 2009 |
| pKO2.0-F3 | pKO2.0 containing in-frame deletion of SO1101 | This study |
| pKO2.0-*luxS* | pKO2.0 containing wild-type of SO1101 | This study |

## Table 2.5. Primers used in this study.

| Primer | Nucleotide Sequence |
|---|---|
| D1 | 5'-GACTGGATCCGATCCGAATGCCAGGGCTTG-3' |
| D2 | 5'-ACTATTGTCGCTTTCTTGACGCCTTCGCGATACAACGCCACTGTCGCTATC-3' |
| D3 | 5'GATAGCGACAGTGGCGTTGTATCGCGAAAGCGTCAAGAAAGCGACAATAGT3' |
| D4 | 5'-GACTGTCGACCCCAAGCAATGAACGGTAACTATCATCATC-3' |
| DTF | 5'-GACAGCACAGGAAATGAACGGC-3' |
| DTR | 5'-CTCATCACCTTGCTATCACCTAAGTTG 3' |

## Supplemental Figures

**A.**

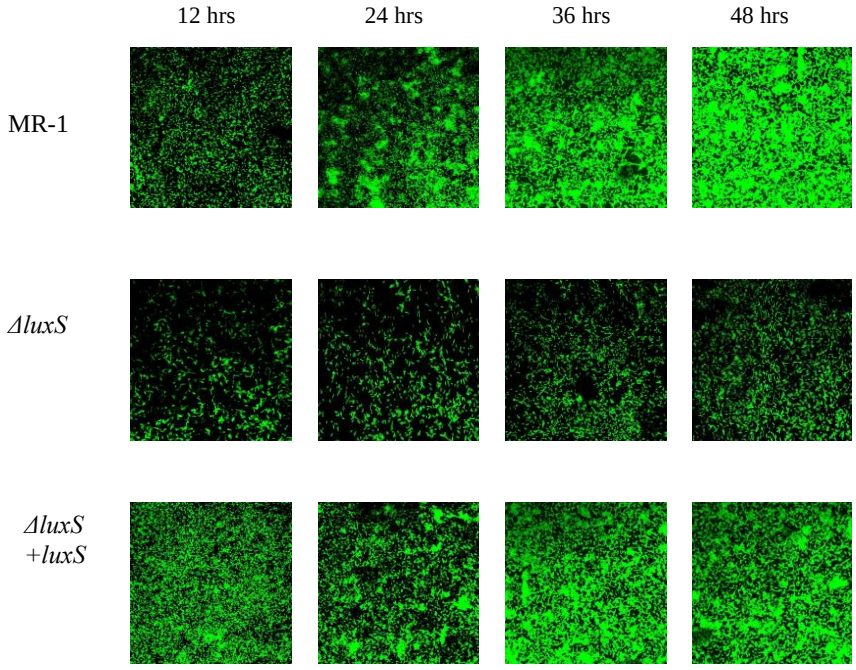


**B.**

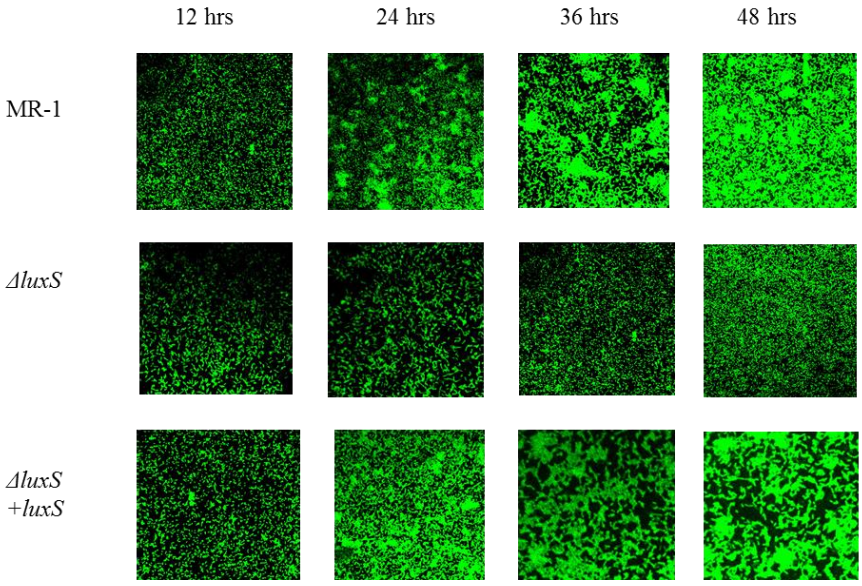

**C.**

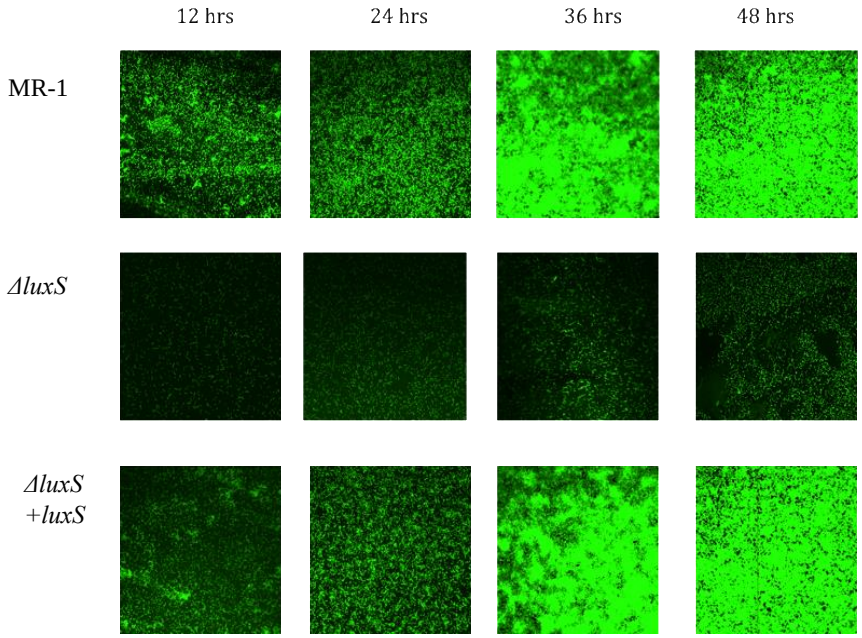


**Figure 2.S1. CLSM images of anaerobic biofilms formed by *S. oneidensis* wild-type (MR-1), Δ*luxS*, and Δ*luxS*+*luxS* strains during a 48 hr anaerobic growth period on bare silica surfaces amended with formate as electron donor and thiosulfate (A), fumarate (B), or Fe(III) oxide-coated silica surfaces (C) as electron acceptor.**

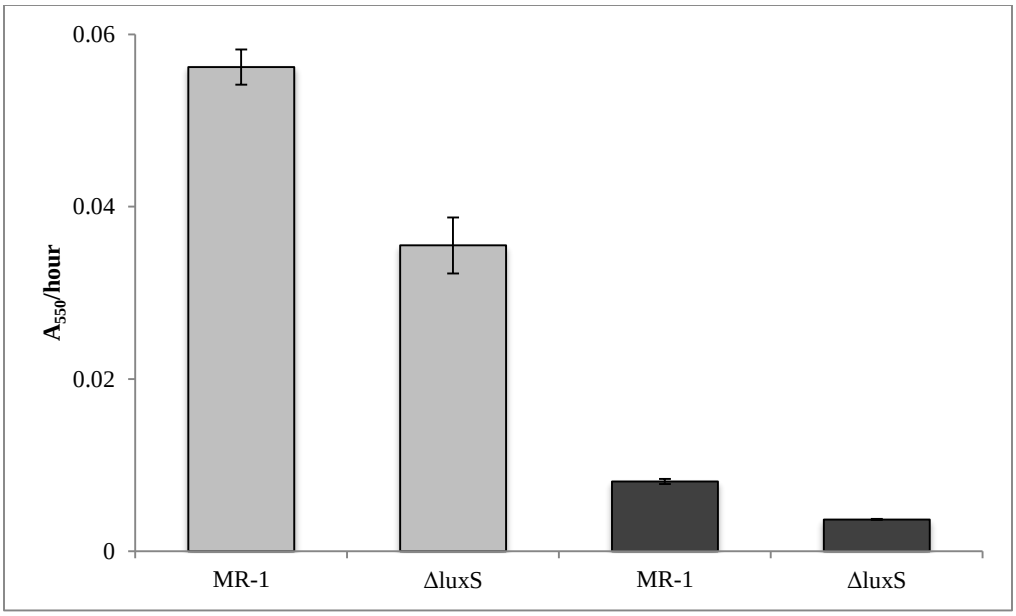


**Figure 2.S2. Rates of aerobic biofilm formation by *S. oneidensis* wild-type and Δ*luxS* mutant strains with lactate (light gray) or formate (dark gray) as electron donor and $O_2$ as electron acceptor.**

**A.**

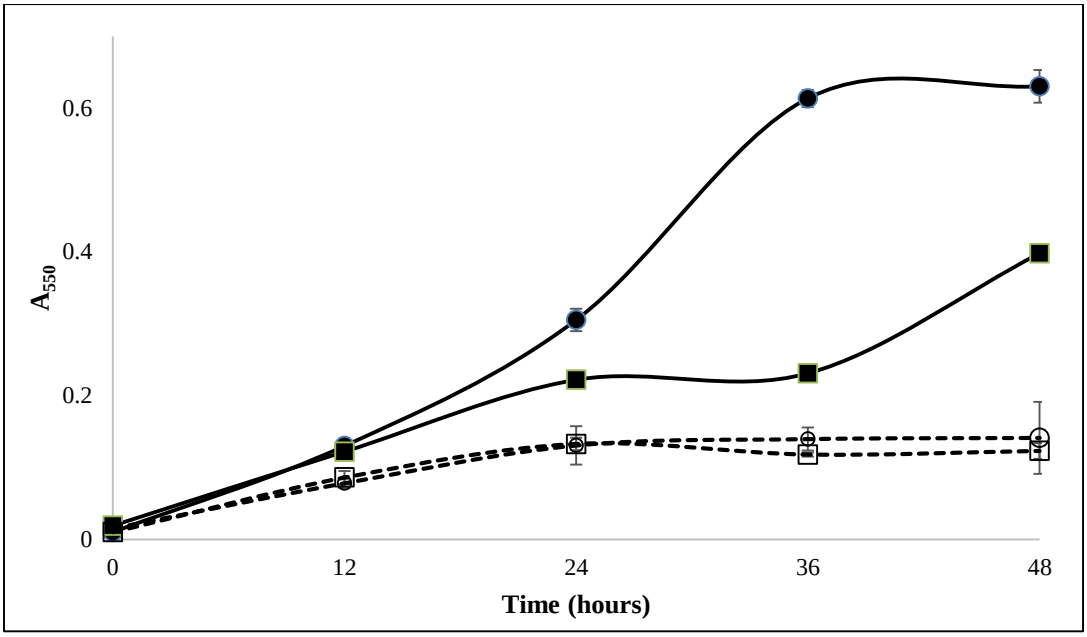


**B.**

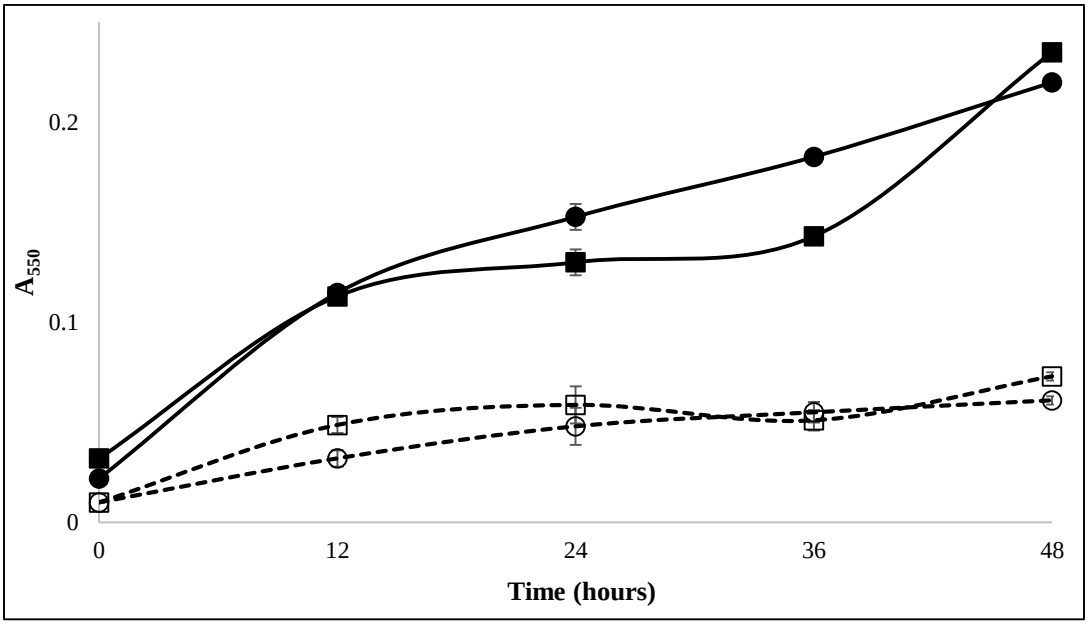


**Figure 2.S3. Anaerobic biofilm formation on polystyrene surfaces measured via conventional CV-based biofilm assays. *S. oneidensis* wild type and Δ*luxS* mutant strains were amended with lactate (wild-type, closed circles; Δ*luxS*, open circles, dashed lines) or formate (wild-type, closed squares; Δ*luxS*, open squares, dashed lines) as electron donor and thiosulfate (A) or fumarate (B) as electron acceptor.**

**A.**

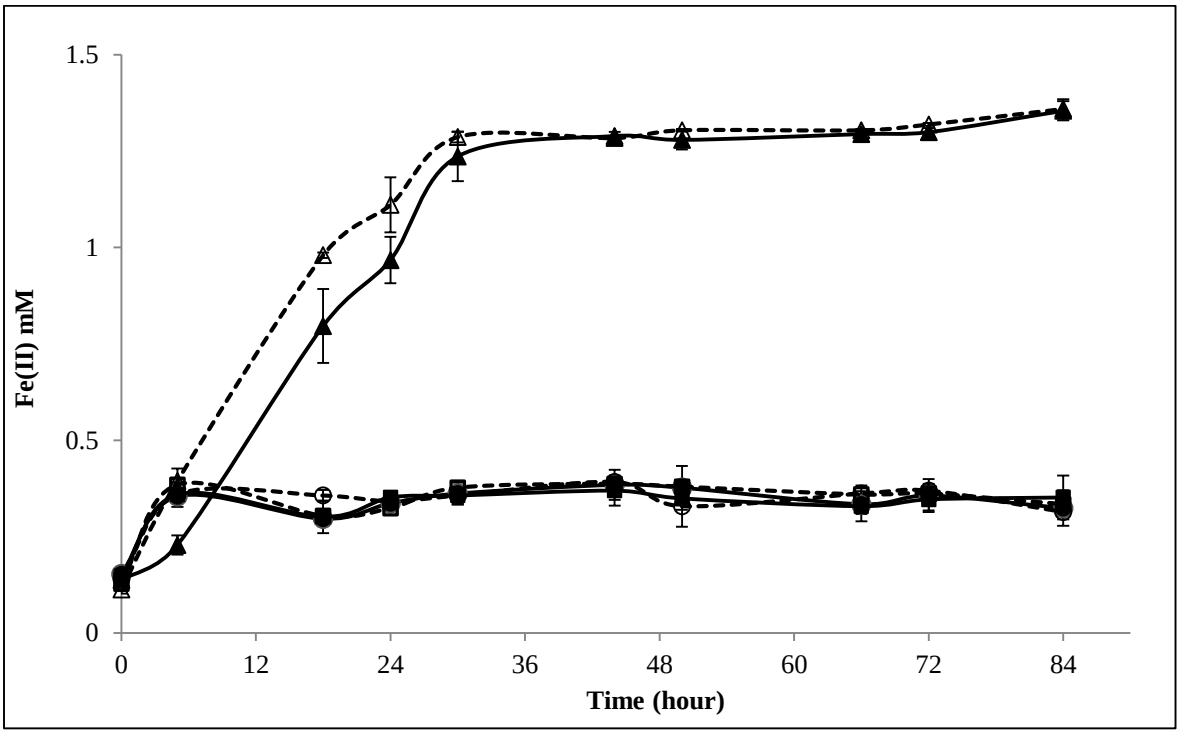
1.5
1
0.5
0
Fe(II) mM
0
12
24
36
48
60
72
84
Time (hour)

**B.**

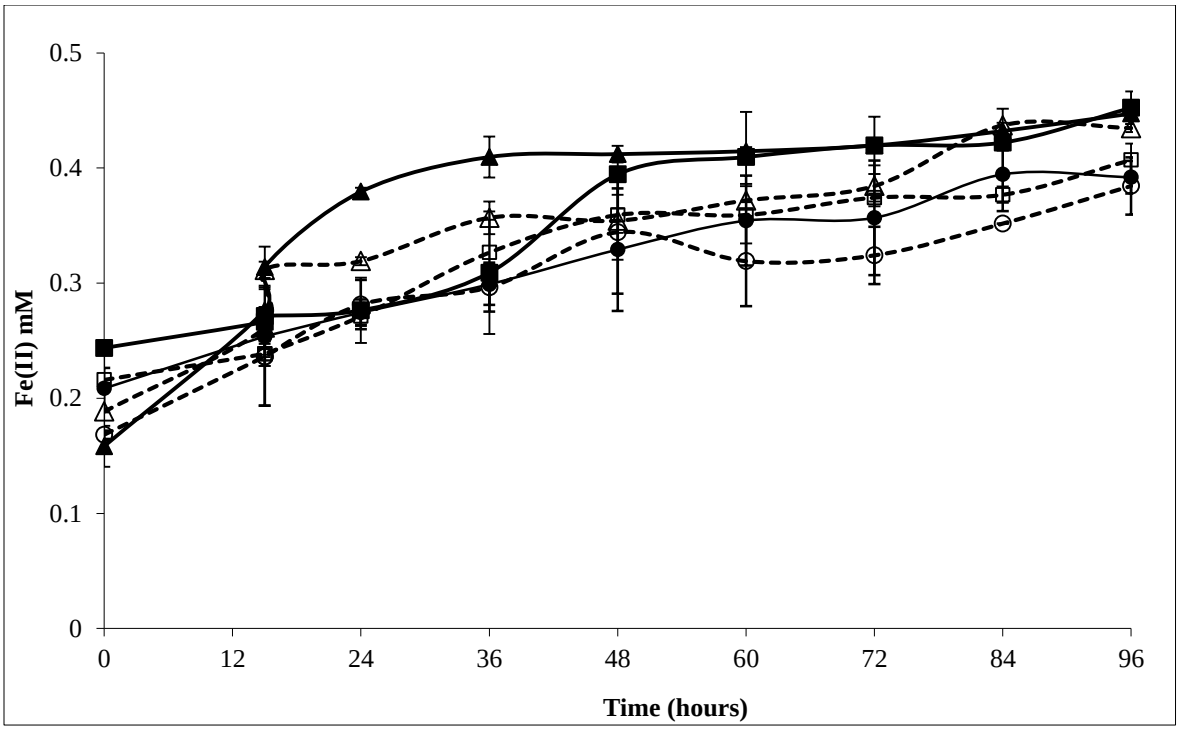
0.5
0.4
0.3
0.2
0.1
0
Fe(II) mM
0
12
24
36
48
60
72
84
96
Time (hours)

**C.**

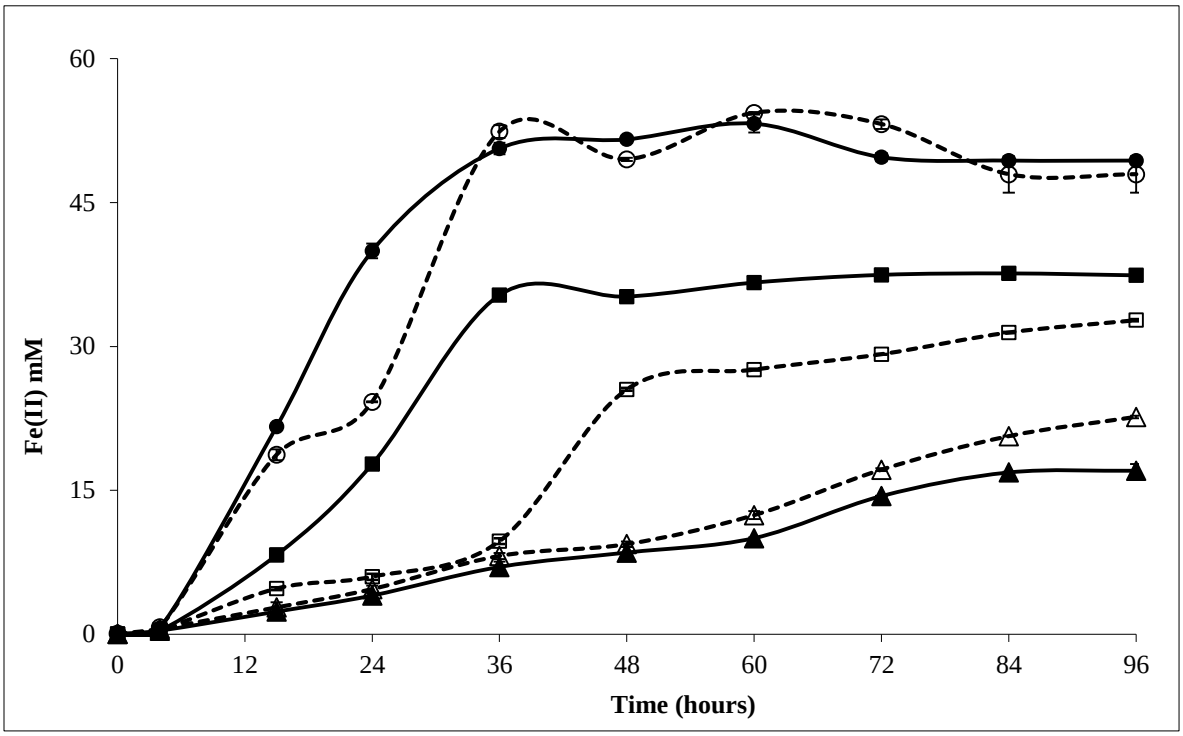


**D.**

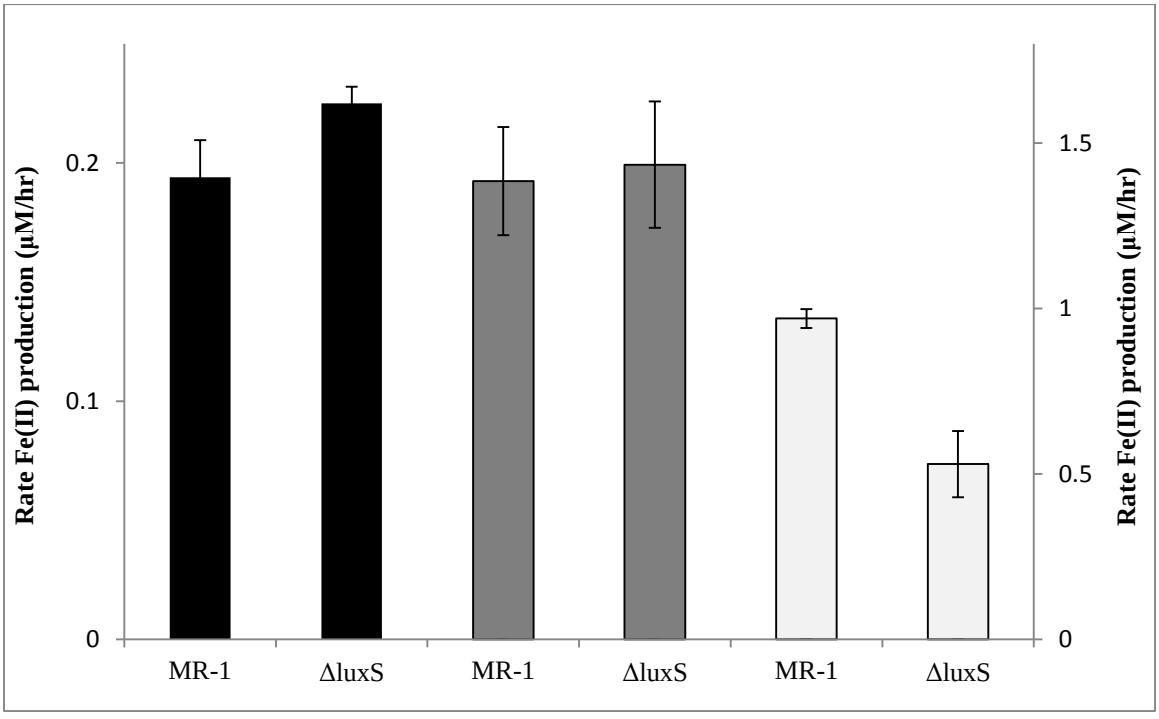


**Figure 2.S4. Fe(III) reduction by *S. oneidensis* wild type and Δ*luxS* mutant strains amended with lactate (wild-type, closed circles; Δ*luxS*, open circles, dashed line), formate (wild-type, closed squares; Δ*luxS*, open squares, dashed line), or $H_2$ (wild-**

**type, closed triangles; Δ*luxS*, open triangles, dashed line) as electron donor and HFO (A), hematite (B) or Fe(III) citrate (C) as electron acceptor. (D) Fe(III) reduction rates by *S. oneidensis* wild-type and Δ*luxS* mutant strains in anaerobic batch cultures with with Fe(III) citrate as electron acceptor with either $H_2$ (black bars, primary axis), lactate (gray bars, secondary axis), or formate (white bars, secondary axis) as electron donor. Values are means of two parallel yet independent anaerobic incubations, and each time point in the two parallel incubations represent triplicate samples. Error bars represent range of errors. In some cases, error bars are smaller than the symbol.**

**A.**

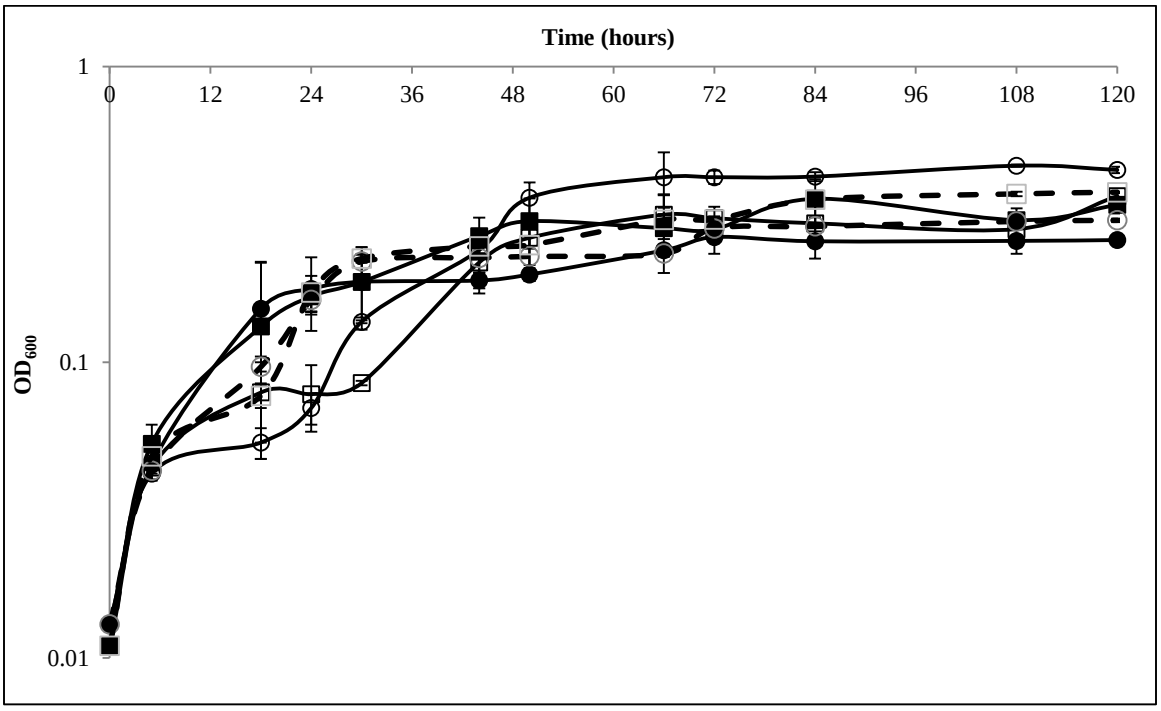
Time (hours)
1
0
12
24
36
48
60
72
84
96
108
120
OD600
0.1
0.01

**B.**

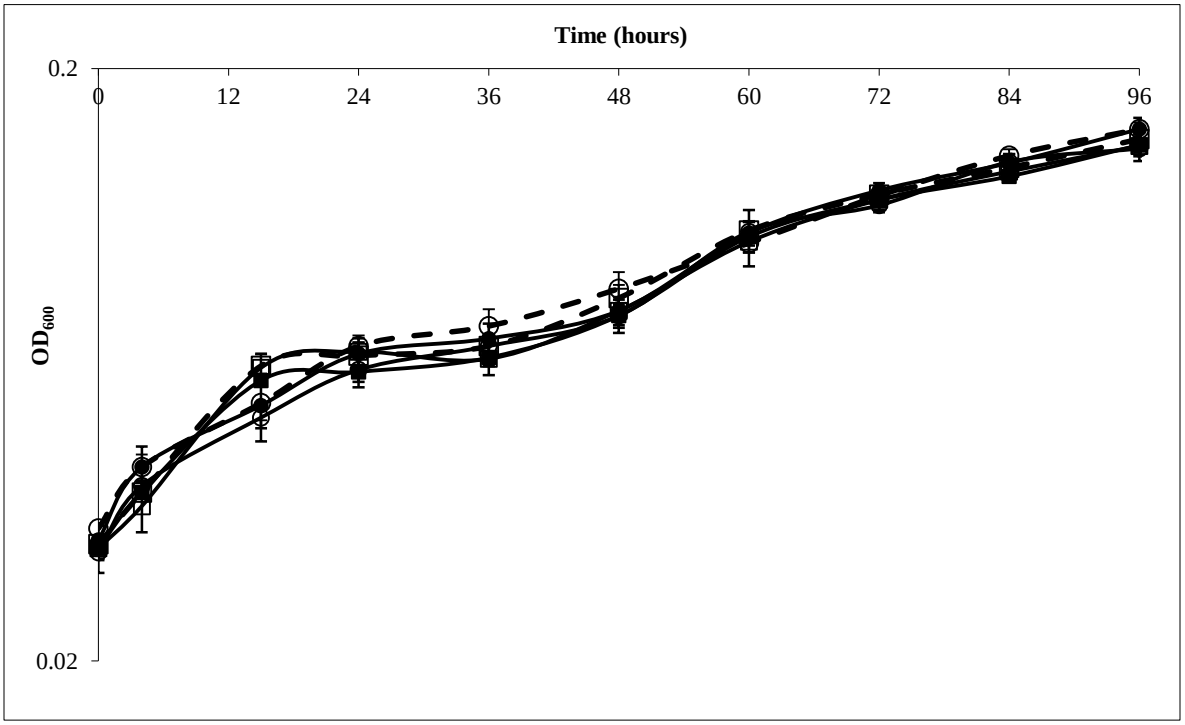
Time (hours)
0.2
0
12
24
36
48
60
72
84
96
OD600
0.02

**C.**

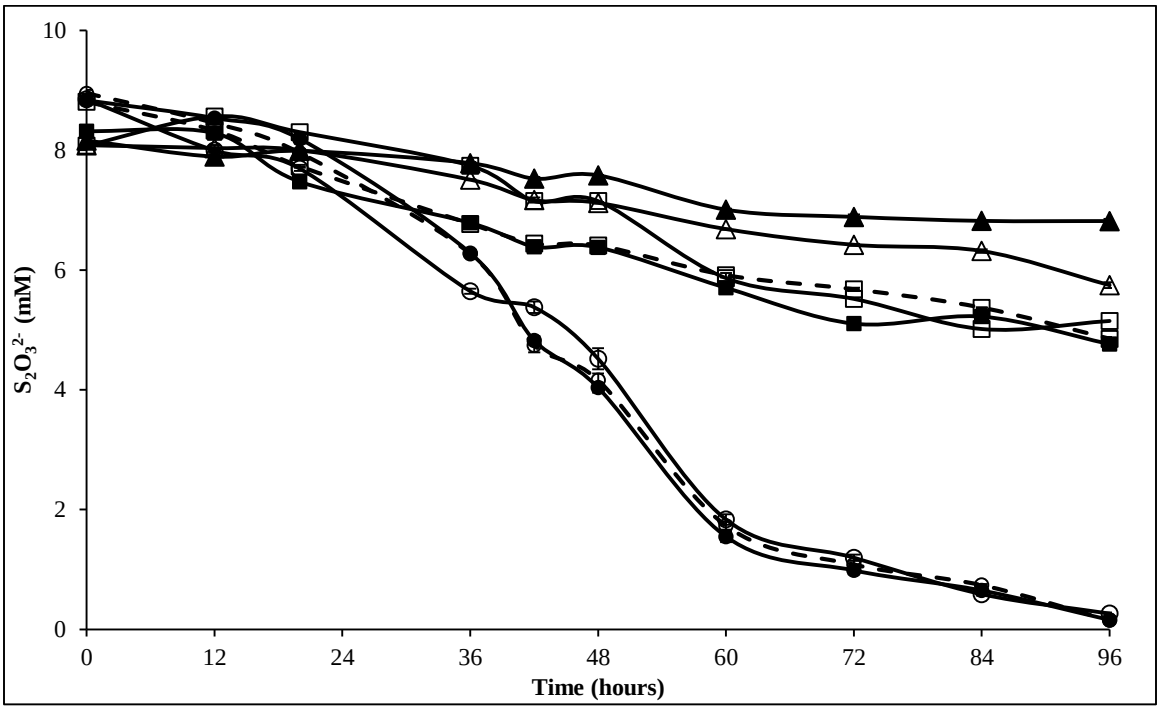
10
8
6
4
2
0
0
12
24
36
48
60
72
84
96
$S_2O_3^{2-}$ (mM)
Time (hours)

**D.**

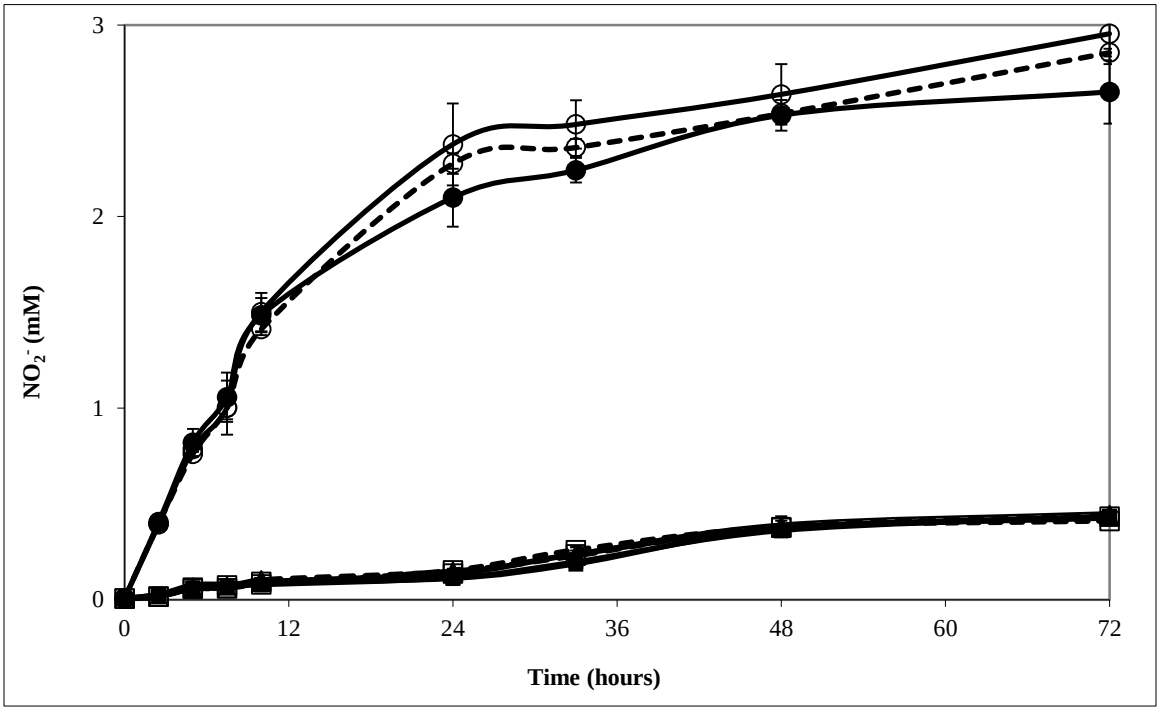
3
2
1
0
0
12
24
36
48
60
72
$NO_2^-$ (mM)
Time (hours)

**E.**

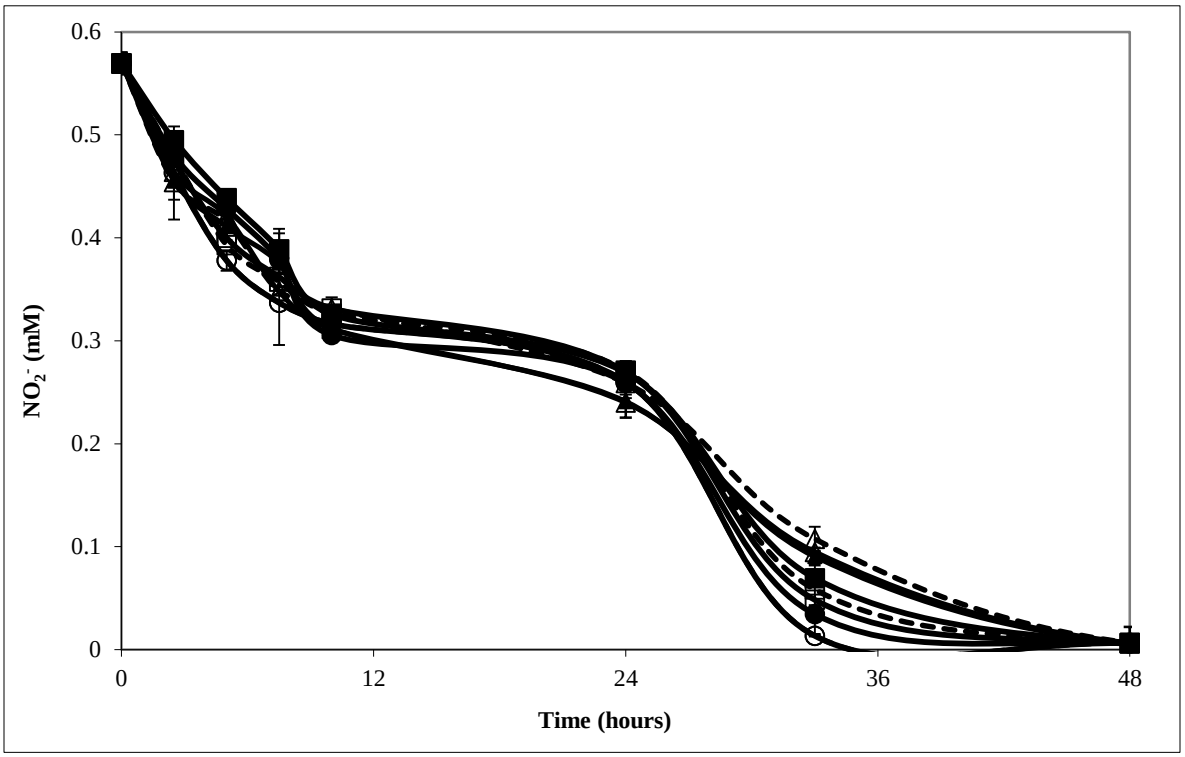


**F.**

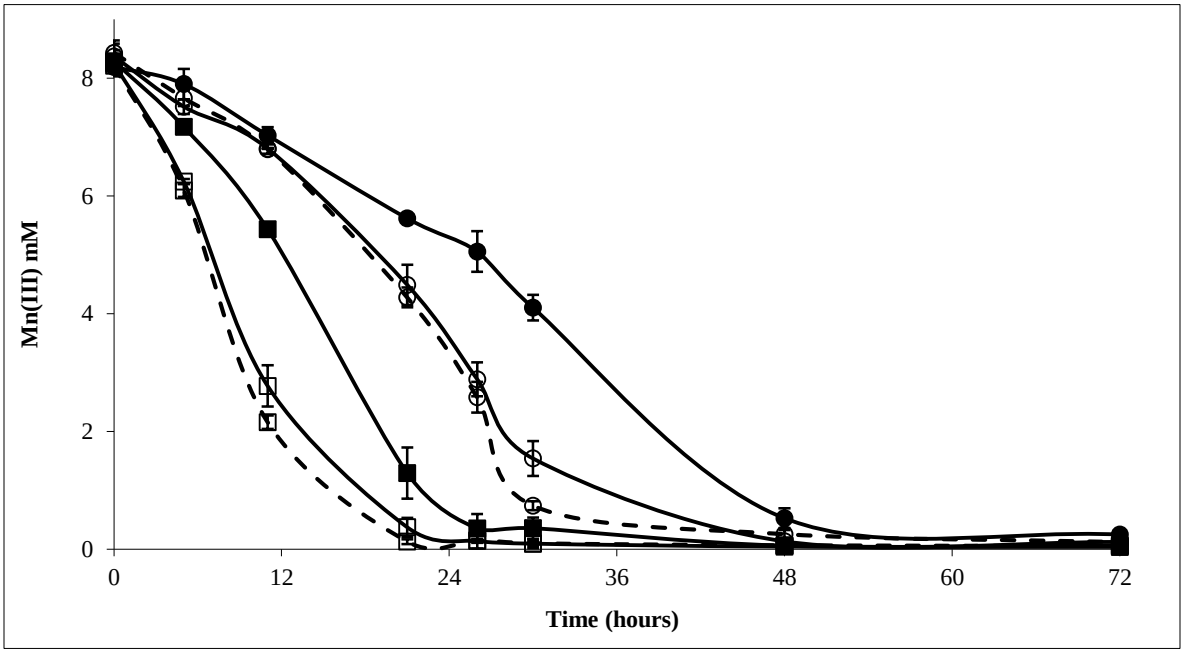


**Figure 2.S5. Anaerobic incubations of *S. oneidensis* wild type, Δ*luxS*, and Δ*luxS*+*luxS* strains amended with lactate (wild-type, closed circles; Δ*luxS*, open circles; Δ*luxS*+*luxS*, dashed line, open circles), formate (wild-type, closed squares; Δ*luxS*, open squares; Δ*luxS*+*luxS*, dashed line, open squares), or $H_2$ (wild-type, closed triangles; Δ*luxS*, open triangles; Δ*luxS*+*luxS*, dashed line, open triangles) as electron donor and TMAO (A), fumarate (B), thiosulfate (C), nitrate (D), nitrite (E), and**

**Mn(III)-pyrophosphate (F) as electron acceptor. Values are means of two parallel yet independent anaerobic incubations, and each time point in the two parallel incubations represent triplicate samples. Error bars represent range of errors. In some cases, error bars are smaller than the symbol.**

# CHAPTER 3

## Quorum Sensing Signal Autoinducer-2 as Sole Carbon and Electron Source For Anaerobic Respiration by *Shewanella oneidensis*

[Submitted for publication, currently under review. The Autoinducer-2 detection via HPLC experiments described in Chapter 3 were carried out in collaboration with Ramanan Sekar, a PhD student in Dr. DiChristina's research group.]


### Summary

Gram-negative bacteria communicate via production of the quorum sensing (QS) signals acylhomoserine lactone (autodinducer-1; AI-1) and furanosyl diester (AI-2) that initiate adaptive responses to changes in cell population density and regulate a variety of bacterial processes, including biofilm formation. AI-1- and AI-2-dependent biofilm formation, however, has been studied exclusively under aerobic (but not anaerobic) growth conditions. The gram negative, γ-proteobacterium *Shewanella oneidensis* produces AI-2 (but not AI-1) throughout aerobic biofilm formation. In the present study, wild-type *S. oneidensis* formed anaerobic biofilms on solid Fe(III) oxide surfaces, while deletion mutant Δ*luxS* (lacking AI-2-producing S-ribosylhomocysteine lyase) displayed a biofilm formation-deficient phenotype. *S. oneidensis* genome analyses, however, failed to uncover canonical AI-1 and AI-2 QS systems, thus suggesting that LuxS-catalyzed AI-2 production is not involved in QS. Wild-type *S. oneidensis* (but not Δ*luxS)* produced AI-2 during initial phases of both aerobic and anaerobic (Fe(III) oxide reduction-linked) growth, and consumed AI-2 during latter phases only after lactate consumption had

ceased. *S. oneidensis* consumed AI-2 (produced by *S. oneidensis* or *Vibrio harveyi*) as sole carbon and electron source during aerobic and anaerobic growth on a variety of electron acceptors. *S. oneidensis* may thus sustain growth by accumulating AI-2 extracellularly during growth on a primary carbon source and subsequently metabolizing the accumulated AI-2 after the primary carbon source has been exhausted. Furthermore, the ability of *S. oneidensis* to metabolize *V. harveyi* AI-2 as sole carbon and electron source indicates that *S. oneidensis* AI-2 metabolism may disrupt cell-cell communication systems of other bacteria in multi-species biofilms.

## Introduction

Microorganisms in marine and freshwater environments are often found as surface-attached biofilm communities (1, 2). The biofilm matrix is composed of exopolymeric substances that promote adhesion to solid surfaces and provide the biofilm microbial communities with hydrated microenvironments that enhance metabolic activity and protect against environmental stresses such as variations in temperature, pH, salinity, and nutrient levels (3-6). Biofilm formation on solid surfaces is especially critical to the gram-negative, γ-proteobacterium *Shewanella oneidensis* during anaerobic electron transfer to solid metal oxides and the anodes of microbial fuel cells (MFCs) (7, 8). The formation of biofilms on the surface of metal oxides or anodes ensures the *S. oneidensis* cells are within the 15A distance required for electron transfer between the cell and the surface of the Fe(III) oxide or anaode surface.

Biofilm community members communicate via production of extracellular quorum sensing (QS) signals such as autoinducers (AIs) that initiate adaptive responses to changes in cell population density and regulate a variety of bacterial processes, including biofilm development (3, 9). In gram-negative bacteria such as members of the genus *Vibrio*, AIs are classified into two main types: acyl homoserine lactones (AHL or AI-1) and furanosyl diesters (AI-2). AI-1 is synthesized by AHL synthases (e.g., *V. harveyi* LuxM) that fuse homoserine lactone rings to acyl side chains of varying length and chemical composition (4, 10). After secretion, *V. harveyi* AI-1 diffuses to neighboring cells and is recognized by the cognate membrane-associated hybrid sensor kinase/phosphatase LuxN that initiates signals for production of LuxR, the transcriptional activator of target gene expression (11). Seven *luxR* homologs have been identified in

the *S. oneidensis* genome, however, all seven *luxR* homologs are classified as members of the *luxR-narL-fixJ* superfamily of transcriptional activators lacking conserved AHL binding motifs (12, 13). In addition, AI-1 is not detected in the extracellular fraction of aerobically-grown cultures, thus *S. oneidensis* is not predicted to carry out AI-1-dependent QS (13, 14). A comprehensive search for genes encoding AI-1-based QS systems in the *S. oneidensis* genome, however, has not been conducted.

In contrast, the *S. oneidensis* genome encodes the activated methyl cycle (AMC) enzyme S-ribosylhomocysteine (SRH) lyase (LuxS), which cleaves SRH to homocysteine and the AI-2 precursor (S)-4,5-dihydroxy-2,3-pentanedione (DPD)(3, 15). DPD spontaneously cyclizes to either the *S* (or *R*) form of 2,4-dihydroxy-2-methyldihydro-3-furanone (DHMF), which undergoes hydration and incorporation of borate to form mature AI-2 (16). In *V. harveyi*, AI-2 signals are communicated to neighboring cells by AI-2 uptake and binding by LuxP, and AI-2-LuxP interaction with the hybrid sensor kinase/phosphatase LuxQ that initiates signals for LuxR production (3, 11, 15). AI-2 is detected in the extracellular fraction of aerobically-grown *S. oneidensis* wild-type (but not Δ*luxS*) cultures (12, 13). A comprehensive search for genes encoding AI-2-based QS systems in the *S. oneidensis* genome, however, has not been conducted.

Microbial QS systems are disrupted by AI-1- and AI-2-specific degradation pathways (17). AI-1 is degraded enzymatically under aerobic conditions by ring-cleaving lactonases, acyl tail-cleaving acylases, and acyl tail-modifying oxidoreductases (17, 18). In *Escherichia coli,* AI-2 uptake and degradation are encoded by the *lsrACDBFG* and *lsrRK* operons. AI-2 (in the form of DPD) is imported by the LsrACDB uptake system and the imported DPD is phosphorylated by LsrK to form phospho-DPD, which induces

expression of the two Lsr operons by binding to and inactivating the Lsr transcriptional repressor LsrR (19). Phospho-DPD is subsequently cleaved by LsrG to produce 2-phosphoglycolate and other unidentified degradation products (19, 20). The *S. oneidensis* wild-type and Δ*luxS* mutant strains both degrade AI-2 during aerobic growth in rich medium (12), however, a comprehensive search for *S. oneidensis lsr* homologs has yet to be conducted. In addition, although AI-1 is metabolized as sole carbon and electron source for aerobic growth by a variety of microorganisms (17, 21-25), AI-2 metabolism as sole carbon and electron source for anaerobic growth by any microorganism has yet to be reported.

The main objective of the present study was to test the two hypotheses that *S. oneidensis* produces AI-2 (designated OAI-2) during anaerobic growth (as a byproduct of LuxS catalyzed conversion of S-ribosylhomocysteine to homocysteine) and that *S. oneidensis* can metabolize the accumulated OAI-2 or AI-2 from other bacteria (e.g., *V. harveyi* AI-2, designated HAI-2) as sole carbon and electron source to fuel anaerobic respiration. The experimental strategy to test the hypothees included i) comprehensive genome-wide searches for *S. oneidensis* genes putatively involved in OAI-2-based QS and OAI-2 degradation, ii) detection of OAI-2 in the extracellular fraction of *S. oneidensis* wild-type (but not Δ*luxS*) cultures grown under anaerobic conditions, iii) linkage of the *S. oneidensis* Δ*luxS* genotype to the anaerobic biofilm formation-deficient phenotype of the *S. oneidensis* Δ*luxS* mutant, and iv) determination of the ability of the *S. oneidensis* wild-type and Δ*luxS* mutant strains to grow aerobically and to respire anaerobically with OAI-2 and HAI-2 as sole carbon and electron source.

**Materials and Methods**

**Bacterial strains and cultivation conditions**. The bacterial strains and plasmids used in this study are listed in Table 3.1. *S. oneidensis* overnight cultures (to be used as inoculum for aerobic and anaerobic growth experiments with HAI-2 and OAI-2 as electron donor) were grown aerobically in M1 minimal medium (26) supplemented with lactate (18 mM) as electron donor. Overnight cultures were washed twice and resuspended in M1 medium prior to inoculating in M1 medium supplemented with either lactate, OAI-2, or HAI-2 as electron donors. Electron acceptors were added from anaerobic stock solutions synthesized as previously described (27-32): Fe(III) citrate (50 mM), ferrihydrite (10 mM), fumarate (10 mM), $NO_3^-$ (15 mM), $NO_2^-$ (2 mM), TMAO (25 mM), and $S_2O_3^{2-}$ (10 mM).

**In-frame gene deletion mutagenesis and genetic rescue of the Δ*luxS* biofilm formation-deficient phenotype**. The gene encoding LuxS (SO_1101) was deleted in-frame from the *S. oneidensis* genome via previously described procedures (33). The primers used for construction of Δ*luxS* are listed in Table 3.2 Regions corresponding to approximately 750 bp upstream and downstream of each open reading frame (ORF) were PCR-amplified with primers D1 and D2 for the upstream region and D3 and D4 for the downstream region with iProof ultrahigh-fidelity polymerase (Bio-Rad, Hercules, CA), generating fragments F1 and F2, which were fused by overlap extension PCR to generate fragment F3. Fragment F3 was cloned into pKO2.0 with BamHI and SalI restriction endonucleases to generate recombinant plasmid pKO2.0-F3, which was electroporated into *E. coli* strain β2155 λ *pir*. pKO2.0-F3 was mobilized into recipient *S. oneidensis* wild-type cells via conjugal transfer from *E. coli* donor strain β2155 λ pir. *S. oneidensis*

recipient strains containing the plasmid integrated into the genome were selected on LB agar medium supplemented with 15 μg $ml^{-1}$ Gm. Single plasmid integrants were identified via PCR with primers D1-DTR and D4-DTF that flank the targeted recombination region. Plasmids were resolved from the genomes of the single integrants by plating on LB agar medium containing sucrose (10% w/v). Following counter selection on sucrose-containing LB agar medium, the corresponding in-frame deletion mutant (designated strain Δ*luxS*) was isolated and confirmed via PCR amplification and direct DNA sequencing (University of Nevada, Reno Genomics Facility). Genetic complementation of Δ*luxS* was carried out by cloning wild-type *luxS* into broad-host-range cloning vector pBBR1MCS (34) and conjugally transferring the recombinant vector into Δ*luxS* via bi-parental mating procedures (35).

**Nucleotide and amino acid sequence analyses.** Genome sequence data for *S. oneidensis* MR-1 was obtained from the National Center for Biotechnology Information (NCBI, http://www.ncbi.nlm.nih.gov) and the Department of Energy Joint Genome Institute (DOE-JGI, http://jgi.doe.gov). Lux and Lsr homologs in the NCBI databases were identified in the *S. oneidensis* genome via BLAST analysis (36) using the corresponding *Vibrio* and *E. coli* proteins as search queries.

**Visual inspection of anaerobic biofilm formation on bare and Fe(III) oxide-coated silica surfaces via confocal laser scanning microscopy (CLSM).** *S. oneidensis* wild-type and Δ*luxS* mutant strains were incubated anaerobically on bare and Fe(III) oxide-coated silica surfaces and biofilm formation was visualized via CLSM. To prepare the

Fe(III) oxide-coated silica surfaces, silica glass microscope slides were washed with 30% (w/v) hydrogen peroxide ($H_2O_2$) and subsequently etched by washing with 5 M NaOH (37, 38). The etched silica surfaces were coated with Fe(III) oxides by slowly oxidizing a 1 M $FeSO_4$ solution with 30% (w/v) $H_2O_2$. The microscope slides were heated to 100ºC to fix the Fe(III) oxide coating to the silica surface and then cleaned via sonication (37, 38).

Biofilm formation experiments (to be used for CLSM imaging) were inoculated using *S. oneidensis* MR-1 or *ΔluxS* grown in LB media at 30˚C to $OD_{600}$ 1.0. 12 mL of the aforementioned culture was added to bare silica surfaces or Fe(III) oxide-coated silica surfaces in sterile petri dishes. The slides were incubated at 30˚C for 45 min. Next, the slides were transferred to fresh media (M1 media supplemented with the appropriate electron donor and acceptor) and placed in an anaerobic chamber. Strains were incubated anaerobically for 48 h at 25˚C in M1 minimal growth medium containing the previously prepared bare silica surfaces. M1 growth medium was amended with either lactate or purified HAI-2 or supernatants containing OAI-2 as electron donor and thiosulfate or Fe(III) oxide-coated silica as electron acceptor. At pre-determined time points, replicate silica slides were sacrificed for CLSM imaging and determination of electron acceptor reduction activity.

For CLSM imaging, the bare silica surfaces were washed with sterile, anaerobic PBS buffer (NaCl (8 g $l^{-1}$), KCl (0.2 g $l^{-1}$), $Na_2HPO_4$ (1.44 g $l^{-1}$), $KH_2PO_4$ (0.24 g $l^{-1}$, pH 7) and attached cells were fixed with 4% paraformaldehyde. The fixed cells were stained with 0.1% (w/v) anaerobic acridine orange solution for 20 min and then washed with anaerobic PBS buffer for 10 min prior to examination of biofilm structure via CLSM.

CLSM imaging was carried out with a Zeiss 510 Vis system comprised of a Zeiss Axio Observer inverted microscope and an argon laser source with excitation wavelengths of 453, 477, 488, and 514 nm. 3D digitized images were generated with Zeiss Zen 2009 software (Carl Zeiss Microscopy, Inc.).

**High Performance Liquid Chromatography (HPLC) and Ion Chromatography (IC).** AI-2 concentrations were measured via HPLC analysis of diaminonaphthalene (DAN; Sigma Aldrich)-derivitized supernatant samples as previously described (39). Aliquots (250 µl) of batch culture supernatants were transferred to autosampler vials containing an equal volume of DAN solution, and the two solutions were mixed for 2 min and subsequently incubated for 40 min at 90°C. After cooling to room temperature, 20 µl of each sample was injected into a Waters HPLC system equipped with a fluorescence detector. Derivatized samples were separated on an Agilent ZORBAX SB-C18 reverse-phase column (259 mm x 4.6 mm length, 5 µm diameter). The mobile phase contained 0.045% formic acid (solvent A) and 55% acetonitrile (solvent B) at a constant flow rate of 0.8 ml/min. The excitation and emission wavelengths of the fluorescence detector were set at 271 and 503 nm, respectively, with a retention time of approximately 3 min. DAN solution was prepared by dissolving 10 mg DAN into 50 ml of 0.1 M HCl. DPD concentrations were estimated from calibration curves with DPD purified from *V. harveyi* strain as standard.

Lactate concentrations in culture supernatants were determined by harvesting 500 uL of cell culture and centrifuging at 6000*g* for 10 min. Lactate concentrations were measured via ion chromatrograph (IC) (Dionex, DX-300 Series) equipped with Dionex

IonPAc ICE-AS6 chromatography column and AMMS ICE 300 suppressor. The Dionex DX-300 utilizes a CDM II detector with suppressed conductivity detection. Anion analysis was performed with 0.4 mM heptafluorobutyric acid as eluent and 5 mM tetrabutylammonium hydroxide as regenerant. Chromatograms were generated for lactate as retention time of 10 min. Calibration curves for lactate were generated from standards to determine the concentration.

**Determination of the overall aerobic and anaerobic respiratory capability of *S. oneidensis* wild type and *ΔluxS* mutant strains with HAI-2 or OAI-2 as sole electron donor.** *S. oneidensis* wild-type and Δ*luxS* mutant strains were grown aerobically and anaerobically (initial inoculum of $1.0 \times 10^7$ cells $ml^{-1}$) in M1 minimal medium supplemented with either lactate (18 mM), purified HAI-2 (5 µM) or OAI-2 (8.5 µM in *S. oneidensis* spent supernatants) as electron donor and either ferrihydrite (10 mM), fumarate (10 mM), $NO_3^-$ (15 mM), or $S_2O_3^{2-}$ (10 mM) as electron acceptor. Fe(II) production was monitored by measurement of HCl-extractable Fe(II) via the Ferrozine method (40). Aerobic growth and anaerobic growth on fumarate were monitored spectrophotometrically by measuring changes in absorbance at 600 nm ($A_{600}$). $NO_2^-$ was measured spectrophotometrically with sulfinilic acid-*N*-1-naphthyl-ethylene-diamine dihydrochloride solution (41). $S_2O_3^{2-}$ concentration was measured by cyanolysis as previously described (33, 42). For growth with OAI-2 as electron donor, 0.22 µm filter-sterilized *S. oneidensis* supernatants were used as electron donor and ferrihydrite (10 mM), fumarate, $NO_3^-$, or $S_2O_3^{2-}$ as electron acceptor.

## Results

**Identification of *S. oneidensis* genes involved in AI-2 quorum sensing and degradation.** The *S. oneidensis* genome was searched for genes similar to those encoding the AI-2 detection and signal relay systems of *V. harveyi, V. fischeri*, and *V. cholerae* (Table 3.3). A homolog of the *V. harveyi* AI-2 sensor kinase/phosphatase *luxQ* was identified in the *S. oneidensis* genome (SO_0859; 32% similarity, 46% identity, e-value of $7e^{-56}$), however, SO_0859 was annotated as a two-component signal transduction system hybrid histidine kinase/response regulator containing a PAS domain without an obvious sensing module (43). A homolog of the *V. harveyi* AHL sensor kinase/phosphatase *luxN* was also identified in the *S. oneidensis* genome (SO_2544; 30% similarity, 47% identity, e-value of $4e^{-19}$), however, SO_2544 was annotated as a two-component signal transduction histidine kinase/response regulator containing an Hpt domain. Genes similar to *luxP*, *luxM*, *luxU*, and *luxI* were not found in the *S. oneidensis* genome. As previously reported, seven *luxR* homologs were detected in the *S. oneidensis* genome, and all seven were classified as *luxR-narL-fixJ* superfamily of transcriptional activators lacking conserved AHL binding motifs (12, 13). In addition, none of the seven *S. oneidensis* LuxR homologs were located proximal to cognate LuxM/LuxI/CqsA homologs, and thus are classified as solo LuxR homologs not involved in QS (Tables 3.4, 3.5, 3.6)(44-46).

The *S. oneidensis* genome was also searched for genes similar to those encoding the *E. coli* AI-2 uptake (LsrACDB) and degradation (LsrG/K) systems (Table 3.7). A

homolog of *E. coli* LsrA (the ATPase component of the *E. coli* AI-2 uptake system) was identified in the *S. oneidensis* genome (SO_0742; 87% similarity, 45% identity, e-value of $8e^{-28}$), however, SO_0742 was annotated as FbpC, the ATPase component of the ABC-type Fe(III) uptake system encoded by the FbpABC operon (43). An *E. coli* LsrK homolog was also identified in the *S. oneidensis* genome (SO_4230; 41% similarity, 26% identity, e-value of $7e^{-24}$), however, SO_4230 was annotated as GlpK, the glycerol kinase component of glycerolipid metabolism (43). Genes encoding the LsrB, C, D, and G homologs of the *E. coli* AI-2 uptake and degradation systems were not detected in the *S. oneidensis* genome (Table 3.7).

**Identification of *S. oneidensis* genes involved in AI-1 degradation.** The *S. oneidensis* genome was also scanned via BLASTp analysis for putative AI-1-degrading lactonase, acylase, and oxidoreductase homologs. Lactonases were not detected in the *S. oneidensis* genome. The BLASTp analyses revealed the presence of a lactonase homolog with a low amino acid sequence identity (28%), similarity (40%), and e-value (0.014) to *Bacillus sp.* AiiA, while an AHL acylase homolog (AaiD; SO_0918) with high amino acid sequence similarity (99%), sequence identity (34%), and e-value ($9e^{-37}$) to *Pseudomonas aeruginosa* PvdQ was detected. A putative oxidoreductase homolog (sulfite reductase (NADPH) flavoprotein subunit CysJ (SO3738) with an amino acid sequence identity (30%), sequence similarity (55%), and e-value ($1e^{-58}$) to *Bacillus megaterium* CYP102A1 was detected.

**Rates of anaerobic biofilm formation on polystyrene surfaces by *S. oneidensis* wild-type and *ΔluxS* mutant strains supplemented with exogenous HAI-2.** Rates of

aerobic and anaerobic biofilm formation on polystyrene surfaces were determined using conventional CV-based biofilm assays carried out in the presence and absence of 10 µM exogenous HAI-2 (Table 3.8; Fig. 3.1, Fig. 3.2). Under aerobic conditions with lactate as carbon and electron source, the rate of Δ*luxS* biofilm formation was 63% of the corresponding wild-type rate (i.e., similar to the previously reported partial Δ*luxS* biofilm formation-deficient phenotype) (13, 47). Addition of exogenous AI-2 restored the rate of aerobic biofilm formation by Δ*luxS* to near wild-type rates (Table 3.8; Fig. 3.1). In addition, under aerobic conditions with HAI-2 replacing lactate as sole carbon and electron source, rates of aerobic biofilm formation by the *S. oneidensis* wild-type and Δ*luxS* strains were identical (Table 3.8; Fig. 3.2). Under anaerobic conditions with lactate as carbon and electron source and thiosulfate as electron acceptor, the rate of anaerobic biofilm formation by Δ*luxS* was 12% of the corresponding wild-type rate. Addition of exogenous HAI-2 also restored the rate of anaerobic biofilm formation by Δ*luxS* to near wild-type rates (Table 3.8; Fig. 3.2). Under anaerobic conditions with HAI-2 replacing lactate as sole carbon and electron source and thiosulfate as electron acceptor, rates of anaerobic biofilm formation by the *S. oneidensis* wild-type and Δ*luxS* strains were identical (Table 3.8; Fig. 3.2).

**Visual inspection of anaerobic biofilm formation by *S. oneidensis* wild-type and *ΔluxS* mutant strains supplemented with exogenous AI-2.** CLSM image analyses indicated that *S. oneidensis* Δ*luxS* mutant strain displayed a biofilm deficient phenotype during anaerobic growth on bare (Figs. 3.3; thiosulfate ($S_2O_3^{2-}$)-amended) and Fe(III) oxide-coated (Fig. 3.3) silica surfaces. The addition of exogenous HAI-2 restored the

biofilm formation phenotype to that observed in the wild-type strain (Fig. 3.3). With lactate as electron donor, *S. oneidensis* wild-type and Δ*luxS* amended with exogenous AI-2 (top and bottom row of images, respectively) formed microcolonies that subsequently developed into larger 3D structures until the bare and Fe(III) oxide-coated silica surfaces were completely covered with cell piles or towers after a 48 h anaerobic incubation period with lactate as electron donor. The Δ*luxS* mutant cells (Fig. 3.3), however, displayed a severely impaired anaerobic biofilm formation phenotype during the 48 h incubation period with lactate as electron donor, with patches of both bare and Fe(III) oxide-coated silica surfaces remaining uncovered.

**Production of extracellular OAI-2 by *S. oneidensis* wild-type and *ΔluxS* mutant strains under anaerobic growth conditions**. *S. oneidensis* wild-type cultures were previously reported to produce OAI-2 (at undetermined concentrations) during aerobic growth in rich growth medium (13). To corroborate this finding, *S. oneidensis* wild-type was grown under aerobic and anaerobic fumarate-reducing conditions with lactate as the electron donor. We found that OAI-2 was produced under aerobic and anaerobic conditions while simultaneous lactate depletion and acetate production was observed (Fig. 3.4, 3.5). When OAI-2 concentrations reached threshold levels, OAI-2 depletion occurred preferentially over acetate depletion (Fig. 3.4, 3.5). In the present study, the wild-type strain produced OAI-2 at a rate of 448 nM $hr^{-1}$ during aerobic growth in defined minimal medium with lactate as electron donor. During anaerobic growth with thiosulfate, nitrate, ferrihydrite, and fumarate as electron acceptor, the wild-type strain produced OAI-2 at rates equal to OAI-2 production rates under aerobic growth conditions (Tables 3.9, 3.10; Fig. 3.6). The Δ*luxS* mutant strain, on the other hand, was unable to

produce OAI-2 under aerobic or anaerobic growth conditions (Tables 3.9, 3.10; Fig. 3.6). Negative control mutant strain *V. harveyi* Δ*luxSluxMluxN* (i.e., lacking the ability to produce, detect and uptake exogenous HAI-2) was unable to produce HAI-2 under aerobic growth conditions, while positive control strain *V. harveyi* Δ*luxMluxN* (i.e., retaining the ability to produce HAI-2, but lacking the ability to detect and uptake exogenous HAI-2) produced HAI-2 under aerobic growth conditions at a rate of 438 nM $hr^{-1}$.

***S. oneidensis* wild-type and *ΔluxS* mutant strains respire anaerobically with OAI-2 and HAI-2 as sole carbon and electron source**. Under aerobic growth conditions with exogenous HAI-2 replacing lactate as sole carbon and electron source, the wild-type and Δ*luxS* mutant strains consumed HAI-2 at similar rates of 209 (+/- 47) nM $hr^{-1}$for the wild-type and 282 (+/-29) nM $hr^{-1}$for the *luxS* mutant and the corresponding doubling times of both strains with HAI-2 as sole carbon and electron source were approximately 20 h (Table 3.11; Fig. 3.7, 3.11). Similar results were obtained when OA-2 used as the sole carbon and electron source under aerobic conditions (Table 3.12; Fig. 3.7, 3.12). In contrast, the doubling times of the wild-type and Δ*luxS* mutant strains under aerobic growth conditions with lactate as sole carbon and electron donor were approximately 10 h (Fig.3.9). Under anaerobic conditions with thiosulfate as electron acceptor, the wild-type strain degraded HAI-2 at rates nearly identical to aerobically-grown wild-type cells, while HAI-2 was degraded by the wild-type strain at rates 1.4-fold faster with fumarate as electron acceptor and 2.6-fold slower with ferrihydrite as electron acceptor. With thiosulfate as electron acceptor, the wild-type strain degraded HAI-2 at rates of 143 (+/-

32) nM $hr^{-1}$ and reduced thiosulfate reduction at rates of 178 (+/- 57) nM $hr^{-1}$, while Δ*luxS* degraded HAI-2 at 159% of wild-type rates and reduced thiosulfate at wild-type rates (Table 3.11; Fig. 3.7, 3.11). With fumarate as electron acceptor, the wild-type strain degraded HAI-2 at rates of 317 (+/- 9) nM $hr^{-1}$ and reduced fumarate at rates of 4 (+/- .471) nM $hr^{-1}$, while Δ*luxS* degraded HAI-2 at 75% of wild-type rates and reduced fumarate at wild-type rates (Table 3.11; Fig. 3.7, 3.11). With ferrihydrite as electron acceptor, the wild-type strain degraded HAI-2 at rates of 132 (+/- 10) nM $hr^{-1}$ and reduced ferrihydrite at rates of 25 (+/- 2) nM $hr^{-1}$, while Δ*luxS* degraded HAI-2 at 76% of wild-type rates and reduced ferrihydrite at wild-type rates (Table 3.11; Fig. 3.7, 3.11). With nitrate as electron acceptor, the wild-type strain degraded HAI-2 at rates of 178 (+/- 19) nM $hr^{-1}$ and reduced nitrate at rates of 174 (+/- 21) nM $hr^{-1}$, while Δ*luxS* degraded HAI-2 at 77% of wild-type rates and reduced nitrate at wild-type rates (Table 3.11; Fig. 3.7, 3.11). Similar results were obtained when OA-2 used as the sole carbon and electron source under anaerobic conditions with thiosufate, fumarate, ferrihydrite, and nitrate as the electron acceptor (Table 3.12; Fig. 3.7, 3.12). Control strain *V. harveyi* Δ*luxS* (lacking the ability to produce HAI-2, but retaining the ability to detect and remove exogenous HAI-2 from the external environment) degraded HAI-2 under aerobic conditions at a rate of 28 (+/- ) nM $hr^{-1}$, which is approximately 55% greater than the rate of HAI-2 degradation by the *S. oneidensis* wild-type and Δ*luxS* mutant strains under aerobic conditions.

**Discussion**

*S. oneidensis* respires a suite of electron acceptors that nearly span the entire continuum of redox potentials found in natural waters and sediments, ranging from

soluble electron acceptors such as oxygen, nitrate, fumarate, and thiosulfate to solid electron acceptors such as Fe(III) oxides (26, 48). *S. oneidensis* transfers electrons to Fe(III) oxides via direct (surface or surface extension-exposed *c*-type cytochromes) and indirect (electron shuttling and Fe(III) solubilization) pathways (49-57). Previous studies have emphasized the requirement for biofilm formation on Fe(III) oxide surfaces as a critical component for *S. oneidensis*-mediated electron transfer to Fe(III) oxide surfaces (7, 8, 58) as a way to ensure the cells are within 15A of the Fe(III) oxide surfaces and electron transfer between the cell and Fe(III) oxide particle can occur. In gram-negative bacteria such as members of the genus *Vibrio*, biofilm formation is regulated by QS-based cell-cell communication systems (9, 59-63). The *S. oneidensis* genome consists of 32% *Vibrio*-like genes (43), thus genome-wide searches for putative *S. oneidensis* QS systems are facilitated by using QS proteins from *V. harveyi*, *V. cholera, and V. fischeri* as search queries.

The AHLs produced by *V. harveyi* (HAI-1), *V. cholera* (CAI-1), and *V. fischeri* (3-oxo-hexanoyl- and octanoyl-AHL) are synthesized by the corresponding AHL synthases LuxM, CqsA, LuxI, and AinS, and are detected by the corresponding AHL sensors LuxN, CqsS, and LuxR (both types of *V. fischeri* AHL) (59, 60, 63-65). Previous studies reported that AHL was not detected in the extracellular fraction of aerobically-grown *S. oneidensis* cultures and that the seven *S. oneidensis* LuxR homologs identified in the *S. oneidensis* genome were not paired with cognate LuxI, LuxM, or CqsA AHL synthases (i.e., classified as solo LuxR homologs) and lacked QS signal binding motifs (13, 14). Genome searches in the present study indicated that homologs of the *Vibrio* AHL synthases and sensors were not present in the *S. oneidensis* genome, thus

reinforcing the previous report that *S. oneidensis* does not carry out AHL-dependent QS (13).

The *S. oneidensis* genome does not contain a *luxM* homolog but does contain seven *luxR* solo homologs (i.e., not paired with cognate AHL synthase-encoding *luxM* or *luxI*)(12, 13, 43-46). LuxR proteins that retain the same modular structure as LuxR proteins involved in QS but lack the cognate AHL synthase (*luxM/I*) are referred to as solo LuxRs (45). Interestingly, of 3550 *luxR* genes identified across a wide range of organisms, only 24% were determined to be members of AHL circuits, while 76% were identified as solo *luxR* genes (44). Solo *luxR* genes are capable of respondng to internal AHL signals produced by non-adjacent *luxI* in the chromosome, or are capable of responding to other exogenous signals. Solo LuxR sequences form distinct clusters that are divergent from the clusters of LuxR sequences that belong to known *luxR-luxI* QS systems and these solo *luxR* genes lack the sequence motifs characteristic of AHL binding LuxR proteins (44). These findings indicates that LuxR homologs in *S. oneidensis* are not similar to the LuxR-type proteins that functions as AHL-dependent transcription regulators (13).

Despite the fact that the *luxS* gene is widespread, there is considerable doubt that the main role of LuxS and AI-2 is its function as a quorum sensing molecule. Conversely, the proposed primary role of LuxS is a metabolic role in the recycling of SAM, with the synthesis of AI-2 simply a by-product of the AMC process. Furthermore, the function of AI-2 in a quorum sensing mechanism is also dependent on the organism containing known AI-2 receptor genes. The AI-2 family of quorum sensing signals, catalyzed by the enzyme *luxS,* is unique in that LuxS is conserved across gram-negative

and gram-positive proteobacteria. This genetic conservation has lead to the supposition that AI-2 is used for interspecies communication (i.e. quorum sensing) (66). LuxS is also involved in the activated methyl cycle (AMC) (67, 68). The metabolic function of LuxS are highly debated regarding whether the mutation in *luxS* displays certain phenotypes as a result of disruption in quorum-sensing activities or disruption of the AMC (16, 69-71).

The AMC is responsible for the synthesis of homocysteine, methionoine, adenosine, S-adenosylhomocysteine (SAH), S-ribosylhomocysteine (SRH), and S-adenosylmethionine (SAM), a predominant methyl donor source within the cell (16). Homocysteine enters the cycle via one of three ways: the conversion of SRH to homocysteine by the *luxS* enzyme, the conversion of cystathionine to homocysteine via cystathionine β-lyase (*metC*), or the conversion of O-acetyl-L-homoserine to homocysteine via O-acetyl-L-homoserine sulfhydrolase (*metY)*. Homocysteine is converted to methionine and then to SAM. SAM is then converted to SAH, which results in the methylation of DNA, RNA, and metabolites. The cycle is completed via conversion SAH to SRH, followed by conversion of SRH to homocysteine and 4,5-dihydroxy-2,3-pentanedione (DPD) via LuxS. DPD can then spontaneously cyclize to form AI-2.

Previous analysis of the *S. oneidensis* genome revealed that the presence of the *luxS* gene (12). *luxS* has been highly characterized in other gram-negative bacteria, such as *Vibrio harveyi*, and has been shown to produce autoinducer-2 (AI-2), a putative signaling molecule used for quorum sensing (72). The role of *luxS* in *S. oneidensis* is not well understood. *S. oneidensis* is capable of forming biofilms, the bacteria live in bacterial communities, and the presence of *luxS* enzyme has led to speculation that AI-2

signaling occurs in *Shewanella*, thus allowing the bacteria to react to bacterial cell density in its immediate environment. However, this generalized role for AI-2 signaling solely based on the presence of the *luxS* enzyme is debatable. The role of LuxS in bacterial species is not necessarily designated as the enzyme responsible for the production of AI-2, instead, the enzyme is an essential component of the AMC required for the conversion S-ribosylhomocysteine (SRH) to homocysteine (73). *S. oneidensis* genome lacks any genetic homologs to the AI-2 receptor found in *Vibrio* species and any transport into the cell appears to be as a result of nutrient limitation (12). Previous studies of aerobic biofilm formation by *luxS* mutant in *S. oneidensis* MR-1 showed a slightly reduced biofilm formation (~70%) compared to the wild-type; complementation with components of the AMC (methionine) restored the mutant biofilm to wild-type indicating any disruption in biofilm formation in the *luxS* mutant is attributed to disruption in the AMC rather than disruption in cell-cell signaling by AI-2 (13)

A homolog of *E. coli* LsrA (ATPase component of the AI-2 uptake system) was identified in the *S. oneidensis* genome (SO_0742), however SO_0742 was annotated as FbpC, the ATPase component of an ABC-type Fe(III) uptake system (43). These findings indicate that *E. coli* LsrA and *S. oneidensis* FbpC function as ATPase components of ABC transport systems dedicated to uptake of different substrates (AI-2 and Fe(III), respectively). An *E. coli* LsrK homolog was also identified in the *S. oneidensis* genome (SO_4230), however SO_4230 was annotated as glycerol kinase (43). In a manner similar to the homology between *E. coli* LsrA and *S. oneidensis* FbpC, these findings indicate that *E. coli* LsrK and *S. oneidensis* glycerol kinase function as the phosphotransfer components of systems involved in degradation of different carbon

substrates (AI-2 and glycerol, respectively). Genes encoding the LsrC, D, and B homologs of the *E. coli* AI-2 uptake system and the LsrG homolog of the *E. coli* AI-2 degradation system were not detected in the *S. oneidensis* genome. These results indicate that AI-2 uptake and degradation system of *S. oneidensis* are different than the corresponding *E. coli* systems.

AI-2s produced by *V. harveyi*, *V. cholera*, and *V. fischeri* (HAI-2, CAI-2, and AI-2, respectively) are synthesized by LuxS homologs and are detected by LuxPQ and LuxR homologs (60). LuxS was previously identified in the *S. oneidensis* genome and OAI-2 was detected in the extracellular fraction of *S. oneidensis* cultures grown aerobically in rich medium (13). In the present study, OAI-2 was detected in the extracellular fraction of *S. oneidensis* cultures grown anaerobically in minimal medium with lactate as electron donor and nitrate, thiosulfate, fumarate, or Fe(III) oxide as electron acceptor (Fig. 3.4, 3.6). OAI-2 was also detected in the extracellular fraction of *S. oneidensis* cultures grown aerobically in defined medium with lactate as electron donor, thus indicating that OAI-2 is produced by *S. oneidensis* under a wide variety of growth conditions, including rich and defined growth media and with electron acceptors of widely varying redox potentials and solubilities.

OAI-2 depletion was first observed in experiments conducted to test the results of previous studies that showed *S. oneidensis* was capable of produced OAI-2. We found that OAI-2 was produced under aerobic and anaerobic conditions while simultaneous lactate depletion and acetate production was observed (Fig. 3.4, 3.5). When OAI-2 concentrations reached threshold levels, OAI-2 depletion occurred preferentially over acetate depletion (Fig. 3.4, 3.5). Preferential use of OAI-2 over acetate under aerobic

growth conditions implies OAI-2 (and other AI-2 molecules, such as HAI-2) can be used as an alternate carbon source and potential electron donor. Rates of OAI-2 production by *S. oneidensis* under anaerobic growth conditions were nearly identical to those observed under aerobic growth conditions. A correlation between rates of OAI-2 production and the mid-point redox potential of the electron acceptor was not observed. Seven solo LuxR homologs were previously found in the *S. oneidensis* genome, yet none contained conserved QS signal binding sites (13). In addition, the *Vibrio*-like AI-2 sensor LuxPQ was missing from the *S. oneidensis* genome (Table 3.3). These results indicated that OAI-2 production by *S. oneidensis* was not involved in QS via canonical *Vibrio*-like AI-2-based QS systems.

In previous studies, Δ*luxS* displayed a partial biofilm formation-deficient mutant phenotype (reaching 66% of wild-type biomass levels) under aerobic conditions in rich growth medium (13). The partial biofilm formation-deficient phenotype was restored to 100% wild-type biomass levels by addition of exogenous homocysteine, but not exogenous AI-2 (produced in vitro by purified *E. coli* LuxS fed SRH as substrate)(13). In the present study, *S. oneidensis* Δ*luxS* also displayed a partial biofilm formation-deficiency under aerobic conditions in defined growth medium with lactate as sole carbon and electron source (63% of wild-type biofilm formation rates). Anaerobic biofilm formation by the gram-negative γ-proteobacterium *Shewanella oneidensis* MR-1, for example, may enhance electron transfer to Fe(III) oxides and MFC anodes via direct (cell surface *c*-type cytochrome) (52, 56, 74, 75) or indirect (electron shuttling and Fe(III) solubilization) pathways (49-51, 53-55, 76).

However, in addition to rescue by homocysteine, the partial aerobic biofilm formation-deficiency of Δ*luxS* in defined growth medium was restored to near wild-type biofilm formation rates by addition of either OAI-2 or HAI-2. Reasons for the previously reported inability of *E. coli*-produced AI-2 to rescue the partial biofilm formation-deficient mutant phenotype of Δ*luxS* under aerobic conditions in rich growth medium are unclear, especially since species-dependent differences in AI-2 structure have not been reported. Furthermore, in the present study, Δ*luxS* displayed a severe biofilm formation-deficiency under anaerobic conditions in defined growth medium (6-23% of wild-type biofilm formation rates on polystyrene and bare and Fe(III) oxide-coated silica surfaces; Fig. 3.2, 3.3). The rates of anaerobic biofilm formation by Δ*luxS* were also restored to near wild-type rates by addition of exogenous homocysteine, OAI-2, or HAI-2. The ability of exogenous homocysteine, OAI-2, and HAI-2 to rescue the severe anaerobic biofilm formation-deficiency of *S. oneidensis* Δ*luxS* links the Δ*luxS* genotype to the anaerobic biofilm formation mutant phenotype. The absence of such a link has hindered past investigations of LuxS-dependent investigations of LuxS-dependent phenotypes.

The absence of genes encoding AHL- and AI-2-based QS systems and the link between the *S. oneidensis* Δ*luxS* genotype and anaerobic biofilm formation-deficient mutant phenotype led us to hypothesize that *S. oneidensis* metabolizes OAI-2 and HAI-2, potentially as sole carbon and electron source for aerobic and anaerobic respiration. Previous studies demonstrated that HAI-2 was depleted by *S. oneidensis* cultures grown aerobically in rich growth medium (12). Results of the present study demonstrated that *S. oneidensis* cultures grew aerobically or anaerobically in minimal growth medium with either OAI-2 or HAI-2 as sole carbon and electron source and either oxygen, nitrate,

fumarate, thiosulfate, or Fe(III) oxide as sole electron acceptor . These findings expand the list of carbon and electron sources respired by *S. oneidensis* to include OAI-2 or AI-2 produced by other bacteria (e.g., HAI-2). The ability to respire OAI-2 provides enhanced growth capability to free-living or biofilm-associated *S. oneidensis* cells: after primary carbon and electron sources such as lactate, succinate, formate, hydrogen, and acetate (aerobic conditions only) have been exhausted, the accumulated extracellular OAI-2 may subsequently imported and metabolized as sole carbon and electron source to sustain aerobic growth and anaerobic reduction activity.

The ability to utilize HAI-2 as sole carbon and electron source under aerobic and anaerobic conditions also provides *S. oneidensis* with the metabolic flexibility to utilize AI-2 produced by other bacteria (i.e., *V. harveyi*) as growth substrate, which potentially represents a form of QS signal-blind metabolic cheating (77). Such capability may sustain the metabolic activity of QS signal-blind *S. oneidensis* cells in multi-species biofilms inhabited by QS-proficient members such as phylogenetically related *Vibrio* species. This ability to utilize HAI-2 as sole carbon and electron source under aerobic and anaerobic conditions also provides *S. oneidensis* with the ability to disrupt the AI-2-based QS communication systems of other bacteria (e.g., *V. harveyi*) in multi-species biofilms (24, 78-80). Such disruptive metabolic capability is important for signal quenching mechanism. However, the absence of *E. coli lsr*-like genes in the *S. oneidensis* genome will necessitate new lines of investigation to uncover the novel structural and functional components of the *S. oneidensis* AI-2 uptake and metabolic systems.

**References**

1. **Karatan E, Watnick P.** 2009. Signals, Regulatory Networks, and Materials That Build and Break Bacterial Biofilms. Microbiol Mol Biol R **73:**310-+.
2. **Flemming HC, Wingender J.** 2010. The biofilm matrix. Nat Rev Microbiol **8:**623-633.
3. **Rutherford ST, Bassler BL.** 2012. Bacterial quorum sensing: its role in virulence and possibilities for its control. Cold Spring Harbor perspectives in medicine **2**.
4. **Solano C, Echeverz M, Lasa I.** 2014. Biofilm dispersion and quorum sensing. Current opinion in microbiology **18:**96-104.
5. **Hall-Stoodley L, Costerton JW, Stoodley P.** 2004. Bacterial biofilms: From the natural environment to infectious diseases. Nat Rev Microbiol **2:**95-108.
6. **Halan B, Buehler K, Schmid A.** 2012. Biofilms as living catalysts in continuous chemical syntheses. Trends Biotechnol **30:**453-465.
7. **McLean JS, Wanger G, Gorby YA, Wainstein M, McQuaid J, Ishii SI, Bretschger O, Beyenal H, Nealson KH.** 2010. Quantification of electron transfer rates to a solid phase electron acceptor through the stages of biofilm formation from single cells to multicellular communities. Environmental science & technology **44:**2721-2727.
8. **Schuetz B, Schicklberger M, Kuermann J, Spormann AM, Gescher J.** 2009. Periplasmic electron transfer via the *c*-type cytochromes MtrA and FccA of *Shewanella oneidensis* MR-1. Appl Environ Microb **75:**7789-7796.
9. **Dickschat JS.** 2010. Quorum sensing and bacterial biofilms. Natural product reports **27:**343-369.
10. **Watson WT, Minogue TD, Val DL, von Bodman SB, Churchill ME.** 2002. Structural basis and specificity of acyl-homoserine lactone signal production in bacterial quorum sensing. Molecular cell **9:**685-694.
11. **Ng WL, Bassler BL.** 2009. Bacterial quorum-sensing network architectures. Annual review of genetics **43:**197-222.
12. **Bodor AM, Jansch L, Wissing J, Wagner-Dobler I.** 2011. The luxS mutation causes loosely-bound biofilms in Shewanella oneidensis. BMC research notes **4:**180.
13. **Learman DR, Yi H, Brown SD, Martin SL, Geesey GG, Stevens AM, Hochella MF.** 2009. Involvement of *Shewanella oneidensis* MR-1 LuxS in Biofilm Development and Sulfur Metabolism. Appl Environ Microb **75:**1301-1307.
14. **Rezzonico F, Duffy B.** 2008. Lack of genomic evidence of AI-2 receptors suggests a non-quorum sensing role for luxS in most bacteria. Bmc Microbiol **8**.
15. **Higgins DA, Pomianek ME, Kraml CM, Taylor RK, Semmelhack MF, Bassler BL.** 2007. The major Vibrio cholerae autoinducer and its role in virulence factor production. Nature **450:**883-886.
16. **Vendeville A, Winzer K, Heurlier K, Tang CM, Hardie KR.** 2005. Making 'sense' of metabolism: autoinducer-2, LuxS and pathogenic bacteria. Nat Rev Microbiol **3:**383-396.
17. **LaSarre B, Federle MJ.** 2013. Exploiting quorum sensing to confuse bacterial pathogens. Microbiology and molecular biology reviews : MMBR **77:**73-111.

18. **Dong YH, Wang LH, Xu JL, Zhang HB, Zhang XF, Zhang LH.** 2001. Quenching quorum-sensing-dependent bacterial infection by an N-acyl homoserine lactonase. Nature **411:**813-817.
19. **Wang L, Li J, March JC, Valdes JJ, Bentley WE.** 2005. luxS-dependent gene regulation in Escherichia coli K-12 revealed by genomic expression profiling. Journal of bacteriology **187:**8350-8360.
20. **Xavier KB, Miller ST, Lu W, Kim JH, Rabinowitz J, Pelczer I, Semmelhack MF, Bassler BL.** 2007. Phosphorylation and processing of the quorum-sensing molecule autoinducer-2 in enteric bacteria. ACS chemical biology **2:**128-136.
21. **Hong KW, Koh CL, Sam CK, Yin WF, Chan KG.** 2012. Quorum quenching revisited--from signal decays to signalling confusion. Sensors **12:**4661-4696.
22. **Uroz S, Chhabra SR, Camara M, Williams P, Oger P, Dessaux Y.** 2005. N-Acylhomoserine lactone quorum-sensing molecules are modified and degraded by Rhodococcus erythropolis W2 by both amidolytic and novel oxidoreductase activities. Microbiology **151:**3313-3322.
23. **Yang WW, Han JI, Leadbetter JR.** 2006. Utilization of homoserine lactone as a sole source of carbon and energy by soil Arthrobacter and Burkholderia species. Archives of microbiology **185:**47-54.
24. **Huang JJ, Han JI, Zhang LH, Leadbetter JR.** 2003. Utilization of acyl-homoserine lactone quorum signals for growth by a soil pseudomonad and Pseudomonas aeruginosa PAO1. Appl Environ Microbiol **69:**5941-5949.
25. **Flagan S, Ching WK, Leadbetter JR.** 2003. Arthrobacter strain VAI-A utilizes acyl-homoserine lactone inactivation products and stimulates quorum signal biodegradation by Variovorax paradoxus. Appl Environ Microbiol **69:**909-916.
26. **Myers CR, Nealson KH.** 1988. Bacterial manganese reduction and growth with manganese oxide as the sole electron acceptor. Science **240:**1319-1321.
27. **Neal AL, Dublin SN, Taylor J, Bates DJ, Burns L, Apkarian R, DiChristina TJ.** 2007. Terminal electron acceptors influence the quantity and chemical composition of capsular exopolymers produced by anaerobically growing *Shewanella* spp. Biomacromolecules **8:**166-174.
28. **Taratus EM, Eubanks SG, DiChristina TJ.** 2000. Design and application of a rapid screening technique for isolation of selenite reduction-deficient mutants of *Shewanella putrefaciens*. Microbiological Research **155:**79-85.
29. **Blakeney MD, Moulaei T, DiChristina TJ.** 2000. Fe(III) reduction activity and cytochrome content of *Shewanella putrefaciens* grown on ten compounds as sole terminal electron acceptor. Microbiological Research **155:**87-94.
30. **Payne AN, DiChristina TJ.** 2006. A rapid mutant screening technique for detection of technetium [Tc(VII)] reduction-deficient mutants of *Shewanella oneidensis* MR-1. FEMS Microbiology Letters **259:**282-287.
31. **Burns JL, Ginn BR, Bates DJ, Dublin SN, Taylor JV, Apkarian RP, Amaro-Garcia S, Neal AL, Dichristina TJ.** 2010. Outer Membrane-Associated Serine Protease Involved in Adhesion of *Shewanella oneidensis* to Fe(III) Oxides. Environmental science & technology **44:**68-73.
32. **Dale JR, Wade R, DiChristina TJ.** 2007. A conserved histidine in cytochrome *c* maturation permease CcmB of *Shewanella putrefaciens* is required for anaerobic

growth below a threshold standard redox potential. Journal of bacteriology **189:**1036-1043.

33. **Burns JL, DiChristina TJ.** 2009. Anaerobic Respiration of Elemental Sulfur and Thiosulfate by *Shewanella oneidensis* MR-1 Requires *psrA*, a Homolog of the *phsA* Gene of *Salmonella enterica* Serovar Typhimurium LT2. Appl Environ Microb **75:**5209-5217.
34. **Kovach ME, Elzer PH, Hill DS, Robertson GT, Farris MA, Roop RM, Peterson KM.** 1995. Four new derivatives of the broad-host-range cloning vector PBBR1MCS, carrying different antibiotic-resistance cassettes. Gene **166:**175-176.
35. **DiChristina TJ, Moore CM, Haller CA.** 2002. Dissimilatory Fe(III) and Mn(IV) reduction by *Shewanella putrefaciens* requires *ferE*, a homolog of the *pulE* (*gspE*) type II protein secretion gene. Journal of bacteriology **184:**142-151.
36. **Altschul SF, Madden TL, Schaffer AA, Zhang JH, Zhang Z, Miller W, Lipman DJ.** 1997. Gapped BLAST and PSI-BLAST: a new generation of protein database search programs. Nucleic Acids Res **25:**3389-3402.
37. **Zhang MN, Dale JR, DiChristina TJ, Stack AG.** 2009. Dissolution Morphology of Iron (Oxy)(Hydr)Oxides Exposed to the Dissimilatory Iron-Reducing Bacterium *Shewanella oneidensis* MR-1. Geomicrobiology Journal **26:**83-92.
38. **Grantham MC, Dove PM, DiChristina TJ.** 1997. Microbially catalyzed dissolution of iron and aluminum oxyhydroxide mineral surface coatings. Geochimica Et Cosmochimica Acta **61:**4467-4477.
39. **Song XN, Qiu HB, Xiao X, Cheng YY, Li WW, Sheng GP, Li XY, Yu HQ.** 2014. Determination of autoinducer-2 in biological samples by high-performance liquid chromatography with fluorescence detection using pre-column derivatization. Journal of chromatography. A **1361:**162-168.
40. **Stookey LL.** 1970. Ferrozine - a new spectrophotometric reagent for iron. Analytical Chemistry **42:**779-781.
41. **Montgomery HAC, Dymock JF.** 1962. Rapid determination of nitrate in fresh and saline waters. Analyst **87:**374-378.
42. **Kelly DP, Wood AP.** 1994. Synthesis and determination of thiosulfate and polythionates. Method Enzymol **243:**475-501.
43. **Heidelberg JF, Paulsen IT, Nelson KE, Gaidos EJ, Nelson WC, Read TD, Eisen JA, Seshadri R, Ward N, Methe B, Clayton RA, Meyer T, Tsapin A, Scott J, Beanan M, Brinkac L, Daugherty S, DeBoy RT, Dodson RJ, Durkin AS, Haft DH, Kolonay JF, Madupu R, Peterson JD, Umayam LA, White O, Wolf AM, Vamathevan J, Weidman J, Impraim M, Lee K, Berry K, Lee C, Mueller J, Khouri H, Gill J, Utterback TR, McDonald LA, Feldblyum TV, Smith HO, Venter JC, Nealson KH, Fraser CM.** 2002. Genome sequence of the dissimilatory metal ion-reducing bacterium Shewanella oneidensis. Nat Biotechnol **20:**1118-1123.
44. **Hudaiberdiev s, Choudhary KS, Alvarez RV, Gelencser Z, Ligeti B, Lamba D, Pongor S.** 2015. Census of solo LuxR genes in prokaryotic genomes. Frontiers in Cellular and Infection Microbiology **5**.

45. **Patel HK, Suarez-Moreno ZR, Degrassi G, Subramoni S, Gonzalez JF, Venturi V.** 2013. Bacterial LuxR solos have evolved to respond to different molecules including signals from plants. Frontiers in Plant Science **4**.
46. **Venturi V, Subramoni S.** 2009. Luxr-family 'solos': bachelor sensors/regulators of signaling molecules. Microbiology **155:**1377-1385.
47. **Cooper RE, Burns JL, DiChristina TJ.** 2015. S-Ribosylhomocysteine lyase (LuxS)-dependent biofilm formation on Fe(III) oxide surfaces dos not enhance Fe(III) oxide reduction activity in *Shewanella oneidensis*. Environmental Microbiology **Submitted**.
48. **Venkateswaran K, Moser DP, Dollhopf ME, Lies DP, Saffarini DA, MacGregor BJ, Ringelberg DB, White DC, Nishijima M, Sano H, Burghardt J, Stackebrandt E, Nealson KH.** 1999. Polyphasic taxonomy of the genus *Shewanella* and description of *Shewanella oneidensis* sp. nov. Int J Syst Bacteriol **49:**705-724.
49. **Fennessey CM, Jones ME, Taillefert M, DiChristina TJ.** 2010. Siderophores are not involved in Fe(III) solubilization during anaerobic Fe(III) respiration by *Shewanella oneidensis* MR-1. Appl Environ Microb **76:**2425-2432.
50. **Jones ME, Fennessey CM, DiChristina TJ, Taillefert M.** 2010. *Shewanella oneidensis* MR-1 mutants selected for their inability to produce soluble organic-Fe(III) complexes are unable to respire Fe(III) as anaerobic electron acceptor. Environmental Microbiology **12:**938-950.
51. **Marsili E, Baron DB, Shikhare ID, Coursolle D, Gralnick JA, Bond DR.** 2008. *Shewanella* secretes flavins that mediate extracellular electron transfer. Proceedings of the National Academy of Sciences of the United States of America **105:**3968-3973.
52. **Pirbadian S, Barchinger SE, Leung KM, Byun HS, Jangir Y, Bouhenni RA, Reed SB, Romine MF, Saffarini DA, Shi L, Gorby YA, Golbeck JH, El-Naggar MY.** 2014. *Shewanella oneidensis* MR-1 nanowires are outer membrane and periplasmic extensions of the extracellular electron transport components. Proceedings of the National Academy of Sciences of the United States of America **111:**12883-12888.
53. **Roden EE, Kappler A, Bauer I, Jiang J, Paul A, Stoesser R, Konishi H, Xu HF.** 2010. Extracellular electron transfer through microbial reduction of solid-phase humic substances. Nat Geosci **3:**417-421.
54. **Taillefert M, Beckler JS, Carey E, Burns JL, Fennessey CM, DiChristina TJ.** 2007. *Shewanella putrefaciens* produces an Fe(III)-solubilizing organic ligand during anaerobic respiration on insoluble Fe(III) oxides. J Inorg Biochem **101:**1760-1767.
55. **von Canstein H, Ogawa J, Shimizu S, Lloyd JR.** 2008. Secretion of flavins by *Shewanella* species and their role in extracellular electron transfer. Appl Environ Microb **74:**615-623.
56. **White GF, Shi Z, Shi L, Wang ZM, Dohnalkova AC, Marshall MJ, Fredrickson JK, Zachara JM, Butt JN, Richardson DJ, Clarke TA.** 2013. Rapid electron exchange between surface-exposed bacterial cytochromes and Fe(III) minerals. Proceedings of the National Academy of Sciences of the United States of America **110:**6346-6351.

57. **Flynn CM, Hunt KA, Gralnick JA, Srienc F.** 2012. Construction and elementary mode analysis of a metabolic model for Shewanella oneidensis MR-1. Biosystems **107:**120-128.
58. **Melton ED, Swanner ED, Behrens S, Schmidt C, Kappler A.** 2014. The interplay of microbially mediated and abiotic reactions in the biogeochemical Fe cycle. Nat Rev Microbiol **12:**797-808.
59. **Lupp C, Ruby EG.** 2005. Vibrio fischeri uses two quorum-sensing systems for the regulation of early and late colonization factors. Journal of bacteriology **187:**3620-3629.
60. **Henke JM, Bassler BL.** 2004. Three parallel quorum-sensing systems regulate gene expression in Vibrio harveyi. Journal of bacteriology **186:**6902-6914.
61. **Bassler B, Hammer BK.** 2003. Quorum sensing controls biofilm formation in Vibrio cholerae. Molecular Microbiology **501:**101-104.
62. **Waters CM, Bassler BL.** 2005. Quorum sensing: Cell-to-cell communication in bacteria. Annu Rev Cell Dev Bi **21:**319-346.
63. **Miller MB, Skorupski K, Lenz DH, Taylor RK, Bassler BL.** 2002. Parallel quorum sensing systems converge to regulate virulence in Vibrio cholerae. Cell **110:**303-314.
64. **Perez PD, Weiss JT, Hagen SJ.** 2011. Noise and crosstalk in two quorum-sensing inputs of Vibrio fischeri. BMC systems biology **5:**153.
65. **Waters CM, Bassler BL.** 2006. The Vibrio harveyi quorum-sensing system uses shared regulatory components to discriminate between multiple autoinducers. Genes & development **20:**2754-2767.
66. **Surette MG, Miller MB, Bassler BL.** 1999. Quorum sensing in Escherichia coli, Salmonella typhimurium, and Vibrio harveyi: a new family of genes responsible for autoinducer production. Proc Natl Acad Sci U S A **96:**1639-1644.
67. **Winzer K, Hardie KR, Williams P.** 2003. LuxS and autoinducer-2: their contribution to quorum sensing and metabolism in bacteria. Advances in applied microbiology **53:**291-396.
68. **Schauder S, Shokat K, Surette MG, Bassler BL.** 2001. The LuxS family of bacterial autoinducers: biosynthesis of a novel quorum-sensing signal molecule. Mol Microbiol **41:**463-476.
69. **De Keersmaecker SC, Sonck K, Vanderleyden J.** 2006. Let LuxS speak up in AI-2 signaling. Trends in microbiology **14:**114-119.
70. **Hardie KR, Heurlier K.** 2008. Establishing bacterial communities by 'word of mouth': LuxS and autoinducer 2 in biofilm development. Nat Rev Microbiol **6:**635-643.
71. **Xavier KB, Bassler BL.** 2003. LuxS quorum sensing: more than just a numbers game. Current opinion in microbiology **6:**191-197.
72. **Bassler B.** 2002. How bacteria talk to each other. Mol Biol Cell **13:**2a-2a.
73. **Winzer K, Hardie KR, Burgess N, Doherty N, Kirke D, Holden MTG, Linforth R, Cornell KA, Taylor AJ, Hill PJ, Williams P.** 2002. LuxS: its role in central metabolism and the in vitro synthesis of 4-hydroxy-5-methyl-3(2H)-furanone. Microbiol-Sgm **148:**909-922.

74. **Cooper RE, Goff JL, Reed BC, Sekar R, DiChristina TJ.** 2014. Breathing metals: Molecular mechanisms of microbial iron reduction, Manual of Environmental Microbiology. ASM Press.
75. **Wee SK, Burns JL, DiChristina TJ.** 2014. Identification of a molecular signature unique to metal-reducing Gammaproteobacteria. FEMS Microbiol Lett **350:**90-99.
76. **Flynn TM, O'Loughlin EJ, Mishra B, DiChristina TJ, Kemner KM.** 2014. Sulfur-mediated electron shuttling during bacterial iron reduction. Science **344:**1039-1042.
77. **Wilder CN, Diggle SP, Schuster M.** 2011. Cooperation and cheating in Pseudomonas aeruginosa: the roles of the las, rhl and pqs quorum-sensing systems. The ISME journal **5:**1332-1343.
78. **Chu YY, Nega M, Wolfle M, Plener L, Grond S, Jung K, Gotz F.** 2013. A new class of quorum quenching molecules from Staphylococcus species affects communication and growth of gram-negative bacteria. PLoS pathogens **9:**e1003654.
79. **Flagan SF, Leadbetter JR.** 2006. Utilization of capsaicin and vanillylamine as growth substrates by Capsicum (hot pepper)-associated bacteria. Environ Microbiol **8:**560-565.
80. **Wang YJ, Huang JJ, Leadbetter JR.** 2007. Acyl-HSL signal decay: intrinsic to bacterial cell-cell communications. Advances in applied microbiology **61:**27-58.
81. **Taga ME, Bassler BL.** 2003. Chemical communication among bacteria. Proc Natl Acad Sci U S A **100 Suppl 2:**14549-14554.

**Figures**

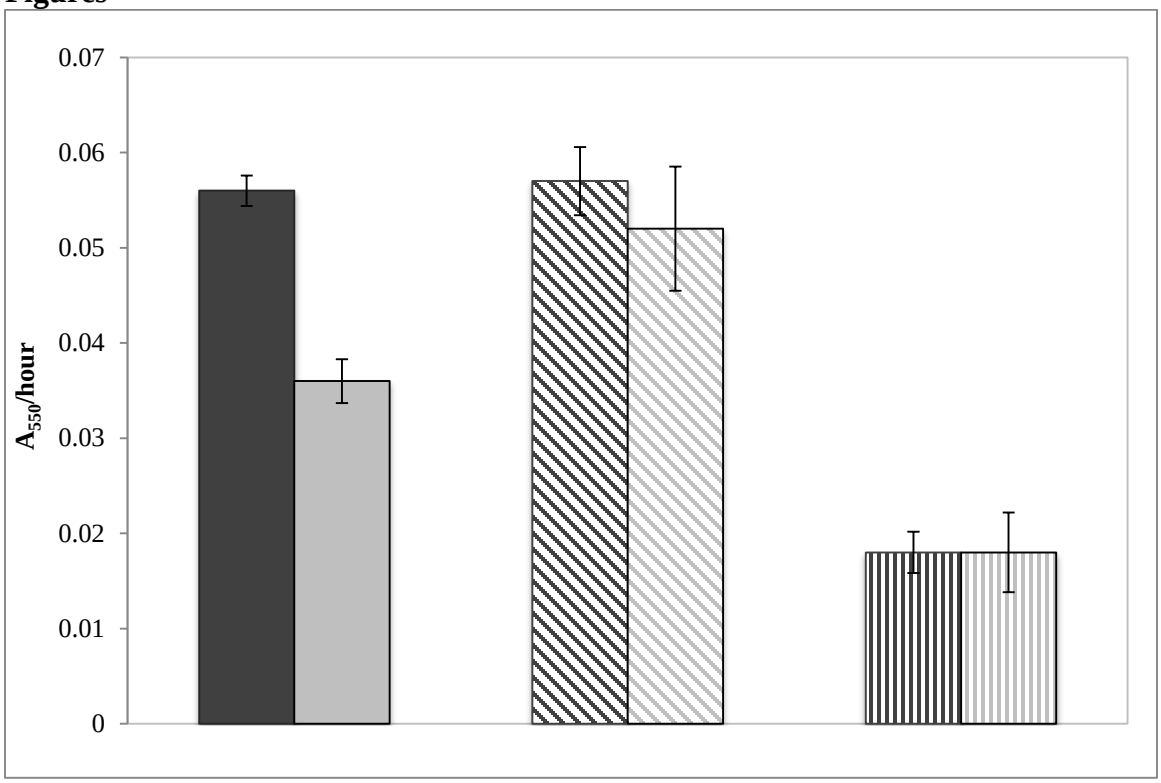


**Figure 3.1. Rates of aerobic biofilm formation (measured via the CV assay as increases in $A_{550}$ per hour) by *S. oneidensis* wild-type (dark gray) and Δ*luxS* (light gray) mutant strains with various electron donors, including lactate (WT dark gray, solid; Δ*luxS* light gray, solid), lactate supplemented with exogenous DPD (HAI-2) (WT dark gray, diagonal lines; Δ*luxS* light gray, diagonal lines), and exogenous DPD (HAI-2) (WT dark gray, vertical lines; Δ*luxS* light gray, vertical lines). Values are means of two parallel yet independent anaerobic incubations. Error bars represent range of errors.**

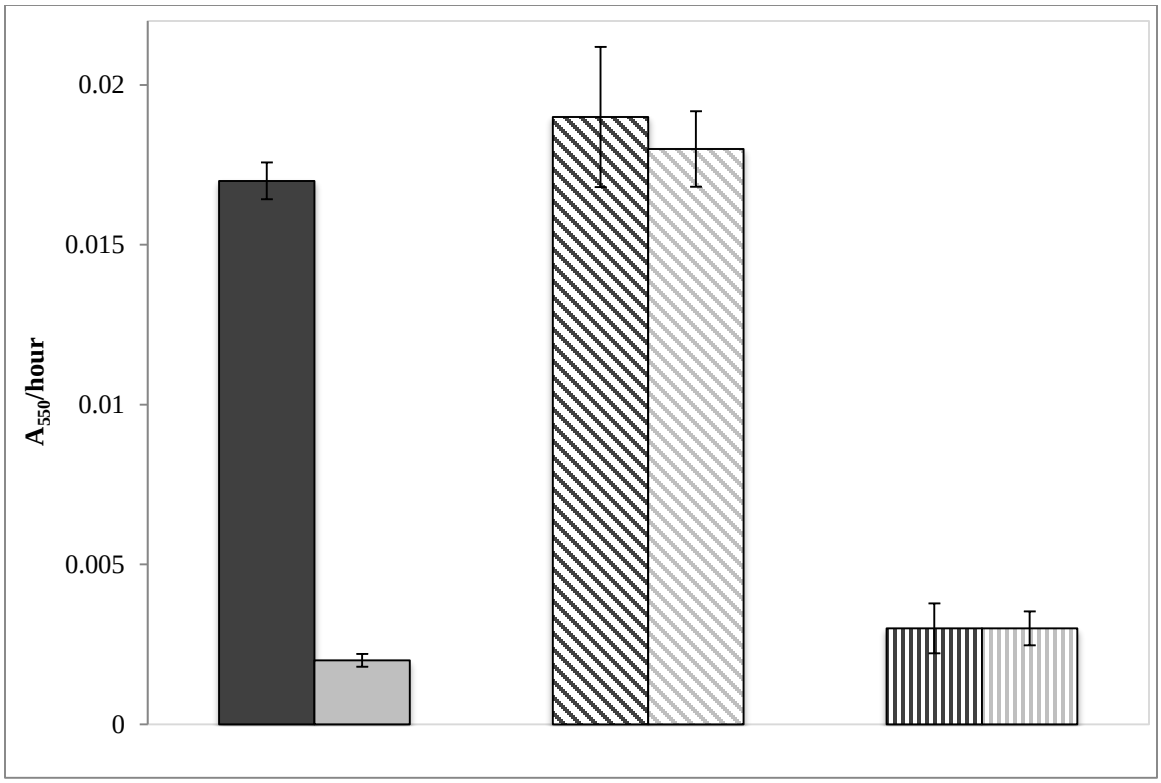


**Figure 3.2. Rates of anaerobic biofilm formation (measured via the CV assay as increases in $A_{550}$ per hour) by *S. oneidensis* wild-type (dark gray) and Δ*luxS* (light gray) mutant strains with thiosulfate as the electron acceptor and various electron donors, including lactate (WT dark gray, solid; Δ*luxS* light gray, solid), lactate supplemented with exogenous DPD (HAI-2) (WT dark gray, diagonal lines; Δ*luxS* light gray, diagonal lines), and exogenous DPD (HAI-2) (WT dark gray, vertical lines; Δ*luxS* light gray, vertical lines). Values are means of two parallel yet independent anaerobic incubations. Error bars represent range of errors.**

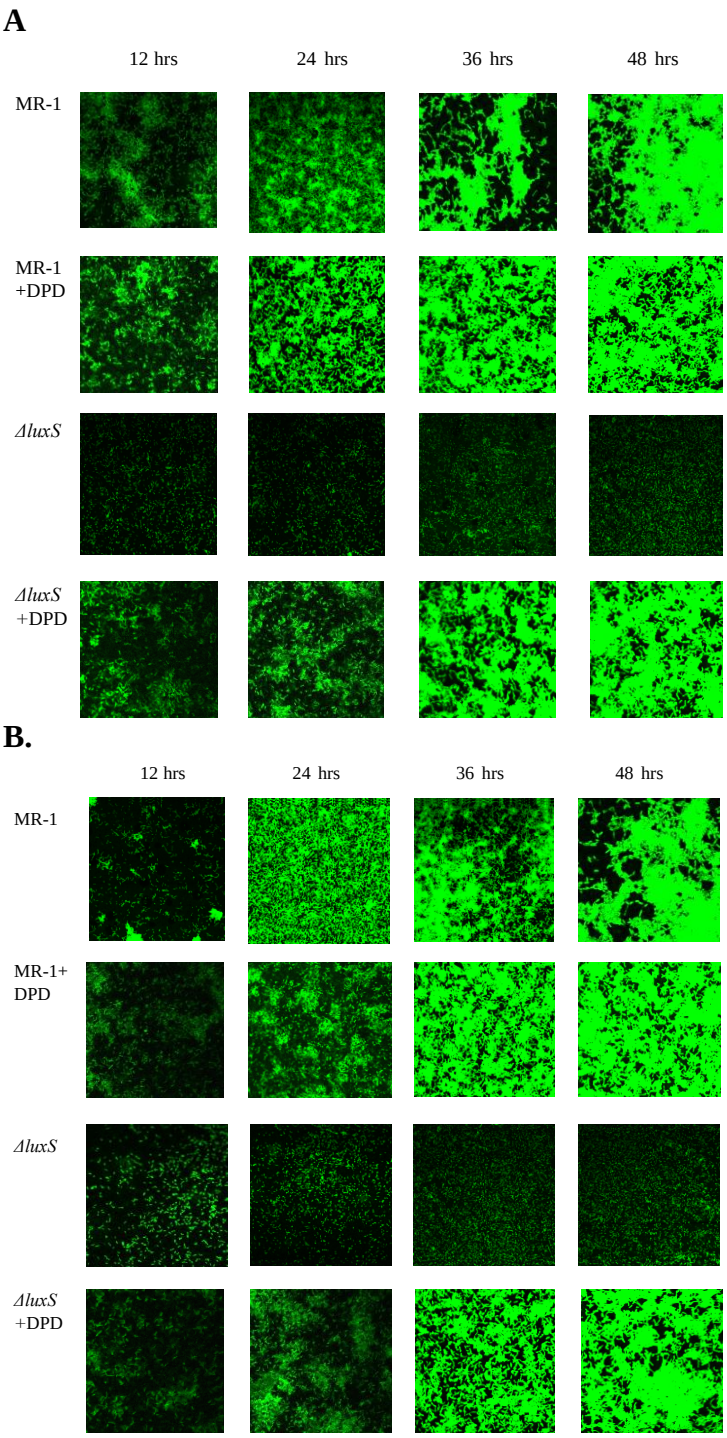


**Figure 3.3. CLSM images of anaerobic biofilms formed by *S. oneidensis* wild-type (MR-1) and Δ*luxS* strains during a 48 hr anaerobic growth period on bare silica surfaces amended with lactate as electron donor and thiosulfate (A) or Fe(III) oxide-coated silica surfaces (B) as electron acceptor with and without the addition of exogenous DPD.**

**A.**

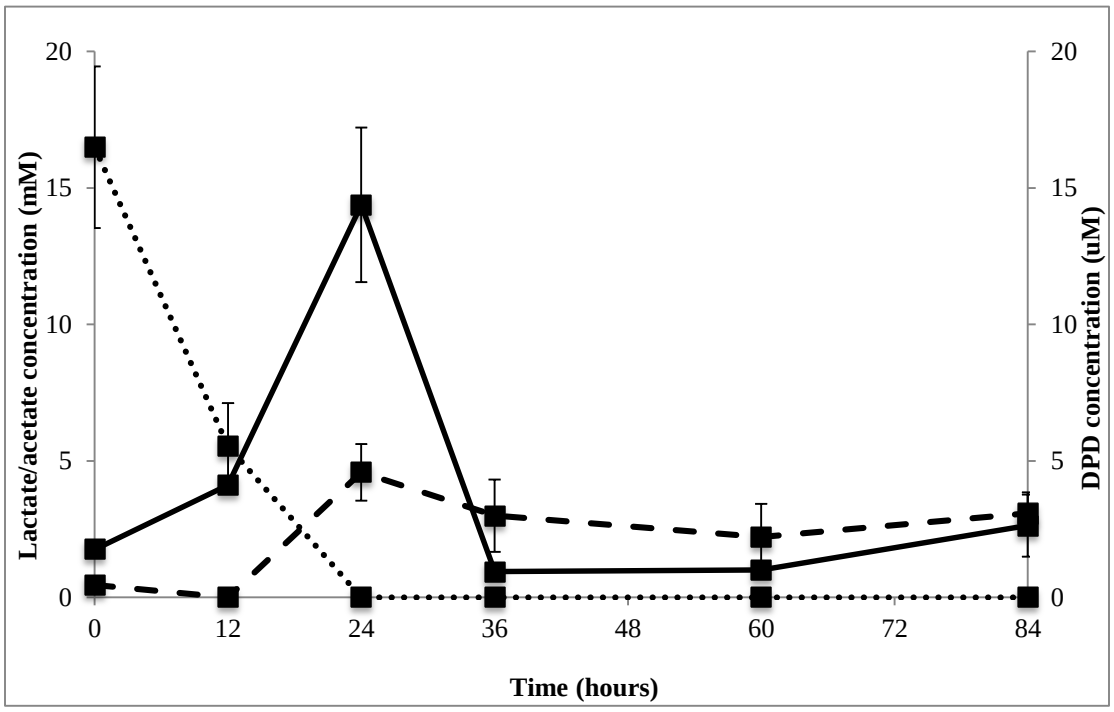


**B.**

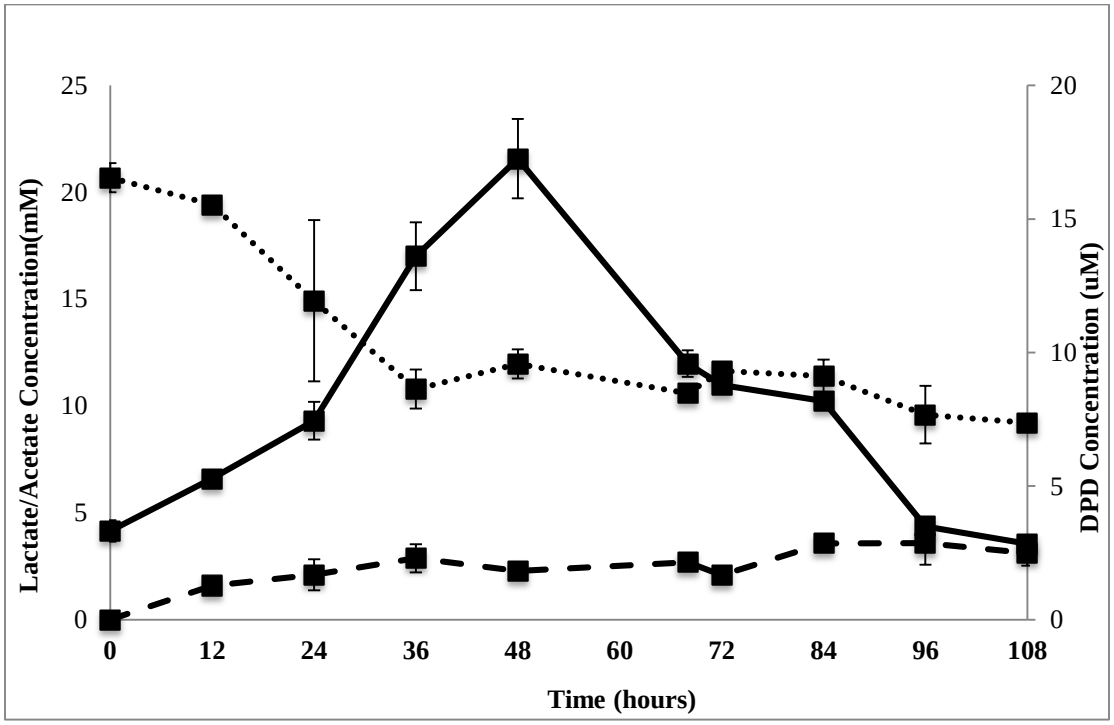


**Figure 3.4. Lactate depletion (dotted line, primary axis), acetate production (dashed line, primary axis), DPD production and subsequent depletion (solid line, secondary axis). (a) *S. oneidensis* wild-type grown under aerobic conditions with lactate as the**

**electron donor. (b) *S. oneidensis* wild-type grown under anaerobic growth conditions with lactate as the electron donor and HFO as the electron acceptor.**

**A.**

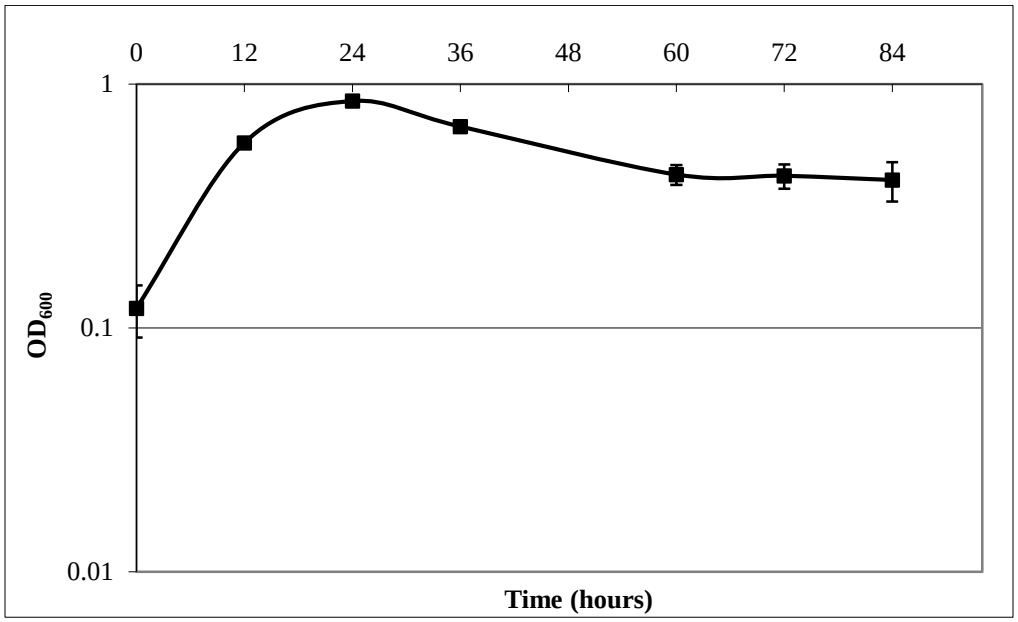


**B.**

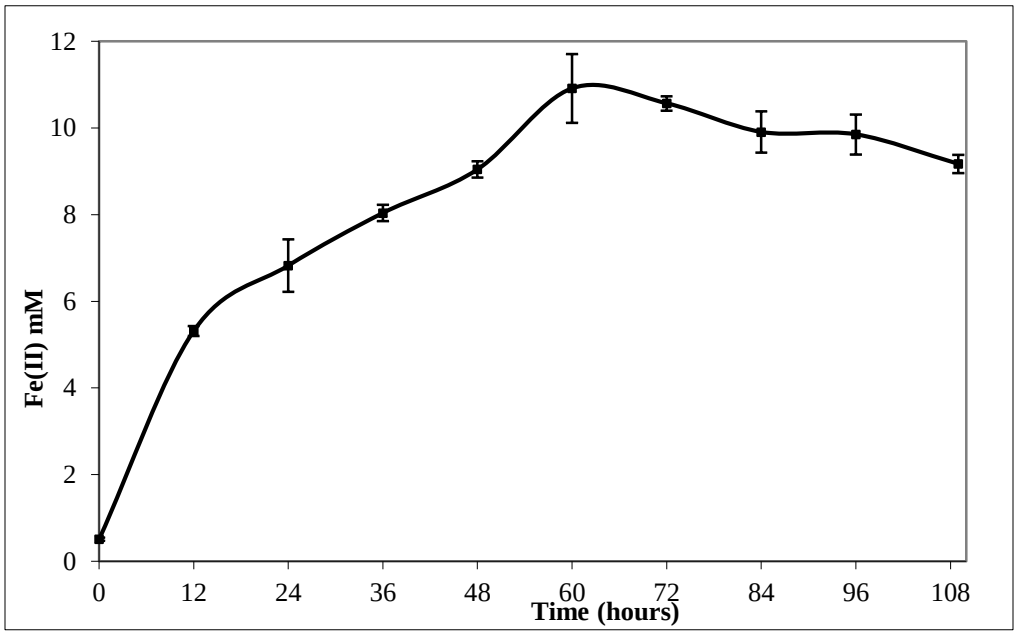


**Figure 3.5. Growth and HFO reduction plots corresponding to Figure 3.4 (lactate depletion, acetate production, DPD production experiments) under aerobic conditions (a) with lactate as the electron donor or anaerobic conditions (b) with lactate as the electron donor and HFO as the electron acceptor.**

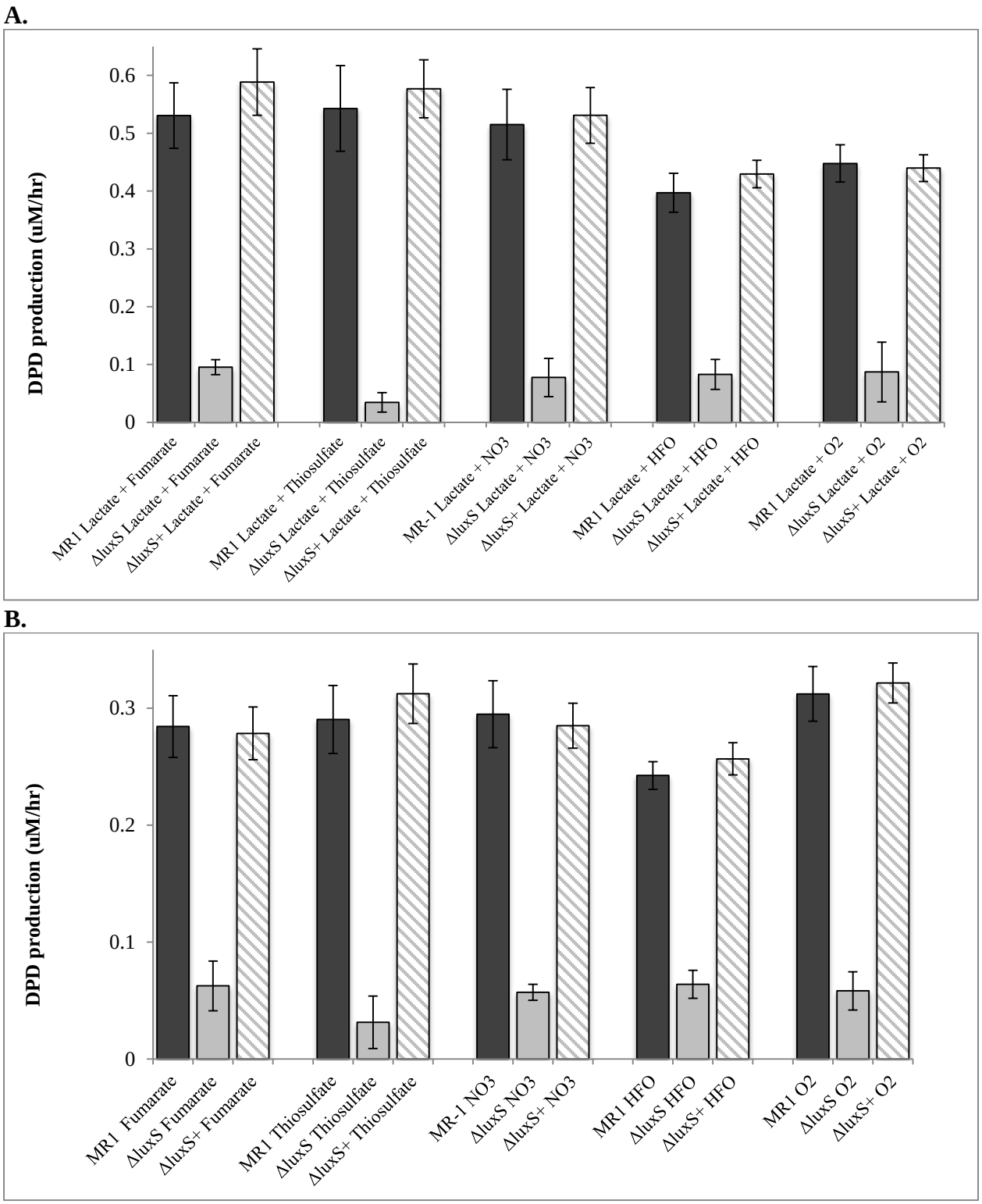


**Figure 3.6**: **Rates of DPD production by *S. oneidensis* wild-type, Δ*luxS,* and Δ*luxS*+ (Δ*luxS* genetic complement) using M1 minimal media under aerobic and anaerobic conditions. (a) DPD production rates with lactate as electron donor. (b) DPD production rates with no electron donor.**

**A.**

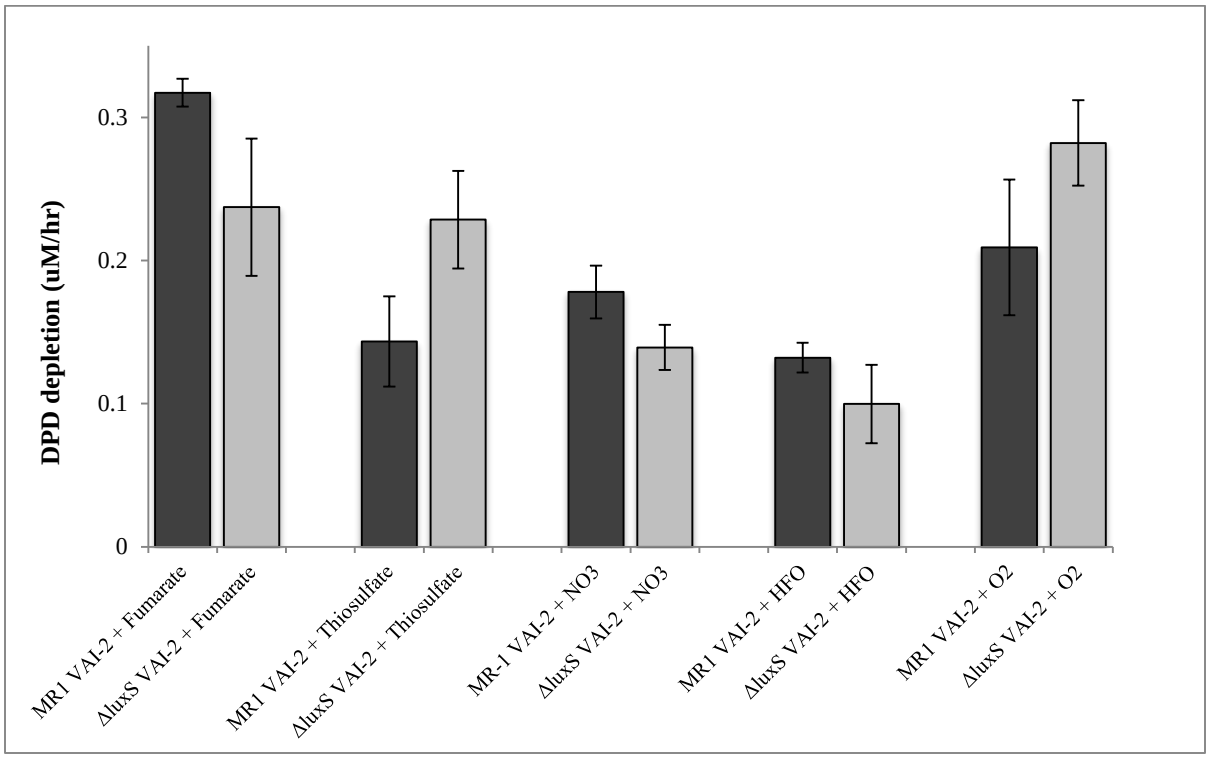


**B.**

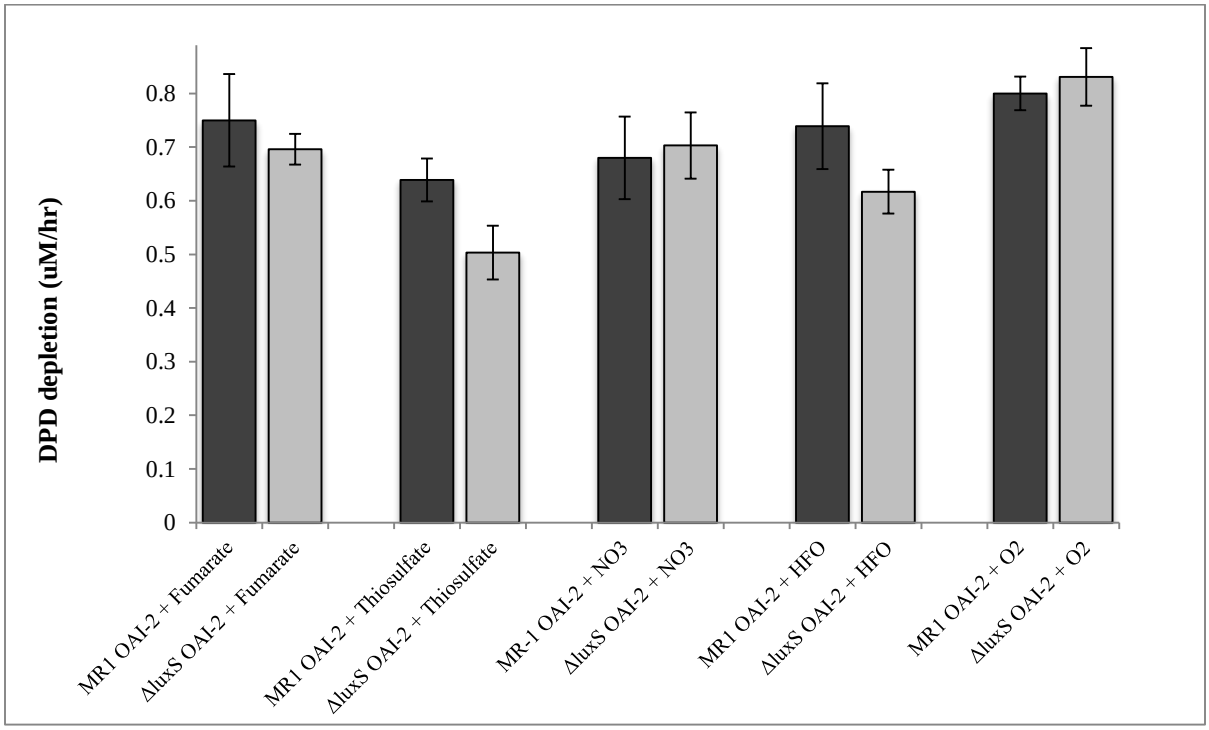


**Figure 3.7: Rates of DPD depletion by *S. oneidensis* wild-type, Δ*luxS,* and Δ*luxS*+ (Δ*luxS* genetic complement) using M1 minimal media under aerobic and anaerobic conditions. (a) *V. harveyi* harvested DPD (HAI-2) depletion rates. (b) *S. oneidensis* harvested DPD (OAI-2) depletion rates.**

**A.**

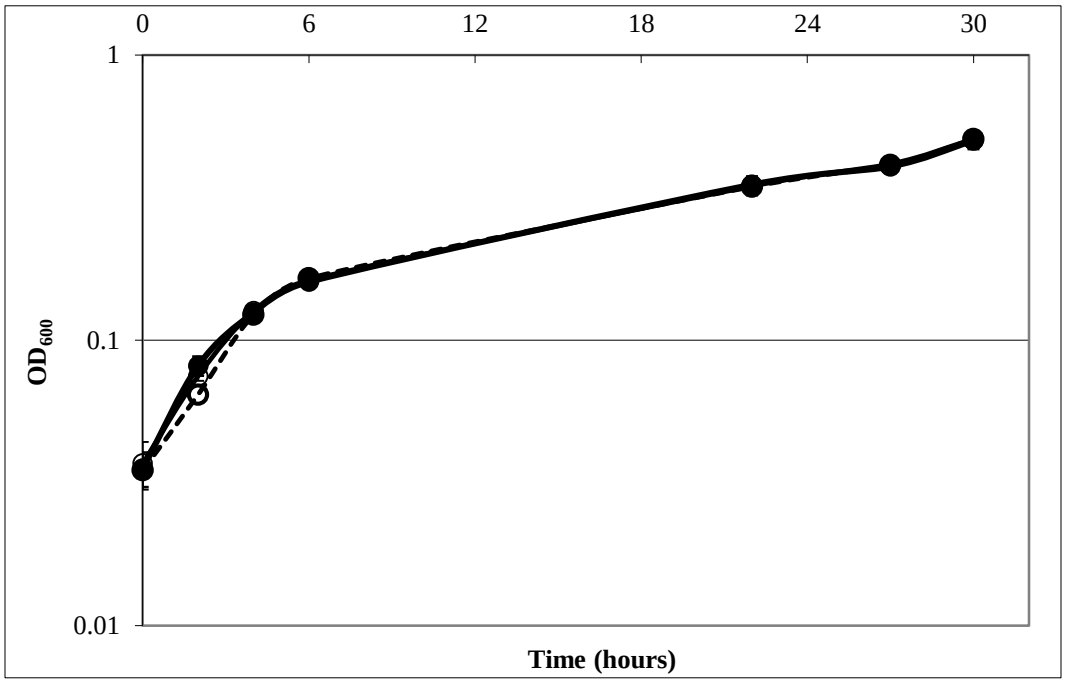
0
6
12
18
24
30
1
0.1
0.01
OD600
Time (hours)

**B.**

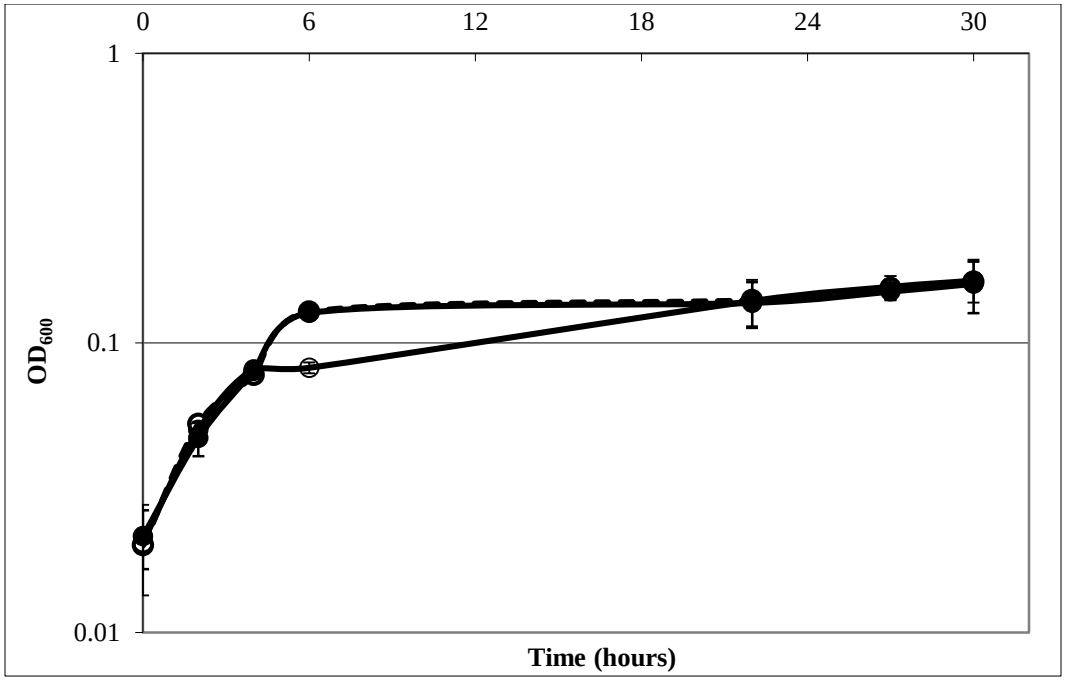
0
6
12
18
24
30
1
0.1
0.01
OD600
Time (hours)

**C.**

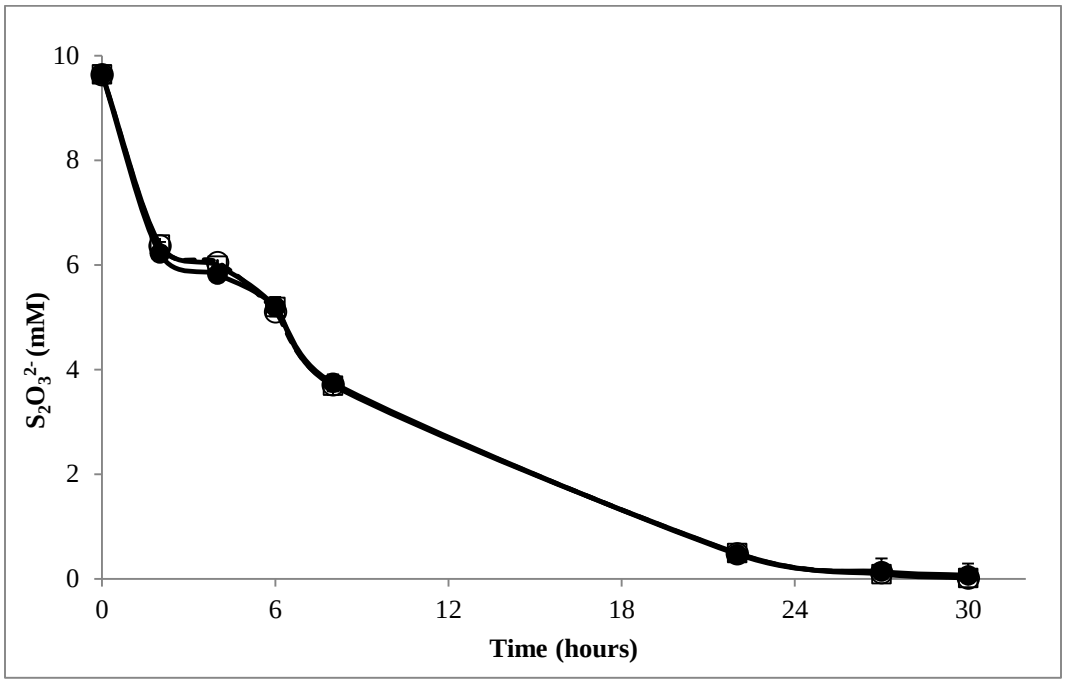
10
8
6
4
2
0
$S_2O_3^{2-}$ (mM)
0
6
12
18
24
30
Time (hours)

**D.**

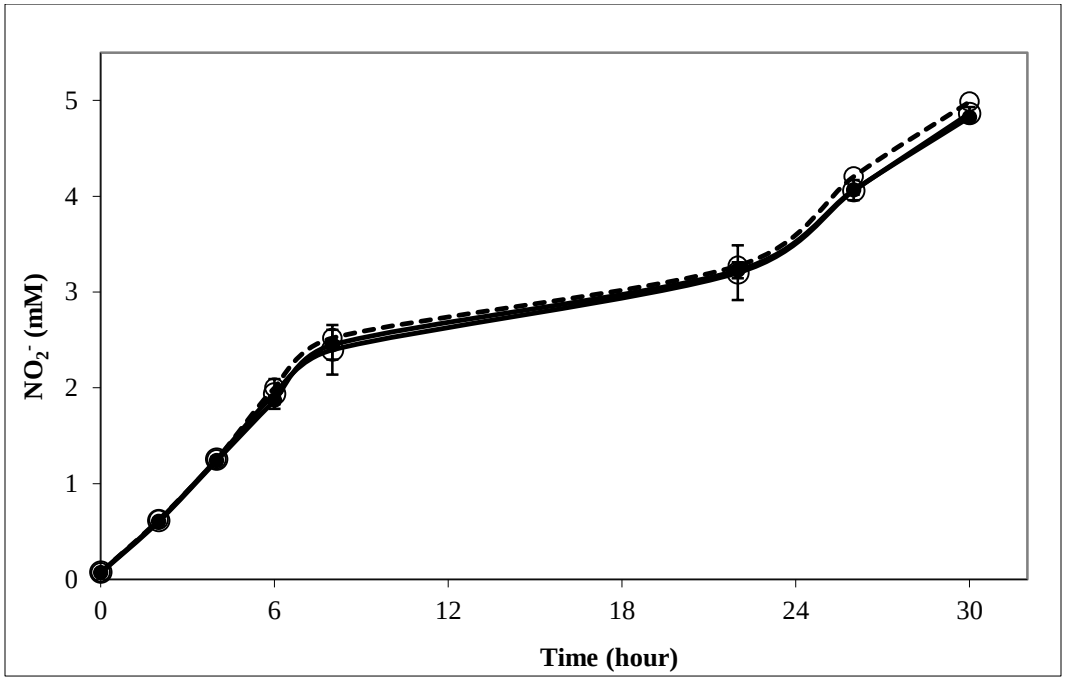
5
4
3
2
1
0
$NO_2^-$ (mM)
0
6
12
18
24
30
Time (hour)

**E.**

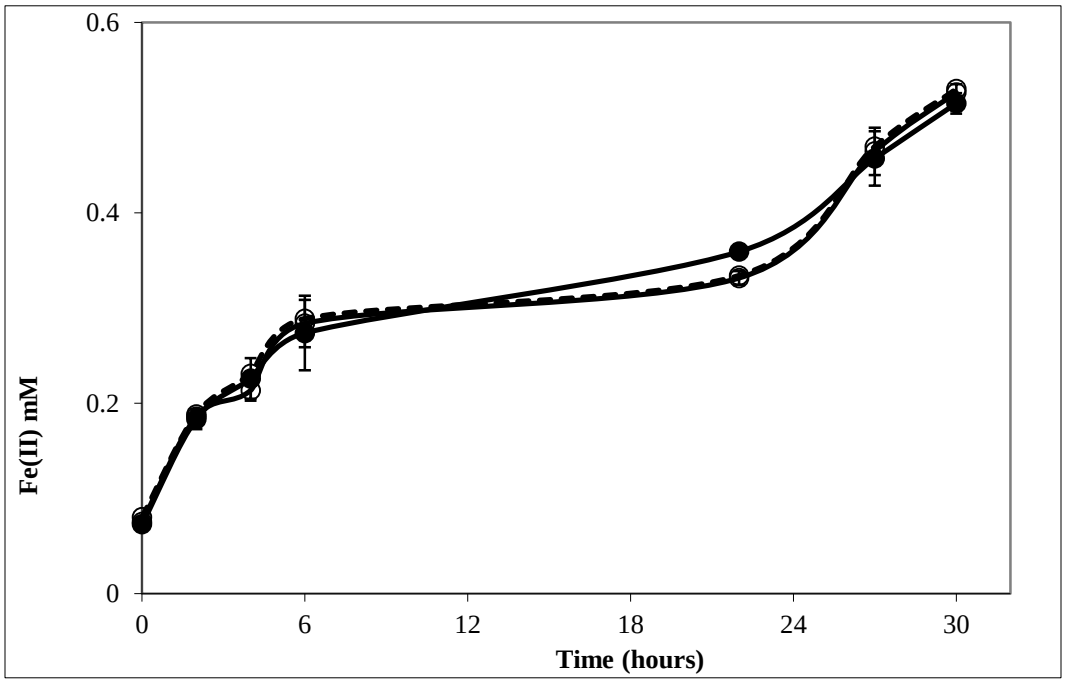


**Figure 3.8. Corresponding aerobic and anaerobic incubations to DPD production experiments involving of *S. oneidensis* wild type, Δ*luxS,* and Δ*luxS+ (ΔluxS* genetic complement) strains amended with lactate (wild-type, closed circles; Δ*luxS,* open circles; Δ*luxS+*, dashed line, open circles) as the electron donor and $O_2$ (a), fumarate (b), thiosulfate (c), nitrate (d), and HFO (e) as electron acceptor. Values are means of two parallel yet independent anaerobic incubations. Error bars represent range of errors. In some cases, error bars are smaller than the symbol.**

**A.**

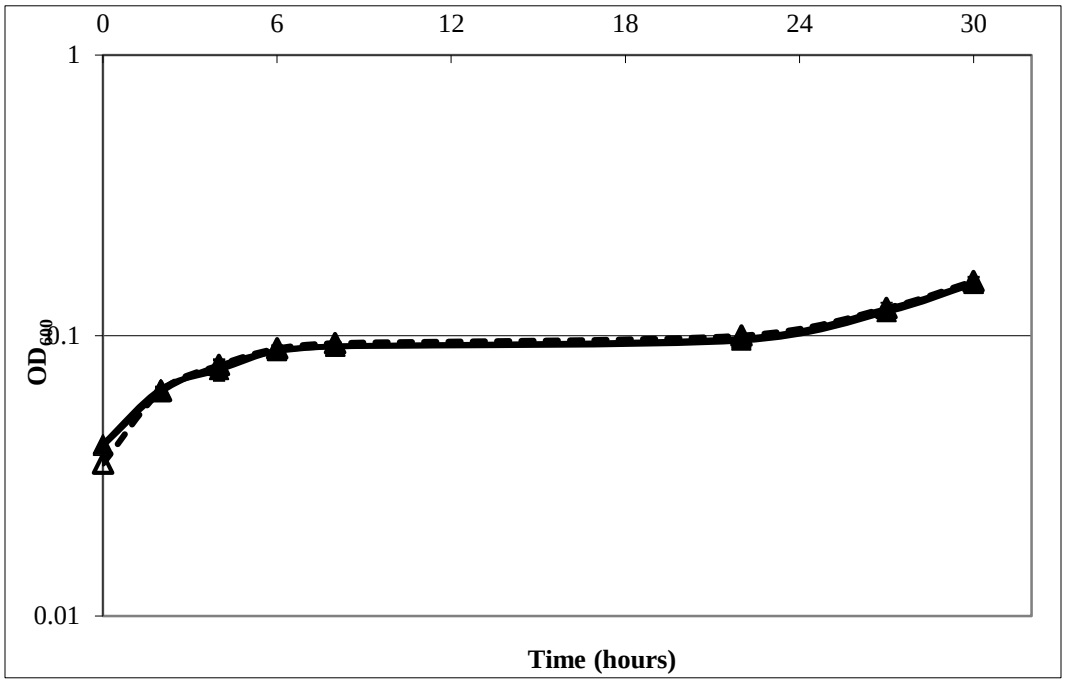
0
6
12
18
24
30
1
0.1
0.01
OD600
Time (hours)

**B.**

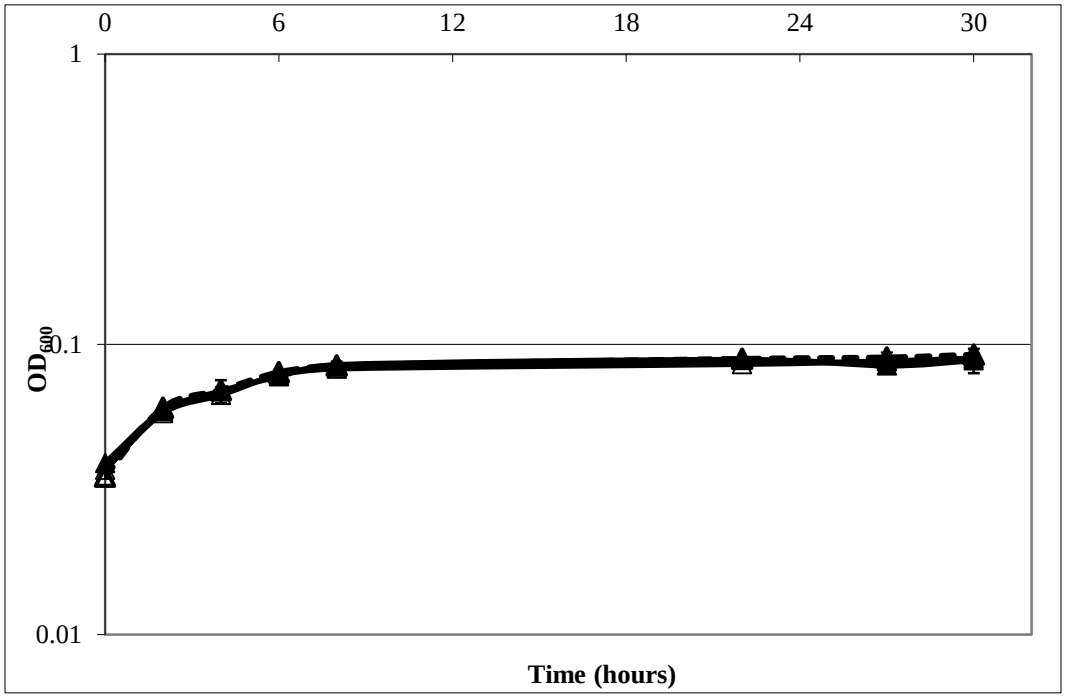
0
6
12
18
24
30
1
0.1
0.01
OD600
Time (hours)

**C.**

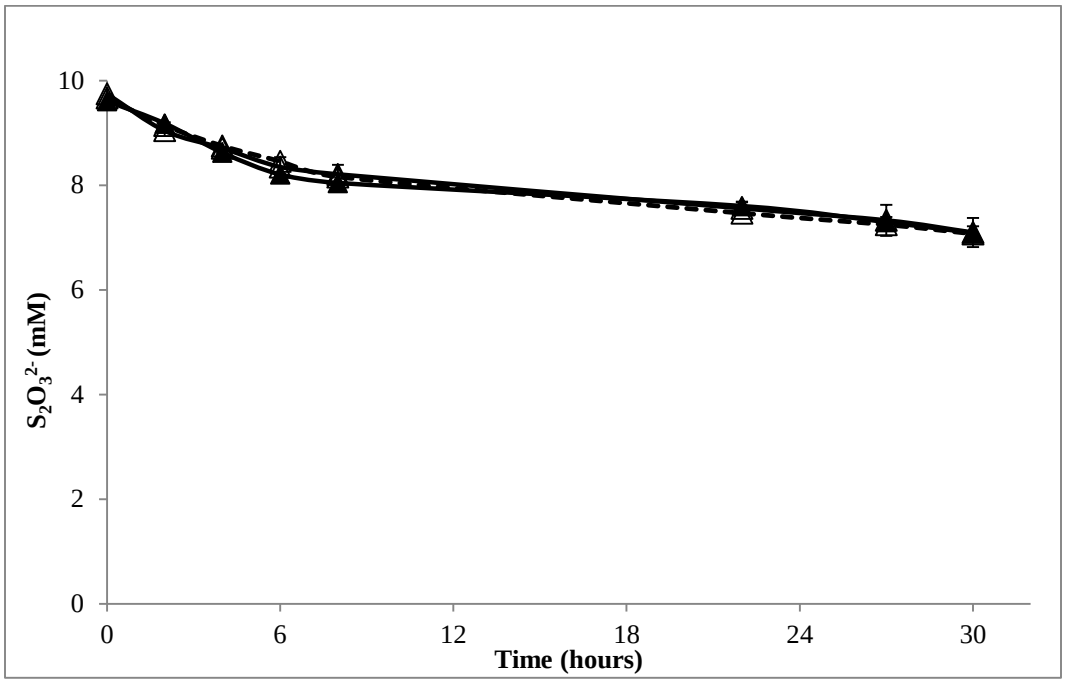
10
8
6
4
2
0
$S_2O_3^{2-}$ (mM)
0
6
12
18
24
30
Time (hours)

**D.**

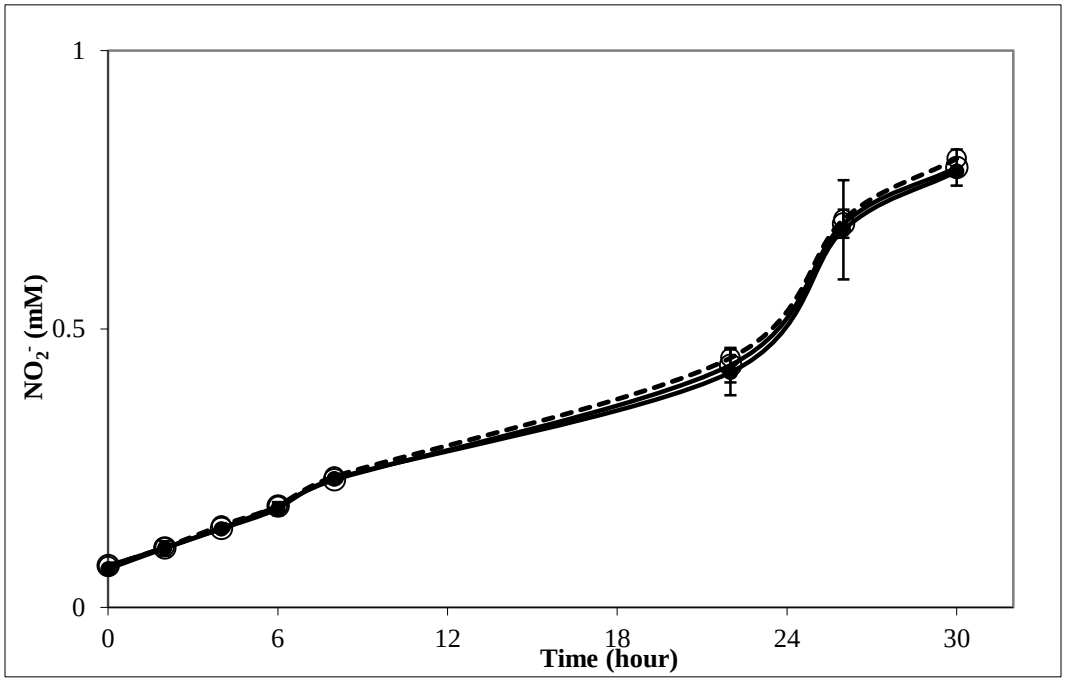
1
0.5
0
$NO_2^-$ (mM)
0
6
12
18
24
30
Time (hour)

**E.**

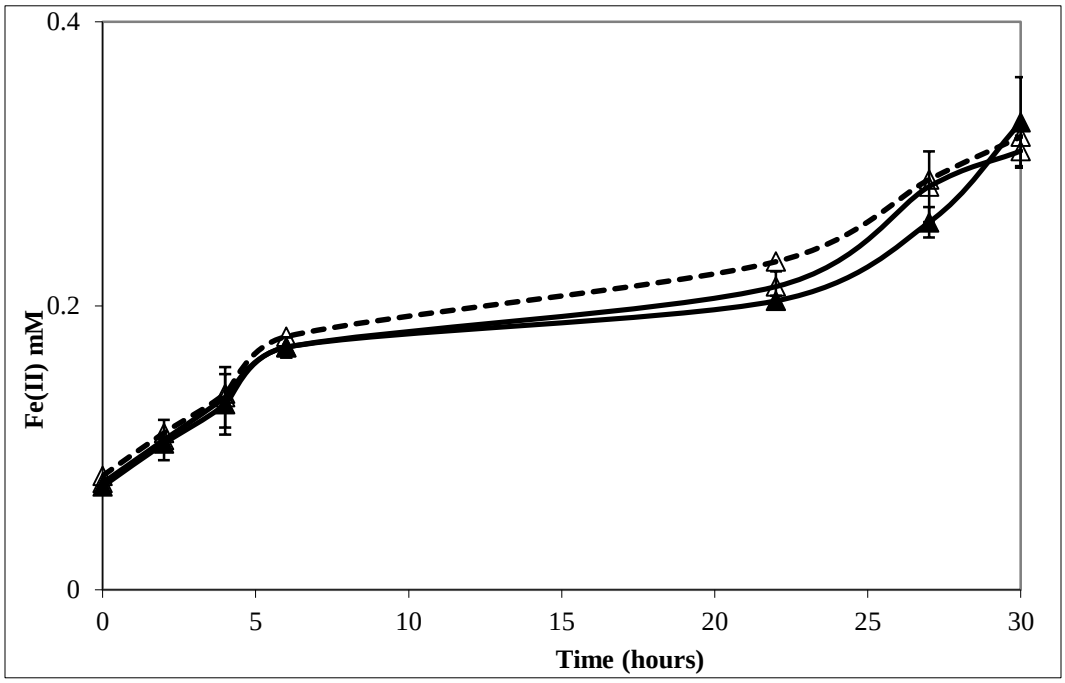


**Figure 3.9. Corresponding aerobic and anaerobic incubations to DPD production experiments involving aerobic and anaerobic incubations of *S. oneidensis* wild type, Δ*luxS*, and Δ*luxS*+ (Δ*luxS* genetic complement) strains with no exogenous electron donor added (wild-type, closed triangles; Δ*luxS*, open triangles; Δ*luxS*+*luxS*, dashed line, open triangles) and $O_2$ (a), fumarate (b), thiosulfate (c), nitrate (d), and HFO (e) as electron acceptor. Values are means of two parallel yet independent anaerobic incubations. Error bars represent range of errors. In some cases, error bars are smaller than the symbol.**

**A.**

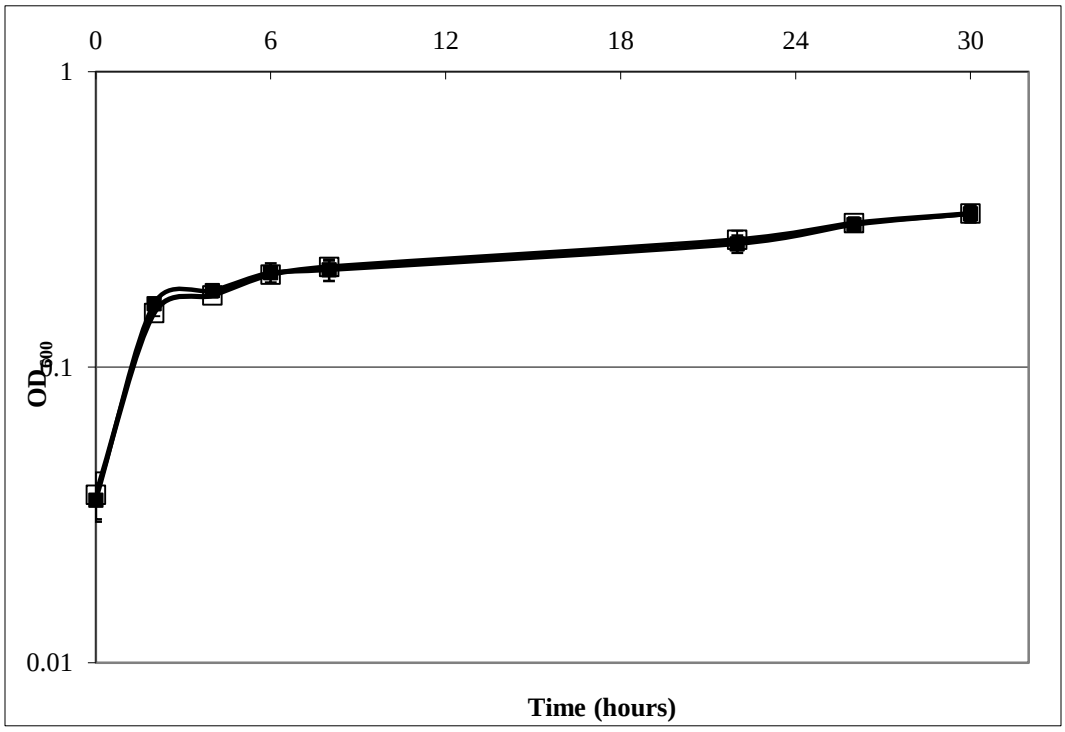
0
6
12
18
24
30
1
0.1
0.01
OD600
Time (hours)

**B.**

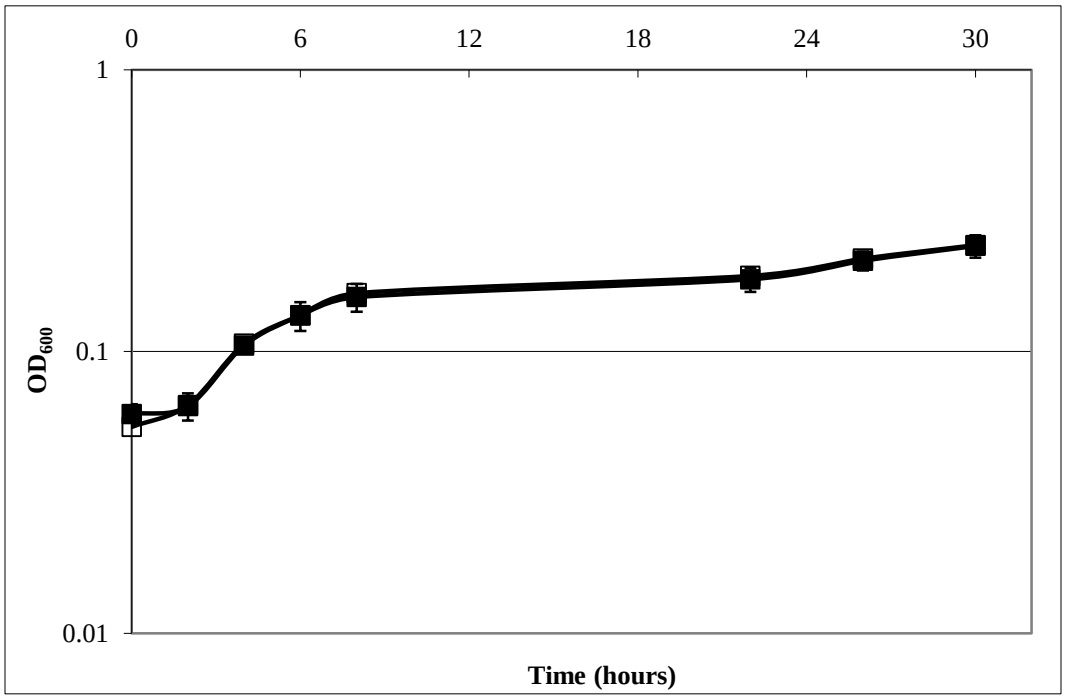
0
6
12
18
24
30
1
0.1
0.01
OD600
Time (hours)

**C.**

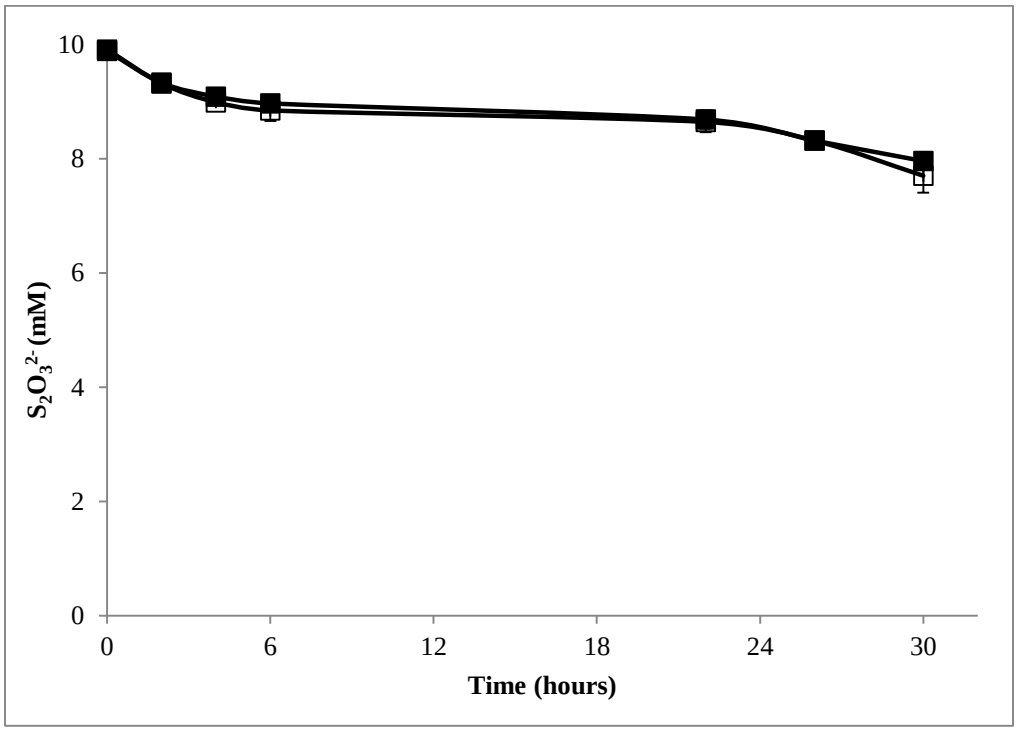
10
8
6
4
2
0
0
6
12
18
24
30
$S_2O_3^{2-}$ (mM)
Time (hours)

**D.**

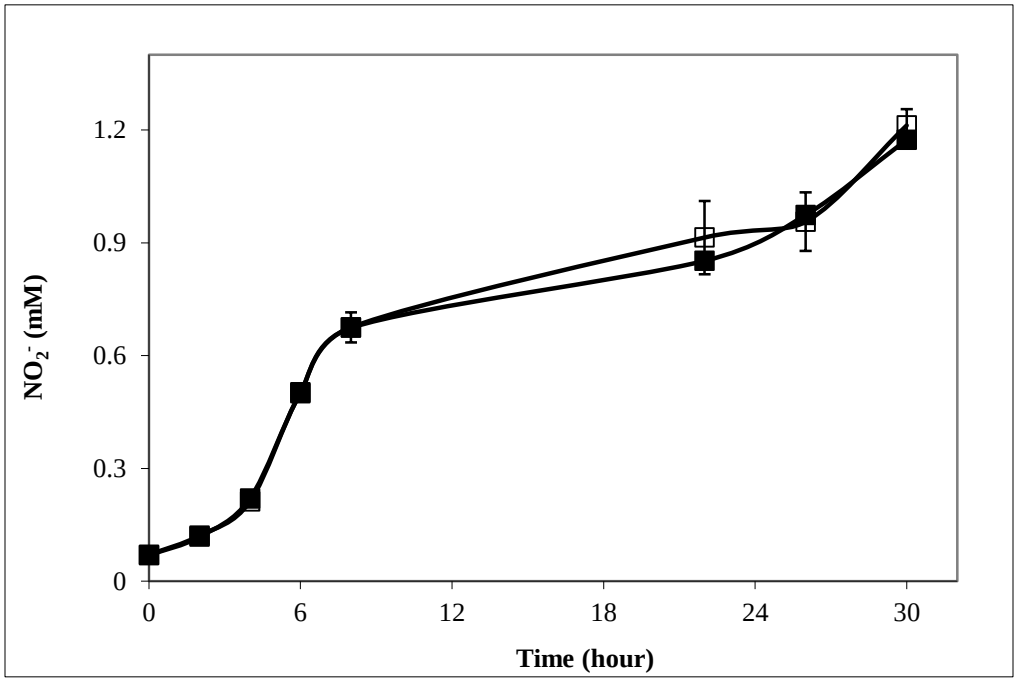
1.2
0.9
0.6
0.3
0
0
6
12
18
24
30
$NO_2^-$ (mM)
Time (hour)

**E.**

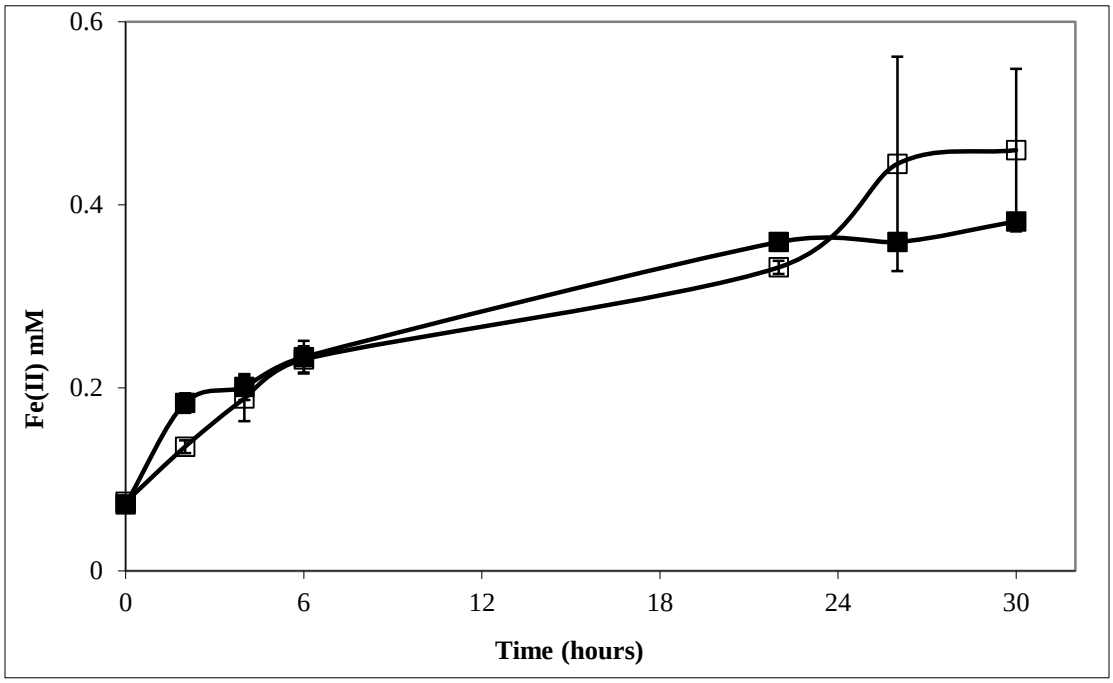


**Figure 3.10. Corresponding aerobic and anaerobic incubations to DPD depletion experiments (*S. oneidensis* produced DPD, OAI-2) involving aerobic and anaerobic incubations of *S. oneidensis* wild type and Δ*luxS* strains amended with exogenous DPD (OAI-2) as electron donor, (wild-type, closed squares; Δ*luxS*, open squares) and $O_2$ (a), fumarate (b), thiosulfate (c), nitrate (d), and HFO (e) as electron acceptor. Values are means of two parallel yet independent anaerobic incubations. Error bars represent range of errors. In some cases, error bars are smaller than the symbol.**

**A.**

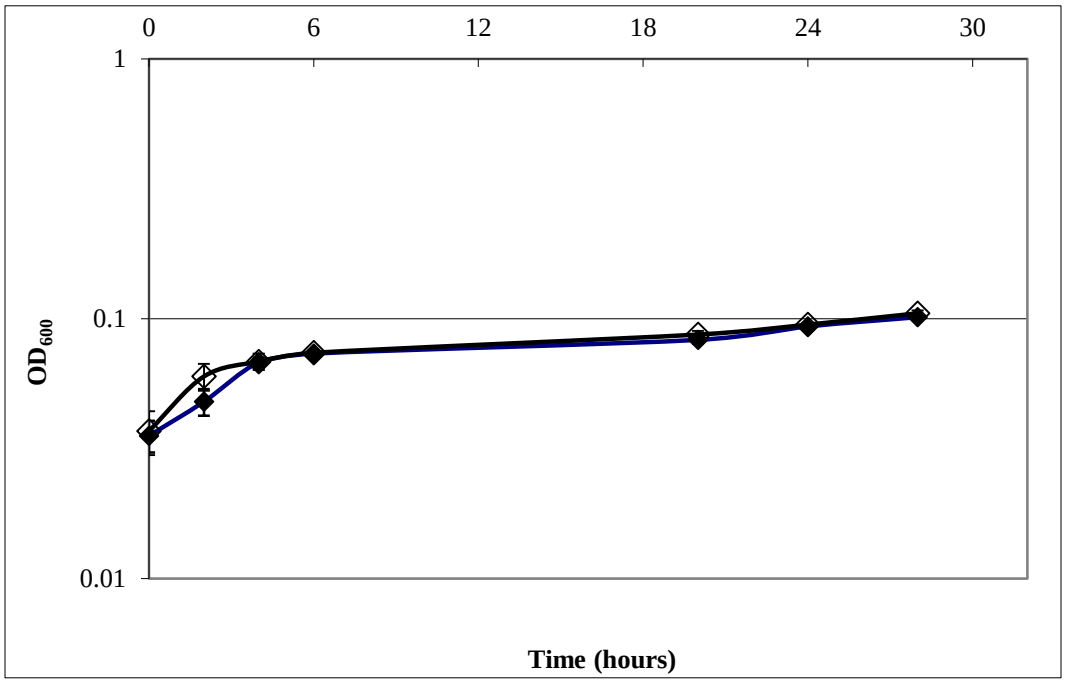
0
6
12
18
24
30
1
0.1
0.01
OD600
Time (hours)

**B.**

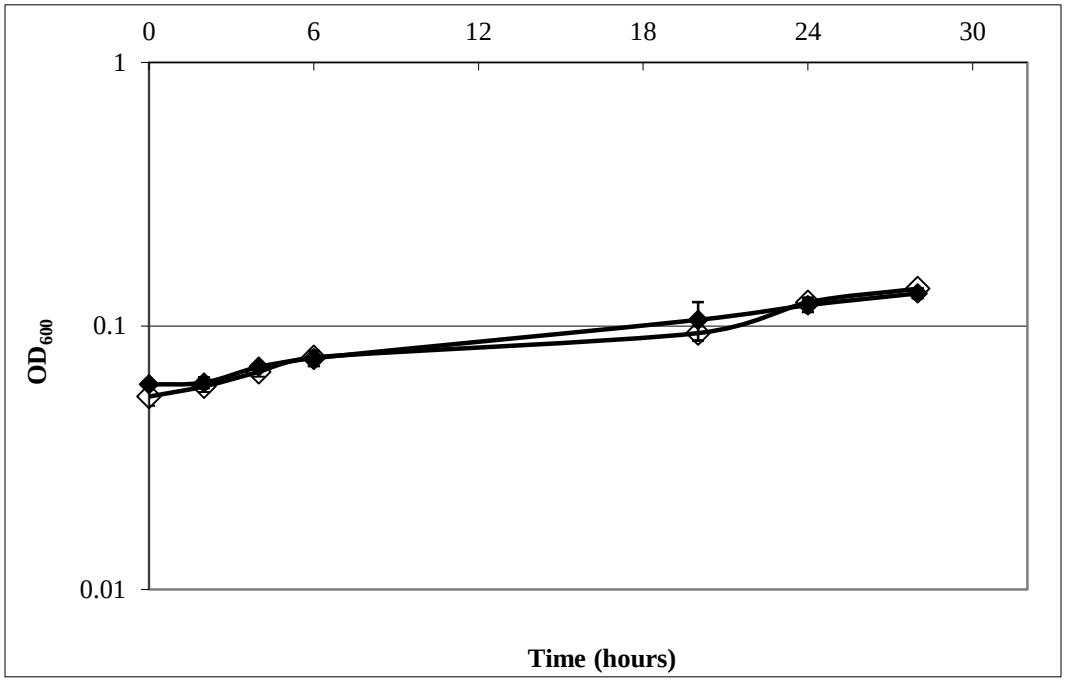
0
6
12
18
24
30
1
0.1
0.01
OD600
Time (hours)

**C.**

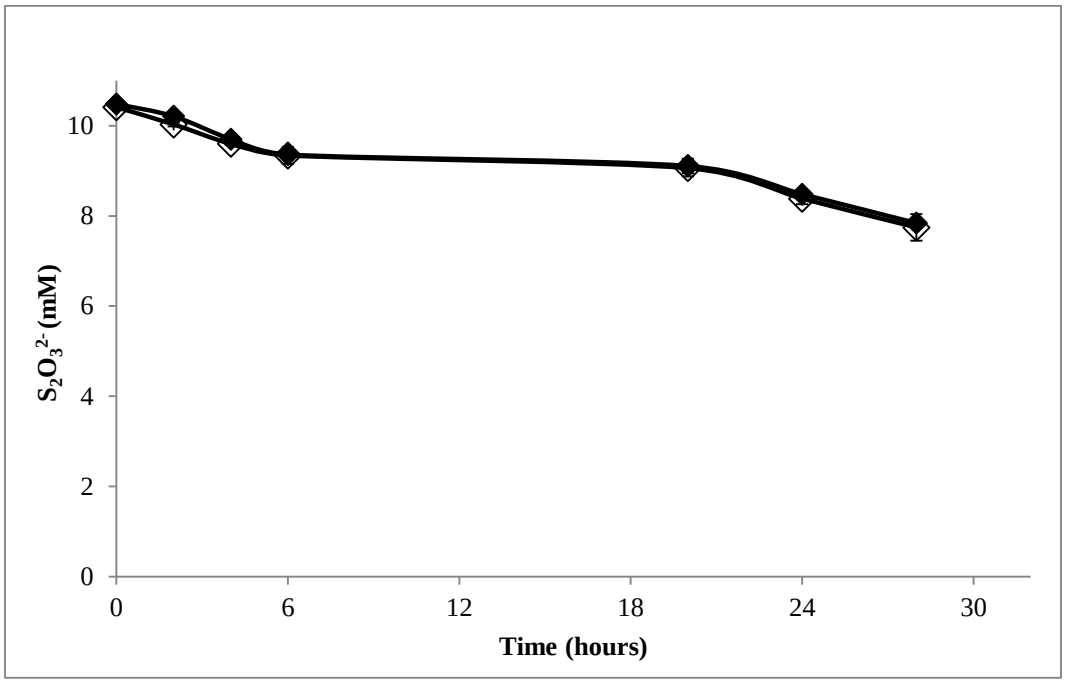
10
8
6
4
2
0
$S_2O_3^{2-}$ (mM)
0
6
12
18
24
30
Time (hours)

**D.**

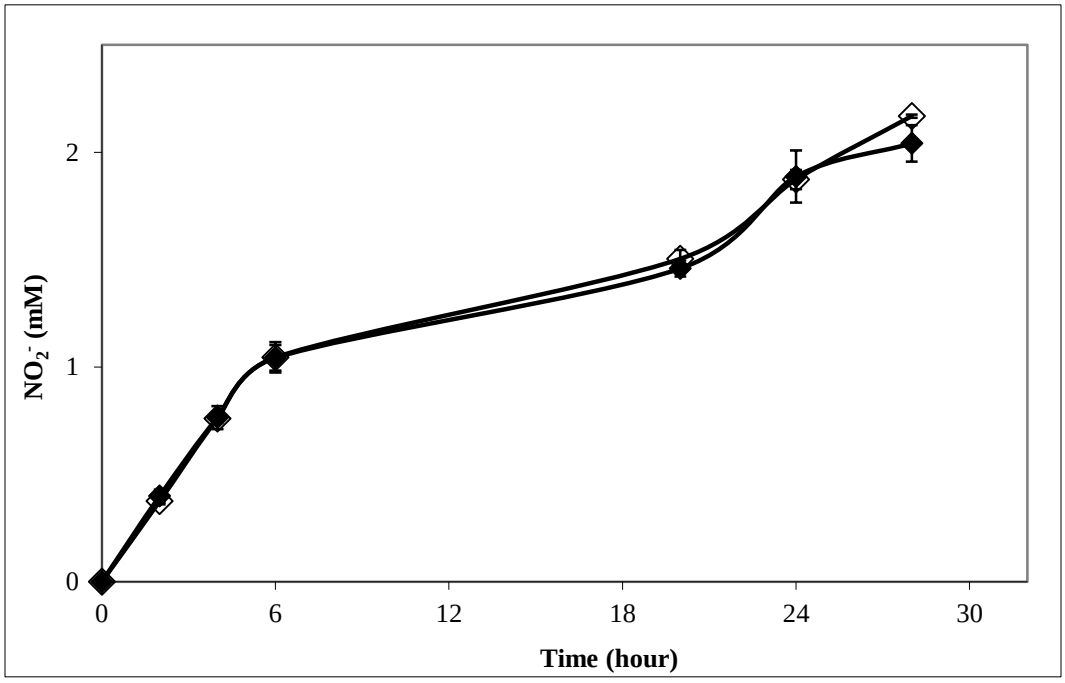
2
1
0
$NO_2^-$ (mM)
0
6
12
18
24
30
Time (hour)

**E.**

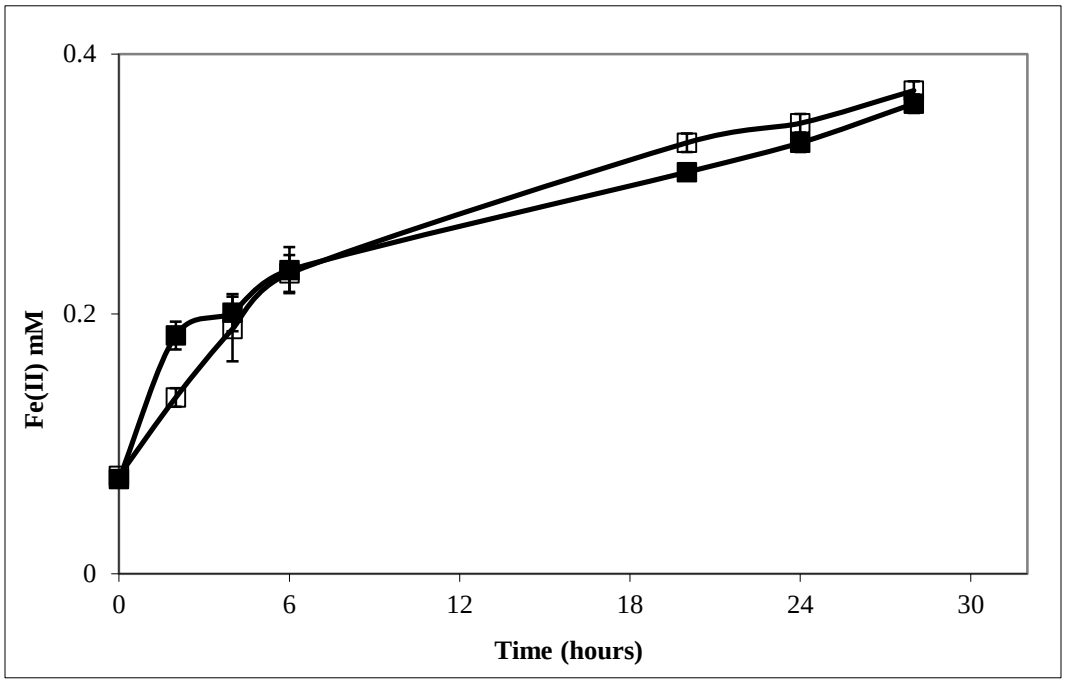


**Figure 3.11. Corresponding aerobic and anaerobic incubations to DPD depletion experiments (*Vibrio* produced DPD, HAI-2) involving aerobic and anaerobic incubations of *S. oneidensis* wild type and Δ*luxS* strains amended with exogenous DPD as electron donor, (wild-type, closed diamonds; Δ*luxS*, open diamonds) and $O_2$ (a), fumarate (b), thiosulfate (c), nitrate (d), and HFO (e) as electron acceptor. Values are means of two parallel yet independent anaerobic incubations. Error bars represent range of errors. In some cases, error bars are smaller than the symbol.**

**Table 3.1: Bacterial strains and plasmids used in this study.**

| Bacterial strain or plasmid | Description | Source or Reference |
|---|---|---|
| *S. oneidensis* | | |
| MR-1 | Wild-type strain | ATCC |
| Δ*luxS* | In-frame deletion mutant | This study |
| ΔSO3800 | In-frame deletion mutant | Burns and DiChristina, 2009 |
| Δ*lux+luxS* | *luxS*-complemented mutant | This study |
| *E. coli* | | |
| EC100D *pir-116* | F⁻ *mcrA* Δ(*mrr-hsdRMS-mcrBC*) φ80d*laxZ*ΔM15 Δ*lacX74 recA1 end A1 araD139* Δ(*ara leu*) *7697 galU galK* λ⁻ *rpsL nupG pir-116*(DHFR) | Epicentre |
| β2155 λ *pir* | *thrB1004 pro thi strA hsdS laxZ*ΔM115 (F9 *lacZ*ΔM115 *lacI*$^{q}$ *traD36 proA1 proB1)* Δ*dapA::erm pir::*RP4 Km$^{r}$ | Dehio and Meyer, 1997 |
| Plasmids | | |
| pKO2.0 | 4.5-kb γR6K *mob*RP4 *sacB* Gm$^{r}$ *lacZ* | Burns and DiChristina, 2009 |
| pKO2.0-F3 | pKO2.0 containing in-frame deletion of SO1101 | This study |
| pKO2.0-*luxS* | pKO2.0 containing wild-type of SO1101 | This study |

## Table 3.2: Primers used in this study.

| Primer | Nucleotide Sequence |
|---|---|
| D1 | 5'-GACTGGATCCGATCCGAATGCCAGGGCTTG-3' |
| D2 | 5'-ACTATTGTCGCTTTCTTGACGCCTTCGCGATACAACGCCACTGTCGCTATC-3' |
| D3 | 5'GATAGCGACAGTGGCGTTGTATCGCGAAAGCGTCAAGAAAGCGACAATAGT3' |
| D4 | 5'-GACTGTCGACCCCAAGCAATGAACGGTAACTATCATCATC-3' |
| DTF | 5'-GACAGCACAGGAAATGAACGGC-3' |
| DTR | 5'-CTCATCACCTTGCTATCACCTAAGTTG 3' |

**Table 3.3: BLAST analyses of QS-associated proteins (AI-2, AI-1) Homologs in *S. oneidensis* MR-1.**

| | *Vibrio* protein function | *S. oneidensis* MR-1 annotation | | e-value | Identity (%) | Similarity (%) |
|---|---|---|---|---|---|---|
| LuxS | S-ribosylhomocysteinase (AI-2 synthase) | S-ribosylhomocysteinase (AI-2 synthase) | SO_1101 | 3e-102 | 80 | 98 |
| LuxP | Autoinducer-2-binding periplasmic protein | transcriptional repressor of maltodextrose utlization (MalR) | SO_2244 | 0.028 | 24 | 29.6 |
| LuxQ | Autoinducer-2 sensor histidine kinase/phosphatase | two-component transduction system hybrid histidine kinase/response regulator with PAS domain | SO_0859 | 3e-55 | 33 | 46 |
| LuxM | Acyl homoserine lactone synthase (HAI-1 synthase) | 20G-Fe(II) oxygenase family protein | SO_1098 | 0.010 | 29 | 14 |
| LuxN | Autoinducer-1 sensor kinase/phosphatase (HAI-1 sensor kinase/phosphatase) | two-component transduction system hybrid histidine kinase/response regulator with Hpt domain | SO_2544 | 4e-19 | 25 | 40 |
| CqsA | CAI-1 Autoinducer synthase | 2-amino-3-ketobutyrate coenzyme A ligase (Kbl) | SO_4674 | 2e-30 | 28 | 84 |
| CqsS | Autoinducer-1 sensor kinase/phosphatase (CAI-1 sensor kinase/phosphatase) | two-component transduction system hybrid histidine kinase/response regulator with PAS domain | SO_0859 | 3e-24 | 24 | 72 |
| LuxO | Repressor protein | nitrogen-responsive two component signal transduction system sigma54-dependent response regulator (GlnG) | SO_4472 | 4e-96 | 42 | 88 |
| LuxU | Phosphorelay protein | 2-oxoglutarate dehydrogenase complex dehydrogenase E1 component (SucA) | SO_1930 | 0.55 | 48 | 23 |
| LuxR | Transcriptional regulator/ bioluminescence regulatory protein | two component signal transduction system response regulator activating acetyl-CaA synthase | SO_2648 | 2e-72 | 56 | 96 |

**Table 3.4: Identification of LuxR-type proteins in *S. oneidensis* MR-1 genome.**

| LuxR Homologs in *S. oneidensis* MR-1 (identified in Learman, et al. 2009) | |
|---|---|
| **SO_0351** | Two-component signal transduction system response regulator LuxR family |
| **SO_0864** | Transcriptional activator of curli operon CsgD |
| **SO_1860** | Two-component signal transduction system response regulator UvrY |
| **SO_2648** | Two-component signal transduction system response regulator activating acetyl-CoA synthase LuxR family |
| **SO_2725** | Transcriptional regulator LuxR family |
| **SO_3305** | Two-component signal transduction system response regulator LuxR family |
| **SO_4624** | Transcriptional regulator LuxR family |

**Table 3.5: BLAST analyses of LuxR-type proteins (identified in Table 3.4) in *S. oneidensis* MR-1 into *V. fischeri.***

| ***S. oneidensis* gene locus** | **Protein Function** | ***V. fischeri* homolog function** | **e-value** | **Identity (%)** | **Similarity (%)** |
|---|---|---|---|---|---|
| **SO_0351** | Two-component signal transduction system response regulator LuxR family | Transcriptional regulator | 4e-24 | 29 | 94 |
| **SO_0864** | Transcriptional activator of curli operon CsgD | LuxR family transcriptional regulator | 1e-18 | 31 | 53 |
| **SO_1860** | Two-component signal transduction system response regulator UvrY | Response regulator | 6e-121 | 78 | 98 |
| **SO_2648** | Two-component signal transduction system response regulator activating acetyl-CoA synthase LuxR family | LuxR family transcriptional regulator | 4e-71 | 58 | 95 |
| **SO_2725** | Transcriptional regulator LuxR family | LuxR family transcriptional regulator | 1e-26 | 31 | 91 |
| **SO_3305** | Two-component signal transduction system response regulator LuxR family | LuxR family transcriptional regulator | 7e-41 | 44 | 100 |
| **SO_4624** | Transcriptional regulator LuxR family | LuxR family transcriptional regulator | 6e-4 | 35 | 20 |

**Table 3.6. BLAST analyses of LuxR Homologs (identified in Table 3.4) in *S. oneidensis* MR-1 into *V. harveyi:***

| ***S.oneidensis* gene locus** | **Protein Function** | ***V. harveyi* homolog function** | **e-value** | **Identity (%)** | **Similarity (%)** |
|---|---|---|---|---|---|
| **SO_0351** | Two-component signal transduction system response regulator LuxR family | LuxR family transcriptional regulator | 1e-17 | 26 | 100 |
| **SO_0864** | Transcriptional activator of curli operon CsgD | LuxR family transcriptional regulator | 2e-16 | 36 | 52 |
| **SO_1860** | Two-component signal transduction system response regulator UvrY | Transcriptional regulator, LuxR family | 1e-119 | 77 | 98 |
| **SO_2648** | Two-component signal transduction system response regulator activating acetyl-CoA synthase LuxR family | Transcriptional regulator LuxR | 1e-68 | 56 | 95 |
| **SO_2725** | Transcriptional regulator LuxR family | Bacterial regulatory LuxR family protein | 7e-19 | 40 | 53 |
| **SO_3305** | Two-component signal transduction system response regulator LuxR family | Transcriptional dual regulator NarL | 5e-13 | 29 | 96 |
| **SO_4624** | Transcriptional regulator LuxR family | Tetrathionate response regulatory protein TtrR | 0.004 | 33 | 20 |

**Table 3.7: BLAST analyses of Lsr Homolog in *S. oneidensis* MR-1.**

| ***E. coli* protein** | ***E. coli* protein function** | ***S. oneidensis* MR-1 annotation** | | **e-value** | **Identity (%)** | **Similarity (%)** |
|---|---|---|---|---|---|---|
| LsrA | ATPase that provides energy for AI-2 transport | ABC-type Fe(III) uptake component (FbpC) | SO_0742 | 8e-28 | 32 | 82 |
| LsrC | Channel proteins | Inner membrane protein (unknown function) | SO_0308 | 0.029 | 28 | 36 |
| LsrD | Channel proteins | phage shock protein B (PspB) | SO_1808 | 1.5 | 45 | 7 |
| LsrB | Periplasmic AI-2 binding protein | ABC-type monosaccharide transport system substrate-binding component | SO_3714 | 6e-13 | 34 | 32 |
| LsrK | AI-2 kinase | glycerol kinase (GlpK) | SO_4230 | 4e-25 | 26 | 87 |
| LsrR | *lsr* repressor | $O_2$ response transcriptional regulator of anaerobiosis response (Fnr) | SO_2356 | 0.59 | 42 | 10 |
| LsrF | Similar finction to aldolases | ROK family protein | SO_1389 | 0.18 | 27 | 22 |
| LsrG | AI-2 degrading protein | putative quinol monooxygenase | SO_0400 | 3e-4 | 19 | 75 |
| Tam | trans-aconitate 2-methyltransferase (SAM-dependent methyltransferase) | SAM-dependent methyltransferase type II | SO_1988 | 2e-6 | 24 | 38 |
| YneE | Inner membrane protein | Peptidase | SO_3650 | 0.67 | 31 | 21 |

**Table 3.8: Rates of aerobic and anaerobic biofilm formation in *S. oneidensis* wild-type and Δ*luxS* with lactate, lactate and exogenous DPD, or exogenous DPD as the electron donor and $O_2$ or thiosulfate as the terminal electron acceptor.**

| | Lactate + $O_2$ | Lactate + $O_2$ + HAI-2 | HAI-2+ $O_2$ | Lactate + Thiosulfate | Lactate + Thiosulfate + HAI-2 | HAI-2 + Thiosulfate |
|---|---|---|---|---|---|---|
| **Wild-type** | 0.056±.002 | 0.057±.004 | 0.018±.002 | 0.017±.0006 | 0.019±.002 | 0.003±.0008 |
| ***ΔluxS*** | 0.036±.002 | 0.052±.007 | 0.018±.004 | 0.002±.0002 | 0.018±.002 | 0.003±.0005 |

**Table 3.9: Rates (nM $hr^{-1}$) of aerobic and anaerobic DPD production in *S. oneidensis* wild-type and Δ*luxS* with lactate as the electron donor and fumarate, thiosulfate, nitrate, ferrihydrite, or $O_2$ as the terminal electron acceptor.**

| | Lactate +Fumarate | Lactate +Thiosulfate | Lactate +Nitrate | Lactate +Ferrihydrite | Lactate +$O_2$ |
|---|---|---|---|---|---|
| ***S. oneidensis* MR-1** | 531±56.6 | 543±74.2 | 515±60.9 | 397±33.8 | 448±32.2 |
| ***S. oneidensis Δ luxS*** | 95.5±12.8 | 34.5±17.0 | 77.6±33.2 | 82.8±26.1 | 87.1±51.7 |
| ***S. oneidensis Δ luxS*+** | 586±57.5 | 577±50.2 | 531±48.2 | 430±23.9 | 440±23.1 |

**Table 3.10: Rates (nM $hr^{-1}$) of aerobic and anaerobic DPD production in *S. oneidensis* wild-type and Δ*luxS* with no exogenous electron donor and fumarate, thiosulfate, nitrate, ferrihydrite, or $O_2$ as the terminal electron acceptor.**

| | Fumarate | Thiosulfate | Nitrate | Ferrihydrite | $O_2$ |
|---|---|---|---|---|---|
| ***S. oneidensis* MR-1** | 284±26.3 | 290±24.1 | 250±28.7 | 243±11.8 | 312±23.4 |
| ***S. oneidensis Δ luxS*** | 62.6±21.3 | 31.4±22.4 | 57.1±6.8 | 63.8±11.9 | 58.3±16.3 |
| ***S. oneidensis Δ luxS*+** | 279±22.6 | 285±19.3 | 285±19.3 | 257±13.7 | 322±17.1 |

**Table 3.11: Rates (nM $hr^{-1}$) of aerobic and anaerobic HAI-2 depletion in *S. oneidensis* wild-type and Δ*luxS* with HAI-2 as the electron donor and fumarate, thiosulfate, nitrate, ferrihydrite, or $O_2$ as the terminal electron acceptor.**

| | HAI-2 +Fumarate | HAI-2 +Thiosulfate | HAI-2 +Nitrate | HAI-2 +Ferrihydrite | HAI-2 +$O_2$ |
|---|---|---|---|---|---|
| ***S. oneidensis* MR-1** | 317±9.77 | 143±31.6 | 178±18.5 | 132±10.5 | 209±47.44 |
| ***S. oneidensis Δ luxS*** | 237±47.9 | 229±34.1 | 139±15.8 | 100±27.3 | 282±29.8 |

**Table 3.12: Rates (nM $hr^{-1}$) of aerobic and anaerobic OAI-2 depletion in *S. oneidensis* wild-type and Δ*luxS* with OAI-2 as the electron donor and fumarate, thiosulfate, nitrate, ferrihydrite, or $O_2$ as the terminal electron acceptor.**

| | OAI-2 +Fumarate | OAI-2 +Thiosulfate | OAI-2 +Nitrate | OAI-2 +Ferrihydrite | OAI-2 +$O_2$ |
|---|---|---|---|---|---|
| ***S. oneidensis* MR-1** | 749±86.2 | 639±40.0 | 680±76.9 | 739±79.9 | 800±31.4 |
| ***S. oneidensis Δ luxS*** | 696±28.7 | 503±50.1 | 703±61.9 | 617±40.9 | 831±53.5 |

# CHAPTER 4

## Bacterial Fe(III) and Mn(III, IV) Reduction Driven by Organic Sulfur Metabolism

[The thiol/disulfide detection via HPLC experiments described in Chapter 4 were carried out in collaboration with Ramanan Sekar, a PhD student in Dr. DiChrstina's research group. *Experiments depicted in Figures 4.11 and 4.12were carried out by Seng Kew Wee of the DiChristina Laboratory and experiments in Figure 4.13 were carried out by Eryn Eitel of the Taillefert Laboratory]

### Summary

The γ-proteobacterium *Shewanella oneidensis* respires a variety of terminal electron acceptors, including solid Fe(III) and Mn(IV) oxides. *S. oneidensis* transfers electrons to solid Fe(III) oxides via direct (*c*-type cytochrome) and indirect (electron shuttling) pathways. To test the hypothesis that thiol compounds produced and secreted by *S. oneidensis* functions as an electron shuttle for Fe (III) reduction, the genes encoding the activated methyl cycle (AMC) and transulfurylation pathway (TSP) enzymes S-ribosylhomocysteine lyase (LuxS), cystathionine synthase (MetB), cystathionine lyase (MetC), and O-acetyl-L-homoserine sulfhydrolase (MetY) were deleted in-frame from the *S. oneidensis* genome to generate the corresponding mutants Δ*luxS,* Δ*metB,* Δ*metC,* and Δ*metY*. Under Fe(III)-reducing conditions (with ferrihydrite, hematite, and goethite) with lactate or $H_2$ as the electron donor, the Fe(III) reduction phenotypes for the wild-type, Δ*luxS,* and Δ*metY* yield nearly identical phenotypes, and Δ*metB* and Δ*metC* displayed

Fe(III) reduction-deficient phenotypes. However, the reduction phenotypes with soluble Mn(III) or insoluble Mn(IV) were not as clear cut. With $H_2$ and Mn(III), Δ*luxS,* Δ*metY,* and Δ*metC* displayed wild-type reduction activity, while Δ*metB* did not. With lactate and Mn(III), Δ*luxS,* and Δ*metY* yield reduction rates similar to the wild-type, and Δ*metB* and Δ*metC* displayed Mn(III) reduction-deficient phenotypes. When insoluble Mn(IV) oxides were used as the terminal electron acceptor and $H_2$ as the electron donor, Δ*luxS,* Δ*metY,* and Δ*metB* displayed wild-type reduction activity, but Δ*metC* showed no reduction activity. Alternatively, lactate and Mn(IV) growth curves yielded wild-type reduction phenotypes for Δ*luxS* and Δ*metY,* but Δ*metB* and Δ*metC* displayed deficient reduction phenotypes. High-performance liquid chromatography (HPLC) was used to identify the thiol compounds, including cysteine, homocysteine, glutathione, and cystaemine, present in the wild-type and mutant strains during various phases of growth. The HPLC analyses indicated that during the initial growth phase, cysteine is the dominant thiol detected in the wild-type, Δ*luxS,* and Δ*metY* strains however, as the bacteria continues to reduce solid Fe (III) eventually reaching stationary phase the dominant thiol present shifts from cysteine to glutathione to homocysteine. Cysteamine is detected throughout, albeit at low concentrations. The presence of reduced glutathione in the thiol profiles of the wild-type and mutant strains is important due to the ability of reduced glutathione to reduce disulfides which in turn reduces metal oxides. The Fe(III) reduction-deficient phenotype displayed by Δ*metB* and Δ*metC* suggests the Transulfurylation pathway is required to promote metal reduction, while the AMC contributes to the biosynthesis of thiols.

**Introduction**

Microbial iron (Fe(III)) respiration is a fundamental component of a variety of environmentally important processes, including biogeochemical cycling of iron and carbon, bioremediation of radionuclide-contaminated water, and degradation of toxic hazardous pollutants (1). Microbial Fe(III) reduction also drives the generation of electricity in microbial fuel cells (2-5). Bacterial energy conservation requires generation of a proton motive force (PMF) across the inner membrane (IM). Electrons originating from oxidation of electron donors are transported down the redox gradient of an electron transport chain to IM- or periplasmic- localized terminal reductases coupled to proton translocation across the IM to generate PMF. PMF drives ATP synthesis as protons are translocated back into the cytoplasm through IM-localized ATPases, catalyzing the phosporylation of ADP to ATP (6). Fe(III)-respiring bacteria are therefore presented with a unique problem: they are required to respire anaerobically on insoluble terminal electron acceptors that are unable to contact IM-localized electron transport systems (1).

Manganese is one of the most abundant transition metals found in the Earth's crust and plays an imperative role in the biogeochemical cycling of carbon, phosphorous, nitrogen, and other metals (7-10). Manganese (IV) produced via oxidation of Mn (II) typically exists as highly insoluble oxides at circum-neutral pH and comprises a significant fraction of soils and sediments (11). Solid Mn (III) oxides are also found in natural environments, however, the stability of solid Mn (III) oxides is dependent on the pH and concentration of $Mn^{2+}$ (11, 12). Mn(II) is thermodynamically more stable under anoxic conditions when it is most often found in the dissolved form as free hydrated cation ($Mn^{2+}$), hydroxyl or carbonate complexes, or as insoluble phosphate or carbonate minerals (9, 13). Under anaerobic conditions, Mn (IV) is reduced to Mn (II) either biologically via

dissimilatory reducing microorganisms at circumneutral pH (14) or chemically via Fe(II) or sulfide (15, 16).

Microbial Mn (IV) reduction is a central component of biogeochemical cycling in manganese aquifers (17), redox stratified water columns (18), fresh water sediments (19), and marine sediments (20). The mechanism of dissimilatory Mn (IV) reduction by metal-reducing bacteria is poorly understood. Microorganisms capable of reducing Mn (IV) oxides span both domains of the prokaryotic world (21), including the metal-reducing bacteria of the genus *Shewanella* which are capable of reducing solid Mn (IV) (14, 22), soluble Mn (III) (23), and a wide variety of alternate electron acceptors, including soluble and insoluble Fe (III) oxides (24, 25).

Fe(III)- and Mn (IV)-reducing gram-negative bacteria are presented with a unique physiological problem: at circumneutral pH, the bacteria are required to reduce electron acceptors found in nature as amorphous or crystalline (oxy)hydroxide particles (26) presumably unable to contact inner membrane (IM)-localized electron transport systems. The gram negative, facultative anaerobe *Shewanella oneidensis* respires a suite of terminal electron acceptors that span nearly the entire continuum of redox potentials found in nature, including oxygen, fumarate, nitrate, nitrite, trimethylamine N-oxide, dimethyl sulfoxide, sulfite, thiosulfate, elemental sulfur, and soluble and insoluble transition metals, such as organic Fe(III), Fe(III) oxide, Mn(IV) oxide and Mn(III) (14, 22, 27-31).

To overcome this physiological problem, the dissimilatory metal-reducing bacteria (DMRB) utilized a variety of novel terminal electron transport strategies not found in other gram-negative bacteria that reduce soluble terminal electron acceptors (21, 24), including direct enzymatic reduction of solid metal oxides via direct contact with metal reductases

located on the outer membrane (OM) (32-34), a two-step, solubilization and reduction pathway in which solid metal oxides are dissolved by organic ligands followed by uptake and reduction of the soluble organic-metal complexes via periplasmic metal reductases (30, 35, 36), and a two-step electron shuttling pathway in which endogenous and exogenous electron shuttling compounds are first enzymatically reduced and then chemically oxidized by the solid metal oxides in a second electron transfer reaction (37-39).

Recent findings by our research group indicate that *S. oneidensis* secretes organic sulfur (thiol) compounds extracellularly under anaerobic growth conditions (40). Extracellular thiols were detected at bulk concentrations of approximately 9 µM via application of the thiol reactive stain 5,5'-Dithiobis-(2-Nitrobenzoic acid) (DTNB, Ellman's reagent; reduced form produces yellow color in Fig. 2) to *S. oneidensis* cultures grown anaerobically on agar or liquid growth media. The detection of extracellular thiols was surprising since thiols are generally involved in a variety of intracellular processes, including maintenance of redox homeostasis and proper protein thiol-disulfide ratios, and to protect against reactive oxygen (ROS), nitrogen (RNS), and electrophilic (RES) species (41). The dominant intracellular thiols in eukaryotes and gram-negative bacteria include cysteine and gluthathione (42, 43). In gram-positive bacteria, glutathione may be replaced by alternative thiols such as mycothiol in *Actinobacteria* (44, 45) and bacilithiol in *Bacillus* (46). We postulated that determining the composition and identifying the metabolic pathways involved in extracellular thiol production may provide clues to their function.

The *S. oneidensis* MR-1 genome contains the genes that make up the activated methyl cycle (AMC), transsulfuration pathway (TSP), and direct sulfhydrylation pathway

(DSP). These three cycles are significant in that they are lead to the biosynthesis of homocysteine. These cycles have been highly characterized in both gram-negative bacteria, such as *Escherichia coli, Helicobacter pylori,* and gram-positive bacteria, such as *Bacillus subtilis.* The AMC is a key metabolic pathway that generates S-adenosylmethionine (SAM) as an intermediate product in the synthesis homocysteine. Here, the biosynthesis of homocysteine occurs via a multi-step process. Methionine is first converted to S-adenosylmethionine (SAM) via the S-adenosyl-methionine synthetase (MetK). SAM then transfers its' methyl group to a substrate molecule via a methyltransferase resulting in S-adenosylhomocystine (SAH). SAH is then converted to S-ribosylhomocysteine (SRH) via 5-methylthioadenosine nucleosidase (MtnN). Lastly, an adenosine group is hydrolyzed from SRH via LuxS to yield homocysteine. Homocysteine can be converted back to methionine via methyltetrahydrofolate (MetF) or to cysteine. The transsulfuration pathway is a metabolic pathway that encompasses the interconversion of cysteine and homocysteine via an intermediate cystathionine. There are both forward and reverse transsulfuration pathways found in gram-positive and gram-negative bacteria. The forward pathway is found in *E. coli, S. oneidensis,* and *B. subtilis* (47). The forward TSP is defined by the transfer of the thiol group from cysteine to homocysteine via cystathionine; this conversion is catalyzed via cysthathionine γ-synthase (MetB) and cystathionine β-lyase (MetC). The reverse pathway is found in *H. pylori* and *Klebsiella pneumoniahardie* (48). The reverse TSP is defined by the transfer of the thiol group from homocysteine to cysteine via cystathionine intermediate; this conversion is catalyzed via cystathionine γ-lyase and cystathionine β-synthase. Direct sulfhydrylation pathway (DSP) are defined by the synthesis of cysteine and/or homocysteine via the replacement of the succinyl or acetyl

group with a free sulfide. *cykM* and *cysM* encode the cysteine synthase which produces cysteine from O-succinyl-L-homoserine via DSP. *metY* encodes O-acetylhomoserine (thiol)-lyase which acts as a homocysteine synthase to convert O-acetyl-L-homoserine to homocystine via DSP.

The *S. oneidensis* AMC and transulfurylation pathways are composed of a series of enzymatic reactions that ultimately lead to the production of methionine (Fig. 1) and the activated methyl donor SAM (Fig. 1). Methionine synthesis requires the production of homocysteine, which is produced via one of three pathways: 1) LuxS-catalyzed hydrolysis of SRH to yield homocysteine (Fig. 1), 2) MetC-catalyzed conversion of cystathionine to yield homocysteine (Fig. 1), and 3) MetY catalyzed formation of homocysteine from O-acetyl-L-homoserine (OAHS) and $H_2S$. (Fig. 1). In addition to homocysteine biosynthesis, the AMC and Transsulfurylation pathways in *S. oneidensis* are responsible for conversion of homoserine into threonine via homoserine kinase and threonine (Fig. 1). Cysteine is produced from CysK- and CysM-catalyzed sulfurylation of O-acetyl-L-serine with either $H_2S$ or thiosulfate as the S-donor (Fig. 1). Cysteine is then incorporated into the Transsulfurylation pathway via MetB-catalyzed addition of cysteine to either O-succinyl-L-homoserine (OSHS) or O-phospho-L-homoserine (OPHS) to produce cystathionine.

Thiols are potent chemical reductants of Fe(III), rapidly coupling Fe(III) reduction to production of the corresponding disulfide (3). Cysteine, for example, reduces Fe(III) oxides abiotically via electron transfer reactions that produce Fe(II) and cystine. The initial rate and extent of Fe(III) reduction correlate linearly with cysteine concentration (3, 49). In previous studies, the addition of cysteine to Fe(III)-reducing *S. oneidensis* cultures

increased the rate and extent of Fe(III) reduction by *S. oneidensis (50)*, and the addition of cysteine to *S. oneidensis*-driven microbial fuel cells increased power generation (4). In addition, exogenous cysteine functioned as an electron carrier between *Geobacter sulfurreducens* and *Wolinella succinogenes* in an acetate-oxidizing, Fe(III)-reducing syntrophic co-culture (51). The detection of extracellular thiols in anaerobic Fe(III)-reducing *S. oneidensis* cultures, and the ability of thiols to rapidly reduce Fe(III) oxides forms the basis of a novel electron shuttling system: thiol-driven (abiotic) reduction of external Fe(III) oxides is sustained via catalytic (biotic) reduction of the resulting disulfides.

In the present study, we test the hypothesis that the gram-negative bacteria *S. oneidensis* MR-1 utilizes thiol compounds, including cysteine, homocysteine, glutathione, and cysteamine, produced and secreted by the bacteria under anaerobic Fe (III)- and Mn(III,IV)-reducing conditions as an electron shuttle. To answer this hypothesis, a series of growth experiments using insoluble Fe (III) and Mn(III,IV) as the terminal electron acceptor and lactate or H2 as the electron donor were conducted with the wild-type and in-frame deletion mutants of genes from the activated methyl cycle (AMC) and transulfurylation pathway (TSP) that function to produce endogenous thiols that can ultimately be secreted to the outside of the cell and utilized as an electron shuttle. Subsequent analyses via high-performance liquid chromatography (HPLC) were used to identify the thiols present during various phases of growth and whether or not the thiol was present in the reduced or oxidized form.

**Materials and Methods**

**Bacterial strains and cultivation conditions.** The bacterial strains and plasmids used in this study are listed in Table 4.1. For genetic manipulations, *S. oneidensis* was cultured at 30°C in Luria-Bertani (LB) medium. For anaerobic growth experiments, cells were grown in M1 minimal medium (14) supplemented with lactate (18 mM), formate (18 mM), or hydrogen (anaerobic gas mixture consisting of 5% $H_2$, 10% $CO_2$, 85% $N_2$) as electron donor. When hydrogen was used as the electron donor, incubations were conducted inside an anaerobic chamber with no additional electron donors present in the anaerobic gas mix or media. Electron acceptors were added from anaerobic stock solutions synthesized as previously described (22, 28, 29, 52, 53): ferrihydrite (10 mM), hematite (10 mM), goethite (10 mM), Mn(III)-pyrophosphate (10mM), or Mn(IV) (10mM). When required, gentamicin (Gm) was added at a final concentration of 15 μg/ml. For growth of *Escherichia coli* β2155 λ *pir*, diaminopimelate (DAP) was added at a final concentration of 100 μg/ml. Aerobic growth was monitored spectrophotometrically by measuring changes in optical density at 600 nm ($OD_{600}$).

**Nucleotide and amino acid sequence analyses.** Genome sequence data for *S. oneidensis* MR-1 was obtained from the National Center for Biotechnology Information (NCBI, http://www.ncbi.nlm.nih.gov) and the Department of Energy Joint Genome Institute (DOE-JGI, http://jgi.doe.gov). AMC and Transsulfurylation pathway homologs in the NCBI databases were identified. Proteins displaying sequence similarity to activated methyl cycle genes (SO1101, SO0818, SO1030, SO0929, SO3006, SO1322), transsulfuration pathways genes (SO1676, SO4056, SO2191), direct sulfhydrylation pathway genes (SO1095, SO2903, SO3598), glutathione synthesis and degradation genes

(SO3559, SO0831, SO4702), cysteine/glutathione transporter genes (SO3779, SO3780), homoserine and threonine synthesis genes (SO3413, SO3414, SO3415, SO4055), cysteamine synthesis gene (SO4249) were identified via BLAST analysis (54) using the corresponding *S. oneidensis* enzymes as the search queries.

**Identification of genes required for disulfide reduction, thiol secretion, and disulfide uptake by *S. oneidensis*.** The aforementioned protein sequences encoded by the *Shewanella oneidensis* MR-1 genomes were analyzed and compared to the genome sequences of 17 other *Shewanella* species, including *S. putrefaciens 200, S. putrefaciens CN32, S. putrefaciens W3-18-1, S. amazonensis SB2B, S. denitrificans OS217, S. baltica OS195, S. frigidimarina NCIMB400, S. pealeana ATCC 700345, S. woodyi ATCC 51908, Shewanella sp. ANA-3, Shewanella sp. MR-4, Shewanella sp. MR-7, S. loihica PV-4, S. halifaxens, S. piezotolerans, S. benthica, and S. sediminis.* Percents sequence similarity (Sim), percents identity (ID), and E values for the *S. oneidensis* protein sequences were obtained. In addition, the protein sequences encoded by the *Shewanella oneidensis* MR-1 genomes were analyzed and compared to the organisms outside of the genus *Shewanella* with the homologs of highest similarity (best hit) as determined by BLASTp analysis of GenBank nonredundant database.

**In-frame gene deletion mutagenesis and genetic complementation analysis.** The gene encoding LuxS (SO_1101), MetB (SO_4056), MetC (SO_2191), and MetY (SO_1095) was deleted in-frame from the *S. oneidensis* genome via previously described procedures (Table 4.2) (55). The primers used for construction of Δ*luxS* are listed in Table 4.2.

Regions corresponding to approximately 750 bp upstream and downstream of each open reading frame (ORF) were PCR-amplified with primers D1 and D2 for the upstream region and D3 and D4 for the downstream region with iProof ultrahigh-fidelity polymerase (Bio-Rad, Hercules, CA), generating fragments F1 and F2, which were fused by overlap extension PCR to generate fragment F3. Fragment F3 was cloned into pKO2.0 (containing *sacB*) with BamHI and SalI restriction endonucleases to generate recombinant plasmid pKO2.0-F3, which was electroporated into *E. coli* strain β2155 λ *pir*. pKO2.0-F3 was mobilized into recipient *S. oneidensis* wild-type cells via conjugal transfer from *E. coli* donor strain β2155 λ pir. *S. oneidensis* recipient strains containing the plasmid integrated into the genome were selected on LB agar medium supplemented with 15 μg $ml^{-1}$ Gm. Single plasmid integrants were identified via PCR with primers D1-DTR and D4-DTF that flank the targeted recombination region. Plasmids were resolved from the genomes of the single integrants by plating on LB agar medium containing sucrose (10% w/v). Following counter selection on sucrose-containing LB agar medium, the corresponding in-frame deletion mutant (designated strain Δ*luxS*) was isolated and confirmed via PCR amplification and direct DNA sequencing (University of Nevada, Reno Genomics Facility). Genetic complementation of Δ*luxS,* Δ*metB,* Δ*metC,* and Δ*metY* were carried out by cloning wild-type *luxS* into broad-host-range cloning vector pBBR1MCS (56) and conjugally transferring the recombinant vector into Δ*luxS,* Δ*metB,* Δ*metC,* or Δ*metY* via bi-parental mating procedures (28, 57).

**Determination of the overall anaerobic respiratory capability of Δ*luxS* in batch cultures.** *S. oneidensis* wild-type and Δ*luxS* mutant strains were grown anaerobically

(initial inoculum of $1.0 \times 10^7$ cells $ml^{-1}$) in M1 minimal medium supplemented with either lactate (18 mM) or $H_2$ (anaerobic gas mixture consisting of 5% $H_2$, 10% $CO_2$, 85% $N_2$) as electron donor and either Fe(III)-citrate (50 mM), ferrihydrite (10 mM), or hematite (10 mM) as electron acceptor. Fe(II) production was monitored by measurement of HCl-extractable Fe(II) via the Ferrozine method (58). Δ*luxS* was also tested for the ability to respire anaerobically on Mn(III) pyrophosphate and Mn(IV) oxide. Mn(III) pyrophosphate was measured colorimetrically as previously described (23). Mn(IV) reduction was measured spectrophotometrically after reaction with benzidine as previously described

**Identification of extracellular thiols produced by *S. oneidensis* wild-type and AMC and transulfurylation pathway mutants during anaerobic growth on Fe(III) oxides, Mn(III), and Mn(IV) oxides as electron acceptor.** Thiols produced by *S. oneidensis* wild-type and mutant strains were identified by high-performance liquid chromatography (HPLC) of derivatized thiols with fluorescence detection or, in the case of novel thiols, liquid chromatography-mass spectrometry (LC-MS) techniques. The HPLC method is adapted from previous techniques employed to identify thiols in natural waters (59), blood plasma (60), and urine (61, 62). Samples from anaerobic Fe(III)-respiring cultures will be harvested and centrifuged at 12,000xg. Supernatants will be incubated with the chemical reductant Tris(2-carboxyethyl) phosphine hydrochloride (TCEP) and the derivatizing agent 7-fluorobenzofurazan-4-sulfonic acid ammonium salt (SBD-F) to derivatize the total (reduced and oxidized) complement of extracellular thiols. In a parallel set of experiments, the supernatants will be incubated only with SBD-F (i.e., with TCEP omitted) to derivatize

only the reduced complement of thiols. Comparison of the thiols identified with and without TCEP will provide crucial information on the oxidation state of the extracellular thiols (i.e., reduced thiol or oxidized disulfide forms). In both cases, the resulting set of derivatized thiols will be separated on a C-18 HPLC column (Supelcosil CL-18-DB, 4.6 x 150 mm, 5 um bead size) with an isocratic eluent 100 mM $KHPO_4$, 6% acetonitrile (ACN) adjusted to pH of 2.1 with phosphoric acid. Derivatized thiols will be detected by fluorescence with an excitation wavelength of 385 nm and a measurement wavelength of 515 nm (sample run time 20 min). For novel thiols (i.e., for those not found in the standard set of thiol controls), a LC-MS approach will be utilized with (63) or without (34) derivitization by differential measurement of thiol and disulfide compounds.

**Results**

**Overall respiratory capability of Δ*luxS*, Δ*metB*, Δ*metC* and Δ*metY* in anaerobic batch cultures**. In anaerobic batch cultures with $H_2$ and lactate as electron donor, Δ*luxS* and Δ*metY* reduced ferrihydrite, hematite, and geothite at near wild-type rates (Fig. 4.2). In anaerobic batch cultures with $H_2$ as the electron donor, Δ*metB* and Δ*metC* reduced HFO at 50% of wild-type rates, Δ*metB* and Δ*metC* reduced hematite at 25% of wild-type rates, and Δ*metB* and Δ*metC* reduced goethite at 33% of wild-type rates. (Fig. 4.2). In anaerobic batch cultures with lactate as the electron donor, Δ*metB* and Δ*metC* reduced HFO at 25% of wild-type rates, Δ*metB* and Δ*metC* reduced hematite at 25% of wild-type rates, and Δ*metB* and Δ*metC* reduced goethite at 50% of wild-type rates (Fig. 4.2). In addition, in anaerobic batch cultures with $H_2$ as the electron donor, Δ*luxS*, Δ*metY*, and Δ*metC* reduced the alternate electron acceptor Mn(III) pyrophosphate at rates greater than

wild-type, but Δ*metB* reduced Mn(III) at approximately 50% of wild-type rate. In anaerobic batch cultures with lactate as the electron donor, Δ*luxS and* Δ*metY* reduced the alternate electron acceptor Mn(III) pyrophosphate at wild-type rates, but Δ*metB* and Δ*metC* reduced Mn(III) at approximately 50% of wild-type rate. Under anaerobic conditions with $H_2$ as the electron donor, Δ*luxS*, Δ*metY*, and Δ*metB* reduced the alternate electron acceptor Mn(IV) at wild-type rates, but Δ*metC* was deficient in Mn(IV) reduction. In anaerobic batch cultures with lactate as the electron donor, Δ*luxS and* Δ*metY* reduced the alternate electron acceptor Mn(IV) at wild-type rates, but Δ*metB* and Δ*metC* reduced Mn(IV) at approximately 50% of wild-type rate Thus, in anaerobic batch cultures, Δ*luxS* and Δ*metY* reduced all electron acceptors at wild type rates, regardless of electron donor.

**Thiol production under Fe(III)-reducing conditions.** *S. oneidensis* produced endogenous thiols and disulfides under anaerobic Fe(III)-reducing conditions. Cysteine is a powerful reductant that can reduce other disulfides, which in turn can reduce Fe(III) oxides. Reduced glutathione can reduce other disulfides present in the cell, including cystine, homocystine, and cystamine. As thiols become oxidized, Fe(III) is simultaneously reduced to Fe(II). Any reduced glutathione detected is the result of chemical reduction of oxidized glutathione by another thiol or disulfide. Under ferrihydrite-reducing conditions, cysteine and cystine (with H2 both forms are present, with lactate cystine present) are the dominant thiol and disulfide present in the first 24 hours of growth in *S. oneidensis* wild-type (Fig. 4.3, 4.4). Similar to the wild-type strain, cysteine (and a small proportion of cystine) is the dominant thiol in the first 24 hours of

growth observed in the *luxS* mutant when grown with $H_2$ as the electron donor (Fig. 4.3). With lactate as the electron donor, homocysteine/homocystine, reduced glutathione/oxidized glutathione, and cysteamine/cystamine are the dominant thiols in Δ*luxS*, with cystine appearing after 56 hours (Fig. 4.4). The presence of homocysteine/homocystine in the Δ*metC* mutant indicates that *metY* and *luxS* can contribute a significant amount of homocysteine to the internal thiol pool in the absence of *metC*. Mutants lacking genes required for thiol production, Δ*metB* and Δ*metC*, exhibit impaired Fe(III) reduction activity and altered thiol production activity in comparison to the wild-type strain. The total concentration of cysteine in the *metC* mutant is 10X lower than the concentration of cysteine in the wild-type (Fig. 4.3. 4.4). Δ*metY* is capable of reducing Fe(III) at wild-type rates, however, the thiols and disulfides profile with H2 as the electron donor follow similar patterns as the wild-type; cystine is the dominant thiol in the first 24 hours (Fig. 4.3), however with lactate as the electron donor, no cysteine or cystine is detected (Fig. 4.4).

Under hematite-reducing conditions, cysteine and cystine are the dominant thiol/disulfide present throught the entire reduction period in the wild-type strain, with small contributions of homocysteine/homocystine, reduced glutathione/oxidized glutathione, and cysteamine/cystamine present throughout (Fig. 4.5). Δ*luxS* produces cysteine as the dominant thiol compound, along with homocysteine, reduced glutathione, and cysteamine in small concentration. The only disulfide detected in the Δ*luxS* strain was cystamine. In hematite-reduction deficient mutants Δ*metB* and Δ*metC*, cysteine and cystine only appear after 51 hours, while the first 51 hours are dominated by oxidized glutathione, cystamine, homocysteine (Δ*metB*), and homocystine (Δ*metC*) (Fig. 4.5).

**Thiol production under Mn(III, IV)-reducing conditions.** Similar to the effect of thiols on Fe(III) reduction, thiols are also proposed to serve as an electron shuttle for Mn(IV) oxide reduction. Under Mn(III) reducing conditions with $H_2$ as the electron donor, cystine is the dominant thiol detected in the wild-type and Δ*luxS* in the first 7.5-10 hours. Homocysteine/homocystine, reduced glutathione/oxidized glutathione, and cysteamine/cystamine are also detected. After 75 hours and 32 hours, no thiols or disulfides were detected in the wild-type or Δ*luxS*, respectively (Fig. 4.7). Cysteine and cystine were absent from the thiol pool in Δ*metB,* Δ*metC,* and *metY* despite Δ*metC,* and *metY* retaining wild-type Mn(III) reduction activity. With lactate as the electron donor, cysteine and cystine are detected in the wild-type, Δ*luxS,* Δ*metB,* Δ*metC* and Δ*metY* strains (Fig. 4.8).

Under Mn(IV)-reducing conditions with $H_2$ as the electron donor, cysteine/cystine and oxidized glutathione are the dominant thiols present in the wild-type strain, Δ*metB,* Δ*metC,* and Δ*metY* (4.9). Cysteine/cystine and reduced glutathione are the dominant thiols present in the Δ*luxS* mutant; the presence of a greater concentration of reduced glutathione compared to oxidized indicates that the majority of oxidized glutathione produced by the bacteria is being chemically reduced by other thiols or disulfides (Fig. 4.9). Cysteine and cystine are the dominant thiols detected in the wild-type when grown with lactate as the electron donor and Mn(IV) as the electron acceptor (Fig. 4.10), but ΔluxS, a Mn(IV)-reduction positive strain only produced cysteine and cystine in the first 21 hours, with homocystine the dominant disulfide detected after 50 hours (Fig. 4.10) and Δ*metY,* another Mn(IV)-reduction positive strain cystine, but not cysteine, is the predominant thiol detected throughout the growth period.

**Increased rate and extent of Fe(III) reduction with the addition of exogenous cysteine.** Previous work carried out by Seng Kew Wee (DiChrstina laboratory) and Eryn Eitel (Taillefert laboratory) has shown that cysteine works as an efficient electron shuttle under anaerobic conditions. It was shown that an increased rate and extent of Fe(III) oxide reduction (and shuttling frequency) of the disulfides correlated with increases in Vmax-Di (Fig. 4.11, 4.12). These results suggest that the rates of abiotic Fe(III) reduction by cysteine are not the limiting reaction in thiol-based electron shuttling pathway to Fe(III) oxides, instead microbial disulfide reduction rates are the limiting reaction in the thiol-based electron shuttling pathway to Fe(III) oxides. To confirm this possibility, the rates of abiotic Fe(III) reduction by cysteine were measured voltammetrically in M1 growth medium supplemented with 600 µM cysteine and 40 mM Fe(III) oxide (Fig. 4.13). The rate of Fe(III) oxide reduction by cysteine was approximately 10-fold greater than the corresponding rate at which *S. oneidensis* reduced 300 µM cystine, again indicating that microbial disulfide reduction activity is the limiting step in the electron shuttling pathway to Fe(III) oxides.

**Discussion**

*S. oneidensis* transfers electrons to Fe(III) oxides located more than 50 µM (i.e., 50 cell diameters) from the cell surface (64, 65). Electron reactions are exceedingly slow at distances >15Å (66-68), therefore, electron transfer to external Fe(III) oxides may be enhanced by exogenous or endogenous electron shuttling compounds. *S. oneidensis* exploits naturally-occurring humic acids (69-71), phenazines (e.g., pyocyanin) (72), and redox-active antibiotics (e.g., tetracyclines) (72) as exogenous electron shuttles to

extracellular Fe(III) oxides (69). Potential endogenous electron shuttles produced by *Shewanella* include menaquinone (39), melanin (73), and flavins (FMN, FAD, riboflavin) (69, 74). The ability of these compounds to function as effective endogenous electron shuttles, however, is currently up for debate. *S. oneidensis* was originally postulated to secrete menaquinone as an endogenous electron shuttle (39), however, these findings were subsequently attributed to inadvertent cell lysis (75). Melanin is also produced extracellularly by *Shewanella* but only in the presence of high amounts (1g/L) of tyrosine, thus limiting its effectiveness as an electron shuttle in natural environments (73, 74). *S. oneidensis* also produces extracellular flavins under aerobic or anaerobic conditions (76). Evidence for electron shuttling by flavins includes the findings that oxidized flavins are reduced by *S. oneidensis c*-type cytochrome MtrC (74, 76) and that reduced flavins abiotically reduce Fe(III) oxides (75). The rate limiting step in flavin-based electron shuttling is the microbial reduction of oxidized flavin, as opposed to the abiotic reduction of Fe(III) oxides by reduced flavin (77). Flavins function as electron shuttles when *S. oneidensis* is within 1 uM of the metal oxide surface, resulting in an enhanced rate of solid Fe(III) respiration (77). Secreted flavins are reduced by the Mtr pathway in *S. oneidensis*; the outer membrane (OM)-associated decaheme c-type cytochrome MtrC potentially has a FMN binding domain located near exposed heme groups. This is significant because the absence of OM cytochromes, *S. oneidensis* is unable to reduce solid metal oxides, which indicates the bacteria is unable to respire insoluble metal oxides via direct contact or electron shuttles without the cytochromes (76). Metal oxide reduction via electron shuttling (by the Mtr pathway) coupled to lactate oxidation is the rate limiting step (in flavin enhanced rate of Fe(III) reduction), not heterogeneous electron transfer to Fe(III)

oxide (77).

Electron shuttling pathways are known to increase the rate and extent of solid Fe(III) oxide reduction by *S. oneidensis.* In addition to the abovementioned potential exogenous and endogenous electron shuttles, thiols are an intriguing candidate for electron shuttling. While extracellular flavins has been described as an effective electron shuttle, there are potential limitations that exist that can inhibit the effectiveness of the shuttle. The mechanisms through which flavins function as an electron shuttle by freely diffusing through the cell membranes or as a co-factor bound to cell surface-exposed MtrC is a topic of discussion. *S. oneidensis* produces a number of thiols and disulfides that can serve as an endogenous electron shuttle, including cysteine and cystine, homocysteine and homocystine, reduced glutathione and oxidized glutathione, and cysteamine and cystamine. *S. oneidensis* utilizes the reduced (thiol) form of the disulfide compounds (cysteine, reduced glutathione, homocysteine, cysteamine) as electron shuttles to transfer electrons to extracellular Fe(III) oxides.

In the present study, *S. oneidensis* was shown to produce and secrete a variety of thiol compounds, including cysteine, homocysteine, glutathione, and cysteamine when grown under Fe(III)-, Mn(III)- and Mn(IV)-reducing conditions. Both reduced and oxidized forms of the aforementioned thiol compounds were detected, indicating that the thiols are in a constant state of flux between the reduced and oxidized forms and that the concentration of reduced thiols to its' oxidized counterpart is indicative of the state of metal reduction by the microorganisms. These results indicate that endogenous thiols produced by *S. oneidensis* when utilizing Fe(III) oxides or Mn (III, IV) oxides as the terminal electron acceptor are used as an effective electron shuttles, which ultimately increase the efficiency

of electron transfer to external metal oxides during anaerobic Fe(III)-, Mn(III)-, and Mn(IV)-oxide respiration. Previous results indicate that biofilm formation and direct contact is not necessary for electron shuttling and Fe(III) reduction to occur. These results, taken into consideration with the identification of endogenous thiol and disulfides under Fe(III)- and Mn(III, IV)-reducing conditions provides novel evidence that electron shuttling is the predominant mechanism utilized by *S. oneidensis* under anaerobic metal-reducing conditions.

Under Fe(III)-reducing conditions (with ferrihydrite, hematite, and goethite), the Fe(III) reduction phenotypes for the wild-type, Δ*luxS*, and Δ*metY* yield nearly identical phenotypes, and Δ*metB* and Δ*metC* displayed Fe(III) reduction-deficient phenotypes. However, the reduction phenotypes with soluble Mn(III) or insoluble Mn(IV) were not as clear cut. With H2 and Mn(III), Δ*luxS*, Δ*metY,* and Δ*metC* displayed wild-type reduction activity, while Δ*metB* did not. With lactate and Mn(III), Δ*luxS*, and Δ*metY* yield nearly identical reduction rates, and Δ*metB* and Δ*metC* displayed Mn(III) reduction-deficient phenotypes. When insoluble Mn(IV) oxides were used as the terminal electron acceptor and $H_2$ as the electron donor, Δ*luxS*, Δ*metY,* and Δ*metB* displayed wild-type reduction activity, but Δ*metC* showed no reduction activity. Alternatively, lactate and Mn(IV) growth curves yielded wild-type reduction phenotypes for Δ*luxS* and Δ*metY,* but Δ*metB* and Δ*metC* displayed deficient reduction phenotypes. Just as the Fe(III) reduction and Mn(III,IV) reduction activities of wild-type, Δ*luxS,* Δ*metB,* Δ*metC* and Δ*metY* strains were not identical, the thiol production profiles of the wild-type, Δ*luxS,* Δ*metB,* Δ*metC* and Δ*metY* strains differed between Fe(III) and Mn(III, IV) oxides. There are, however, more similarities between thiols produced by insoluble Fe(III)- and Mn(IV)-oxides than with

soluble Mn(III). The IM/periplasmic embedded MtrCAB complex not only functions as the terminal Fe(III) or Mn(IV) reductase, but also has the potential to function as a terminal disulfide reductase, which provides a basis for electron shuttling to metal oxides via thiols.

The *S. oneidensis* genome contains genes that comprise the activated methyl cycle (AMC) and transsulfurylation pathways (TSP). The AMC is a metabolic cycle that produces the methyl donor S-adenosyl-L-methionine (SAM) and recycles methionine via S-adenosyl homocysteine (SAH) and homocysteine. The TSP is a metabolic pathway responsible for the interconversion of cysteine and homocysteine via cystathionine. In *S. oneidensis,* theses cycles are imperative the production of thiol compounds, including homocysteine, glutathione, and cysteine, that can serve as electron shuttles for Fe(III) oxide reduction. The results indicate that the components of the AMC and TSP of *S. oneidensis* yield extracellular thiols during anaerobic growth on Fe(III) oxides as the terminal electron acceptors and these extracellular thiols can also be used as an electron shuttle. Based on Fe(III) and Mn respiratory phenotypes observed in the AMC and TSP pathway mutants (Δ*luxS,* Δ*metB,* Δ*metC* and Δ*metY*) we can infer that cysteine, glutathione, and cysteamine contribute to metal reduction by serving as efficient electron shuttling molecules, while homocysteine is critical for maintenance of the AMC, propagation of thiol biosynthesis, and maintenance of cellular metabolism via the AMC intermediate SAM. Furthermore, these findings suggest that all metal-reducing bacteria require thiol formation to reduce solid metal oxides. Direct contact mechanism is not the dominant means through electrons are transferred and metals are reduced, instead electron shuttles are the main reduction mechanism.

## References


1. **DiChristina TJ, Fredrickson JK, Zachara JM.** 2005. Enzymology of electron transport: Energy generation with geochemical consequences. Molecular Geomicrobiology **59:**27-52.
2. **Bretschger O, Obraztsova A, Sturm CA, Chang IS, Gorby YA, Reed SB, Culley DE, Reardon CL, Barua S, Romine MF, Zhou J, Beliaev AS, Bouhenni R, Saffarini D, Mansfeld F, Kim BH, Fredrickson JK, Nealson KH.** 2007. Current production and metal oxide reduction by *Shewanella oneidensis* MR-1 wild type and mutants. Appl. Environ. Microbiol. **73:**7003-7012.
3. **Doong RA, Schink B.** 2002. Cysteine-mediated reductive dissolution of poorly crystalline iron(III) oxides by Geobacter sulfurreducens. Environ. Sci. Technol. **36:**2939-2945.
4. **Logan BE, Murano C, Scott K, Gray ND, Head IM.** 2005. Electricity generation from cysteine in a microbial fuel cell. Water Res **39:**942-952.
5. **Logan BE, Hamelers B, Rozendal RA, Schrorder U, Keller J, Freguia S, Aelterman P, Verstraete W, Rabaey K.** 2006. Microbial fuel cells: Methodology and technology. Environ. Sci. Technol. **40:**5181-5192.
6. **Madigan MT, J.M. Martinko, and T.D. Brock.** 2005. *Brock Biology of Microorganisms*, 11th ed. Prentice Hall/Pearson Education, Upper Saddle River, NJ.
7. **Luther GW, Sundby B, Lewis BL, Brendel PJ, Silverberg N.** 1997. Interactions of manganese with the nitrogen cycle: Alternative pathways to dinitrogen. Geochim. Cosmochim. Acta **61:**4043-4052.
8. **Neretin LN, Pohl C, Jost G, Leipe T, Pollehne F.** 2003. Manganese cycling in the Gotland Deep, Baltic Sea. Mar. Chem. **82:**125-143.
9. **Tebo BM, Bargar JR, Clement BG, Dick GJ, Murray KJ, Parker D, Verity R, Webb SM.** 2004. Biogenic manganese oxides: Properties and mechanisms of formation. Annu Rev Earth Pl Sc **32:**287-328.
10. **White DJ, Noll MR, Makarewicz JC.** 2008. Does Manganese Influence Phosphorus Cycling under Suboxic Lake Water Conditions? J Great Lakes Res **34:**571-580.
11. **Davison W.** 1993. Iron and Manganese in Lakes. Earth-Sci Rev **34:**119-163.
12. **Bricker O.** 1965. Some Stability Relations in System Mn-O2-H2o at 25 Degrees and 1 Atmosphere Total Pressure. Am Mineral **50:**1296-&.
13. **Otero XL, Ferreira TO, Huerta-Diaz MA, Partiti CSM, Souza V, Vidal-Torrado P, Macias F.** 2009. Geochemistry of iron and manganese in soils and sediments of a mangrove system, Island of Pai Matos (Cananeia - SP, Brazil). Geoderma **148:**318-335.
14. **Myers CR, Nealson KH.** 1988. Bacterial manganese reduction and growth with manganese oxide as the sole electron acceptor. Science **240:**1319-1321.
15. **Yao WS, Millero FJ.** 1993. The Rate of Sulfide Oxidation by Delta-Mno2 in Seawater. Geochim. Cosmochim. Acta **57:**3359-3365.
16. **Villinski JE, Saiers JE, Conklin MH.** 2003. The effects of reaction-product formation on the reductive dissolution of MnO2 by Fe(II). Environ. Sci. Technol. **37:**5589-5596.

17. **Coates JD, Michaelidou U, Bruce RA, O'Connor SM, Crespi JN, Achenbach LA.** 1999. Ubiquity and diversity of dissimilatory (per)chlorate-reducing bacteria. Appl. Environ. Microbiol. **65:**5234-5241.
18. **Van Cappellen P, Viollier E, Roychoudhury A, Clark L, Ingall E, Lowe K, Dichristina T.** 1998. Biogeochemical cycles of manganese and iron at the oxic-anoxic transition of a stratified marine basin (Orca Basin, Gulf of Mexico). Environ. Sci. Technol. **32:**2931-2939.
19. **Krishnan KP, Sinha RK, Krishna K, Nair S, Singh SM.** 2009. Microbially mediated redox transformations of manganese (II) along with some other trace elements: a study from Antarctic lakes. Polar Biol. **32:**1765-1778.
20. **Thamdrup B.** 2000. *Bacterial manganese and iron reduction in aquatic sediments*, p. 86-103. *In* Schink B (ed.), *Advances in Microbial Ecology*. Kluwer Academic Publishers, Dordrecht.
21. **Lovley DR, Holmes DE, Nevin KP.** 2004. Dissimilatory Fe(III) and Mn(IV) reduction. Advances in Microbial Physiology, Vol. 49 **49:**219-286.
22. **Burnes BS, Mulberry MJ, DiChristina TJ.** 1998. Design and application of two rapid screening techniques for isolation of Mn(IV) reduction-deficient mutants of *Shewanella putrefaciens*. Appl. Environ. Microbiol. **64:**2716-2720.
23. **Kostka JE, Luther GW, Nealson KH.** 1995. Chemical and biological reduction of Mn(III)-pyrophosphate complexes - potential importance of dissolved Mn(III) as an environmental oxidant. Geochim. Cosmochim. Acta **59:**885-894.
24. **DiChristina TJ.** 2005. New insights into the molecular mechanism of microbial metal respiration. Geochim. Cosmochim. Acta **69:**A670-A670.
25. **Hau HH, Gralnick JA.** 2007. Ecology and biotechnology of the genus *Shewanella*. Annu. Rev. Microbiol. **61:**237-258.
26. **Morgan JJ.** 2000. Metal Ions in Biological Systems Manganese and Its Role in Biological Processes, vol. 37.
27. **Moser DP, Nealson KH.** 1996. Growth of the facultative anaerobe Shewanella putrefaciens by elemental sulfur reduction. Appl. Environ. Microbiol. **62:**2100-2105.
28. **Saffarini DA, DiChristina TJ, Bermudes D, Nealson KH.** 1994. Anaerobic respiration of *Shewanella putrefaciens* requires both chromosomal and plasmid-borne genes. FEMS Microbiol. Lett. **119:**271-277.
29. **Taratus EM, Eubanks SG, DiChristina TJ.** 2000. Design and application of a rapid screening technique for isolation of selenite reduction-deficient mutants of *Shewanella putrefaciens*. Microbiol. Res. **155:**79-85.
30. **Taillefert M, Beckler JS, Carey E, Burns JL, Fennessey CM, DiChristina TJ.** 2007. *Shewanella putrefaciens* produces an Fe(III)-solubilizing organic ligand during anaerobic respiration on insoluble Fe(III) oxides. J. Inorg. Biochem. **101:**1760-1767.
31. **Heidelberg JF, Paulsen IT, Nelson KE, Gaidos EJ, Nelson WC, Read TD, Eisen JA, Seshadri R, Ward N, Methe B, Clayton RA, Meyer T, Tsapin A, Scott J, Beanan M, Brinkac L, Daugherty S, DeBoy RT, Dodson RJ, Durkin AS, Haft DH, Kolonay JF, Madupu R, Peterson JD, Umayam LA, White O, Wolf AM, Vamathevan J, Weidman J, Impraim M, Lee K, Berry K, Lee C, Mueller J, Khouri H, Gill J, Utterback TR, McDonald LA, Feldblyum TV,**

**Smith HO, Venter JC, Nealson KH, Fraser CM.** 2002. Genome sequence of the dissimilatory metal ion-reducing bacterium Shewanella oneidensis. Nat. Biotechnol. **20:**1118-1123.

32. **DiChristina TJ.** 2002. New insights into the molecular mechanism of microbial metal reduction. Abstr Pap Am Chem S **223:**U595-U595.
33. **Myers JM, Myers CR.** 2003. Overlapping role of the outer membrane cytochromes of Shewanella oneidensis MR-1 in the reduction of manganese(IV) oxide. Lett. Appl. Microbiol. **37:**21-25.
34. **Shi L, Deng S, Marshall MJ, Wang ZM, Kennedy DW, Dohnalkova AC, Mottaz HM, Hill EA, Gorby YA, Beliaev AS, Richardson DJ, Zachara JM, Fredrickson JK.** 2008. Direct involvement of type II secretion system in extracellular translocation of *Shewanella oneidensis* outer membrane cytochromes MtrC and OmcA. J. Bacteriol. **190:**5512-5516.
35. **Fennessey CM, Jones ME, Taillefert M, DiChristina TJ.** 2010. Siderophores are not involved in Fe(III) solubilization during anaerobic Fe(III) respiration by *Shewanella oneidensis* MR-1. Appl. Environ. Microbiol. **76:**2425-2432.
36. **Jones ME, Fennessey CM, DiChristina TJ, Taillefert M.** 2010. *Shewanella oneidensis* MR-1 mutants selected for their inability to produce soluble organic-Fe(III) complexes are unable to respire Fe(III) as anaerobic electron acceptor. Environmental Microbiology **12:**938-950.
37. **Lovley DR, Woodward JC, Chapelle FH.** 1996. Rapid anaerobic benzene oxidation with a variety of chelated Fe(III) forms. Appl. Environ. Microbiol. **62:**288-291.
38. **Marsili E, Baron DB, Shikhare ID, Coursolle D, Gralnick JA, Bond DR.** 2008. Shewanella Secretes flavins that mediate extracellular electron transfer. Proc. Natl. Acad. Sci. U. S. A. **105:**3968-3973.
39. **Newman DK, Kolter R.** 2000. A role for excreted quinones in extracellular electron transfer. Nature **405:**94-97.
40. **Wee SK.** 2014. Novel pathway for microbial Fe(III) reduction: electron shuttling through naturally occuring thiols. Georgia Institute of Technology.
41. **Hand CE, Honek JF.** 2005. Biological chemistry of naturally occurring thiols of microbial and marine origin. J. Nat. Prod. **68:**293-308.
42. **Fahey RC.** 2001. Novel thiols of prokaryotes. Annu. Rev. Microbiol. **55:**333-356.
43. **Fahey RC, Sundquist AR.** 1991. Evolution of Glutathione Metabolism. Adv. Enzymol. Relat. Areas Mol. Biol. **64:**1-53.
44. **Newton GL, Buchmeier N, Fahey RC.** 2008. Biosynthesis and functions of mycothiol, the unique protective thiol of *Actinobacteria*. Microbiol. Mol. Biol. Rev. **72:**471-+.
45. **Rawat M, Av-Gay Y.** 2007. Mycothiol-dependent proteins in actinomycetes. FEMS Microbiol. Rev. **31:**278-292.
46. **Newton GL, Rawat M, La Clair JJ, Jothivasan VK, Budiarto T, Hamilton CJ, Claiborne A, Helmann JD, Fahey RC.** 2009. Bacillithiol is an antioxidant thiol produced in Bacilli. Nat. Chem. Biol. **5:**625-627.
47. **Aitken SM, Lodha PH, Morneau DJK.** 2011. The enzymes of the transsulfuration pathways: Active-site characterizations. Bba-Proteins Proteom **1814:**1511-1517.

48. **Doherty NC, Shen F, Halliday NM, Barrett DA, Hardie KR, Winzer K, Atherton JC.** 2009. In Helicobacter pylori, LuxS is a key enzyme in cysteine provision through a reverse transsulfuration pathway. J. Bacteriol. **192:**1184-1192.
49. **Amirbahman A, Sigg L, vonGunten U.** 1997. Reductive dissolution of Fe(III) (hydr)oxides by cysteine: Kinetics and mechanism. J. Colloid Interface Sci. **194:**194-206.
50. **Doong RA, Chiang HC.** 2005. Transformation of carbon tetrachloride by thiol reductants in the presence of quinone compounds. Environ. Sci. Technol. **39:**7460-7468.
51. **Kaden J, Galushko AS, Schink B.** 2002. Cysteine-mediated electron transfer in syntrophic acetate oxidation by cocultures of Geobacter sulfurreducens and Wolinella succinogenes. Arch. Microbiol. **178:**53-58.
52. **Neal AL, Dublin SN, Taylor J, Bates DJ, Burns L, Apkarian R, DiChristina TJ.** 2007. Terminal electron acceptors influence the quantity and chemical composition of capsular exopolymers produced by anaerobically growing *Shewanella* spp. Biomacromolecules **8:**166-174.
53. **Blakeney MD, Moulaei T, DiChristina TJ.** 2000. Fe(III) reduction activity and cytochrome content of *Shewanella putrefaciens* grown on ten compounds as sole terminal electron acceptor. Microbiol. Res. **155:**87-94.
54. **Altschul SF, Madden TL, Schaffer AA, Zhang JH, Zhang Z, Miller W, Lipman DJ.** 1997. Gapped BLAST and PSI-BLAST: a new generation of protein database search programs. Nucleic Acids Res. **25:**3389-3402.
55. **Burns JL, DiChristina TJ.** 2009. Anaerobic Respiration of Elemental Sulfur and Thiosulfate by *Shewanella oneidensis* MR-1 Requires *psrA*, a Homolog of the *phsA* Gene of *Salmonella enterica* Serovar Typhimurium LT2. Appl. Environ. Microbiol. **75:**5209-5217.
56. **Kovach ME, Elzer PH, Hill DS, Robertson GT, Farris MA, Roop RM, Peterson KM.** 1995. Four new derivatives of the broad-host-range cloning vector PBBR1MCS, carrying different antibiotic-resistance cassettes. Gene **166:**175-176.
57. **DiChristina TJ, Moore CM, Haller CA.** 2002. Dissimilatory Fe(III) and Mn(IV) reduction by *Shewanella putrefaciens* requires *ferE*, a homolog of the *pulE* (*gspE*) type II protein secretion gene. J. Bacteriol. **184:**142-151.
58. **Stookey LL.** 1970. Ferrozine - a new spectrophotometric reagent for iron. Anal. Chem. **42:**779-781.
59. **Tang DG, Hung CC, Warnken KW, Santschi PH.** 2000. The distribution of biogenic thiols in surface waters of Galveston Bay. Limnol Oceanogr **45:**1289-1297.
60. **Rizzo V, Montalbetti L, Valli M, Bosoni T, Scoglio E, Moratti R.** 1998. Study of factors affecting the determination of total plasma 7-fluorobenzo-2-oxa-1,3-diazole-4-sulfonate (SBD)-thiol derivatives by liquid chromatography. Journal of Chromatography B **706:**209-215.
61. **Oe T, Ohyagi T, Naganuma A.** 1998. Determination of gamma-glutamylglutathione and other low-molecular-mass biological thiol compounds by isocratic high-performance liquid chromatography with fluorimetric detection. Journal of Chromatography B **708:**285-289.

62. **Pastore A, Massoud R, Motti C, Lo Russo A, Fucci G, Cortese C, Federici G.** 1998. Fully automated assay for total homocysteine, cysteine, cysteinylglycine, glutathione, cysteamine, and 2-mercaptopropionylglycine in plasma and urine. Clin. Chem. **44:**825-832.
63. **Seiwert B, Karst U.** 2007. Simultaneous LC/MS/MS determination of thiols and disulfides in urine samples based on differential labeling with ferrocene-based maleimides. Anal. Chem. **79:**7131-7138.
64. **Lies DP, Hernandez ME, Kappler A, Mielke RE, Gralnick JA, Newman DK.** 2005. *Shewanella oneidensis* MR-1 uses overlapping pathways for iron reduction at a distance and by direct contact under conditions relevant for biofilms. Appl. Environ. Microbiol. **71:**4414-4426.
65. **Nevin KP, Lovley DR.** 2002. Mechanisms for Fe(III) oxide reduction in sedimentary environments. Geomicrobiol J **19:**141-159.
66. **L. G, A. L, T. L, D. MF, T. R, I. G.** 1999. DIrect electron transfer between heme-containing enzymes and electrodes as a basis for third generation biosensors. Anal. Chim. Acta **400:**91-108.
67. **S. FR, A. PC, D. ML, T. KL.** 2003. DIrect electron transfer: an approach for electrochemical biosensors with higher selectivity and sensitivity. Journal of the Brazilian Chemical Society **14:**230-243.
68. **B. GH, R. WJ.** 1996. Electron transfer in proteins. Annu. Rev. Biochem. **65:**537-561.
69. **Lovley DR, Coates JD, BluntHarris EL, Phillips EJP, Woodward JC.** 1996. Humic substances as electron acceptors for microbial respiration. Nature **382:**445-448.
70. **Lovley DR, Kashefi K, Vargas M, Tor JM, Blunt-Harris EL.** 2000. Reduction of humic substances and Fe(III) by hyperthermophilic microorganisms. Chem Geol **169:**289-298.
71. **Roden EE.** 2012. Microbial iron-redox cycling in subsurface environments. Biochem. Soc. Trans. **40:**1249-1256.
72. **Hernandez ME, Kappler A, Newman DK.** 2004. Phenazines and other redox-active antibiotics promote microbial mineral reduction. Appl. Environ. Microbiol. **70:**921-928.
73. **Turick CE, Tisa LS, Caccavo F.** 2002. Melanin production and use as a soluble electron shuttle for Fe(III) oxide reduction and as a terminal electron acceptor by Shewanella algae BrY. Appl. Environ. Microbiol. **68:**2436-2444.
74. **von Canstein H, Ogawa J, Shimizu S, Lloyd JR.** 2008. Secretion of flavins by *Shewanella* species and their role in extracellular electron transfer. Appl. Environ. Microbiol. **74:**615-623.
75. **Myers CR, Myers JA.** 2004. *Shewanella oneidensis* MR-1 restores menaquinone synthesis to a menaquinone-negative mutant. Appl. Environ. Microbiol. **70:**5415-5425.
76. **Coursolle D, Baron DB, Bond DR, Gralnick JA.** 2010. The Mtr Respiratory Pathway Is Essential for Reducing Flavins and Electrodes in Shewanella oneidensis. Journal of Bacteriology **192:**467-474.
77. **Shi Z, Zachara JM, Shi L, Wang ZM, Moore DA, Kennedy DW, Fredrickson JK.** 2012. Redox Reactions of Reduced Flavin Mononucleotide (FMN), Riboflavin

(RBF), and Anthraquinone-2,6-disulfonate (AQDS) with Ferrihydrite and Lepidocrocite. Environ. Sci. Technol. **46:**11644-11652.

## Figures

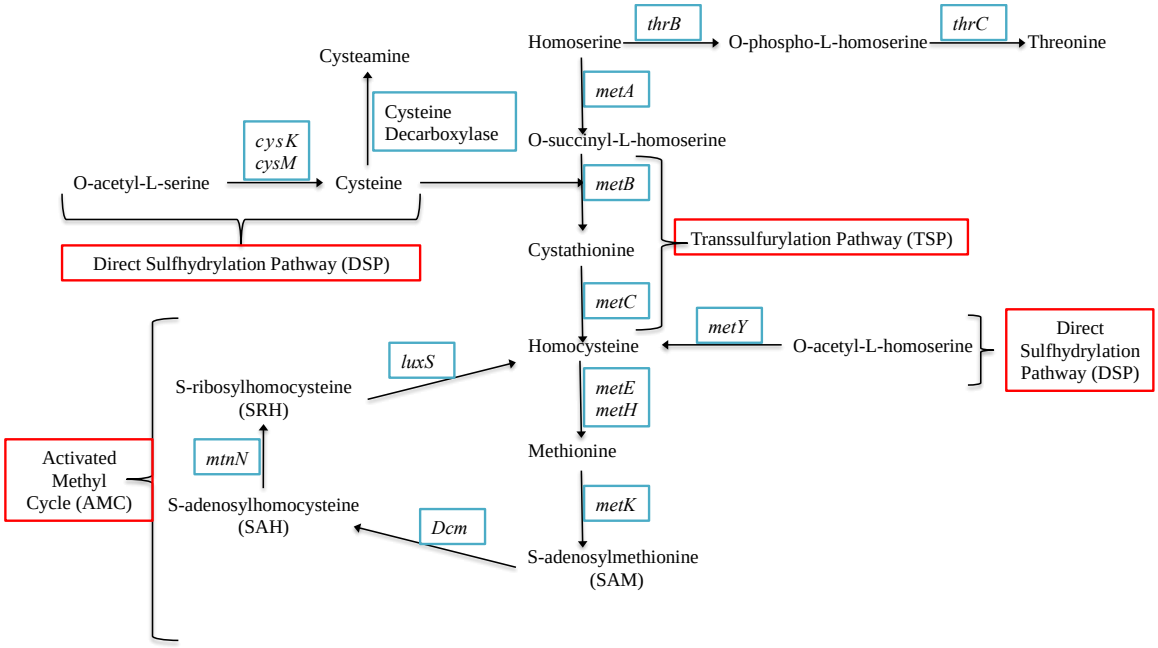


**Figure 4.1. Biosynthesis pathways of homocysteine in *Shewanella.* In *Shewanella,* formation of homocysteine can occur from one of three different pathways: the activated methyl cycle (AMC) is mediated by *luxS*, the transsulfuration pathway (TSP) is mediated by *metB* and *metC*, and the direct sulfhydrylation pathway (DSP) is mediated by *metY* and and *cysK/cysM*.**

**A.**

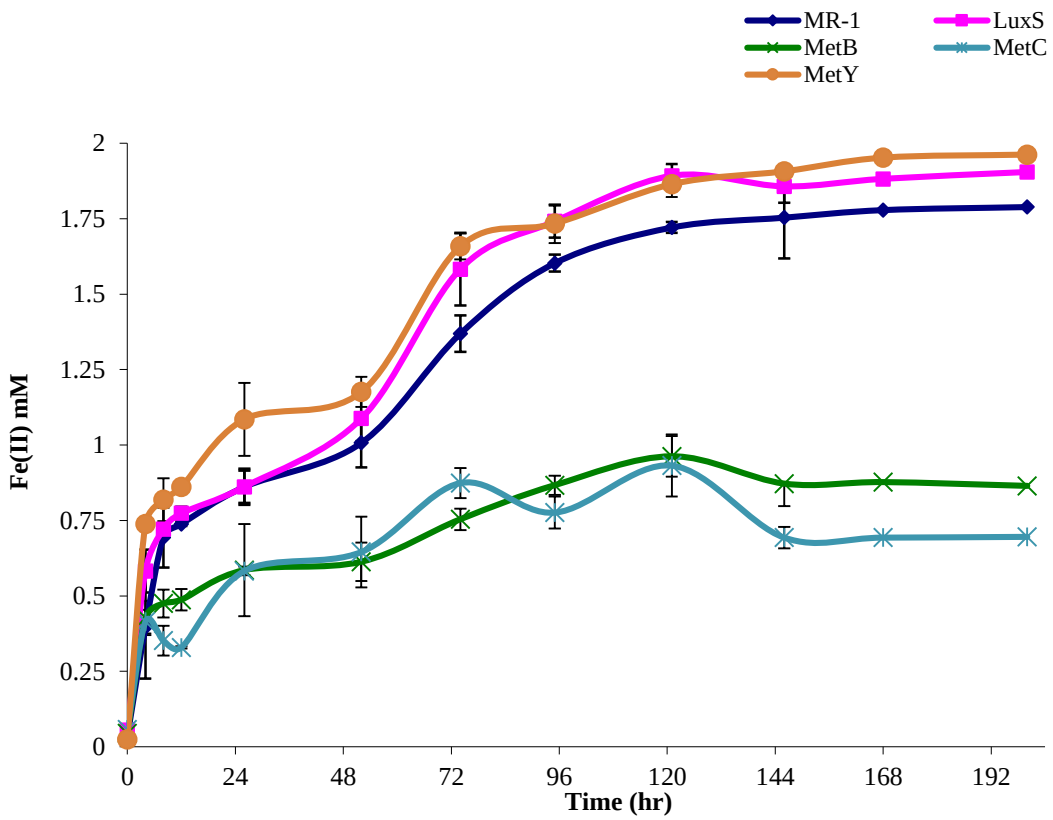
MR-1
LuxS
MetB
MetC
MetY
Fe(II) mM
Time (hr)
0
0.25
0.5
0.75
1
1.25
1.5
1.75
2
0
24
48
72
96
120
144
168
192

**B.**

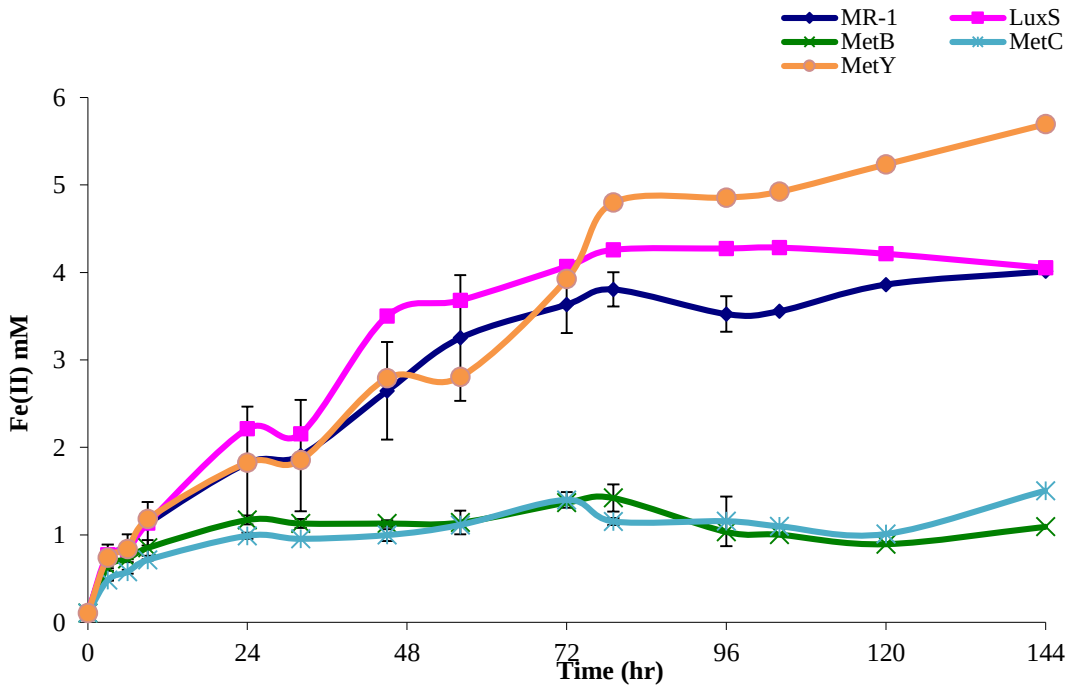
MR-1
LuxS
MetB
MetC
MetY
Fe(II) mM
Time (hr)
0
1
2
3
4
5
6
0
24
48
72
96
120
144

**C.**

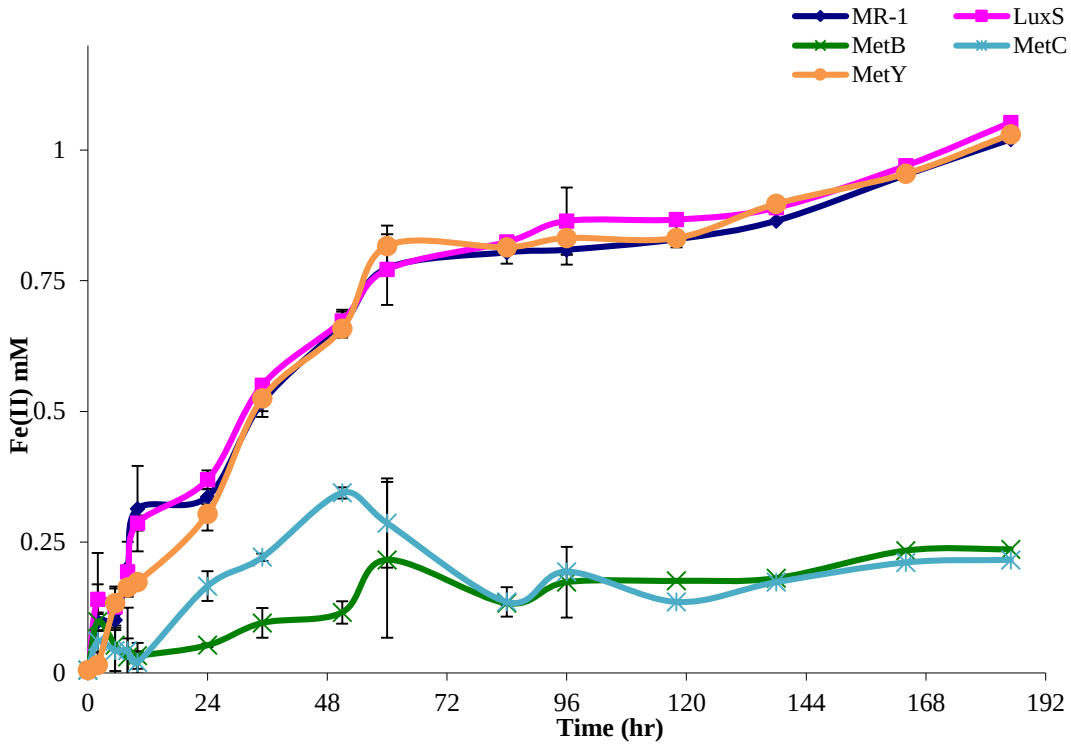
MR-1
LuxS
MetB
MetC
MetY
Fe(II) mM
0
0.25
0.5
0.75
1
0
24
48
72
96
120
144
168
192
Time (hr)

**D.**

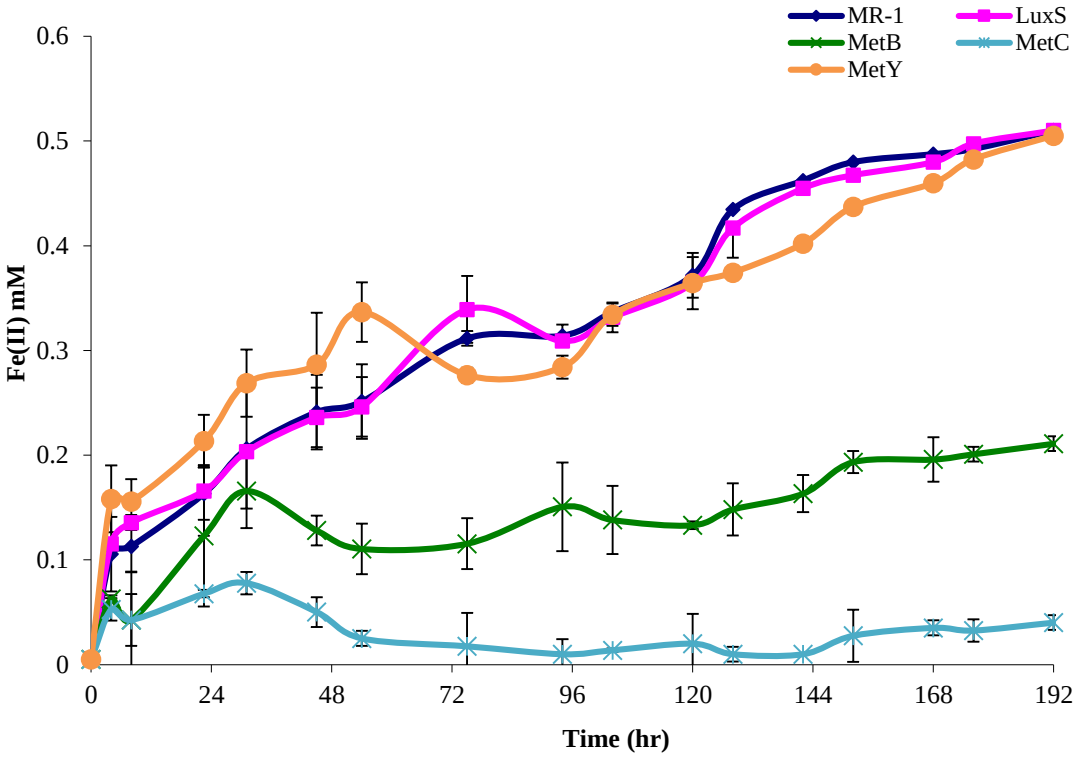
MR-1
LuxS
MetB
MetC
MetY
Fe(II) mM
0
0.1
0.2
0.3
0.4
0.5
0.6
0
24
48
72
96
120
144
168
192
Time (hr)

**E.**

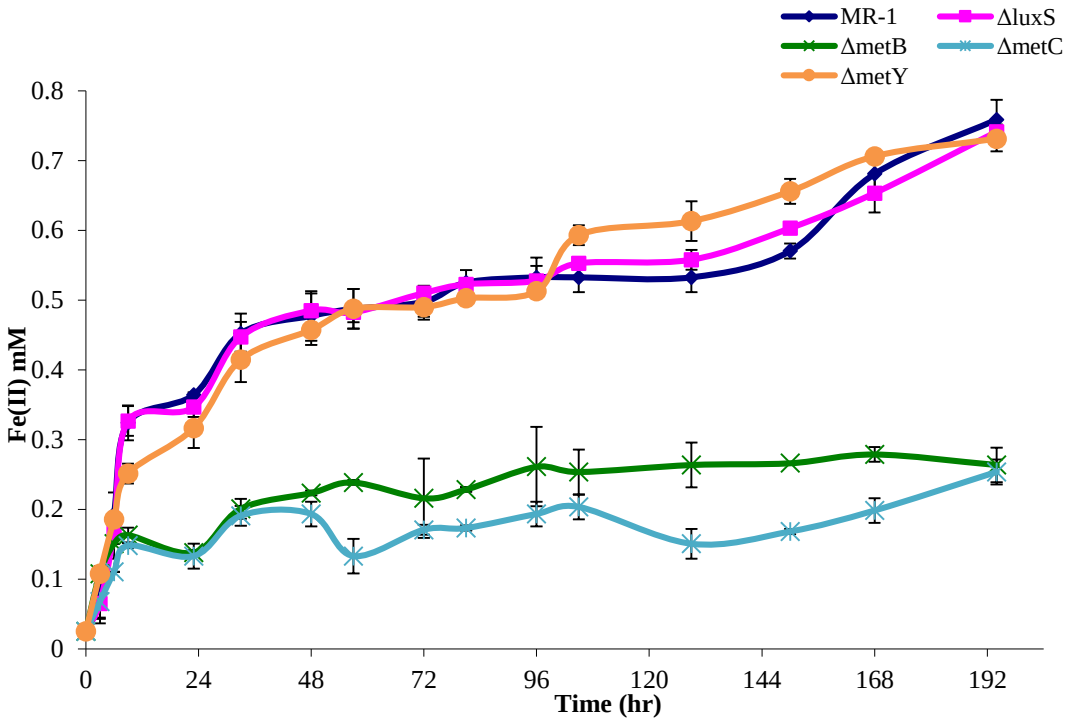
MR-1
ΔluxS
ΔmetB
ΔmetC
ΔmetY
Fe(II) mM
0
0.1
0.2
0.3
0.4
0.5
0.6
0.7
0.8
0
24
48
72
96
120
144
168
192
Time (hr)

**F.**

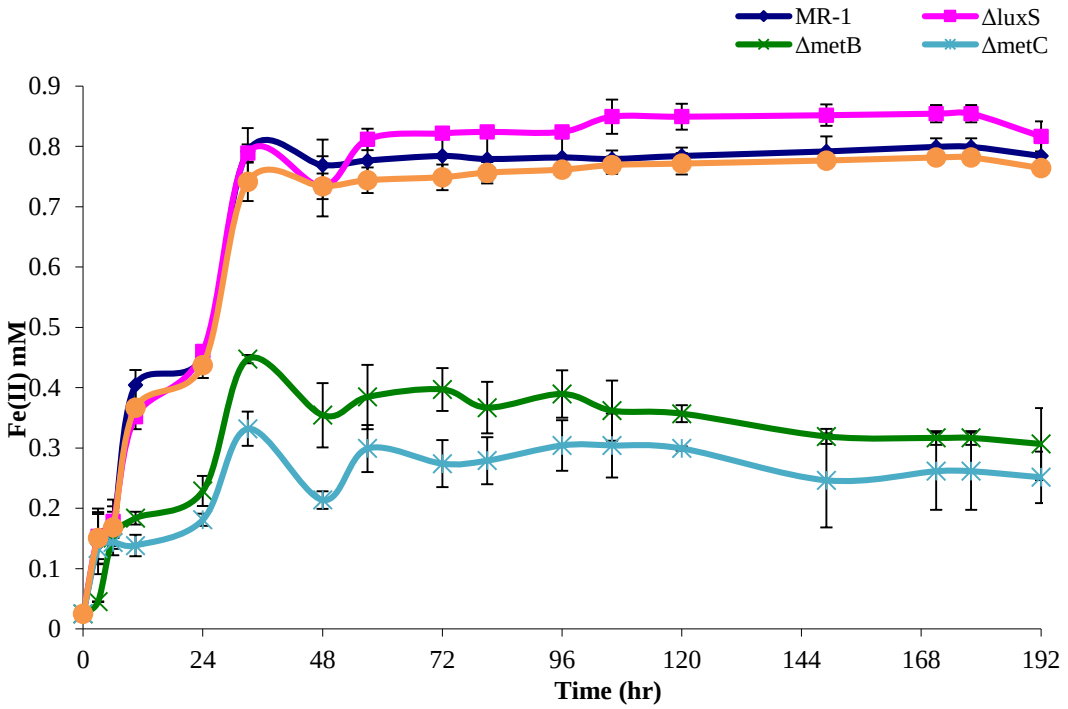
MR-1
ΔluxS
ΔmetB
ΔmetC
Fe(II) mM
0
0.1
0.2
0.3
0.4
0.5
0.6
0.7
0.8
0.9
0
24
48
72
96
120
144
168
192
Time (hr)

**Figure 4.2. Anaerobic Fe(III) reduction by *S. oneidensis* wild-type and Δ*luxS*, Δ*metB*, Δ*metC*, and Δ*metY* mutant strains amended with (A) HFO as the electron acceptor and $H_2$ as the electron donor, (B) HFO as the electron acceptor and lactate as the electron donor, (C) hematite as the electron acceptor and $H_2$ as the electron donor, (D) hematite as the electron acceptor and lactate as the electron donor, (E) Goethite as electron acceptor and $H_2$ as the electron donor, (F) Goethite as electron acceptor and lactate as the electron donor. Values are means of two parallel yet independent anaerobic incubations, and each time point in the two parallel incubations represent triplicate samples. Error bars represent range of errors. In some cases, error bars are smaller than the symbol.**

**A.**

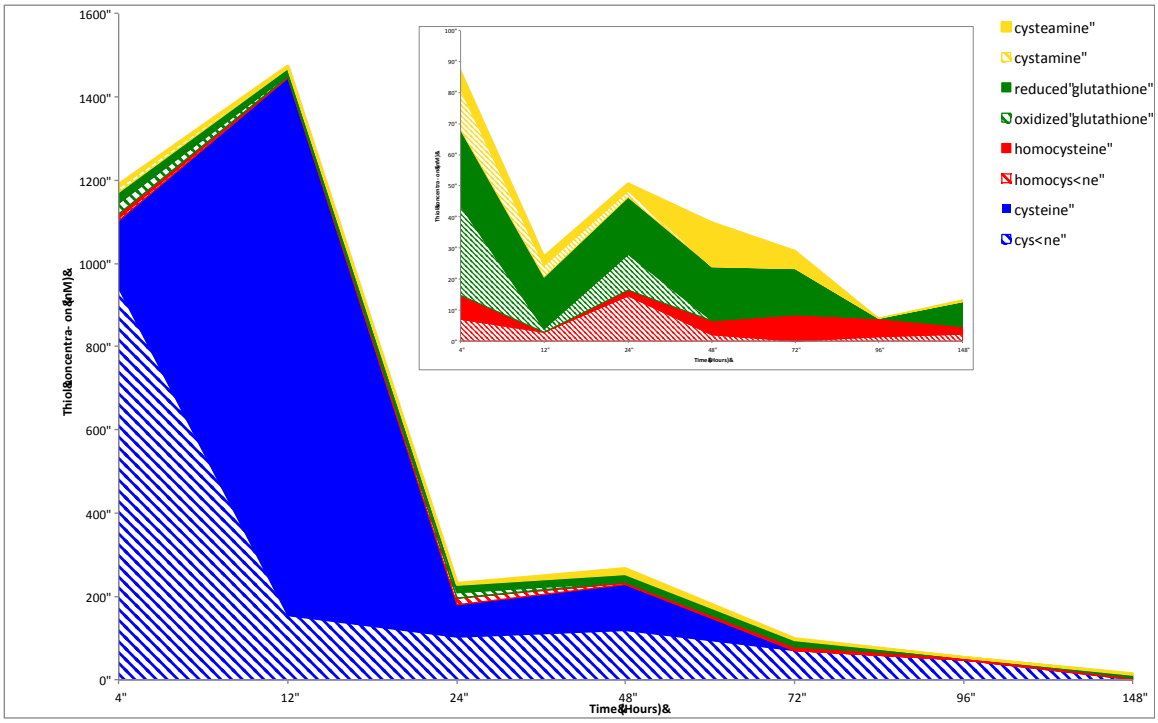
1600"
1400"
1200"
1000"
800"
600"
400"
200"
0"
Thiol&concentra- on&(nM)&
4"
12"
24"
48"
72"
96"
148"
Time&(Hours)&
cysteamine"
cystamine"
reduced"glutathione"
oxidized"glutathione"
homocysteine"
homocys<ne"
cysteine"
cys<ne"

**B.**

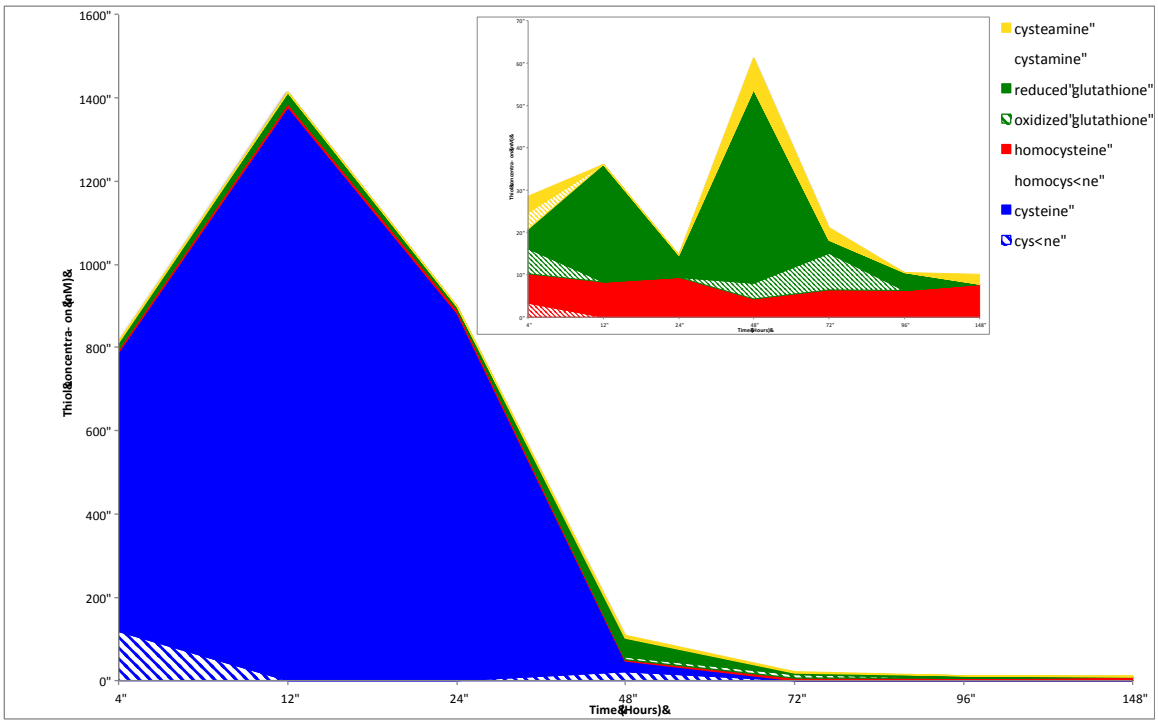
1600"
1400"
1200"
1000"
800"
600"
400"
200"
0"
Thiol&concentra- on&(nM)&
4"
12"
24"
48"
72"
96"
148"
Time&(Hours)&
cysteamine"
cystamine"
reduced"glutathione"
oxidized"glutathione"
homocysteine"
homocys<ne"
cysteine"
cys<ne"

**C.**

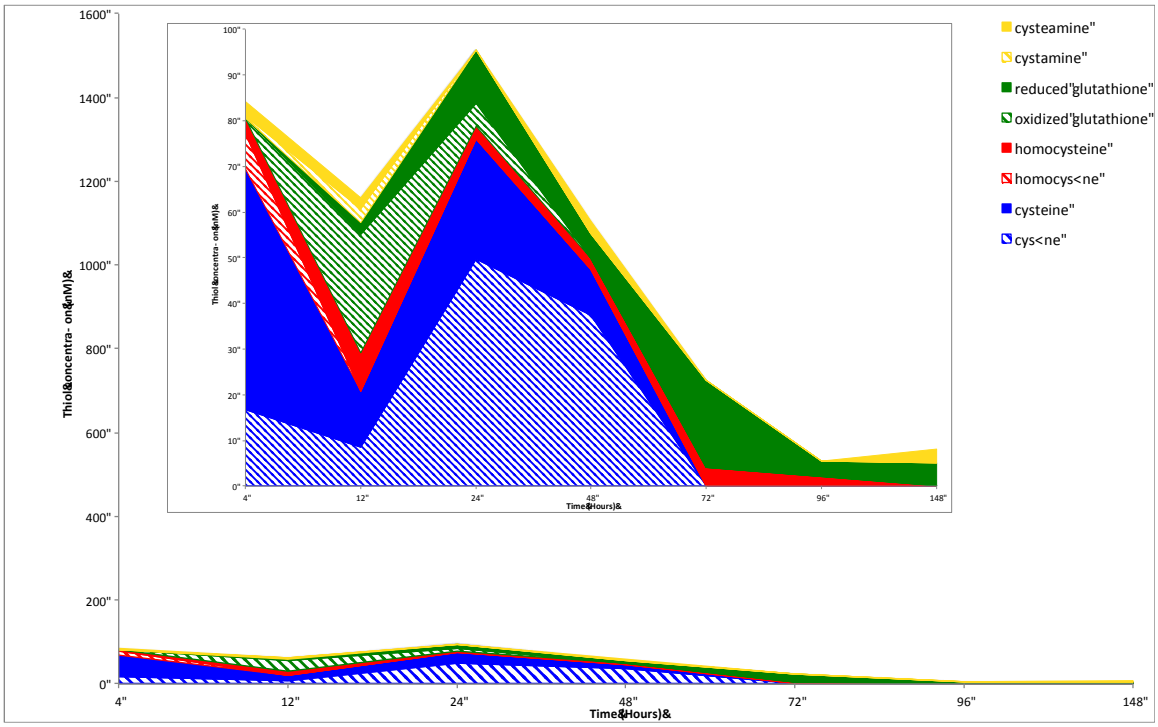
cysteamine"
cystamine"
reduced"glutathione"
oxidized"glutathione"
homocysteine"
homocys<ne"
cysteine"
cys<ne"
Thiol&concentra- on&(nM)&
Time&(Hours)&
1600"
1400"
1200"
1000"
800"
600"
400"
200"
0"
4"
12"
24"
48"
72"
96"
148"

**D.**

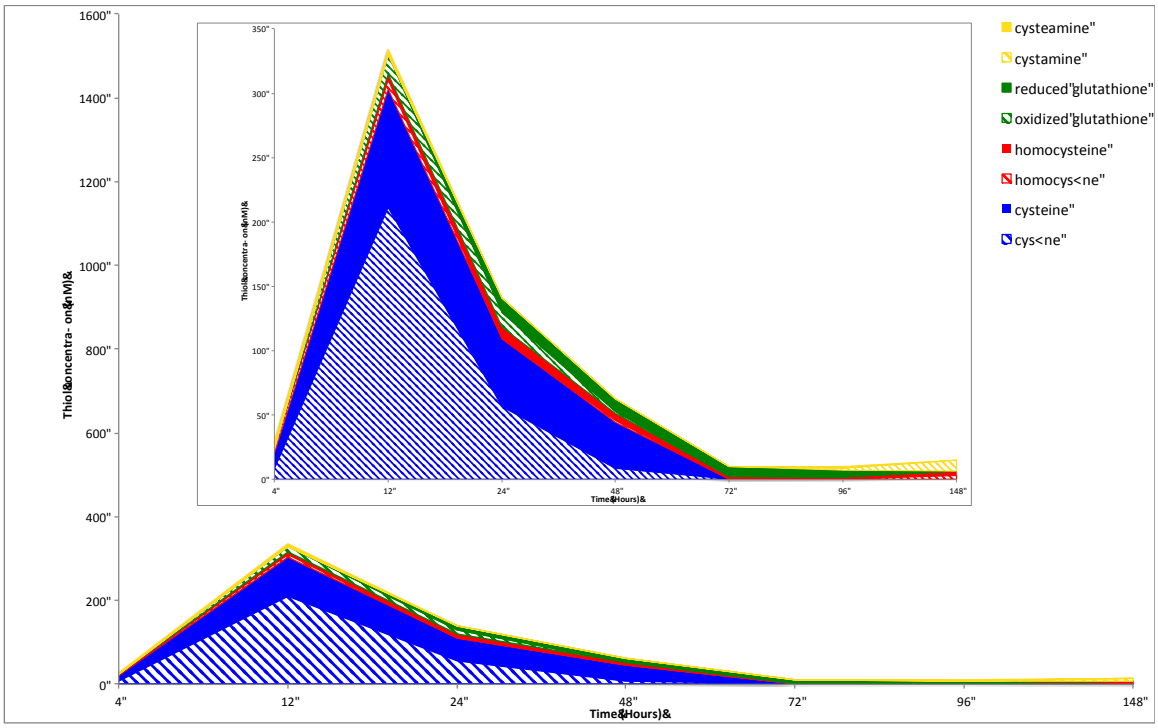
cysteamine"
cystamine"
reduced"glutathione"
oxidized"glutathione"
homocysteine"
homocys<ne"
cysteine"
cys<ne"
Thiol&concentra- on&(nM)&
Time&(Hours)&
1600"
1400"
1200"
1000"
800"
600"
400"
200"
0"
4"
12"
24"
48"
72"
96"
148"

**E.**

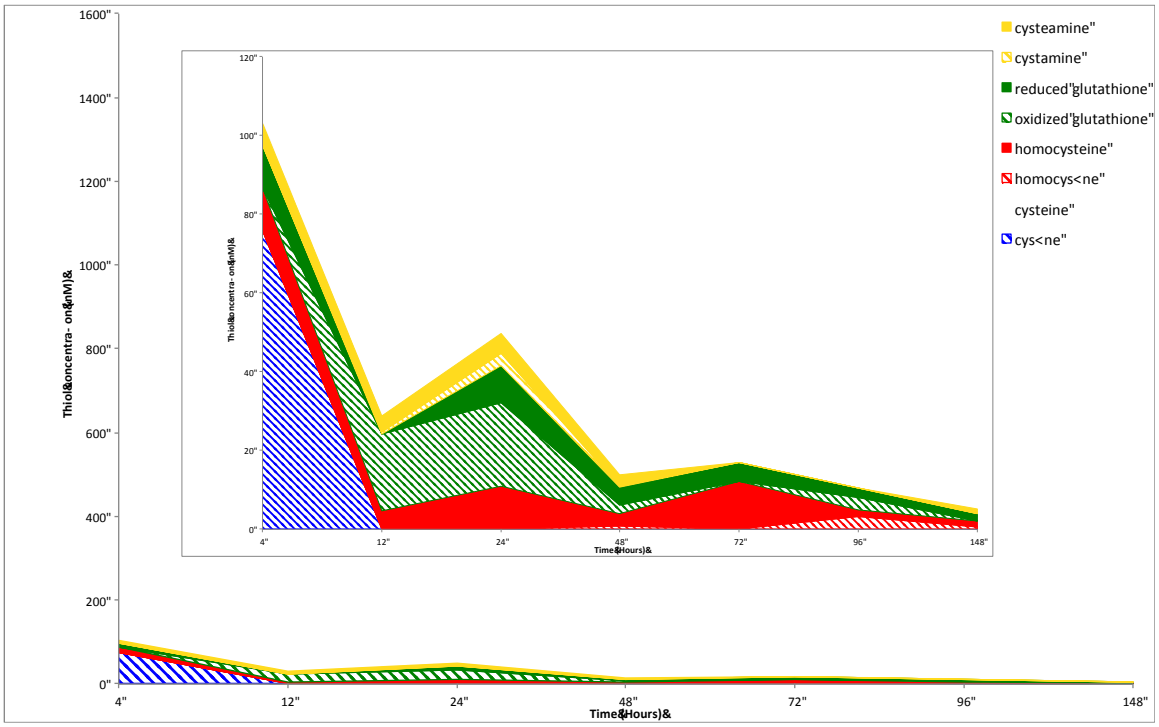


**Figure 4.3. Identification of extracellular thiols produced by *S. oneidensis* wild-type (A) and AMC and transulfurylation pathway mutants strains lacking *luxS* (B), *metB (C)*, *metC (D)*, and *metY (E)* during anaerobic growth with $H_2$ as the electron donor and solid Fe(III) oxides (HFO) as electron acceptor.**

**A.**

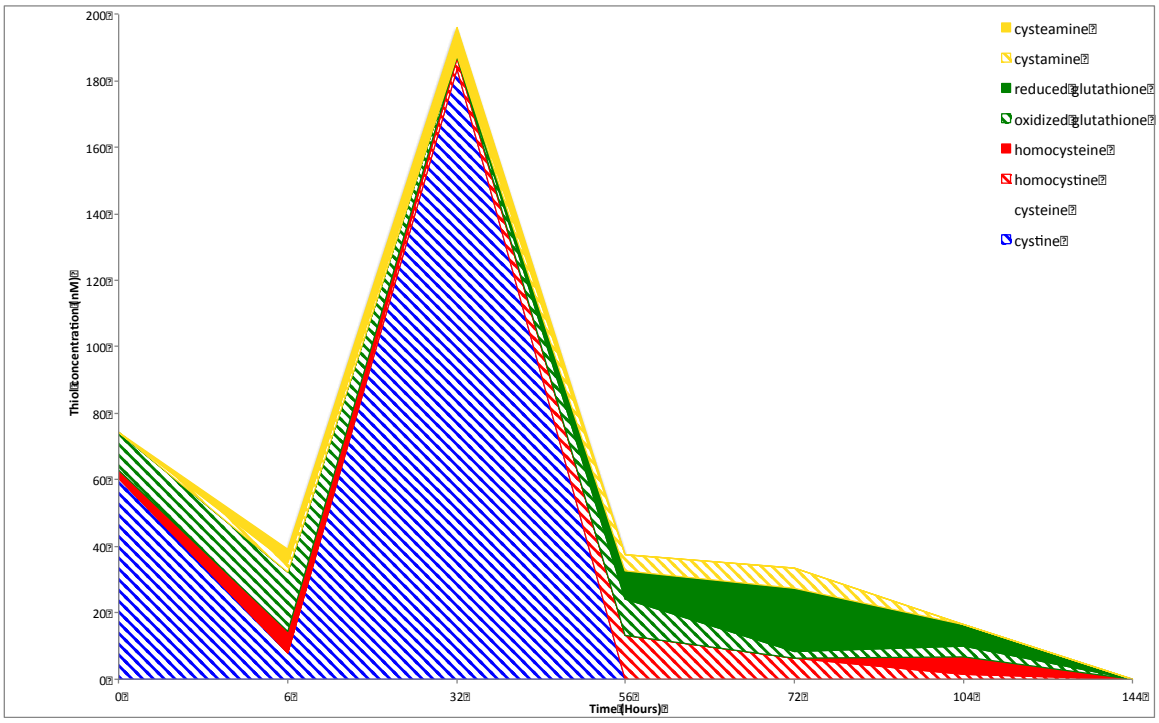
cysteamine
cystamine
reduced glutathione
oxidized glutathione
homocysteine
homocystine
cysteine
cystine
Thiol concentration (nM)
Time (Hours)
0
20
40
60
80
100
120
140
160
180
200
0
6
32
56
72
104
144

**B.**

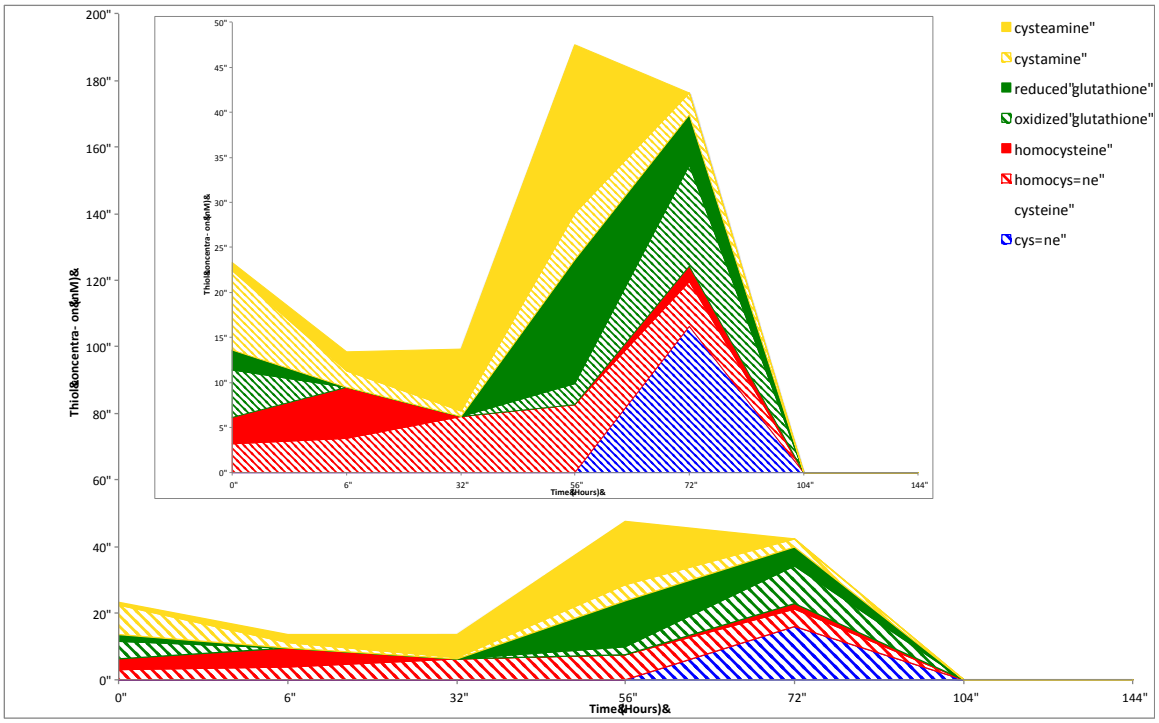
cysteamine
cystamine
reduced glutathione
oxidized glutathione
homocysteine
homocys=ne
cysteine
cys=ne
Time (Hours)

**C.**

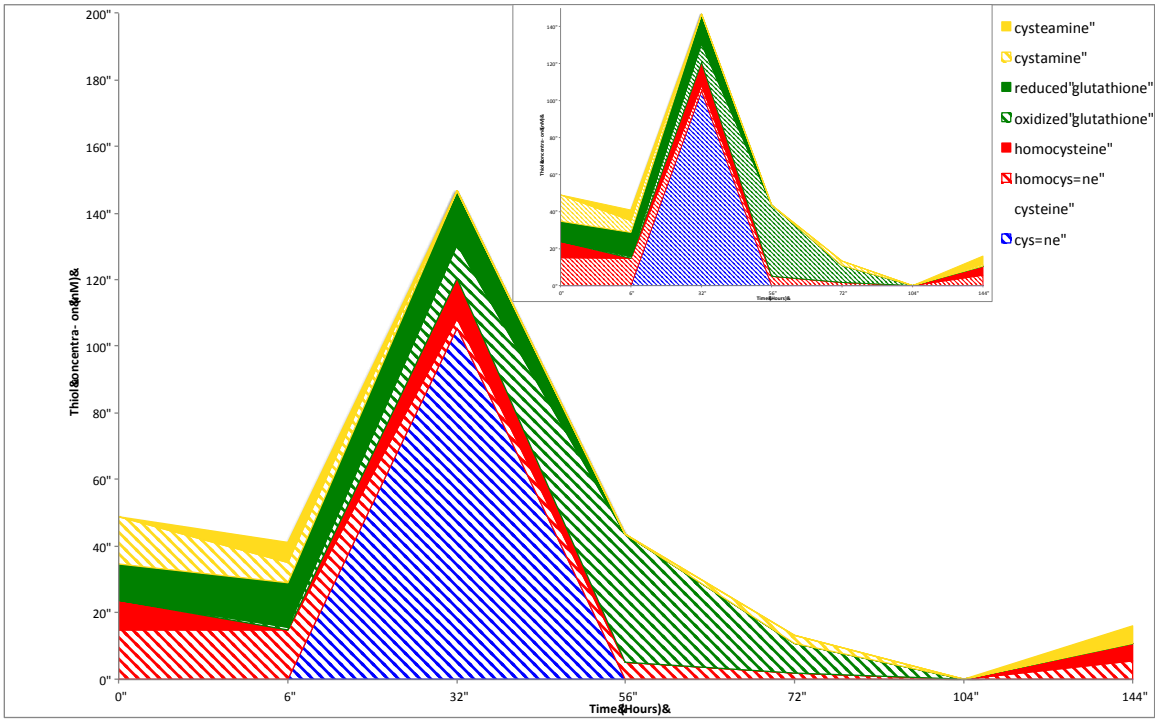
200"
180"
160"
140"
120"
100"
80"
60"
40"
20"
0"
Thiol&concentra- on&(nM)&
0"
6"
32"
56"
72"
104"
144"
Time&(Hours)&
cysteamine"
cystamine"
reduced"glutathione"
oxidized"glutathione"
homocysteine"
homocys=ne"
cysteine"
cys=ne"

**D.**

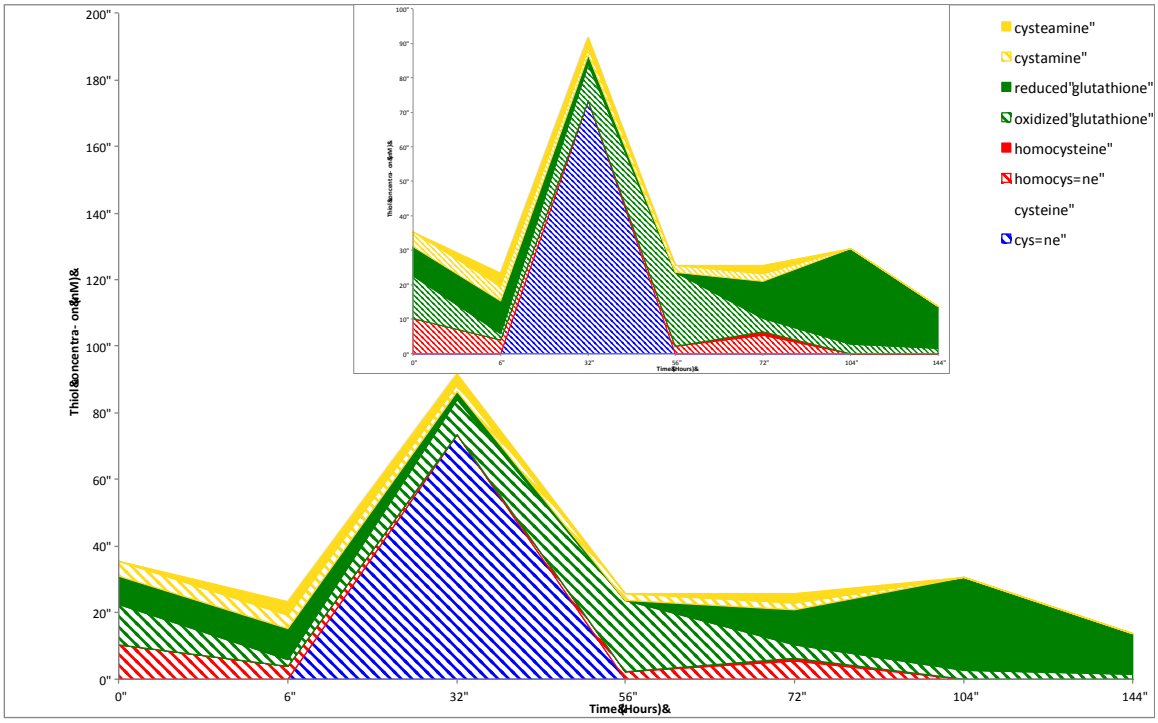
200"
180"
160"
140"
120"
100"
80"
60"
40"
20"
0"
Thiol&concentra- on&(nM)&
0"
6"
32"
56"
72"
104"
144"
Time&(Hours)&
cysteamine"
cystamine"
reduced"glutathione"
oxidized"glutathione"
homocysteine"
homocys=ne"
cysteine"
cys=ne"

**E.**

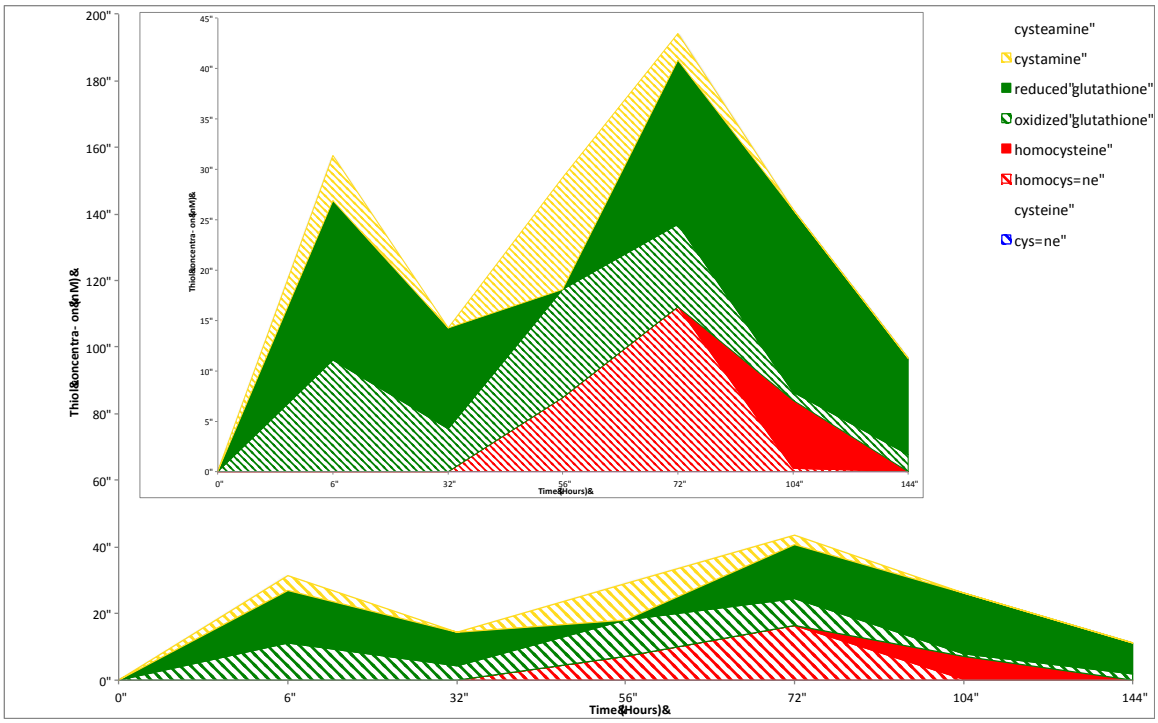


**Figure 4.4. Identification of extracellular thiols produced by *S. oneidensis* wild-type (A) and AMC and transulfurylation pathway mutants strains lacking *luxS* (B), *metB (C)*, *metC (D)*, and *metY (E)* during anaerobic growth with lactate as the electron donor and solid Fe(III) oxides (HFO) as electron acceptor.**

**A.**

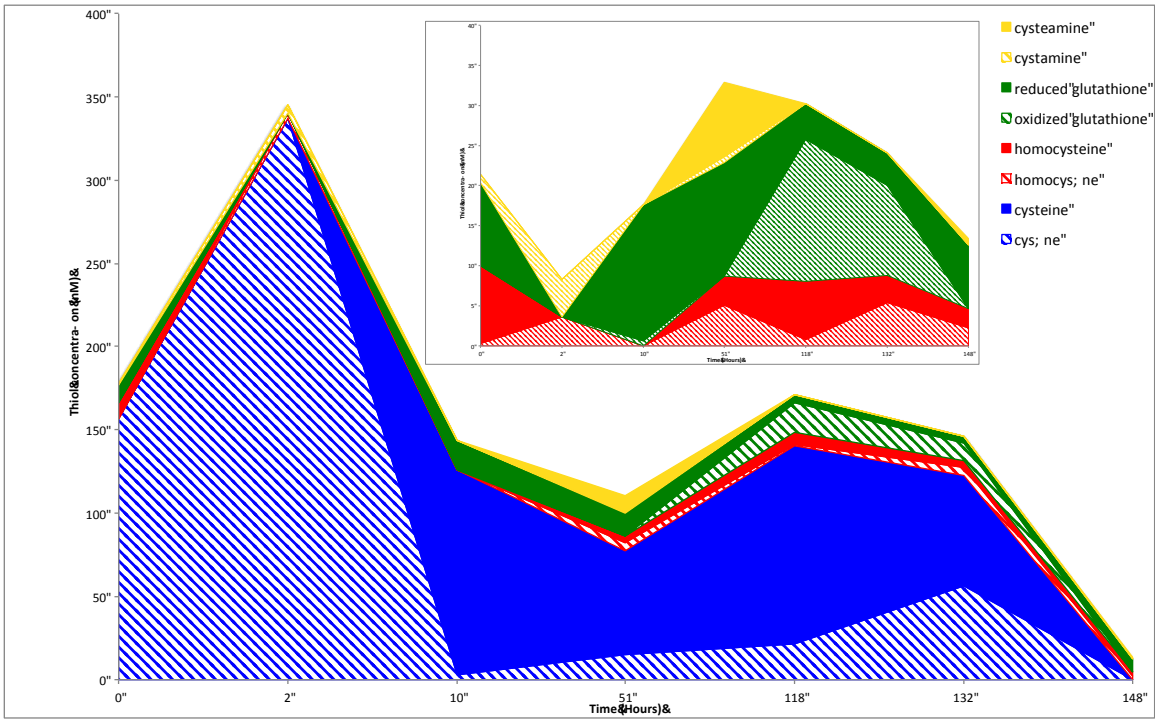
cysteamine"
cystamine"
reduced"glutathione"
oxidized"glutathione"
homocysteine"
homocys; ne"
cysteine"
cys; ne"
Thiol&concentra- on&(nM)&
Time&(Hours)&
0"
2"
10"
51"
118"
132"
148"
50"
100"
150"
200"
250"
300"
350"
400"

**B.**

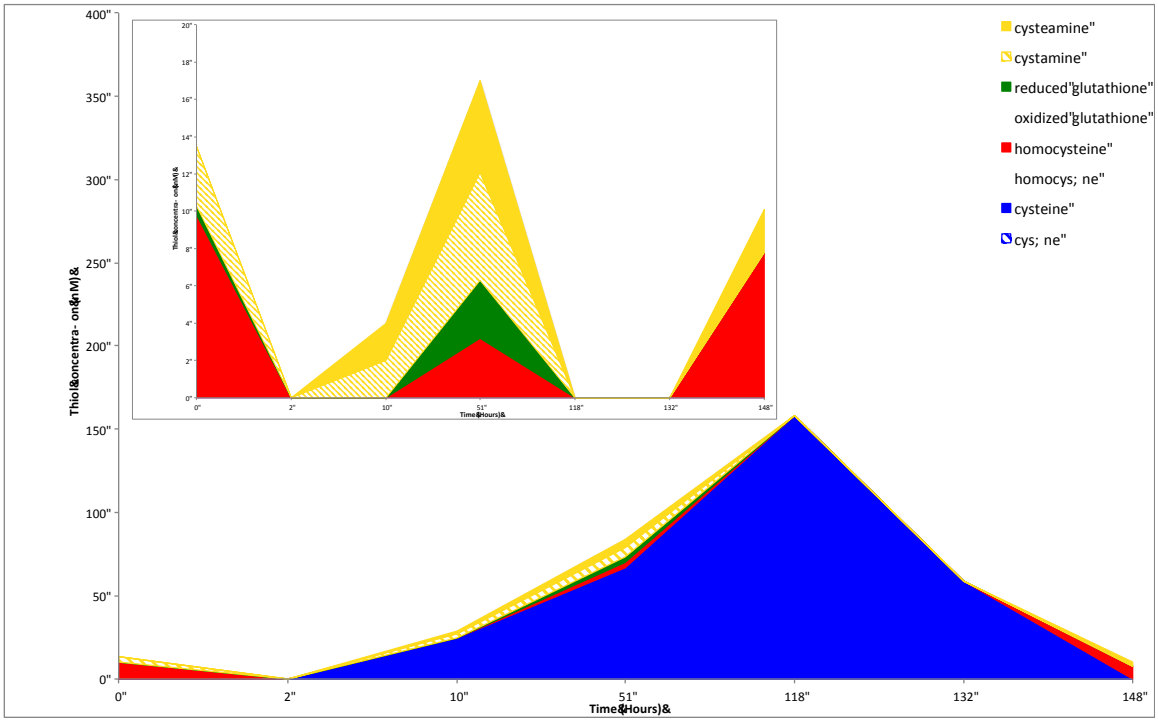
cysteamine"
cystamine"
reduced"glutathione"
oxidized"glutathione"
homocysteine"
homocys; ne"
cysteine"
cys; ne"
Thiol&concentra- on&(nM)&
Time&(Hours)&
0"
2"
10"
51"
118"
132"
148"
50"
100"
150"
200"
250"
300"
350"
400"

**C.**

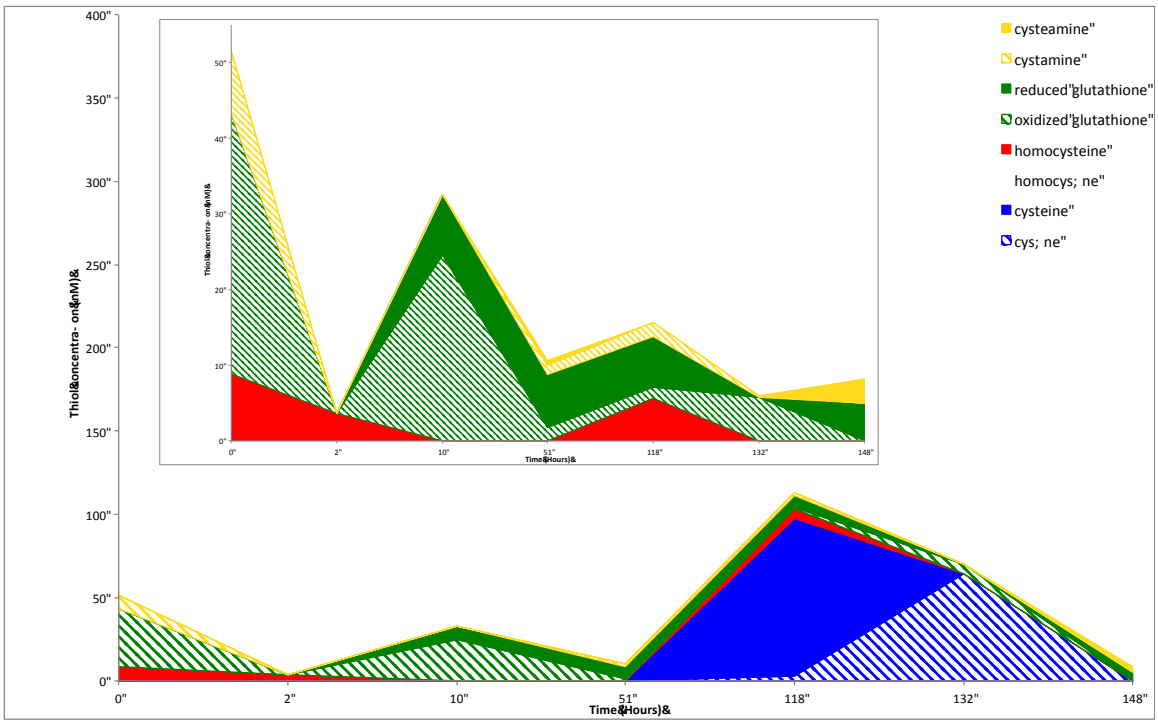
cysteamine"
cystamine"
reduced"glutathione"
oxidized"glutathione"
homocysteine"
homocys; ne"
cysteine"
cys; ne"
Thiol&oncentra- on&nM)&
Time&Hours)&
0"
2"
10"
51"
118"
132"
148"
400"
350"
300"
250"
200"
150"
100"
50"

**D.**

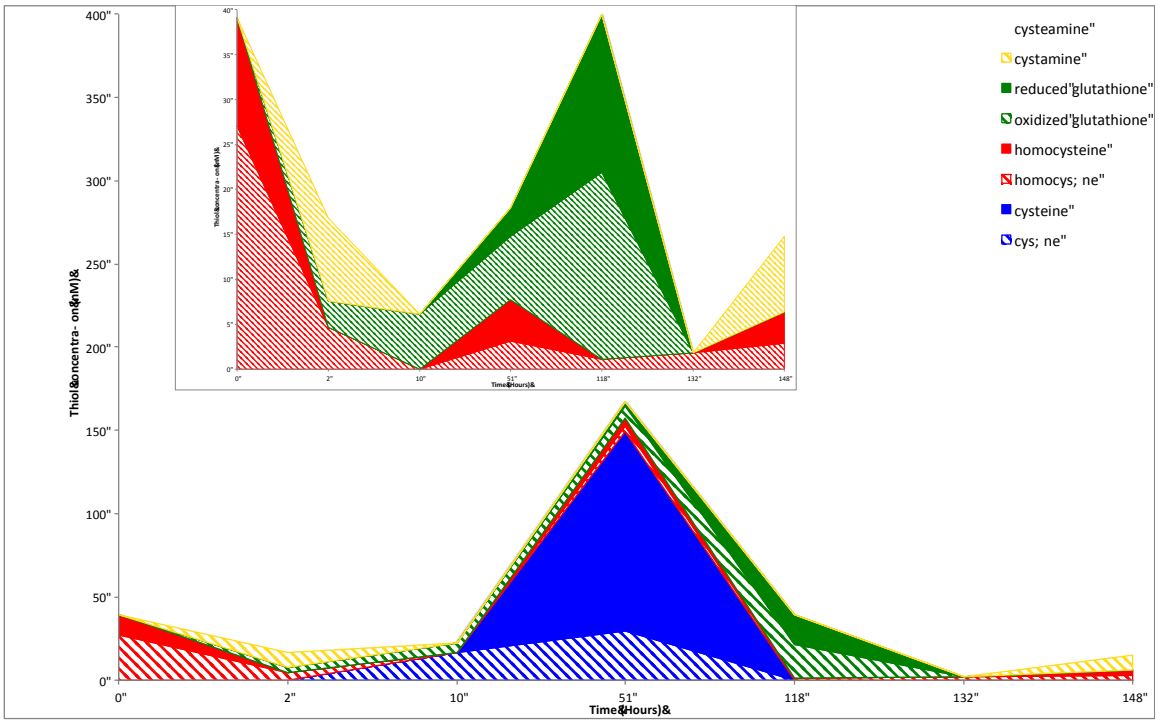
cysteamine"
cystamine"
reduced"glutathione"
oxidized"glutathione"
homocysteine"
homocys; ne"
cysteine"
cys; ne"
Thiol&oncentra- on&nM)&
Time&Hours)&
0"
2"
10"
51"
118"
132"
148"
400"
350"
300"
250"
200"
150"
100"
50"

**E.**

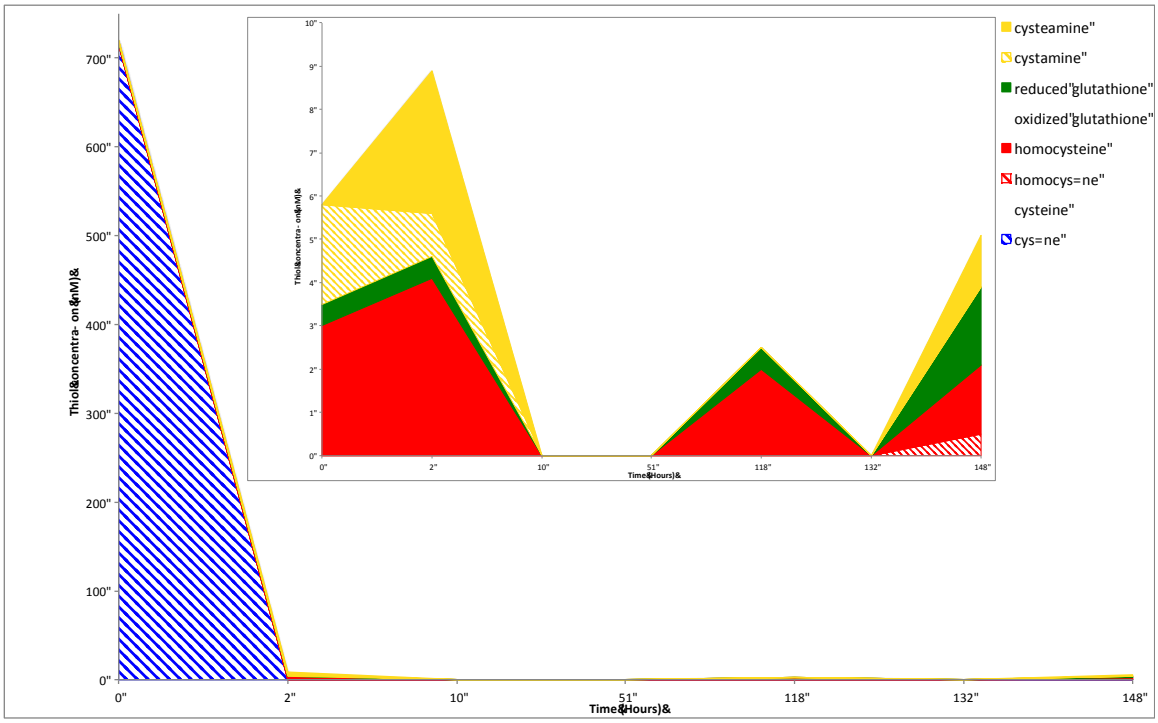


**Figure 4.5. Identification of extracellular thiols produced by *S. oneidensis* wild-type (A) and AMC and transulfurylation pathway mutants strains lacking *luxS* (B), *metB (C), metC (D),* and *metY (E)* during anaerobic growth with $H_2$ as the electron donor and Hematite as electron acceptor.**

**A.**

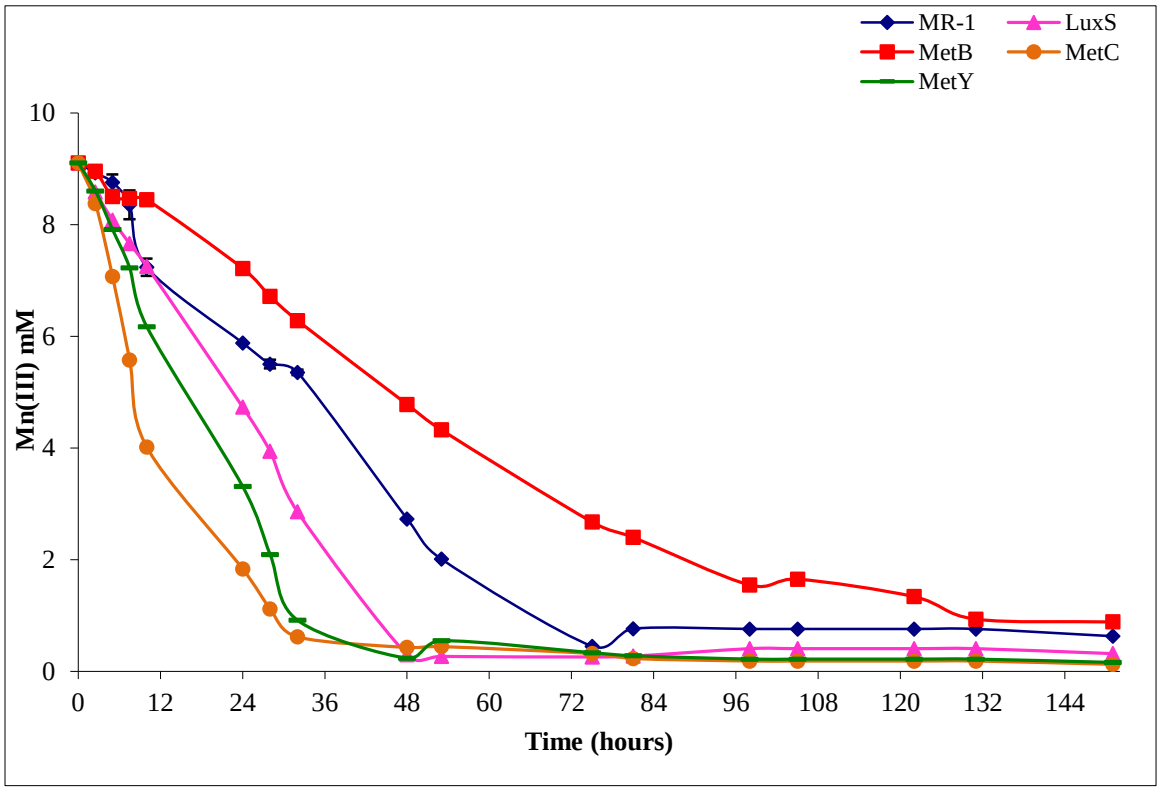
MR-1
LuxS
MetB
MetC
MetY
Mn(III) mM
Time (hours)
0
2
4
6
8
10
0
12
24
36
48
60
72
84
96
108
120
132
144

**B.**

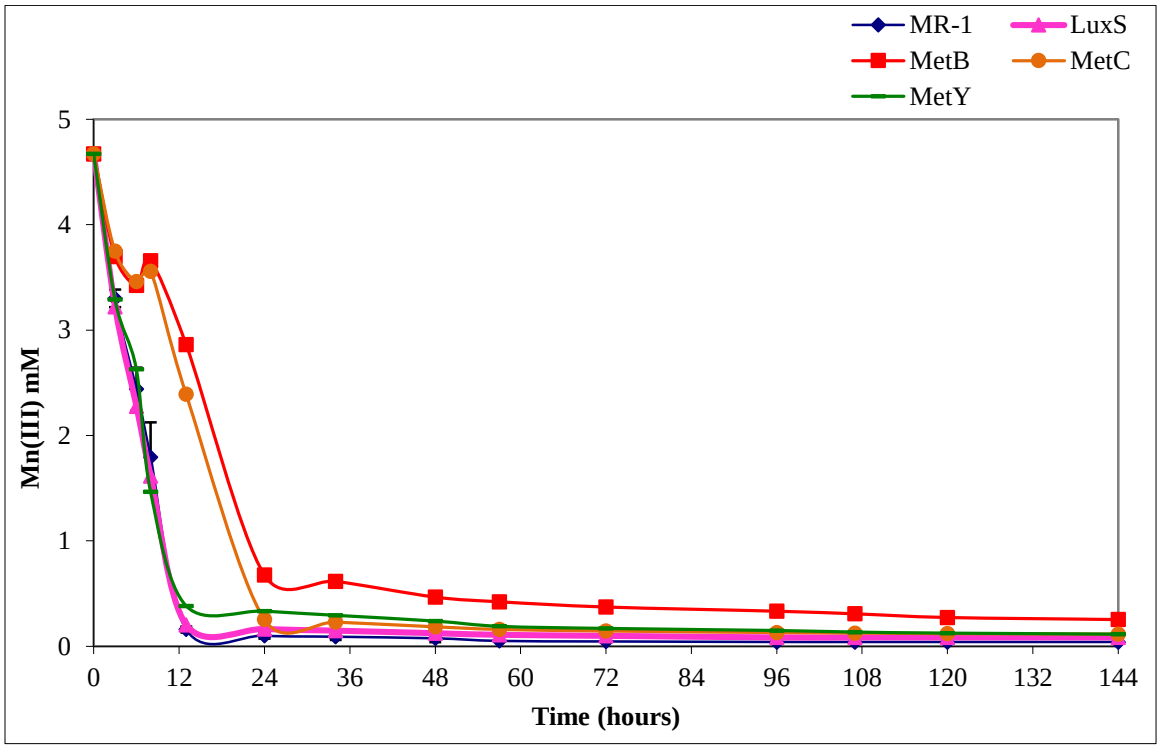
MR-1
LuxS
MetB
MetC
MetY
Mn(III) mM
Time (hours)
0
1
2
3
4
5
0
12
24
36
48
60
72
84
96
108
120
132
144

**C.**

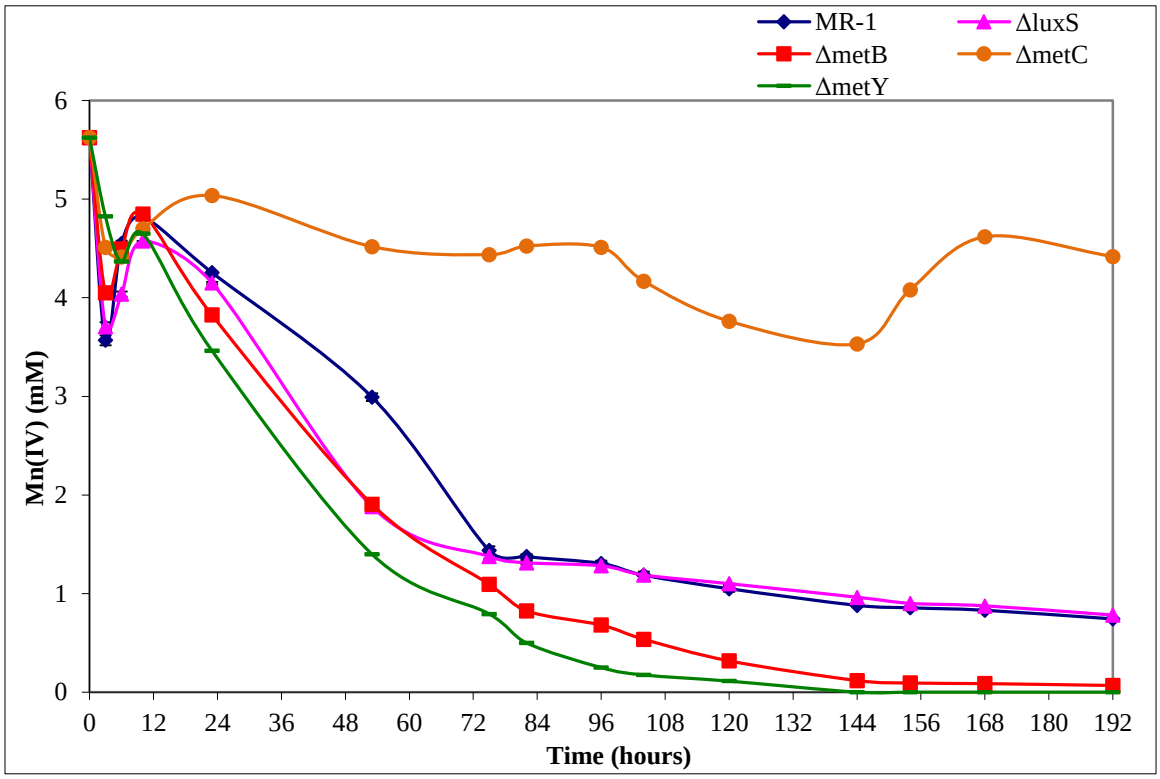
MR-1
ΔluxS
ΔmetB
ΔmetC
ΔmetY
Mn(IV) (mM)
0
1
2
3
4
5
6
0
12
24
36
48
60
72
84
96
108
120
132
144
156
168
180
192
Time (hours)

**D.**

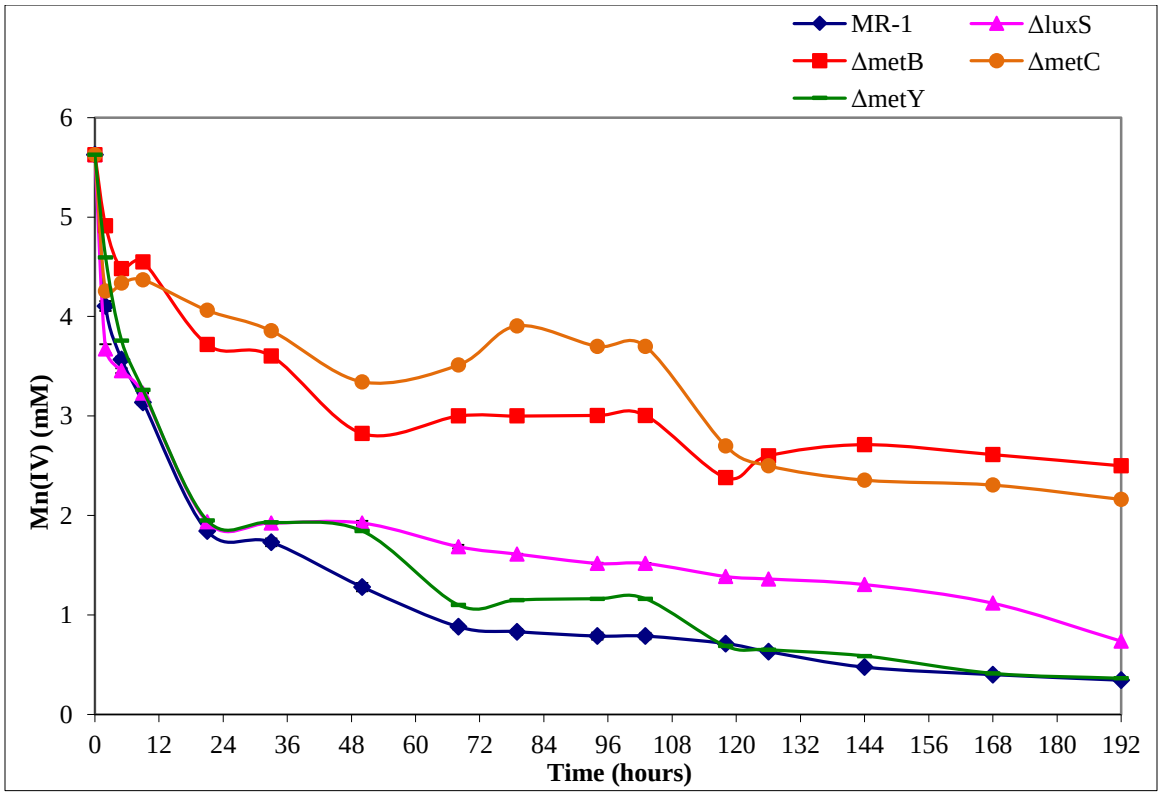
MR-1
ΔluxS
ΔmetB
ΔmetC
ΔmetY
Mn(IV) (mM)
0
1
2
3
4
5
6
0
12
24
36
48
60
72
84
96
108
120
132
144
156
168
180
192
Time (hours)

**Figure 4.6: Mn reduction by *S. oneidensis* wild type, Δ*luxS*, Δ*metB*, Δ*metC*, and Δ*metC* mutant strains amended with Mn(III)-pyrophosphate and $H_2$ (A), Mn(III)-pyrophosphate and lactate (B), Mn(IV) and $H_2$ (C), and Mn(IV) and lactate(D). Values are means of two parallel yet independent anaerobic incubations, and each time point in the two parallel incubations represent triplicate samples. Error bars represent range of errors. In some cases, error bars are smaller than the symbol.**

**A.**

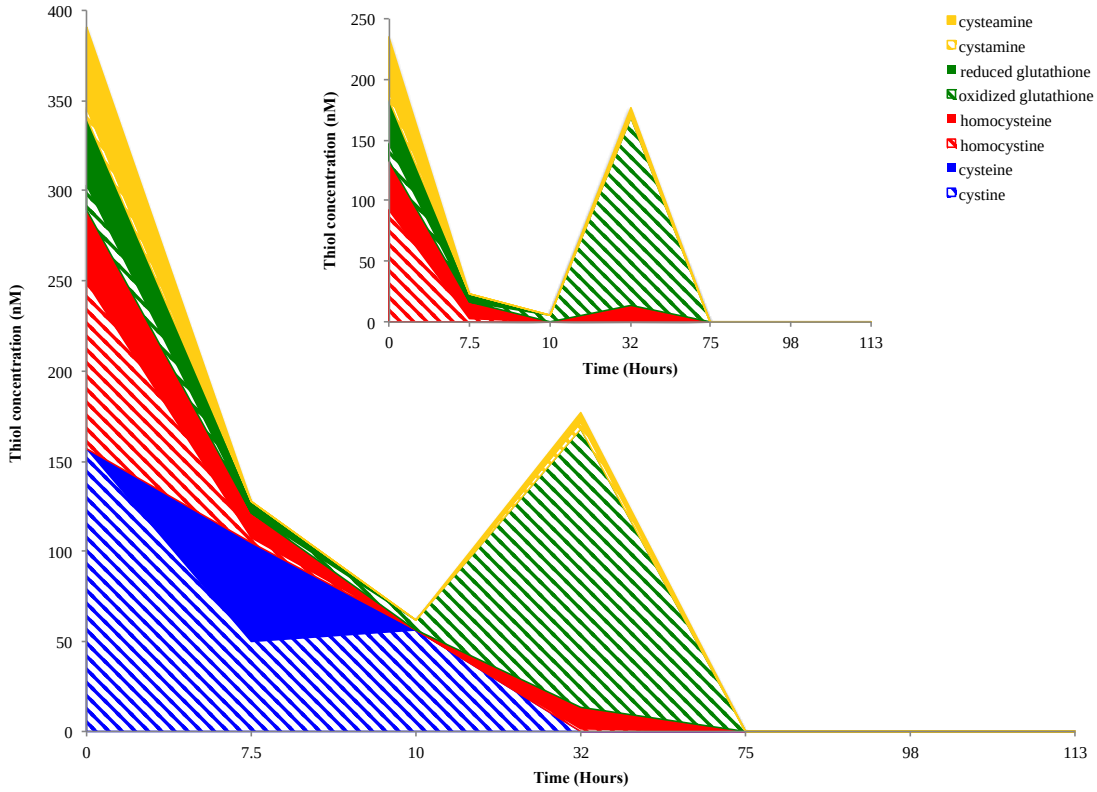
Thiol concentration (nM)
Time (Hours)
cysteamine
cystamine
reduced glutathione
oxidized glutathione
homocysteine
homocystine
cysteine
cystine

**B.**

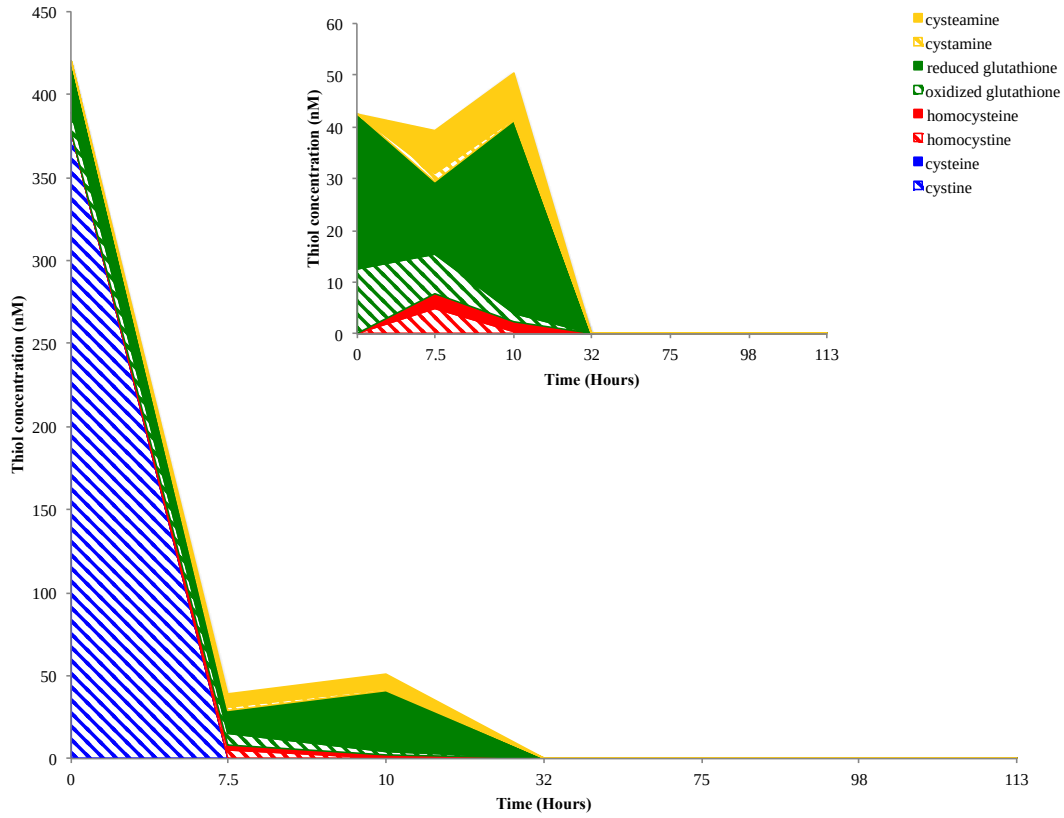
Thiol concentration (nM)
Time (Hours)
cysteamine
cystamine
reduced glutathione
oxidized glutathione
homocysteine
homocystine
cysteine
cystine

**C.**

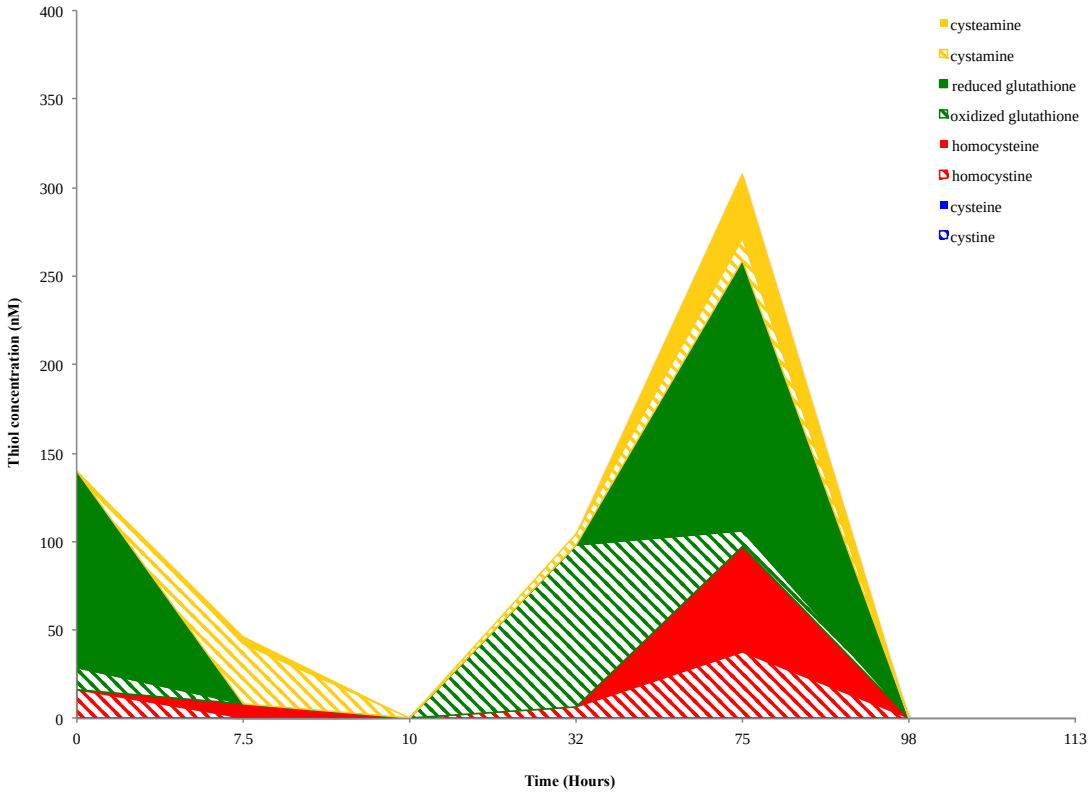
400
350
300
250
200
150
100
50
0
Thiol concentration (nM)
0
7.5
10
32
75
98
113
Time (Hours)
cysteamine
cystamine
reduced glutathione
oxidized glutathione
homocysteine
homocystine
cysteine
cystine

**D.**

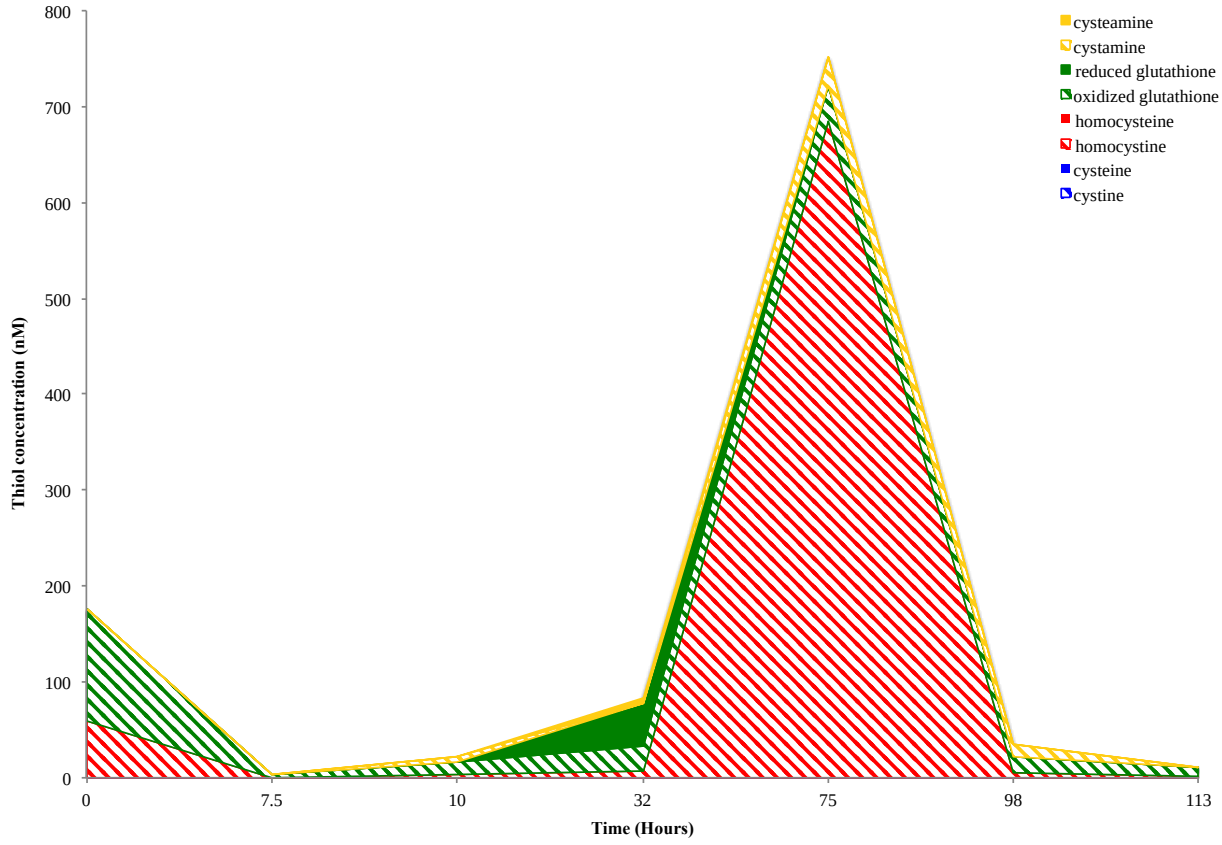
800
700
600
500
400
300
200
100
0
Thiol concentration (nM)
0
7.5
10
32
75
98
113
Time (Hours)
cysteamine
cystamine
reduced glutathione
oxidized glutathione
homocysteine
homocystine
cysteine
cystine

**E.**

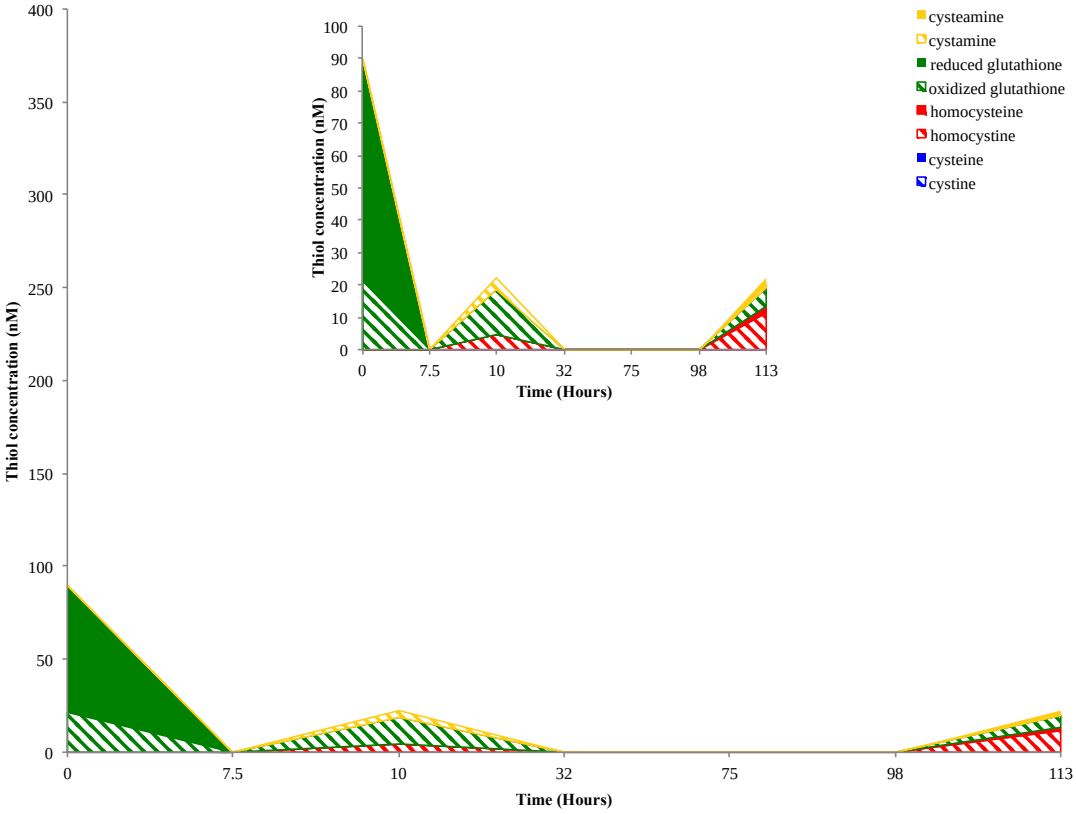


**Figure 4.7: Thiol and disulfide production by *S. oneidensis* wild type (A), Δ*luxS* (B), Δ*metB* (C), Δ*metC* (D), and Δ*metY* (E) mutant strains amended with $H_2$ as the electron donor and Mn(III) as the electron acceptor. Values are means of two parallel yet independent anaerobic incubations, and each time point in the two parallel incubations represent triplicate samples.**

**A.**

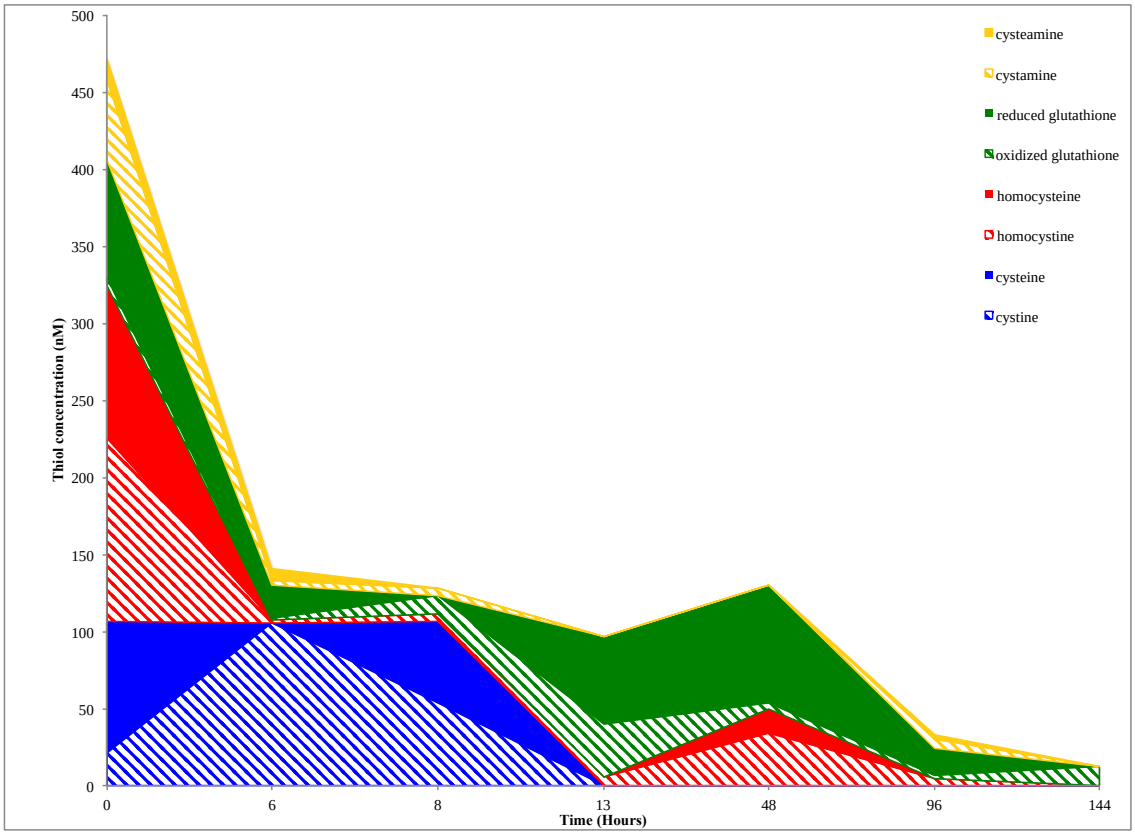
Thiol concentration (nM)
500
450
400
350
300
250
200
150
100
50
0
0
6
8
13
48
96
144
Time (Hours)
cysteamine
cystamine
reduced glutathione
oxidized glutathione
homocysteine
homocystine
cysteine
cystine

**B.**

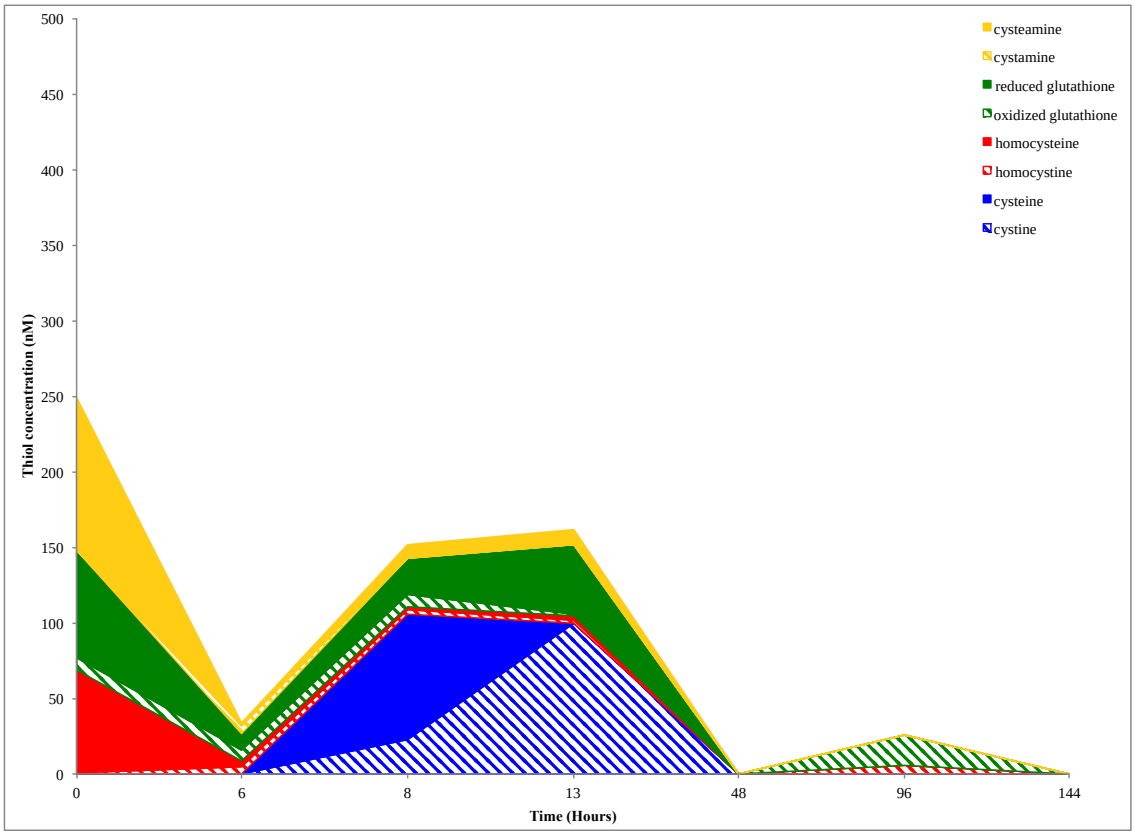
Thiol concentration (nM)
500
450
400
350
300
250
200
150
100
50
0
0
6
8
13
48
96
144
Time (Hours)
cysteamine
cystamine
reduced glutathione
oxidized glutathione
homocysteine
homocystine
cysteine
cystine

**C.**

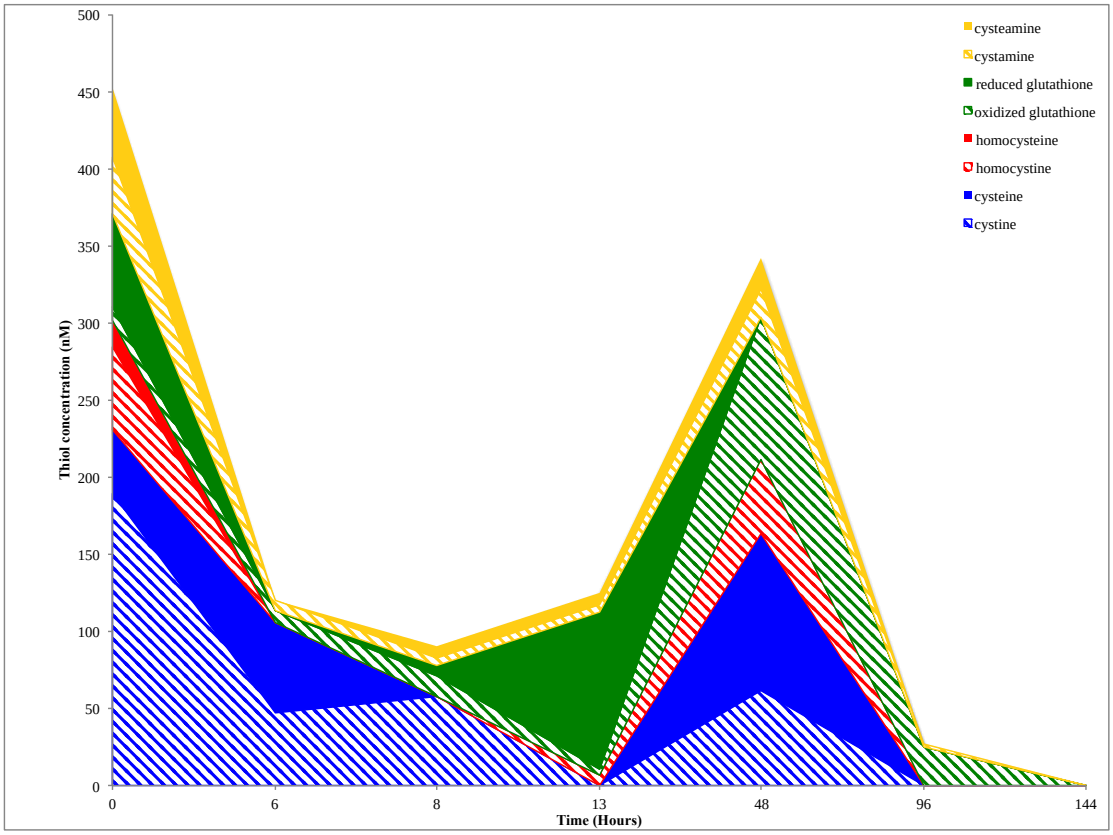
500
450
400
350
300
250
200
150
100
50
0
Thiol concentration (nM)
0
6
8
13
48
96
144
Time (Hours)
cysteamine
cystamine
reduced glutathione
oxidized glutathione
homocysteine
homocystine
cysteine
cystine

**D.**

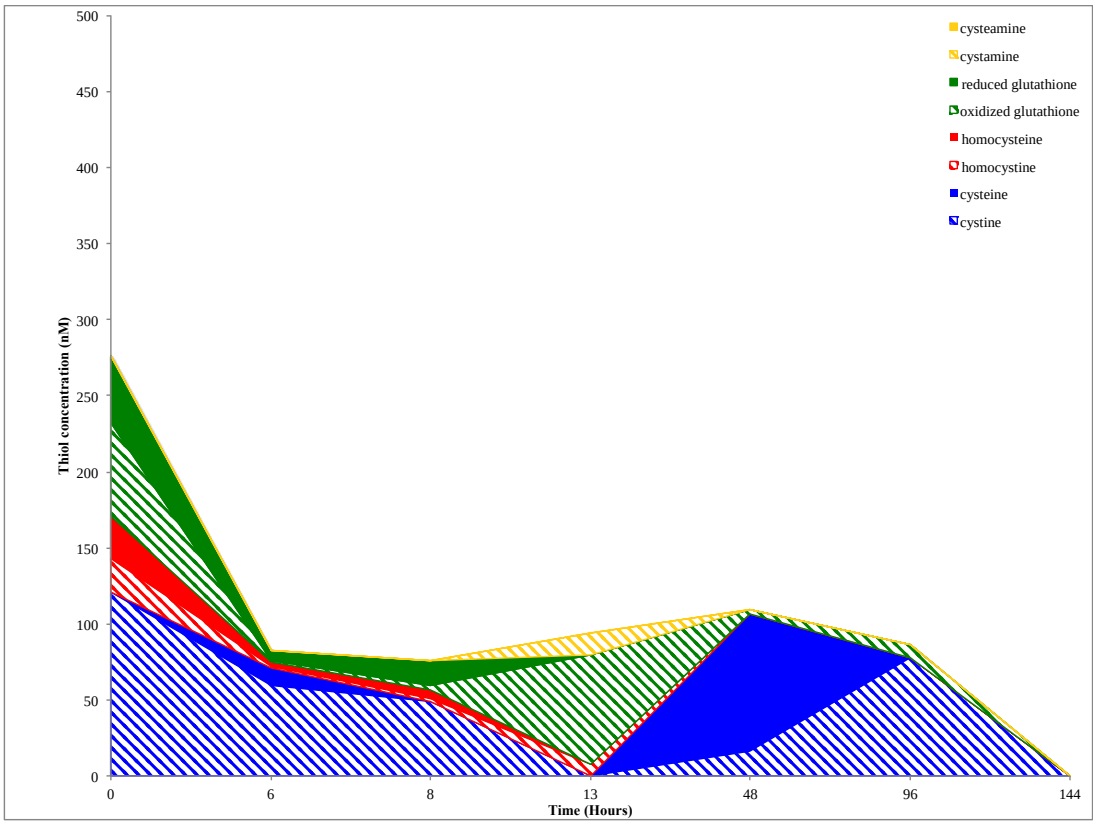
500
450
400
350
300
250
200
150
100
50
0
Thiol concentration (nM)
0
6
8
13
48
96
144
Time (Hours)
cysteamine
cystamine
reduced glutathione
oxidized glutathione
homocysteine
homocystine
cysteine
cystine

**E.**

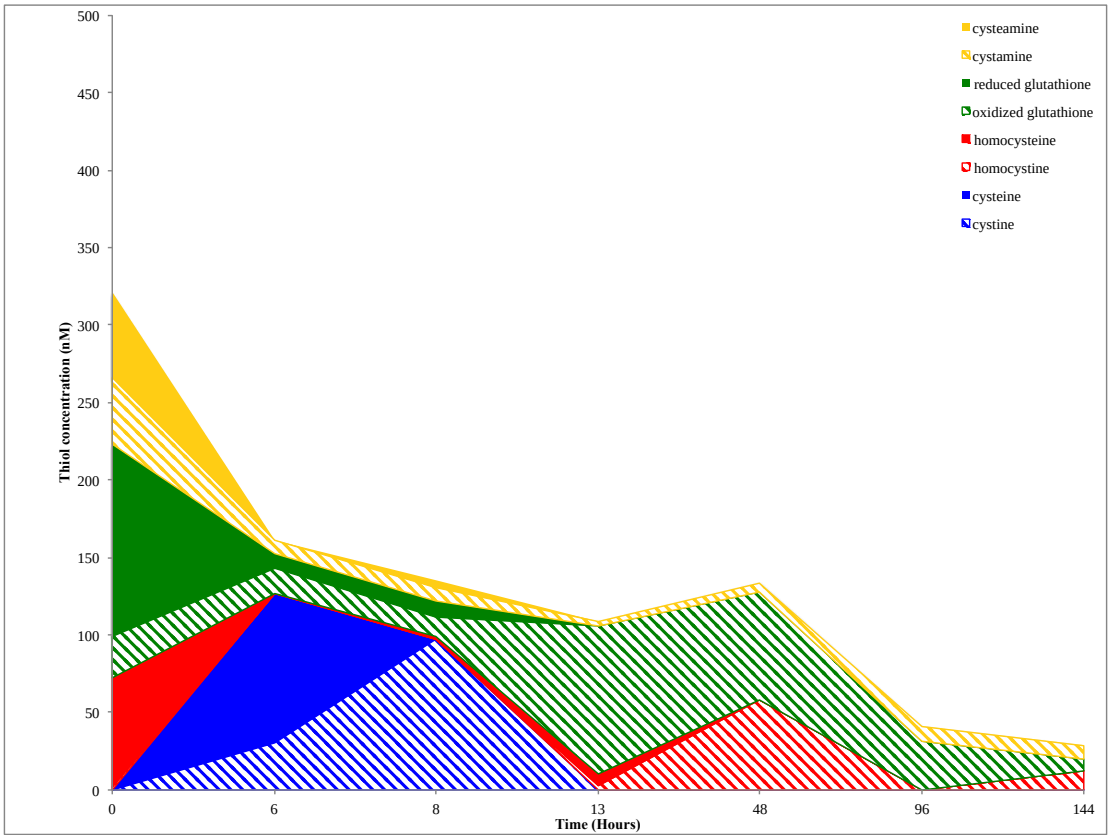


**Figure 4.8: Thiol and disulfide production by *S. oneidensis* wild type (A), Δ*luxS* (B), Δ*metB* (C), Δ*metC* (D), and Δ*metY* (E) mutant strains amended with <u>lactate</u> as the electron donor and <u>Mn(III)</u> as the electron acceptor. Values are means of two parallel yet independent anaerobic incubations, and each time point in the two parallel incubations represent triplicate samples.**

**A.**

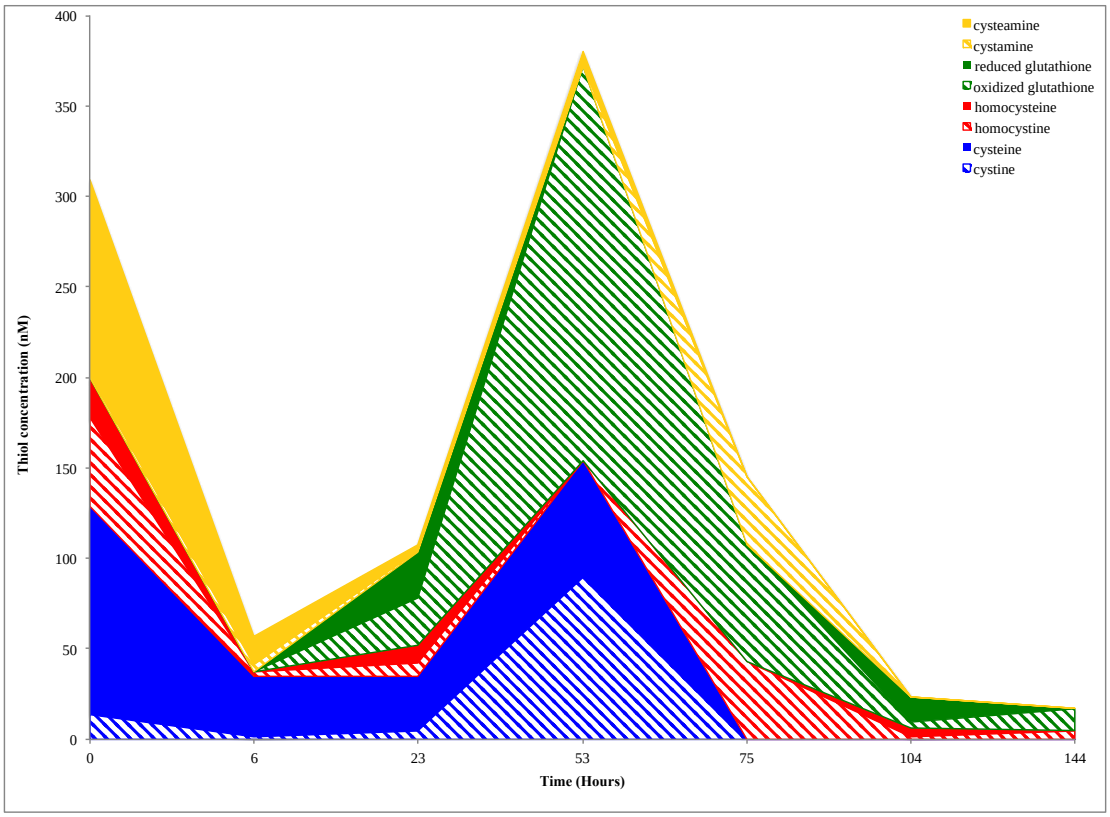
cysteamine
cystamine
reduced glutathione
oxidized glutathione
homocysteine
homocystine
cysteine
cystine
Thiol concentration (nM)
0
50
100
150
200
250
300
350
400
0
6
23
53
75
104
144
Time (Hours)

**B.**

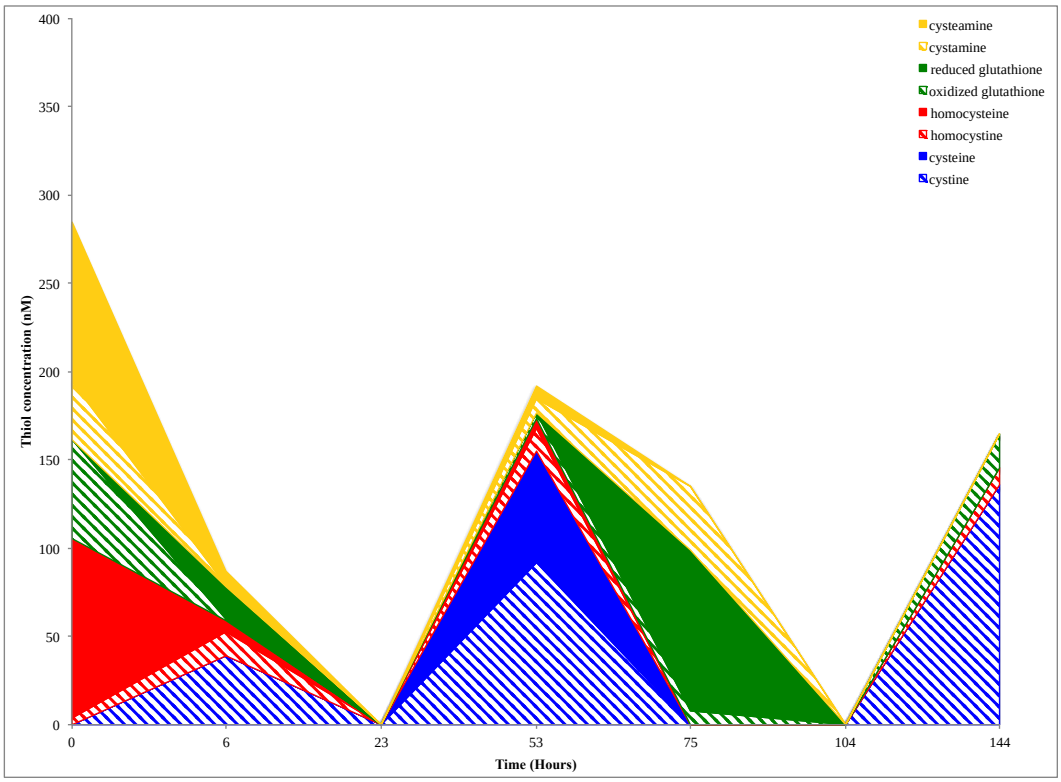
cysteamine
cystamine
reduced glutathione
oxidized glutathione
homocysteine
homocystine
cysteine
cystine
Thiol concentration (nM)
0
50
100
150
200
250
300
350
400
0
6
23
53
75
104
144
Time (Hours)

**C.**

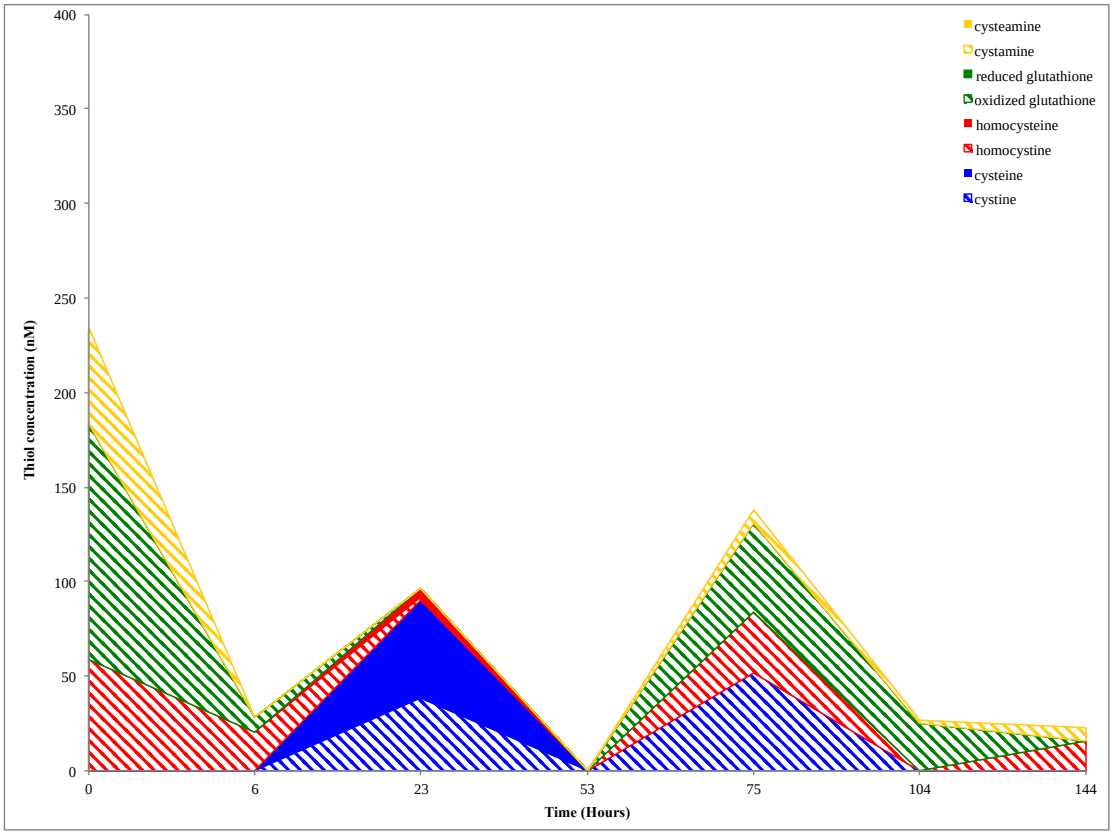
cysteamine
cystamine
reduced glutathione
oxidized glutathione
homocysteine
homocystine
cysteine
cystine
Thiol concentration (nM)
400
350
300
250
200
150
100
50
0
0
6
23
53
75
104
144
Time (Hours)

**D.**

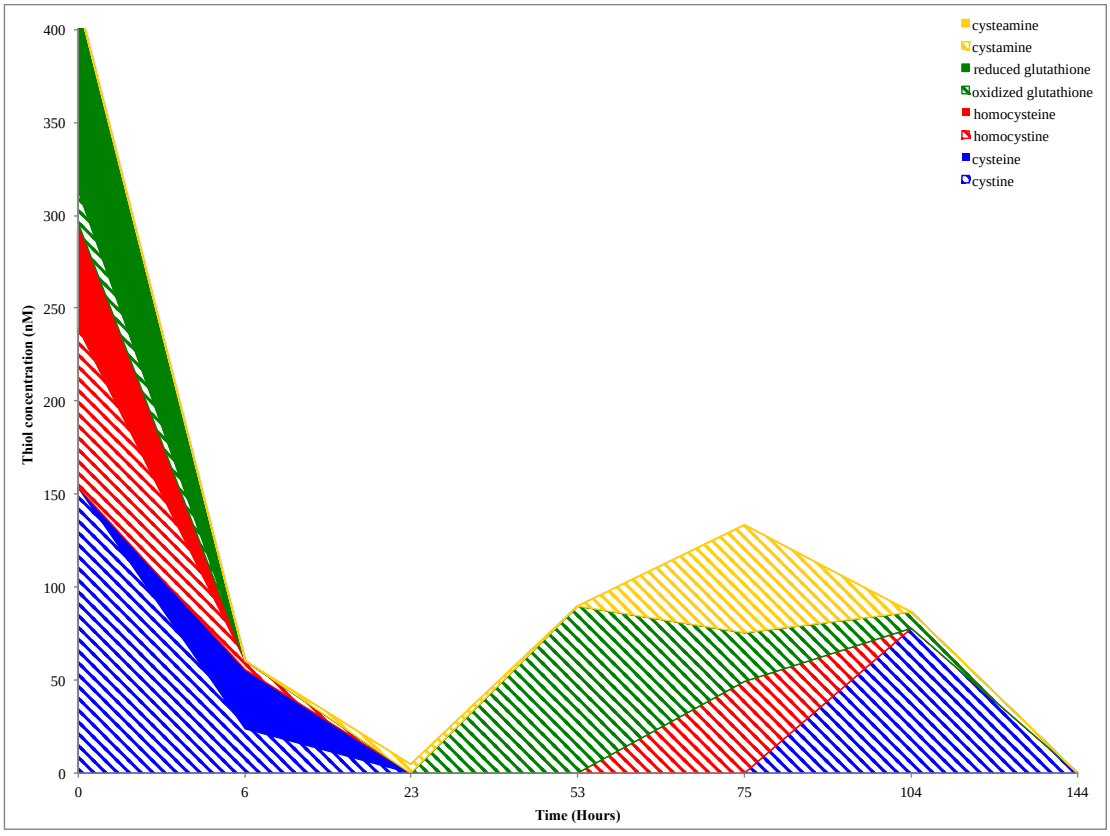
cysteamine
cystamine
reduced glutathione
oxidized glutathione
homocysteine
homocystine
cysteine
cystine
Thiol concentration (nM)
400
350
300
250
200
150
100
50
0
0
6
23
53
75
104
144
Time (Hours)

**E.**

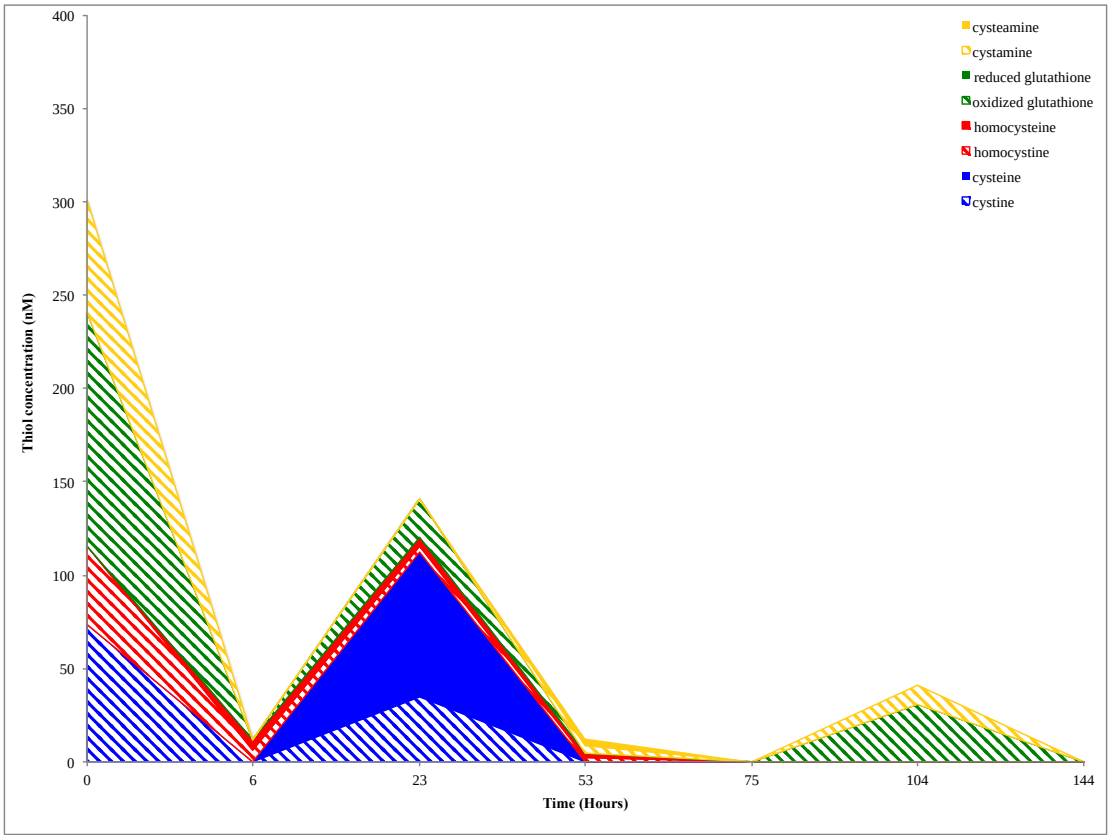


**Figure 4.9: Thiol and disulfide production by *S. oneidensis* wild type (A), Δ*luxS* (B), Δ*metB* (C), Δ*metC* (D), and Δ*metY* (E) mutant strains amended with $H_2$ as the electron donor and Mn(IV) as the electron acceptor. Values are means of two parallel yet independent anaerobic incubations, and each time point in the two parallel incubations represent triplicate samples.**

**A.**

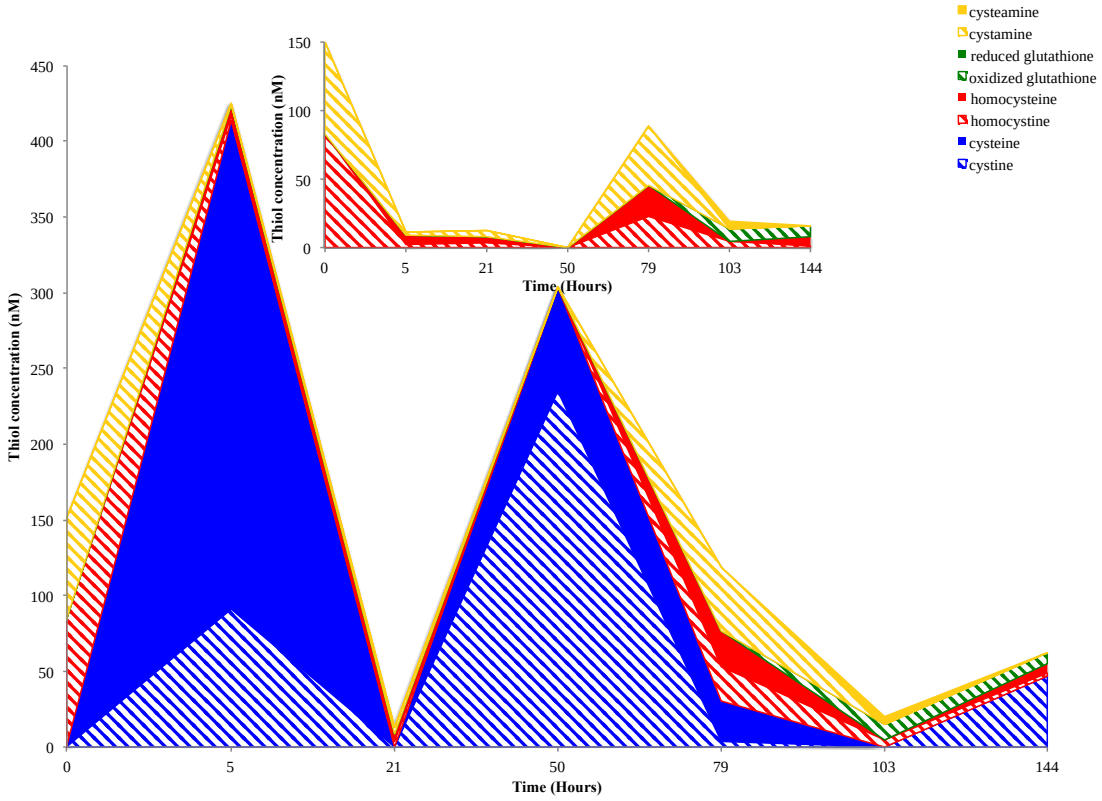
cysteamine
cystamine
reduced glutathione
oxidized glutathione
homocysteine
homocystine
cysteine
cystine
Thiol concentration (nM)
Time (Hours)
0
5
21
50
79
103
144
0
50
100
150
200
250
300
350
400
450

**B.**

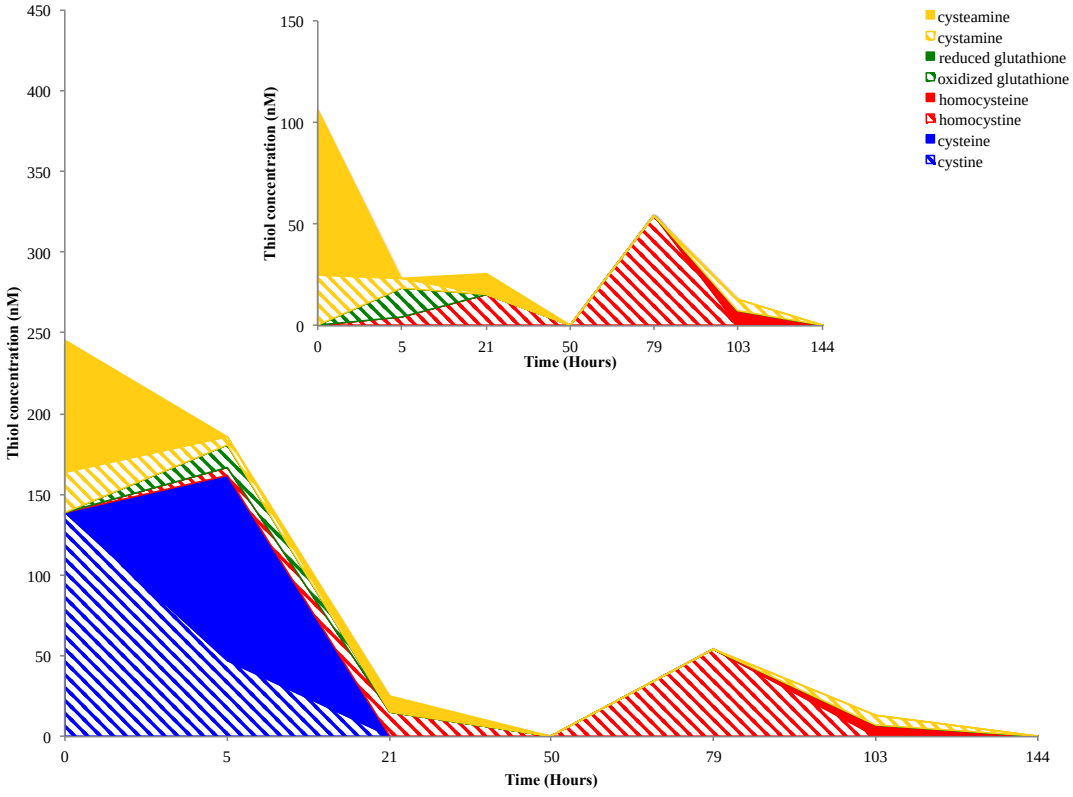
cysteamine
cystamine
reduced glutathione
oxidized glutathione
homocysteine
homocystine
cysteine
cystine
Thiol concentration (nM)
Time (Hours)
0
5
21
50
79
103
144
0
50
100
150
200
250
300
350
400
450

**C.**

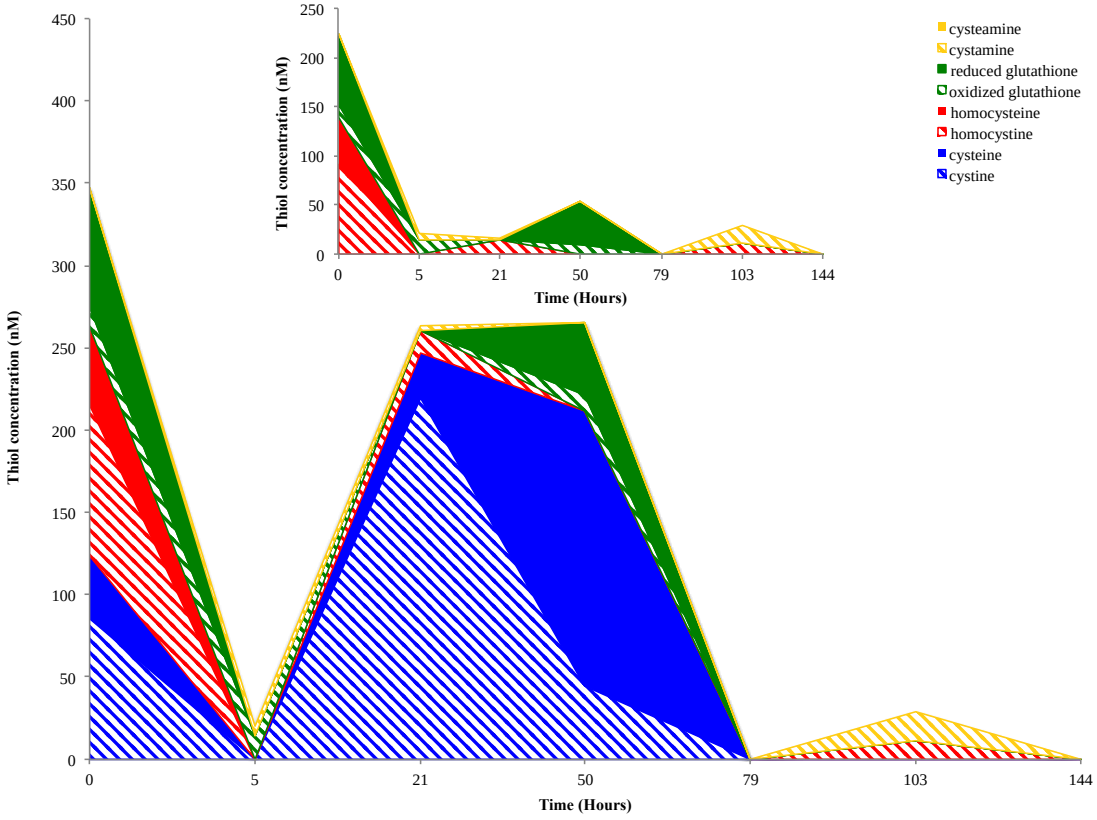
Thiol concentration (nM)
Time (Hours)
cysteamine
cystamine
reduced glutathione
oxidized glutathione
homocysteine
homocystine
cysteine
cystine

**D.**

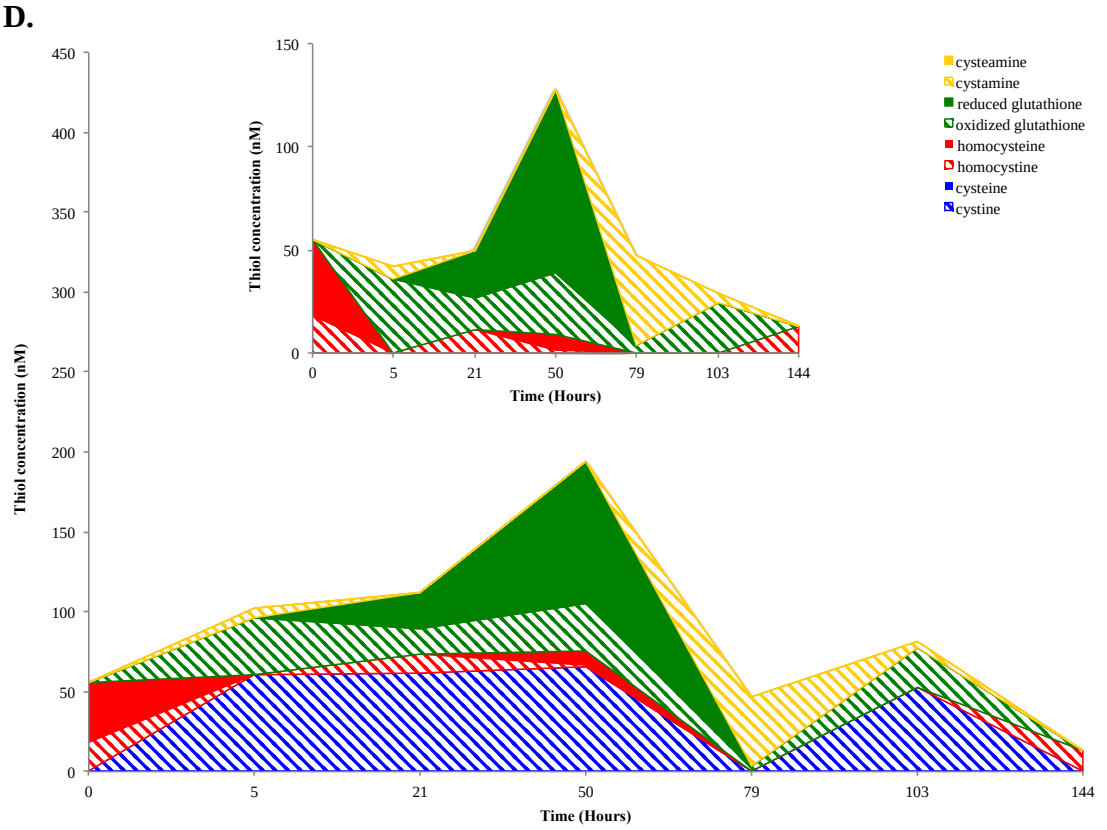
Thiol concentration (nM)
Time (Hours)
cysteamine
cystamine
reduced glutathione
oxidized glutathione
homocysteine
homocystine
cysteine
cystine

**E.**

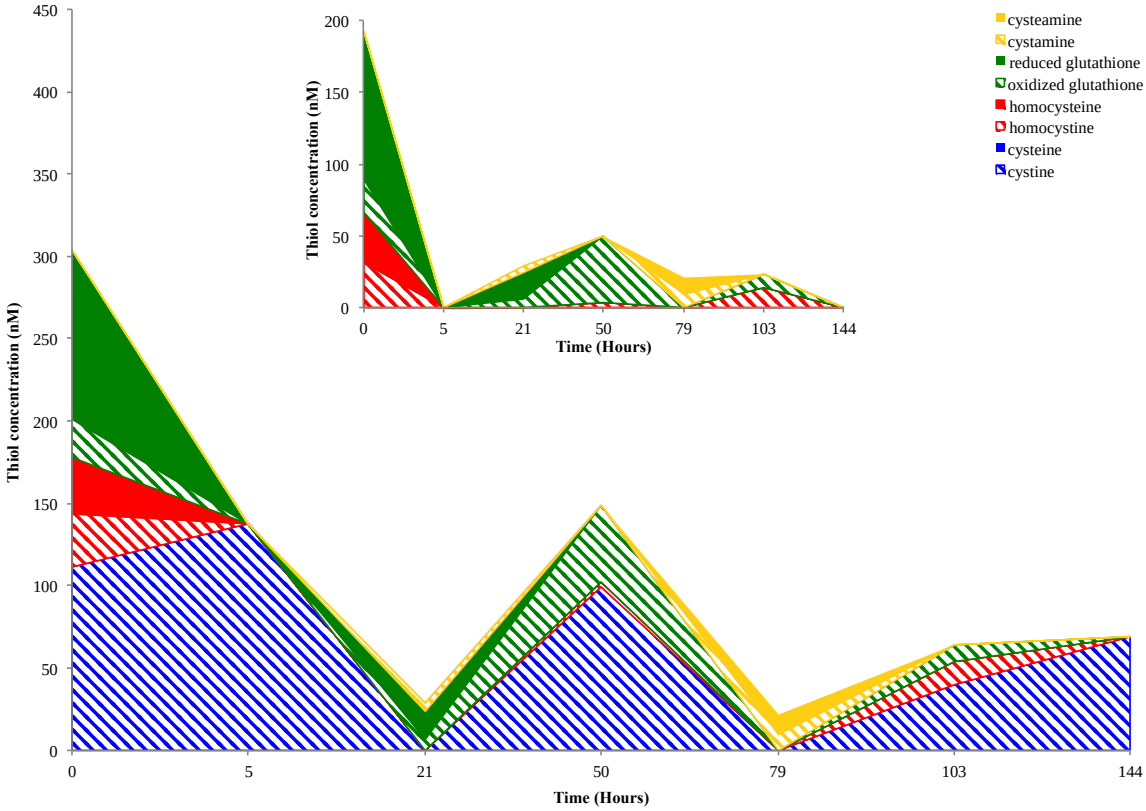


**Figure 4.10: Thiol and disulfide production by *S. oneidensis* wild type (A), Δ*luxS* (B), Δ*metB* (C), Δ*metC* (D), and Δ*metY* (E) mutant strains amended with <u>lactate</u> as the electron donor and <u>Mn(IV)</u> as the electron acceptor. Values are means of two parallel yet independent anaerobic incubations, and each time point in the two parallel incubations represent triplicate samples.**

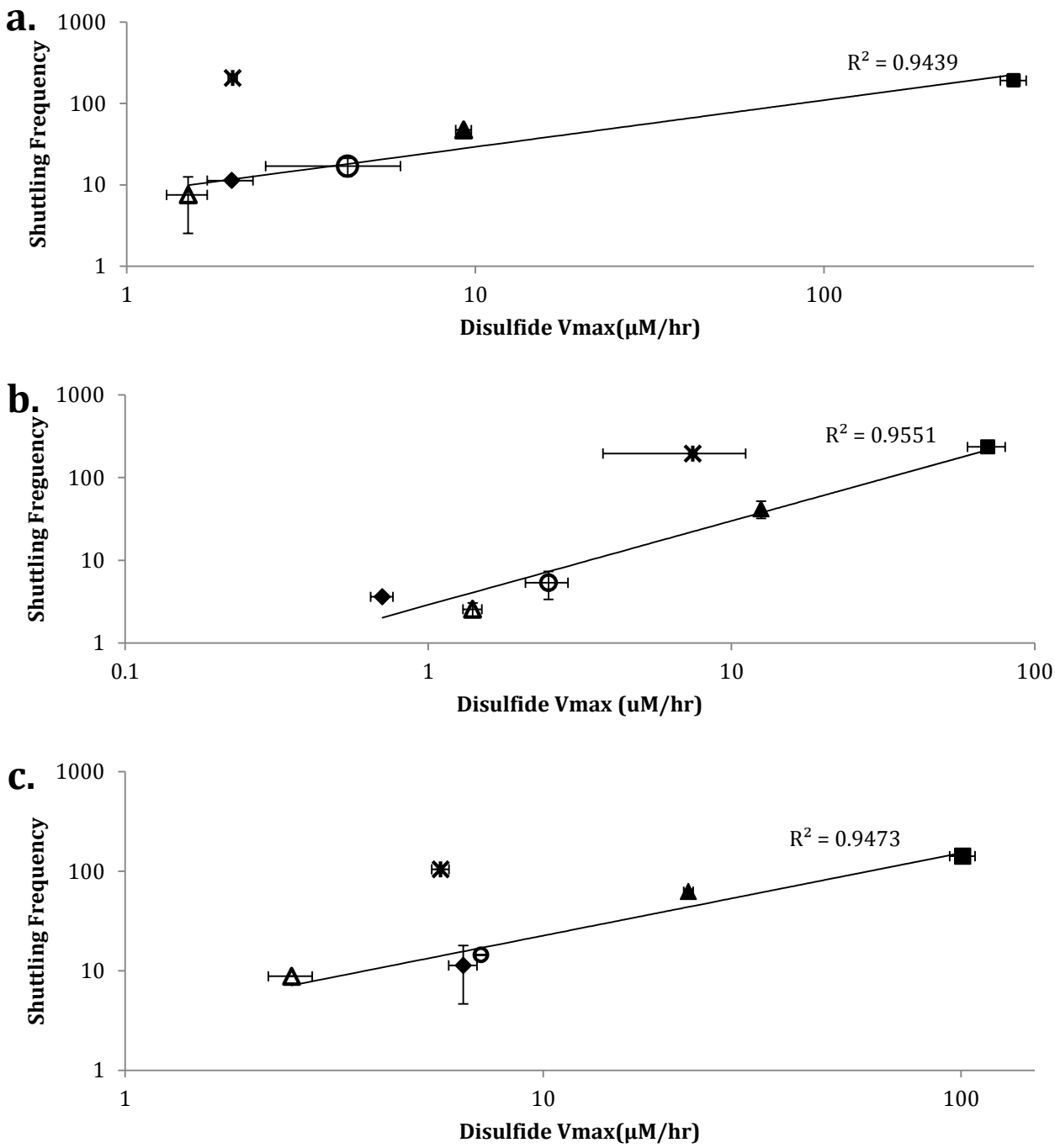


***Figure 4.11. Calculated disulfide shuttling frequencies as a function of *V*max-Di with (a) $H_2$ , (b) lactate, and (c) formate as electron donor. Filled Square: CSSC; filled triangle: Cystamine; Filled Diamond: GSSG; open circle: DTDG; open triangle: DTDP; cross: DMDS (*Experiments carried out by Seng Kew Wee of the DiChristina Laboratory).**

**a.**

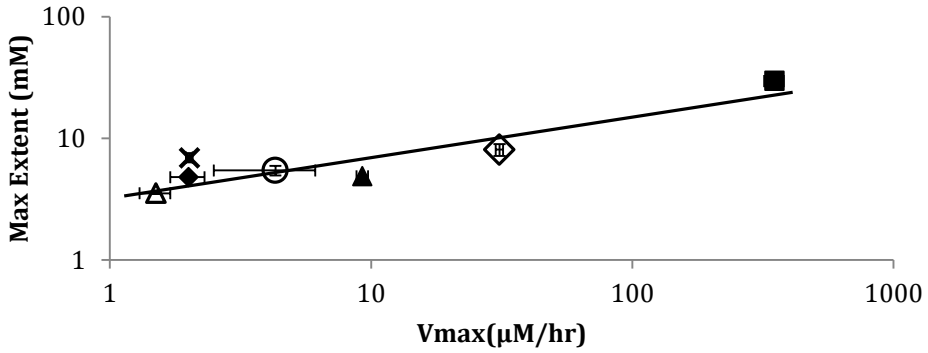


**b.**

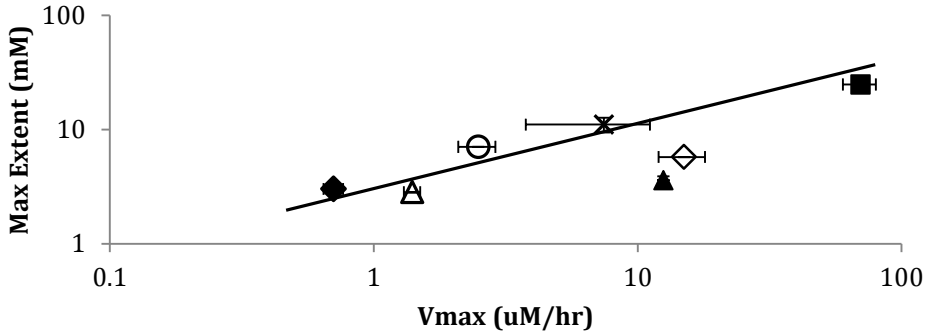


**c.**

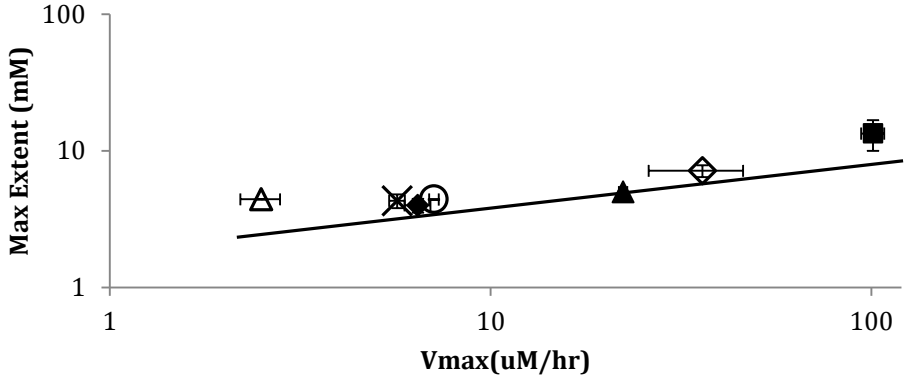


***Figure 4.12. Maximum extent of Fe(III) reduction as a function of Vmax-Di with (a) $H_2$ , (b) lactate, and (c) formate as electron donor. Filled Square: CSSC; filled triangle: Cystamine; Filled Diamond: GSSG; open circle: DTDG; open triangle: DTDP; cross: DMDS. Filled Square: CSSC; filled triangle: Cystamine; Filled Diamond: GSSG; open diamond: Ellman's; open circle: DTDG; open triangle: DTDP; cross: DMDS (*Experiments carried out by Seng Kew Wee of the DiChristina Laboratory).**

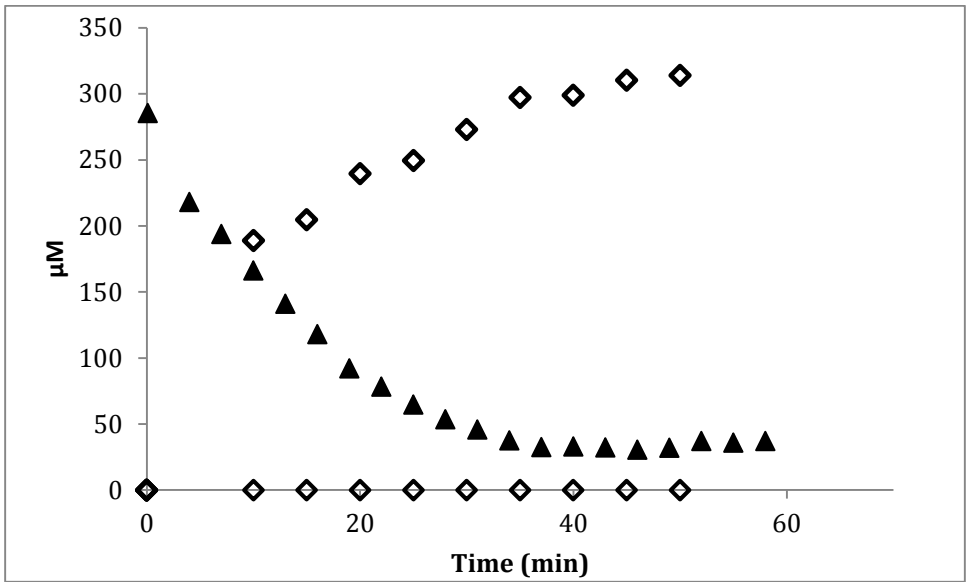


***Figure 4.13. Abiotic reduction of 40 mM Fe(III) oxide by 500 µM cysteine carried out under anaerobic conditions in M1 growth medium. Solid triangles, cysteine; open diamonds, Fe(II) measured by the ferrozine method with HCl extraction. (*Experiments carried out by Eryn Eitel of the Taillefert Laboratory).**

## Table 4.1. Bacterial strains and plasmids used in this study.

| Bcterial strain or plasmid | Description | Source or Reference |
|---|---|---|
| *S. oneidensis* | | |
| MR-1 | Wild-type strain | ATCC |
| Δ*luxS* | In-frame deletion mutant | Cooper, *et al*., 2015 |
| Δ*metB* | In-frame deletion mutant | This study |
| Δ*metC* | In-frame deletion mutant | This study |
| Δ*metY* | In-frame deletion mutant | This study |
| *E. coli* | | |
| EC100D *pir-116* | F- *mcrA* Δ(*mrr-hsdRMS-mcrBC*) ϕ80d*lacZ*ΔM15 Δ*lacX74 recA1 endA1 araD139* Δ(*ara leu*)*7697 galU galK* λ$^-$ *rpsL nupG pir-116*(DHFR) | Epicentre |
| β2155 λ *pir* | *thrB1004 pro thi strA hsdS lacZ*ΔM15 (F9 *lacZ*ΔM15 *lacI*$^q$ *traD36 proA1 proB1*) Δ*dapA*::*erm pir*::RP4 Km$^r$ | Dehio and Meyer, 1997 |
| Plasmids | | |
| pKO2.0 | 4.5-kb γR6K mobRP4 sacB Gmr lacZ | Burns and DiChristina, 2009 |
| pKO2.0-F3 (*luxS)* | pKO2.0 containing in-frame deletion of SO1101 | This study |
| pKO2.0-F3 (*metB)* | pKO2.0 containing in-frame deletion of SO4056 | This study |
| pKO2.0-F3 (*metC)* | pKO2.0 containing in-frame deletion of SO2191 | This study |
| pKO2.0-F3 (*metY)* | pKO2.0 containing in-frame deletion of SO1095 | This study |

## Table 4.2. Primers used in this study.

| Primers | Nucleotide Sequence |
|---|---|
| SO1101D1 | 5'-GACTGGATCCGATCCGAATGCCAGGGCTTG-3' |
| SO1101D2 | 5'-ACTATTGTCGCTTTCTTGACGCTTTCGCGATACAACGCCACTGTCGCTATC-3' |
| SO1101D3 | 5'-GATAGCGACAGTGGCGTTGTATCGCGAAAGCGTCAAGAAAGCGACAATAGT-3' |
| SO1101D4 | 5'-GACTGTCGACCCCAAGCAATGAACGGTAACTATCATCATC-3' |
| SO1101TR | 5'-GACAGCACAGGAAATGAACGGC-3' |
| SO1101TF | 5'-GACAGCACAGGAAATGAACGGC-3' |
| SO4056D1 | 5'-GACTGGATCCCGTTCACGCAATAGGGTGAGTAGC-3' |
| SO4056D2 | 5'-GCTGGAACCACCAAATTTATGTAAGTGACCCTAAGTTCGCAAAGAGATGTCTGGAC-3' |
| SO4056D3 | 5'-GTCCAGACATCTCTTTGCGAACTTAGGGTCACTTACATAAATTTGGTGGTTCCAGC-3' |
| SO4056D4 | 5'-GACTGTCGACGCTCTTGAGTAATTTCGCATCGTTGATC-3' |
| SO4056TR | 5'-GTGTTAAACAGCGGCTGCAAAGT-3' |
| SO4056TF | 5'-GGTTTTGTTCACTGGTAAGCTAAA-3' |
| SO2191D1 | 5'-GACTGGATCCGCTTATCCCATGAGCTACGTACTCCT-3' |
| SO2191D2 | 5'-CGCCTTCGCTGTTTTACATATAAGGGGCACTACCTTGGCGAGTCTGTAT-3' |
| SO2191D3 | 5'-ATACAGACTCGCCAAGGTAGTGCCCCTTATATGTAAAACAGCGAAGGC-3' |
| SO2191D4 | 5'-GACTGTCGACGATAACTAGCCTTTATCCCGATACGCC-3' |
| SO2191TR | 5'-GTCACTGGGTAAGATCGAAGCCT-3' |
| SO2191TF | 5'-GTCGGGTGCGTAACCATCTA-3' |
| SO1095D1 | 5'-GACTGGATCCGCGGTATTCCTGCTGATCCTGTTG-3' |
| SO1095D2 | 5'-GATGTTTATCGCTCAAACGCAAAAGGCGCCTTGTGCAGATGGATACTAAAACCG-3' |
| SO1095D3 | 5'-CGGTTTTAGCCATCTGCACAAGGCGCCTTTTGCGTTTGAGCGATAAACATC-3' |
| SO1095D4 | 5'-GACTGTCGACGCTGGTATTAGCCGTACTTGTGTATGGA-3' |
| SO1095TR | 5'-GCTGCTGATTGGCACACTT-3' |
| SO1095TF | 5'-CAGCATATTCACCTTTAGAGCG-3' |

**Table 4.3. *S. oneidensis* AMC, Transulfurylation Pathway, and Direct Sulfhydrylation Pathway Genes.**

| ORF/Gene | Putative Function |
|---|---|
| SO1101 (*luxS*) | S-ribosylhomocysteinase (Autoinducer-2 synthase) |
| SO0818 (*metE*) | B-12 cobalamine-independent homocyseine methyltransferase |
| SO1030 (*metH*) | B12-dependentmethyltetrahydrofolte homocysteine methyltransferase |
| SO0929 (*metK*) | S-adenosylmethionine synthetase |
| SO3006 (Dcm Transmethylase) | C-5 cytosine-specific DNA methylase family protein |
| SO1322 (*mtnN*) | 5-methylthioadenosine nucleosidase |
| SO1676 (*metA*) | Homoserine O-succinyltransferase |
| SO4056 (*metB*) | Cystathionine gamma-synthase |
| SO2191 (*metC*) | Cystathionine beta-lyase |
| SO4054 (*metF*) | 5,10-methylenetetrahydrofolate reductase |
| SO4057 (*metJ*) | Transcriptional regulator of methionine metabolism |
| SO4055 (*metL*) | Homoserine dehydrogenase , methionine-sensitive |
| SO1095 (*metY*) | O-acetylhomoserine (thiol)-lyase |
| SO2903 (*cysK)* | Cysteine synthase |
| SO3598 (*cysM)* | Cysteine synthase B |
| SO3559 (*gshA*) | Glutamate-cysteine ligase |
| SO0831 (*gshB*) | ATP-dependent glutathione synthetase |
| SO4702 (*gor*) | Glutathione disulfide reductase |
| SO3779 (*cydC*) | Cysteine/Glutathione ABC transporter ATP-binding protein, ATPase/permease |
| SO3780 (*cydD*) | Cysteine/Glutathione ABC transporter ATP-binding protein, ATPase/permease |
| SO3415 (*thrA*) | Bifunctional aspartokinase I / homoserine dehydrogenase |
| SO3414 (*thrB*) | Homoserine kinase |
| SO3413 (*thrC*) | Threonine synthase |
| SO1812 (*mdeA*) | Methionine gamma-lyase |

**Table 4.4. BLAST analysis *S. oneidensis* AMC, Transulfurylation Pathway, and Direct Sulfhydrylation Pathway Genes.**

| ORF/Gene | Result for *Shewanella* spp[a] | | | Result for GenBank Analysis[b] | | | | |
|---|---|---|---|---|---|---|---|---|
| | Sim | ID | E value | Best Hit | Sim | ID | E value | Putative Function |
| SO1101 (*luxS*) | 100-100 | 76-97 | $10^{-97}$-$10^{-123}$ | *Vibrio parahaemolyticus* | 100 | 82 | $1^{-100}$ | S-ribosylhomocysteinase |
| SO0818 (*metE*) | 24-100 | 14-98 | $10^{-27}$-0.0 | *Proteus mirabilis* | 99 | 59 | 0.0 | 5-methyltetrahydropterolytriglutamate/ homocysteine S-methyltransferase |
| SO1030 (*metH*) | 97-100 | 82-97 | 0.0-0.0 | *Ferrimonas balearica* | 98 | 74 | 0.0 | B12-dependent methionine synthase |
| SO0929 (*metK*) | 100-100 | 89-99 | 0.0-0.0 | *Ferrimonas balearica* | 100 | 88 | 0.0 | Methionine adenosyltransferase |
| SO3006 (Dcm Transmethylase) | 23-100 | 8-85 | $10^{-137}$-1.7 | *Yersinia pseudotuberculosis* | 99 | 57 | 0.0 | C-5 cytosine-specific DNA methylase family protein |
| SO1322 (*mtnN*) | 97-100 | 77-97 | $10^{-129}$-$10^{-170}$ | *Ferrimonas kyonanensis* | 97 | 70 | $4^{-113}$ | 5-methylthioadenosine nucleosidase |
| SO1676 (*metA*) | 99-100 | 83-97 | 0.0-0.0 | *Ferrimonas balearica* | 99 | 70 | $1^{-164}$ | Homoserine O-succinyltransferase |
| SO4056 (*metB*) | 96-100 | 83-97 | 0.0-0.0 | *Ferrimonas balearica* | 96 | 71 | 0.0 | Cystathionine gamma-synthase |
| SO2191 (*metC*) | 96-100 | 77-97 | 0.0-0.0 | *Psychromonas hadalis* | 97 | 81 | 0.0 | Cystathionine beta-lyase |
| SO4054 (*metF*) | 49-100 | 26-99 | 0.0-0.028 | *Grimontia* sp. AK16 | 99 | 74 | $4^{-165}$ | 5,10-methylenetetrahydrofolate reductase |
| SO4057 (*metJ*) | 100-100 | 85-98 | $10^{-64}$-$10^{-75}$ | *Photobacterium produndum* SS9 | 99 | 86 | $1^{-161}$ | Transcriptional repressor of methionine metabolism |
| SO4055 (*metL*) | 100-100 | 78-98 | 0.0-0.0 | *Ferrimonas balearica* | 99 | 52 | 0.0 | Aspartate kinase |
| SO1095 (*metY*) | 98-100 | 38-97 | $10^{-78}$-0.0 | *Cobetia martina* | 99 | 87 | 0.0 | O-acetylhomoserine aminocarboxypropyltransferase |
| SO2903 (*cysK)* | 100-100 | 88-98 | 0.0-0.0 | *Oceanimonas smirnovii* | 99 | 82 | 0.0 | Cysteine synthase |
| SO3598 (*cysM)* | 95-100 | 31-96 | $10^{-55}$-0.0 | *Vibrio cholerae* | 100 | 80 | $9^{-171}$ | Cysteine synthase B |
| SO3559 (*gshA*) | 90-99 | 66-92 | 0.0-0.0 | *Aeromonas diversa* | 94 | 54 | 0.0 | Glutamate-cysteine ligase |
| SO0831 (*gshB*) | 99-100 | 83-97 | 0.0-0.0 | *Aliagarivorams taiwanensis* | 99 | 75 | $4^{-179}$ | Glutathione synthetase |
| SO4702 (*gor*) | 92-100 | 29-99 | $10^{-43}$-0.0 | *Ferrimonas balearica* | 100 | 74 | 0.0 | Glutathione reductase |
| SO3779 (*cydC*) | 95-100 | 52-91 | 0.0-0.0 | *Psychromonas hadalis* | 99 | 61 | 0.0 | Glutathione ABC transporter ATP-binding protein |
| SO3780 (*cydD*) | 93-100 | 53-85 | 0.0-0.0 | *Psychromonas hadalis* | 96 | 62 | 0.0 | Cysteine ABC transporter ATP-binding protein |
| SO3415 (*thrA*) | 99-100 | 76-97 | 0.0-0.0 | *Oceanimonas* sp. GK1 | 99 | 59 | 0.0 | Bifunctional aspartokinase I / homoserine dehydrogenase |
| SO3414 (*thrB*) | 99-100 | 72-96 | $10^{-176}$-0.0 | *Leminorella grimontii* | 99 | 57 | $3^{-123}$ | Serine Kinase |
| SO3413 (*thrC*) | 99-100 | 72-96 | 0.0-0.0 | *Ferrimonas futtsuensis* | 99 | 65 | 0.0 | Threonine synthase |
| SO1812 (*mdeA*) | 98-99 | 72-91 | 0.0-0.0 | *Colwellia piezophila* | 99 | 68 | 0.0 | Methionine gamma-lyase |

[a]**Percents sequence similarity (Sim), percents identity (ID), and E values for S. oneidensis AMC, Transulfurylation pathway, and direct sulfurylation pathway gene sequences obtained from TIGR are shown. Ranges were determined by pairwise comparison with translated sequence data from genome sequences of recently sequenced *Shewanella* groups, including *S. putrefaciens* 200, S. *putrefaciens* CN32, *S. putrefaciens* W3-18-1, *S. amazonensis* SB2B, *S. denitrificans* OS217, *S. baltica* OS195, *S. frigidimarina* NCIMB400, *S. pealeana* ATCC 700345, *S. woodyi* ATCC 51908, *Shewanella sp*. ANA-3, *Shewanella sp.* MR-4, *Shewanella sp.* MR-7, *S. loihica* PV-4, *S. halifaxens, S. piezotolerans, S. benthica*, and *S. sediminis*.**

[b]**Organisms outside the genus Shewanella with the homologs of the highest similarity (best hit) as determined by BLASTp analysis of the GenBank nonredundant database are shown.**

**Table 4.5. Rates of Fe(II) production (mM $hr^{-1}$) in *S. oneidensis* wild-type and *luxS, metB, metC,* and *metY* with $H_2$ or lactate as the electron donor and HFO, Hematite, or Goethite as the terminal electron acceptor.**

| | $H_2$ | | | Lactate | | |
|---|---|---|---|---|---|---|
| | **HFO** | **Hematite** | **Geothite** | **HFO** | **Hematite** | **Geothite** |
| **WT** | 0.0191 | 0.0124 | 0.0039 | 0.0419 | 0.0029 | 0.0232 |
| **Δ*luxS*** | 0.0218 | 0.0118 | 0.0041 | 0.0478 | 0.0026 | 0.0231 |
| **Δ*metB*** | 0.0101 | 0.0030 | 0.0015 | 0.0107 | 0.0010 | 0.0128 |
| **Δ*metC*** | 0.0117 | 0.0045 | 0.0012 | 0.0133 | 0.0007 | 0.0093 |
| **Δ*metY*** | 0.0233 | 0.0125 | 0.0053 | 0.0462 | 0.0036 | 0.0217 |

# CHAPTER 5

## THESIS SUMMARY AND FUTURE RESEARCH DIRECTIONS

Microbial iron respiration is a central component of a variety of environmentally important processes, including bioremediation of radionuclide-contaminated water, biogeochemical cycling of iron and carbon, degradation of toxic hazardous pollutants, and generation of electricity in microbial fuel cells. Bacterial energy conservation requires generation of a proton motive force (PMF) across the inner membrane (IM). Electrons originating from oxidation of electron donors are transported down the redox gradient of an electron transport chain to IM- or periplasmic- localized terminal reductases coupled to proton translocation across the IM to generate PMF. PMF drives ATP synthesis as protons are translocated back into the cytoplasm through IM-localized ATPases, catalyzing the phosporylation of ADP to ATP. Fe(III)-respiring bacteria are presented with a unique physiological problem: they are required to respire anaerobically on insoluble terminal electron acceptors that are unable to contact IM-localized electron transport systems

*S. oneidensis* employs a variety of novel respiratory strategies to overcome the problem of respiring solid Fe(III) oxides including i) direct enzymatic reduction via outer membrane (OM) or nanowire-localized metal reductases, ii) Fe(III) chelation (solubilization) pathways in which the solid Fe(III) oxides are first non-reductively dissolved by endogenously synthesized organic ligands prior to reduction, iii) nanowire pathways in which electrically conductive pili (nanowires) transfer electrons to external

metal oxides, and iv) electron shuttling pathways mediated by exogenous or endogenous electron shuttling compounds.

The formation of biofilms is a widely known mechanism utilized by both gram-negative and gram-positive bacteria. Biofilms, which can form on both biotic and abiotic surfaces, have been shown to control bioluminescence, sporulation, competence, antibiotic production and resistance, and virulence factor production via quorum sensing mechanisms. Mechanisms that control anaerobic biofilm formation in *S. oneidensis* are poorly understood and the connection between biofilm formation and Fe(III) oxide reduction activity is even less understood. Chapter 2 provides evidence that electron shuttling is the primary mechanism though which Fe(III) reduction occurs. Our results indicate that the mutant Δ*luxS* was incapable of forming biofilms under anaerobic conditions, yet retains wild-type anaerobic Fe(III) reduction activity under all conditions tested. These results imply biofilm formation and direct contact to the surface of metal oxides is not important for electron shuttling and Fe(III) reduction.

Autoinducer molecules are chemical signals produced and used by bacteria to regulate quorum sensing. In most studies involving autoinducer molecules (i.e. autoinducer-2, autoinducer-1, and acylhomoserine lactone) are believed to regulate biofilm formation via quorum sensing. However, the *S. oneidensis* genome only contains the autoinducer-2 synthase gene, *luxS*. The results of Chapter 3 indicate autoinducer-2 is not used to regulate biofilm formation; instead, the molecule is used by *S. oneidensis* as an alternate carbon energy source or electron donor source under anaerobic growth conditions.

Thiols are potent chemical reductants of Fe(III), rapidly coupling Fe(III) reduction to production of the corresponding disulfide. Cysteine, for example, reduces Fe(III) oxides abiotically via electron transfer reactions that produce Fe(II) and cystine.

The initial rate and extent of Fe(III) reduction correlate linearly with cysteine concentration. In previous studies, the addition of cysteine to Fe(III)-reducing *S. oneidensis* cultures increased the rate and extent of Fe(III) reduction by *S. oneidensis*, and the addition of cysteine to *S. oneidensis*-driven microbial fuel cells increased power generation. In addition, exogenous cysteine functioned as an electron carrier between *Geobacter sulfurreducens* and *Wolinella succinogenes* in an acetate-oxidizing, Fe(III)-reducing syntrophic co-culture. The detection of extracellular thiols in anaerobic Fe(III)-reducing *S. oneidensis* cultures, and the ability of thiols to rapidly reduce Fe(III) oxides forms the basis of a novel electron shuttling system: thiol-driven (abiotic) reduction of external Fe(III) oxides is sustained via catalytic (biotic) reduction of the resulting disulfides .

To build on the results presented in Chapters 2 and 3, the thiol and disulfide production activity of *luxS, metB, metC,* and *metY* in-frame deletion mutants was analyzed during anaerobic respiration on Fe(III) oxides, Mn(III), and Mn(IV) oxides. The results of Chapter 4 indicate various intermediates of the activated methyl cycle and transulfurylation pathway and the Fe(III) and Mn respiratory phenotypes are impacted upon deletion of *luxS, metB, metC,* and *metY* from the genome. Fluctuations in thiol/disulfide concentrations are indicative of the use of thiol (i.e. cysteine, homocysteine, reduced glutathione, and cysteamine) compounds as an electron shuttle. Increased thiol concentration (or maintained thiol pools) results in Fe(III) reduction, Fe(II) production, and disulfide formation. Interestingly, reduced glutathione was found throughout the experimental time phase for wild-type, Δ*luxS, ΔmetB, ΔmetC,* and Δ*metY*. The presence of reduced glutathione centers around the ability of reduced glutathione ability to reduce disulfides,

which in turn reduces metal oxides. Reduced glutathione functions as a huttle for the electron shuttles. The Fe(III) reduction-deficient phenotype displayed by Δ*metB* and Δ*metC* suggests the Transulfurylation pathway is required to promote metal reduction, while the AMC contributes to the biosynthesis of thiols.

Furthermore, thiols serve as a redox buffer to allow *S. oneidensis* to transition between electron acceptors (with varying redox potentials) while maintaining homeostasis levels of thiols within the cell, which ultimately drives electron shuttling. Current work is focused on analyzing abiotic thiol and disulfide activity on insoluble Fe(III) and Mn(IV) oxides and characterizing what initiates and catalyzes the multi-step electron shuttling pathway which begins with enzymatic disulfide reduction at the cell surface and terminates with abiotic Fe(III) oxide reduction outside the cell. Future experiments will focus on identifying the thiols and disulfides present under anaerobic growth conditions with alternative electron acceptors, including fumarate, nitrate, nitrite, and thiosulfate. We will also will explore the role of redox homeostasis in production and maintenance of biofilm formation under anaerobic formation, the impact of endogenous and exogenous thiols on biofilm formation, and the role of thiols as a redox buffer by *S. oneidensis*. The use of thiols as a redox buffer allows *S. oneidensis* to transition between electron acceptors, including those with similar redox potentials and those with highly varied redox potentials, which ultimately allows the bacteria to maintain internal thiol concentrations. In addition, future studies will seek to identify the reductase that interacts with the thiols and disulfides that serve as electron shuttles to Fe(III) and Mn(IV) oxides. We will focus on the MtrCAB complex that is believed to play a role as the terminal reductase under direct contact mechanism of metal reduction.

Purified MtrCAB complex has been shown to reduce Fe(III) oxides ex vivo. Our aim is to show that MtrC can reduce the thiol electron shuttle, for example if MtrC can function as the thiol reductase and reduce oxidized glutathione, the reduced glutathione can then reduce other disulfides such as cystamine, cystine, and homocystine which then serve as the electron shuttle to the Fe(III) and Mn(IV) oxides.

Future research should also focus on the role of electroactive biofilms formed by *S. oneidensis* and the role they play in extracellular electron transfer to both insoluble metal oxides and the surface of poised electrodes. Biofilms can form on the surface of these metal oxides and electrodes creating a electron shuttling mechanism through which secreted redox mediators, such as thiols (i.e. cysteine, glutathione, homocysteine) accumulate at the surface of these particles and electrons. The accumulation of thiols on the surface of biofilms provides a recyclable electron shuttle for Fe(III) oxides, Mn(IV) oxides, and electrode surfaces. Studies should look further into the impact of biofilm age (attachment, growth, detachment), variations in the concentration of thiols produced and secreted during the various biofilm phases, and any impact on electron shuttling (i.e. do rates of thiol production and electron shuttling increase or decrease depending on the biofilm age). The aim of this work should be to show that biofilm attachment to the surface of electrodes and metal oxides provides an environment for electron shuttling via production and secretion of redox mediators (i.e. thiols). We have shown in previous experiments that biofilm formation-deficiency does not prevent Fe(III) oxide reduction activity, but the introduction of exogenous redox mediators restores biofilm formation activity and can ultimately provide a boost in reduction activity via electron shuttling. These studies have important implications in the optimization of microbial fuel cells and

other biofilm-based electrochemical systems, such as biosensors. In addition to the role of biofilm-mediated electron shuttles and optimization of microbial fuel cells, the secretion of redox mediators by biofilms in redox stratified marine and freshwater sediments may aid in metal reduction and cycling in areas were availability of specific substrates or electron shuttles are not in the immediate vicinity of metabolically active metal-reducing bacteria. In redox stratified marine and freshwater environments, biofilms have the potential to provide continuous, recyclable electron shuttles (i.e. thiols) a phenomenon that should be studied in future experiments.

# VITA

## Rebecca Elizabeth Cooper

Rebecca Elizabeth Cooper was born in Longview, Texas, but moved to Savannah, GA as a toddler. She attended St. Andrew's School in her hometown of Savannah before moving to Atlanta to begin her undergraduate studies. She received a B.S. in Biology from Georgia Institute of Technology, Atlanta, GA in 2008 and M.Sc. from Appalachian State University, Boone, NC in 2010 before returning to Georgia Tech to pursue a doctorate in 2010. When she is not working on her research, Ms. Cooper enjoys running, playing tennis, and visiting her family's mountain home in Boone, NC.